UNIVERSITY OF LIVERPOOL

AN INSIGHT INTO THE MECHANISMS OF ABACAVIR INDUCED HYPERSENSITIVITY REACTIONS WITH A VIEW TO DESIGNING SAFER THERAPEUTICS.

This thesis is submitted in accordance with the requirements of the University of Liverpool for the degree of Doctor of Philosophy by

Paul James Thomson

August 2018

To my family, here and there, one and all.

Declaration

I declare that the work presented in this thesis is all my own work and has not been submitted for any other degree.

……………………………………………………………………………………………….

Paul James Thomson (MSc, BSc)

Acknowledgements

Firstly, I would like to unreservedly thank my two supervisors Professor Dean Naisbitt and Professor Kevin Park for all their help and support throughout my PhD. Throughout the years many hurdles appeared in my project and Deans door was always open for him to provide support and guidance on how to move forward when things went wrong. I would also like to thank Professor Paul O'Neill and Dr Neil Berry from the Department of Chemistry for the assistance with the abacavir analogues and for teaching me the molecular modelling. I would also like to thank the team at Monash University in Melbourne for all their hard work and advice with the peptides, Nicole and Tony. Staying with the Melbourne group, I am forever indebted to Dr Patricia Illing for her tremendous work and assistance with the peptide elutions with the abacavir analogues, her support and assistance was fantastic and is something I will never forget.

I would also like to thank all members of the CDSS both past and present for their help and support throughout my time in the department. Sally Wood and Dr Lee Faulkner for teaching me all the techniques that I used throughout my studies and John Farrell who assisted me greatly throughout the years. I would also like to thank my colleagues in the lab and throughout the department, who over the years have become great friends. Particular thanks goes to my weekend buddies Monday Ogese and Samantha Jones, who much like me spent many a weekend in the lab and were always up for a chat. Staying with my colleagues, special mention goes to James, Joel, Arun, Adrianna and Andy who kept Thursday drinks going throughout the years, usually followed by some cheap food in town, a much needed distraction from lab work! I would also like to thank my two students in the lab Laila and Kanoot, who will soon be about to start this all for themselves. Working with you both on a day to day basis has helped me greatly in preparing for whatever I do next! Special mention also goes to Alejandra Monroy, who came to our department for 6 months to learn techniques and left as one of my greatest friends, who has stayed in regular contact with me throughout my time here! Indeed, our constant bickering about who owns the hood in the side lab (it's mine btw!) and how a haggis is clearly an animal native to Scotland, has cheered me up so many times!

I must also extend my gratitude and admiration to the City of Liverpool in general, I came here as a loner Scotsman and this wonderful city and its wonderful people have made me feel most welcome.

Finally, I would like to take this opportunity to extend my unconditional gratitude to my family, who have supported me throughout my almost 10 years as a student, completing 3 separate degrees at as many Universities up and down the United Kingdom. To my sister Amy, who after a few hiccups has finally settled herself at University and is currently on track to achieve a First Class degree! To my grandparents who have always phoned me to see how I am getting on and been up for a needed chat to take my mind off things when it all got a bit stressful. Lastly, but by no means least, to my Mum and Dad who have been there for me throughout and always provided help unconditionally when it was needed in whatever capacity. I couldn't have done the last ten years without yous!

Contents

List of abbreviations

ABC	Abacavir
ACEi	Angiotensin Converting
ACP	Acyl Carrier Protein
ADR	Adverse Drug Reaction
AHR	Aryl Hydrocarbon Receptor
ALP	Alkaline Phosphate
AMP	Adenosine Monophosphate
APC	Antigen Presenting Cell
AUC	Area Under Curve
BCL	B-cell Lymphoma
BLAST	Basic Local Alignment Search Tool
β₂m	β_2-microglobulin
BSA	Bovine Serum Albumin
CCR	Co-receptor
CD	Cluster of Differentiation
CFSE	Carboxyfluorescein Succinimidyl Ester
Ci	Curie
CMV	Cytomegalovirus
cpm	Counts per minute
CSA	Cyclosporin A
CTLA	Cytotoxic T-lymphocyte-Associated Protein 4
CYP	Cytochrome P450
DAMP	Damage-associated Molecular Pattern
DAP	Diaminopimelic Acid
DC	Dendritic Cell
dGTP	Deoxyguanosine Triphosphate
DILI	Drug Induced Liver Injury
DIPEA	Diisopropylethylamine
DISC	Death-Inducing Signaling Complex
DNA	Deoxyribose Nucleic Acid
DNFB	Fluoro dinitrobenzene
DoTs	Dose over Time and Susceptibility
DRESS	Drug Reaction with Eosinophilia and Systemic Symptoms
EBV	Epstein Barr Virus
ELISA	Enzyme-Linked Immunosorbent Assay
ELIspot	Enzyme-Linked Immunospot Assay
EPI	Enhanced Product Ion
ER	Endoplasmic Reticulum
EtOH	Ethanol
FACS	Fluorescence Activated Cell Sorting
FasL	Fas Ligand
FcεRI	High-Affinity IgE Receptor
FDA	Food and Drug Administration
FDR	False Discovery Rate

FOXP3	Forkhead Box P3
g	Gram
GI	Gastrointestinal
GLD	Glutaraldehyde
GM-CSF	Granulocyte-Macrophage Colony-Stimulating Factor
GrB	Granzyme B
GSTP	Glutathione S-transferase P
GWAS	Genome Wide Association Study
h	Hour
HBSS	Hanks Balanced Salt Solution
HEPES	Hydroxyethyl Piperazineethanesulfonic Acid
HHV	Human Herpesvirus
HIV	Human Immunodeficiency Virus
HLA	Human Leukocyte Antigen
HMGB1	High Mobility Group Box 1
HPLC	High Performance Liquid Chromatography
HSA	Human Serum Albumin
HSP	Heat Shock Protein
HSV	Herpes Simplex Virus
IBD	Inflammatory Bowel Disease
IFN	Interferon
Ig	Immunoglobulin
IL	Interleukin
i-PrOH	Isopropyl alcohol
ITIM	Immunoreceptor Tyrosine-Based Inhibitory Motif
KLRG-1	Killer cell Lectin-like Receptor Subfamily G Member 1
L	Litres
LAIR-1	Leukocyte-Associated Immunoglobulin-like Receptor 1
LCMS	Liquid chromatography mass spectrometry
LPS	Lipopolysaccharide
LTT	Lymphocyte Transformation Test
Mb	Megabase
mg	Milligram
MHC	Major Histocompatibility Complex
mL	Millilitres
MPE	Maculopapular Exanthema
MRM	Multiple Reaction Monitoring
mRNA	Messenger Ribonucleic Acid
MS	Mass Spectrometry
µg	Microgram
µL	Microliters
µM	Micro molar
MW	Molecular Weight
NHS	National Health Service
NK	Natural Killer Cell
NMR	Nuclear magnetic resonance
NNT	Number Needed to Treat

NPV	Negative Predictive Value
NRTI	Nucleoside Reverse-Transcriptase Inhibitors
NSAID	Nonsteroidal anti-inflammatory Drug
PAMP	Pathogen-associated Molecular Pattern
PBMC	Peripheral Blood Mononuclear Cells
PBS	Phosphate-buffered saline
PDB	Protein Data Bank
pH	Power of Hydrogen
PHA	Phytohemagglutinin
PI	Pharmacological Interaction
PPV	Positive Predicative Value
PRR	Pattern Recognition Receptor
pΩ	C-terminal anchor residue
QALY	Quality-Adjusted Life Year
RORYT	RAR-related orphan receptor gamma
rpm	Revolutions per minute
RPMI	Roswell Park Memorial Institute
SCAR	Severe Cutaneous Adverse Reactions
SD	Standard Deviation
SEM	Standard Error of Mean
SFU	Spot Forming Units
SI	Stimulation Index
SJS	Stevens Johnson Syndrome
SMX	Sulfamethoxazole
SMX-NHOH	Sulfamethoxazole Hydroxylamine
SMX-NO	Nitroso sulphamethoxazole
SNP	Single Nucleotide Polymorphism
SOCS	Suppressor of Cytokine Signalling
SSRI	Selective Serotonin Reuptake Inhibitor
STAT	Signal Transducer and Activator of Transcription Protein
TAP	Transporter Associated with Antigen Presentation
TCC	T-cell clone
TCR	T-cell Receptor
TEN	Toxic Epidermal Necrolysis
Tfh	Follicular B helper T cells
TGF	Transforming Growth Factor
Th	T helper cell
TLR	Toll Like Receptor
TMB	Tetramethylbenzidine
T-MWA	T-cell Multi-Well Assay
TNF	Tumour Necrosis Factor
Treg	Regulatory T-cell
U.K.	United Kingdom
WHO	World Health Organisation

Manuscripts in preparation

Paul J Thomson, Patricia T Illing, John Farrell, Mohammad Alhaidari, Neil Berry, Paul M O'Neill, Anthony W Purcell, Kevin B Park, Dean J Naisbitt.

Modification of the cyclopropyl moiety of abacavir provides insight into the relationship between HLA-B*57:01 binding and T-cell activation.

Paul J Thomson Patricia T Illing, John Farrell, Mohammad Alhaidari, Nicole A Mifsud, Anthony W Purcell,, Kevin B Park, Dean J Naisbitt.

Abacavir altered self-peptides can be recognised by CD8$^+$ T-cells, leading to the induction of a hypersensitivity reaction.

Published Abstracts

EAACI Drug Hypersensitivity Meeting 2018, Amsterdam, Netherlands. 19th-21st April 2018.

Poster Title: Modifications of the cyclopropyl moiety if abacavir provides an insight into the relationship between the drug interaction within the HLA-B*57:01 antigen binding cleft and T-cell activation.

Poster Title: Abacavir altered self-peptides can be recognised by CD8+ T-cells, leading to the induction of a hypersensitivity reaction. **(Travel Grant Winner).**

Basic Immunology Research in Allergy and Clinical Immunology, 15th EAACI Immunology Winter School, 2017, Sierra Nevada, Spain 26-26th January 2017.

Poster Title: Eradication of unwanted CD8+ T-cell responses to abacavir via the modification of the 6-amino cyclopropyl moiety.

EAACI Drug Hypersensitivity Meeting 2016, Malaga, Spain. 21st-23rd of April 2016.

Poster title: Development of novel chemicals that do not bind to HLA-B*57:01 or activate CD8+ T-cells through modification of the 6-amino cyclopropyl group of abacavir. **(Travel Grant Winner).**

Abstract

Immune-mediated hypersensitivity reactions to the antiretroviral drug abacavir are observed exclusively in individuals carrying the HLA-B*57:01 risk allele. Abacavir is hypothesised to bind within the peptide binding groove of HLA-B*57:01 and alter the array of peptides presented on the cell surface. Indeed, presentation of these unique abacavir-self-peptide complexes is thought to initiate a CD8^{+} mediated T-cell response to the drug in hypersensitive patients.

Consistent with previous findings abacavir-specific T-cell clones from healthy donors expressing HLA-B*57:01 were found to be activated via 2 independent mechanisms, relying on and exclusive of antigen processing respectively. Furthermore, clones yielded a varied T-cell receptor expression and cytokine secretion properties when stimulated with abacavir, indicating the presence of multiple unique subsets of abacavir-responsive T-cells.

Eighteen abacavir substituted analogues were synthesised with modifications to the cyclopropyl moiety of the compound, namely derivatives of the azetidine group. Eight of these analogues completely lacked any T-cell activity, while others strongly induced IFN-γ secretion from the abacavir-responsive clones. Interestingly, activation of T-cells was demonstrated to be enantiomeric-specific around the cyclopropyl and cyclopentyl moiety. However, no analogue bereft of T-cell activity possessed sufficient antiviral potency to be considered a replacement for abacavir in the therapeutic setting. Molecular modelling revealed the unfavourable binding characteristics of non-cross-reacting analogues within the peptide binding groove of HLA-B*57:01, something not observed with T-cell activating analogues. Furthermore, peptide elution studies revealed a distinct shift towards small chain terminating peptides in the presence of cross-reacting abacavir analogues but not non-cross reactive analogues. Raising clones to the respective analogues of abacavir yielded a plethora of T-cells with reactivity towards the analogues including those that initially did not cross react with abacavir clones, indicating the importance of T-cell cloning assays in the analysis of the immunogenicity of HLA-binding drugs.

While the role of altered self-peptides presented on the surface of the MHC in the presence of abacavir is thought to drive the CD8^{+} mediated T-cell reactions, the peptide sequences that activate T-cells in the presence of abacavir has not been fully defined. Further studies with a previously presumed immunogenic peptide (NTVELRVKI) demonstrated little to no reactivity towards abacavir clones in its natural form, whilst producing non-specific T-cell activity in the amidated form. Dissecting the contribution of the abacavir-induced-self-peptides in T-cell responses to abacavir is difficult as these peptides are naturally loaded onto MHCs for presentation on the cell surface. However, using a panel of five abacavir induced-self peptides which had underwent kinetic studies previously to examine their dependence on abacavir for presentation on the surface of antigen presenting cells over time, peptide responsive T-cell clones were generated in the presence of abacavir. At low concentrations of the drug, these clones demonstrated an enhanced response to abacavir in the presence of the individual self-peptides. Finally, two clones raised solely to abacavir, displayed strong IFN-γ secretion to two of the self-peptides in the absence of the drug. These findings suggest that the abacavir-dependent self-peptides do seem to contribute to the activation of T-cells.

This work highlights the involvement of peptides in the CD8^{+} T-cell-mediated hypersensitivity reactions to abacavir in HLA-B*57:01^{+} individuals. Furthermore, it emphasises the

importance of a holistic approach to the design and subsequent analysis of the safety of a new compound for integration into the therapeutic setting.

Chapter 1 General Introduction

1.1. Adverse drug reactions

The definition of adverse drug reactions (ADRs) given by the World Health Organisation (WHO), which has been used for over 30 years, is "a response to a drug that is noxious, unintended and occurs at doses normally used in man for the prophylaxis, diagnosis or therapy of a disease, or for the modification of physiological function" (WHO, 1972). However in 2000, *Edwards & Aronson* criticised WHO's definition of ADRs due to the ambiguity of the word "noxious". They argued that this word did not encompass all adverse reactions, specifically those which are an inconvenience to the patient but not necessarily harmful. They also stated that this particular definition did not include reactions that occur to drugs at a dose out of the therapeutic range i.e. overdoses and trace amounts (Edwards & Aronson 2000). Therefore it was proposed that ADRs be defined as "an appreciably harmful or unpleasant reaction, resulting from an intervention related to the use of a medicinal product which predicts hazard from future administration and warrants prevention of specific treatment, alteration of the dosage regimen or withdrawal of the product" (Edwards & Aronson 2000).

ADRs represent a major problem both clinically and financially due to the increase in morbidity and mortality that they cause. ADRs account for 6.5% of hospital admissions in adults in the UK and 2.1% in children (Pirmohamed et al. 2004). Furthermore 6.7% of patients will suffer a serious ADR whilst in hospital, 0.15% of which will be fatal, accounting for 5700 deaths per year (Lazarou et al. 2015). ADRs account for 1 in 16 hospital admissions in the UK, and on average prompt a hospital stay of around 8 days. This represents around 4% of the total capacity of all hospital beds, translating to a financial burden of £466 million on the National Health Service (NHS) (Pirmohamed et al. 2004).

ADRs can also significantly affect a patient's compliance to drug therapy which can have a detrimental effect on their quality of life. Furthermore, the incidence of ADRs significantly

reduce the availability of the choice of drug treatment for the patient, as well as leading to diagnostic confusion. This may reduce the patient's confidence in the healthcare professionals leading to further compliance issues.

1.2. Classification.

ADRs can be classified under two main headings, common and uncommon ADRs and can be categorised using the A-G classification system.

Type A (Augmented) reactions are predictable, dose related ADRs which are generally related to the pharmacology of the drug. These reactions are usually less severe than type B reactions but are more frequent. They account for 80% of the overall proportion of ADRs (Farcas & Bojita 2009). Type A reactions are related to the primary pharmacology and the secondary actions of the drug which may differ from its therapeutic action but is still known from the drugs pharmacological profile. For example, the treatment of hypertension with β-blockers is known to induce bradycardia due to the blockade of β-adrenergic receptors in cardiac tissues leading to a reduction in heart rate. However non-selective β-blockers can block β_2 receptors in pulmonary tissues, thereby preventing the binding of epinephrine and norepinephrine leading to bronchospasm (Ahmed & Branley 2009).

Type B (Bizarre) reactions are uncommon but often well recognised ADRs. These manifest in a minority of patients and usually consist of sensitive or idiosyncratic reactions (Rohilla & Yadav 2013). Type B reactions are not obviously dose dependent or related to the primary pharmacology of the drug making them difficult to predict during drug development. Therefore, these reactions may only be recognised following licensing as a result of post marketing pharmacovigilance (Pirmohamed & Park 2003). Type B reactions are very important as they are often severe and in some cases can result in mortality (Farcas & Bojita 2009) (Pirmohamed 2005). Type B reactions can affect multiple organs within the body an include reactions such as hypersensitivity, Stevens Johnson syndrome (SJS), toxic epidermal

necrolysis (TEN), anaphylaxis and drug induced liver injury (DILI) (Wei, Michael lee, et al. 2012). These reactions often occur in susceptible individuals with an association between specific HLA-alleles and a range of culprit drugs being a prime example. This includes antibiotics (e.g. penicillins), non-steroidal anti-inflammatory drugs (NSAIDs e.g. celecoxib), anti-convulsants (e.g. carbamazepine), allopurinol and anti-retrovirals (e.g. abacavir). These reactions are mediated by the adaptive immune system involving the presentation of drug antigens by major histocompatibility complexes (MHC) leading to the subsequent activation of T-cells.

Type C (Chronic) reactions are caused by repeated exposure to a drug over a long period of time. They are uncommon reactions and are related to the aggregating dose of the drug (Farcas & Bojita 2009). For example, glucocorticoids are prescribed to patients for their immunosuppressive and anti-inflammatory properties to treat auto-immune diseases. However, chronic use of these glucocorticoids induces a decrease in calcium absorption in bones leading to a reduction in bone remodelling and a decrease in bone turnover which can result in osteoporosis (Fraser & Adachi 2009).

Type D (Delayed) reactions are uncommon, usually dose-dependent reactions only detected following repeated exposure to the drug or exposure at a critical time point in a patient's life. Immunosuppressant drugs prescribed to treat inflammatory bowel disease (IBD) has been shown to be associated with an increase in incidence of lymphoma in patients subjected to repeated exposure (Farrell et al. 2000; Bewtra & Lewis 2011).

Type E (End of Treatment) reactions are uncommon reactions that can occur following cessation of the drug therapy. This generally refers to negative symptoms experienced upon withdrawal of drugs such as opiates and selective serotonin reuptake inhibitors (SSRI's). Opiate withdrawal syndrome is a prime example of this kind of reaction where patients will

often experience symptoms such as headaches, muscle aches and cramps, hot and cold sweats and irritability upon withdrawal of drugs such as morphine (Farcas & Bojita 2009).

Type F (Failure of Therapy) reactions are more common dose-related reactions that are often caused by drug-drug interactions. These reactions have been described as an "unexpected failure of therapy" (Hartigan-Go & Wong 2000). For example antibiotics such as rifampicin and some anti-convulsants such as phenytoin, which possess enzyme inducing activity, can lead to an inadequate dosage of the female oral contraceptive pill hindering its ability to suppress ovulation, which may result in unwanted pregnancy (D'Arcy 1986). Indeed, female patients are now advised to seek other forms of contraception when prescribed enzyme inducing therapeutics.

Type G (Genetic) reactions are very rare but still important as they cause irreversible genetic and DNA damage. An obvious example of this is the teratogenic reactions caused by anti-emetic drug thalidomide on unborn foetuses including limb anomalies, congenital heart disease, deformation of the inner and outer ear and malformations in the eyes (Kim & Scialli 2011).

The A-G adverse drug reaction classifications is summarised in Table 1.1.

Type of Reaction	Drugs	Example
Augmented	β-blockers	Bronchospasm
Bizarre	Anti-epileptics (Carbamazepine)	Stevens Johnsons syndrome
Chronic	Glucocorticoids	Osteoporosis
Delayed	Immunosuppressants	Lymphoma
End of Treatment	Opiates, Benzodiazepines	Withdrawal syndrome
Failure of Therapy	Rifampicin, Phenytoin	Unwanted pregnancy
Genetic	Thalidomide	Teratogenicity

Table 1.1. Classifications of adverse drug reactions with culprit drugs and examples.

1.3. Dose, time and susceptibility used as tools for classifying ADRs

In 2003 *Aronson & Ferner* indicated that the traditional A-G classification system of adverse drug reactions only took into consideration the properties of the drug and the dose dependence of its effects. They suggested other factors should be considered including the time course and severity of the reaction along with the properties of the individual concerned including genetic, pathological and biological factors. All of which may increase an individual's susceptibility to a reaction (Aronson & Ferner 2003). Therefore, a classification system comprising of three main factors: dose, time and susceptibility (DoTS) was proposed.

1.3.1. Dose

This approach assumes that all ADRs, including those that are immunologically mediated, are dose dependent. These reactions are split into those that occur at doses above the therapeutic index (supratherapeutic) including toxicity and overdosage effects, standard therapeutic doses including collateral effects and doses below the therapeutic index (subtherapeutic) such as hypersensitivity reactions occurring in susceptible individuals (Callreus 2006).

1.3.2. Time

Two categories exist for the classification of ADRs based on their time course, time dependent reactions and time independent reactions (Callreus 2006; Aronson & Ferner 2003). Time independent reactions can take place at any point during the treatment regimen independent of the length of the course. This often happens when the concentration of the drug is altered at the site of action i.e. digoxin toxicity occurs when elimination of the drug is reduced due to renal impairment (Aronson & Ferner 2003).

Time dependent reactions can be classified into six subtypes:

1) Rapid reactions occur when the drug is administered too quickly, for instance the rapid injection of vancomycin has been known to cause red man syndrome (Sivagnanam & Deleu 2003).

2) First dose reactions will take place after the first dose of a drug in the treatment regimen. An example of this includes anaphylaxis with penicillin treatment (Drain & Volcheck 2001) or hypotension following first dose of angiotensin converting enzyme inhibitors (ACEi) in hypertensive patients (Vitovec & Spinar 2000).

3) Early reactions take place within the first few doses of treatment and usually cease with continued dosing when the individual has developed a tolerance. For instance nitrate induced headaches generally plateau after repeated doses (Wall et al. 1996).

4) Intermediate reactions generally occur after a some delay, however if the reaction has not taken place within a certain period of time then there is a low risk of the reaction taking place at all (Aronson & Ferner 2003). An example would be neutropenia with the prodrug carbimazole (Bux et al. 2000).

5) Late reactions seldom occur at the beginning of the treatment regimen but the risk of a reaction increases upon continuing exposure to the drug. For example Cushings Syndrome with continued glucocorticoid therapy (Sharma & Nieman 2011). This subtype also includes the withdrawal reactions experienced upon cessation of the drug treatment such as the headaches dizziness and nausea that can be experienced upon opiate withdrawal.

6) Delayed reactions can be observed a long period of time after exposure to the drug, even upon drug withdrawal prior to a reaction taking place. Teratogenetic reactions that were associated with thalidomide treatment in pregnant women is an obvious example (Kim & Scialli 2011).

1.3.3. Susceptibility

The third section of the DoTS paradigm takes into account the various factors that could affect an individual's susceptibility to a reaction. These include genetics, age, sex physiological state, exogenous drugs or foods and other disease states (Aronson & Ferner 2003; Callreus 2006). This is summarised in Table 1.2.

Susceptibility Variable	Example
Genetics	Patients positive for HLA-B*57:01 are more susceptible to hypersensitivity reactions with abacavir.
Age	Increased susceptibility to adverse reactions in older patients with renal failure which is more prevalent in 65<.
Sex	Increased risk of cutaneous reactions among females.
Physiological State	Anti-epileptic drugs can be excreted faster in pregnant women resulting in increased seizures.
Exogenous Factors	The consumption of grapefruit juice can adversely affect the bioavailabilty of numerous drugs that are metabolised via CYP3A4.
Disease	Hepatic cirrhosis affects morphine metabolism.

Table 1.2. Factors influencing an individual's susceptibility to an adverse drug reaction.

1.4. Drug induced hypersensitivity reactions

Drug induced hypersensitivity reactions are ADRs that are observed in susceptible individuals after exposure to certain drugs (Alfirevic & Pirmohamed 2010). Hypersensitivity reactions are type B reactions which can often be severe and in some cases life threatening (Sukasem 2014). As previously mentioned these reactions are not detected during drug discovery or clinical trials and generally only come to light during post marketing surveillance when exposed to susceptible individuals. This often results in the affected patient being prescribed alternate therapies which may have a reduced efficacy as well as being more expensive, which has a negative impact from both a patients and a healthcare professionals point of view (Alfirevic & Pirmohamed 2010).

Many hypersensitivity reactions are immunologically mediated (Phillips & Mallal 2011) and can often present symptoms including skin rash, anaphylaxis, gastrointestinal (GI) disturbances and severe cutaneous reactions including SJS and TEN (Phillips & Mallal 2011; Sukasem 2014). Hypersensitivity reactions can be classified into two groups; immune mediated reactions and non-immune mediated reactions.

Immune mediated reactions were classified into four main categories by *Gell and Coombs* (1963), ranging from Type I-IV.

Type I reactions are immediate type reactions that are produced by drug/antigen specific IgE antibodies and can manifest as angioedema, anaphylaxis and bronchoconstriction (Sukasem 2014).

Type II reactions referred to as cytotoxic mechanism reactions are caused by IgG and IgM cytotoxic events which can lead to cellular destruction and detachment affecting target cells such as erythrocytes, leukocytes and platelets (Pichler 2007). This can lead to haemolytic anaemia and thrombocytopenia.

Type III reactions are mediated by IgG and IgM and depend on the formation of immune complexes, which may take place during drug treatment, giving rise to an immune response (Pichler 2007). This can manifest as small vessel vasculitis and serum sickness.

Type IV reactions are known as delayed hypersensitivity reactions and are mediated via T-cells. SJS and TEN are prime examples of type IV hypersensitivity reactions, however based on the subgroups of T-lymphocytes involved and the cytokine expression profile, this group of reactions has been divided into an additional four subsets (IVa-IVd) (Sukasem 2014). The further (a-d) classification of these reactions is dependent on the respective involvement of monocytes (IVa), eosinophils (IVb), cytotoxic T-cells (IVc) and neutrophils (IVd) (Adam et al. 2011).

1.5. Clinical manifestations

The skin is the most common site of hypersensitivity reactions to drugs, due to it being a highly immunologically privileged site. Therefore it is a prime target for reactions mediated by the immune system as well as the fact that rashes present on the skin, even mild, are visible to the patient and are therefore more likely to be reported when compared with other organs where mild reactions may go unnoticed (Uetrecht & Naisbitt 2013). Maculopapular eruptions are the most common ADRs observed in the skin. Often reported as drug rashes or eruptions they account for 90% of cutaneous ADRs (Hunziker et al. 1997) . These reactions start on the trunk, upper extremities and increasingly become more widespread. This usually takes place 4-14 days following initiation of treatment with a drug and may still be apparent for 1-2 days following termination of therapy (Roujeau 2005).

Drug reaction with eosinophilia and systemic syndrome (DRESS) is a much rarer drug induced hypersensitivity reaction characterised by severe eruption, fever and rash, along with at least one symptom affecting other organs including lymphadenopathy, hepatitis, nephritis,

pneumonitis, carditis, thyroiditis and haematological anomalies such as thrombocytopenia and leukopenia. This reaction is reported to occur in between 1:1000 and 1:10000 patients with exposures to culprit drugs including anticonvulsants (lamotrigine, phenytoin and carbamazepine), antimicrobials (flucloxacillin, ampicillin, dapsone, sulfamethoxazole) and antivirals (abacavir and nevirapine) (Spriet & Banks 2015). Symptoms develop in 2-6 weeks post first use, which is typically later than other reactions and have been reported to be most frequent in people of African descent. Subsequent re-exposure can evoke a reaction in a much shorter period of time (24 hours) (Roujeau 2005; Verma et al. 2013). Abnormalities in the liver are apparent in up to 70% of patients expressing symptoms of DRESS, which is usually characterised by a clear increase in serum alanine aminotransferase levels often resulting in hepatitis directly associated with the 20% mortality rate of DRESS (Shiohara et al. 2006). DRESS reactions to drugs have been shown to be regulated by the cellular actions of eosinophils mediated via the secretion of IL-5 from T-cells, which was demonstrated to be elevated in patients with DRESS (Choquet-Kastylevsky et al. 1998). Viral reactivation is associated with the more severe symptoms of DRESS and is often used as a diagnostic tool (Pritchett et al. 2012). Human herpes virus-6 (HHV-6) is detected in a majority of patients with severe DRESS symptoms. Indeed, an increased HHV-6 DNA has been detected in the serum of fatal cases of DRESS associated with renal failure (Descamps et al. 2003). The presence of cytomegalovirus (CMV) and Epstein Barr virus (EBV) have also been shown to participate in some cases of DRESS with drugs including allopurinol and phenytoin (Aihara et al. 2001; Descamps et al. 2003).

SJS and TEN are severe adverse cutaneous reactions which primarily affect the skin and mucosal membranes. TEN is the most severe of the cutaneous reactions yielding a mortality rate of approximately 30% while SJS is a milder form of the same reaction. TEN has an incidence of 0.4-1.2 cases per million persons per year while SJS is slightly higher at 1-2 cases

per million persons per year (Rzany et al. 1996). The presentation of SJS is identified by the presence of small blistering emerging on purple macules. Widespread lesions are also apparent and usually predominate on the trunk. The spread of these blisters can result in separation of the epidermis from the dermis and overall detachment in <10% of the bodily surface area (Roujeau 2005; Uetrecht & Naisbitt 2013). The same lesions are characteristic of TEN but with a higher prevalence of blisters resulting in overall detachment of large epidermal sheets on >30% of the bodily surface area. Cases where the detachment lies between 10 and 30% are referred to as overlap SJS-TEN (Bastuji-Garin et al. 1993). Various mucosal sites including the mouth, genitals, eyes and intestines are implicated in both SJS and TEN which can result in blindness.

The pathogenesis of SJS/TEN is thought to be immune mediated due to the fact that re-challenge with culprit drugs can result in swift reappearance of symptoms (Harr & French 2010). SJS/TEN lesions demonstrate keratinocyte apoptosis followed by necrosis, which is a marker of epidermal detachment. Blister fluid analysis reveals the presence of cytotoxic lymphocytes suggesting a MHC Class I-restricted CD8$^+$ T-cell-mediated reaction is involved (Le Cleach et al. 2000). Keratinocyte apoptosis appears to be regulated via the death ligand FasL and its associated receptor Fas, which keratinocytes demonstrate exceptional sensitivity to and is shown to be enhanced in the presence of the proinflammatory cytokine IFN-γ, present in the skin during TEN (Abe et al. 2003). Blister fluid cells also express high levels of granulysin mRNA, which when administered in mice has been shown to mimic SJS/TEN (Harr & French 2010). Indeed, granulysin levels are found to be elevated in serum from blister fluid from ADRs compared to the low expression taken in absence of blistering ADR suggesting an imperative role for granulysin in SJS/TEN (Chung et al. 2008).

1.6. In-vitro diagnostic tests for delayed hypersensitivity reactions

The fundamental aim of the diagnosis of a drug allergy is to firstly confirm that the symptoms presented correlate with a drug hypersensitivity reaction but also to identify the culprit therapeutic for the reaction experienced. To identify the drug in question *in vivo* tests such as skin and drug provocation may be utilised. A variety of skin tests are readily available for clinical use including patch, prick and intracutaneous tests, however all are accompanied with problems (Porebski et al. 2011). Skin tests have low sensitivity and often yield negative results in patients, even if a history of DHR is known, and are also invasive in nature (Romano et al. 2004; Bousquet et al. 2008; Padial et al. 2008; Aberer et al. 2003). While drug provocation tests can be useful in diagnosis, they are not well tolerated by patients due to the potential to further elicit a recurrence of severe reactions (Romano et al. 2004; Aberer et al. 2003) and the fact that they can only be performed after an appropriate period of time when the symptoms of the initial reaction have subsided (Porebski et al. 2011).

In vitro tests provide a much safer alternative as they avoid invasiveness of the skin tests and the risks of severe reactions that accompany the provocation tests. *In vitro* tests also provide a greater insight into the mechanisms involved in hypersensitivity reactions while allowing for the evaluation of many immune responses from multiple therapeutics concurrently (Porebski et al. 2011). The standard *in vitro* tests used as diagnostic tools include the lymphocyte transformation test (LTT), enzyme linked immunospot (ELIspot) assay and others including the use of flow cytometry to detect markers on cells along with intracellular cytokine synthesis.

These tests are not without limitations; firstly, they are not useful in detecting class II and III reactions (Porebski et al. 2011). Secondly, they are dependent on the access to and ethical approval of patient peripheral blood mononuclear cells (PBMCs) and the relevant

infrastructure to both study and cryopreserve these cells. A researcher must also be appropriately trained to isolate PBMCs from patient samples and incorporate them into the aforementioned assays, most of which require sterile techniques. However, as many of these limitations also exist with the skin and drug provocation assays, these *in vitro* techniques still represent a safer alternative.

1.6.1. Lymphocyte transformation test (LTT)

The LTT, also referred to as the lymphocyte proliferation or stimulation test, is a commonly used *in vitro* test for the diagnosis of T-cell responses specific to a drug (Nyfeler & Pichler 1997; Pichler & Tilch 2004). Use of this diagnostic assay involves the isolation of PBMCs from hypersensitive patients in response to treatment with the drug in question. PBMCs are re-challenged with the specific drug and proliferation of T-cells is measured via ^{3}H-thymidine uptake in dividing cells during DNA synthesis. A heightened proliferative response in the presence of the assumed allergenic drug is taken as a marker of drug specific T-cell activation. Proliferation is expressed as a stimulation index (SI) and an SI value of ≥2 is considered positive. Such proliferative responses are not observed in PBMCs isolated from drug naïve individuals, indicating that said proliferation is indeed a sign of prior sensitization and subsequent activation of memory cells. *Luque et al* demonstrated that the LTT assay is an effective screening tool for the diagnosis of both immediate and delayed hypersensitivity reactions to beta lactam drugs (Luque et al. 2001). The LTT assay is useful for a variety of groups of therapeutics including antibiotics (beta-lactams, sulfonamides), antiepileptics (lamotrigine, carbamazepine, phenytoin), antituberculosus drugs (rifampicin, isoniazide) and antihypersensitives (enalapril) among others (Pichler & Tilch 2004). Therapeutics known to cause hypersensitivity reactions via the hapten model (section 1.9.1), and PI model (section 1.9.2) have been shown to produce positive results in the LTT.

The readout stage of this assay can be adjusted to measure other markers of T-cell activation. This includes the measurement of both the synthesis and release of cytokines including IL-5, IL-10 and IFN-γ (Merk 2005). Furthermore, the measurement of CD69 expression can serve as a marker of T-cell activation (Simms & Ellis 1996). The sensitivity of the LTT is thought to range between 56% to 78% while its specificity ranges from 85% to 93% (Elzagallaai & Rieder 2015; Nyfeler & Pichler 1997). There are various factors that are known to influence the ability of the LTT assay at identifying drug hypersensitivity. These include the timing of the test following the initial reaction in the patient, the clinical manifestation of the reaction, the nature of the drug involved in the reaction, the test procedure itself specifically with the lack of standardization to the procedure and the read out system employed by the researcher (Elzagallaai et al. 2009).

The LTT assay requires experience by a researcher with knowledge of cellular techniques and also the relevant infrastructure to allow the assays to be carried out correctly. The use of radioactive thymidine at the readout stage is one obvious drawback due to the use of radioactive material. While a positive LTT is a valued contributor to drug allergy diagnosis, the sensitivity of the assay is still limited and more importantly a negative LTT does not rule out a drug hypersensitivity reaction in the patient (Pichler & Tilch 2004).

1.6.2. Flow cytometry

Flow cytometry is a widely used technique for the analysis of the expression of cell surface markers and intracellular molecules. It allows for the multiparametric analysis of an assorted population of cells concurrently, making it an effective high throughput diagnostic tool. Activated T-cells display unique surface markers not observed in naïve T-cells. This includes receptor proteins, costimulatory molecules, chemokine receptors and MHC class II molecules (Shipkova & Wieland 2012). The upregulation of these surface markers is a commonly used hallmark for T-cell activation. The upregulation and surface expression of the early antigen

activation receptor protein CD69 has been demonstrated to occur rapidly following activation of T-cells and displays a distinct difference from baseline values (Porebski et al. 2011). It has been known to be a useful readout of T-cell activation in response to therapeutics including amoxicillin, carbamazepine (Beeler et al. 2008) and abacavir (Yerly et al. 2017). Other cell surface markers of T-cell activation include CD25 (IL-2 receptor), CD71 (transferrin receptor) and HLA-DR (MHC Class II) (Shipkova & Wieland 2012; Caruso et al. 1997). Flow cytometry may also be used to measure the proliferative responses of T-cells to a particular antigen. This is carried out using the carboxyfluorescin diacetate succinimidyl ester (CFSE) assay. CFSE permeates the cellular membrane and interacts with the amino groups of the intracellular proteins forming a stable covalent bond. Each cellular division results in a halving of the CFSE fluorescence allowing lymphocyte proliferation to be measured via flow cytometry (Quah et al. 2007; Faulkner et al. 2012; Gibson et al. 2014).

1.6.3. ELISA

Enzyme-linked immunosorbent assay (ELISA) is a diagnostic tool that allows for the detection and measurement of substances including peptides, proteins and cytokines, the latter of which can be quantified as a measure of T-cell activity. This assay involves the use of monoclonal antibodies which bind to the surface of wells in a 96-well plate. The addition of supernatant from a given sample will cause cytokines to bind to the capture antibodies. Unbound cytokines are removed by washing and a detection antibody is added, specific for the cytokine in question, followed by enzyme horseradish peroxidase, substrate solution tetramethylbenzidine (TMB) and finally H_2SO_4 stop solution. The resultant colour change can be measured and compared against a baseline value as a marker of T-cell activation. Many studies have used the ELISA assay as a method for various cytokines and effector molecules, for measuring of T-cell activation in response to various antigens (Salehi et al. 2016; Zhao et al. 2017; Toksoy et al. 2017). However, this assay is limited due to its inability to measure

cytokine secretion at the single cell level along with its low sensitivity when compared with the ELIspot assay, discussed below (Cox et al. 2006; Czerkinsky et al. 1988).

1.6.4. ELIspot assay

Enzyme-linked immunospot (ELIspot) assay is a fast, quantitative assay that allows for the quantification of T-cell activation via the detection and subsequent measurement of secreted cytokines or effector molecules such as the granzymes and perforin. This provides an insight into the biological function of the cells as well as the mechanistic properties of the antigens. First described in 1988 the ELIspot assay employs the use of epitope-specific monoclonal antibodies for the detection of individual cytokine secreting cells (Czerkinsky et al. 1988). Monoclonal or polyclonal antibodies, which are specific for each cytokine, are coated onto a white ELIspot plate, T-cells are then added to the plate and co-incubated in the presence of a particular antigen. During the incubation period, the T-cells secrete cytokines that are captured by the antibody coated on the plate. Cells are then removed via washing, and a detection antibody is added and, following subsequent washing, the strepdavidin conjugate is added followed later by BCIP/NBT substrate. The precipitation of this substrate manifests as spots at the sites of cytokine secretion, which can be quantified as a measure of T-cell activity (Cox et al. 2006; Lehmann & Zhang 2012). The most utilized ELIspot assay is for the detection of IFN-γ secretion as a primary readout for the activation of CD4$^+$ and/or CD8$^+$ T-cells (Rasmussen et al. 2013; Naisbitt et al. 2015; Monshi et al. 2013). However, this assay may be adjusted to distinguish between the various subsets of T-cells via the detection of the multitude of cytokines they are known to secrete (Fujihashi *et al.*, 1993; Wang *et al.*, 1994; Bell *et al.*, 2013). This includes Th1 helper cells which secrete cytokines IL-2, IFN-γ and TNF-α, Th2 cells which secrete IL-4, IL-5, IL-10 and IL-13, or Th17 cells which secrete IL-17 (Fujihashi et al. 1993; Hiro et al. 1994; Faulkner et al. 2016). The use of the ELIspot assay displays numerous advantages including its rapidness, wide range of

cytokines available for detection and ability to address questions on the mechanistic profile of the antigen in question at the same time. The ELIspot assay has been shown to have a sensitivity of around 200 times greater than the ELISA assay (Tanguay & Killion 1994). The main limitation of the ELIspot assay is cost, mainly due to the fact that only single cytokines can be detected in each well, meaning individual antibodies for each cytokine must be purchased, however this limitation is also apparent with the ELISA assay.
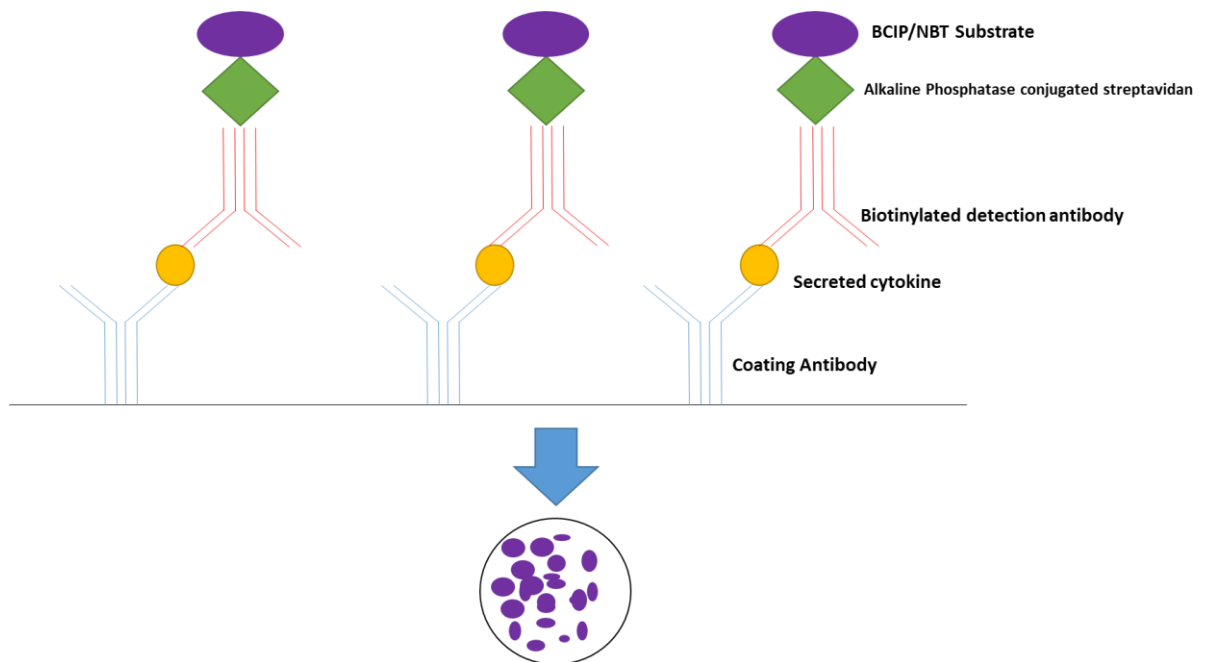
Figure 1.1. Schematic of the ELIspot assay used for the detection of cytokine secretion in response to an antigen.

1.6.5. Luminex

Multiplex assays such as luminex allow for the simultaneous recognition and measurement of multiple secreted proteins including cytokines and effector molecules. This assay employs a similar principle to that of the ELISA and ELIspot assays. Beads which have been pre-coated with a capture antibody specific to the analyte of interest are coated onto a plate allowing for the capture of the secreted analyte. Detection antibodies are then added which bind to the secreted antigen and finally a conjugated strepdavidin is added allowing for the quantification of multiple cytokine secretions via dual laser flow-based detection (Khalifian et al. 2015).

1.6.6. T-cell cloning

T-cell cloning is a well-established effective procedure for the detection of antigen specificity in T-cells *in vitro*. It allows for the expansion of the drug-specific population of T-cells which often represents only a small subset of the overall T-cell population, thereby overcoming the issue of low cell numbers. Expansion of the antigen-specific T-cell population allows for further analysis of the T-lymphocytes including mechanistic studies, analysis of protein surface expression and characterisation on the cellular phenotypes and effector functions. This process represents a mainstay for studying the antigen-specific T-cell functions and has been shown to be imperative in understanding the cellular pathophysiology of reactions associated with exposure to drugs such as carbamazepine (Lichtenfels et al. 2014), flucloxacillin (Monshi et al. 2013), dapsone (Alzahrani et al. 2017) and abacavir (Bell *et al.*, 2013; Adam *et al.*, 2014; Naisbitt *et al.*, 2015).

1.7. The immune system

The immune system comprises an interactive network of lymphoid organs, cells and cytokines for the protection against organisms that the host is exposed to throughout its life. The primary objective of the immune system is to control and eliminate these microorganism and toxins. This relies on the complex detection of structural features present on a pathogen or toxin to distinguish from cells belonging to the host, this is essential for the host to eliminate a foreign pathogen without injuring its own tissues (Parkin & Cohen 2001). The immune system can be classified into two parts. Innate, non-specific, immune system which contributes an immediate response to an antigen with the adaptive immune system complementing and ultimately driving the immune response (Medzhitov & Janeway 1997).

1.7.1. Cellular components of the innate immune system

The innate immune system encompasses the first line of defence for the host against invading pathogens during infection playing a critical role in the primary recognition and successive initiation of a proinflammatory response to these pathogens. As well as composing of physical and chemical barriers to infection, this system relies on the recognition of conserved structures present on pathogens known as pathogen associated molecular patterns (PAMPs) via recognition receptors encoded within the germ line (Akira et al. 2006). The response primarily initiated by the innate immune system is regarded as non-specific, unlike adaptive immunity, and takes place via phagocytotic cells and antigen presenting cells including dendritic cells, macrophages and granulocytes.

1.7.1.2. Mast Cells

Mast cells are granulocytes that originate from myeloid stem cells and are primarily found in the skin and mucosal tissues during homeostasis. These cells play an important role in many allergic reactions and inflammatory responses. Mast cells originate in the bone marrow where their expansion is mediated by the binding of stem cell factor to its receptor and a number of cytokines including IL-3, IL-4, IL-9 and IL-10. They are characterised by the presence of organelles in the cytoplasm, which contain inflammatory mediators known as leukotrienes, histamine and cytokines. During an allergic reaction, IgE (released from B-cells) will attach to the mast cells covering the cells plasma membrane. Following binding to the mast cell receptor, the antigen binding segment of IgE is able to interact with and bind the antigen (Mekori & Metcalfe 2000). Further exposure to the same antigen results in cross linking of the cellular bound IgE and consequently induces the release of histamine and cytokines including GM-CSF, IL-8, IL-9 and TNF-α, resulting in allergic inflammation (Mekori & Metcalfe 2000; Chaplin 2010). Mast cells have been shown to play an imperative role in diseases such as asthma, ear infection and pulmonary fibrosis (Amin 2012; Bradding et al. 2006) as well as more recently being demonstrated to be important in allergic immune reactions such as anaphylaxis (Galli & Tsai 2013).

1.7.1.3. Macrophages

Macrophages are white blood cells that are responsible for engulfing and digesting foreign substances including cellular debris, microbes and other pathogens in a process known as phagocytosis, playing a critical role in both the innate and adaptive immune responses. They are produced via the differentiation of monocytes and are known to express cellular proteins CD14, CD40, CD11b, CD64 and CD68 (Khazen et al. 2005). The process of phagocytosis is initiated via the attachment of PAMPs to the pathogen recognition receptors (PRRs) present

on the macrophages. This results in the engulfment of the pathogen which then fuses with the lysosome. Once engulfed the pathogen is degraded via reactive oxidative species, nitric oxide and lysosomal enzymes (Aderem & Underhill 1999).

As previously stated, macrophages also have a role in adaptive immunity by acting as antigen presenting cells. Following the ingestion of a pathogen the macrophage will display an antigen on the cellular surface through attachment to the cellular membrane on an MHC Class II molecule. This antigen is then presented to Th1 helper cells resulting in the proliferation of these cells and the production of pro-inflammatory cytokines (Unanue 1984).

1.7.1.4. Neutrophils

Neutrophils are white blood cells belonging to the granulocyte family due to their multi-lobed nuclei. They are the most abundant in the granulocyte family and the most abundant of the leukocytes accounting for around 70% and form the first line of defence against pathogens including protozoa, fungal and bacterial particles. These cells are known to be one of the major factors in acute inflammation, due to being one of the first classes of leukocyte recruited to the site of inflammation (Kolaczkowska & Kubes 2013). They undergo a process known as chemotaxis which allows them to migrate towards the site of inflammation. This process involves the use of cellular receptors by neutrophils to detect the chemical concentrations of IL-8, which has been shown to play a pivotal role in this process, to relocate to the site of inflammation (Bickel 1993; Baggiolini & Clark-Lewis 1992). Upon encountering a pathogen a neutrophil will engulf it via phagocytosis and once encapsulated the pathogen is destroyed using reactive oxidative species and antibacterial proteins including cathepsins and lysozymes (Segal 2005).

1.7.1.4. Basophils

Basophils are the least common granulocytes, accounting for less than 1% of leukocytes. Activation of basophils, via binding of IgE to the FcεRI receptor, initiates the process of degranulation leading to the secretion of histamine, heparin, proteolytic enzymes, GM-CSF as well as cytokines including IL-4 and IL-13 causing a pro-inflammatory response (Parkin & Cohen 2001) . These cells are known to be involved in allergic reactions including asthma, atopic dermatitis and anaphylaxis (Siracusa et al. 2013).

1.7.1.5. Eosinophils

Eosinophils are granulocytes that comprise between 1-6% of leukocytes. They originate from stem cells in a process known as hematopoiesis in the bone marrow and relocate to the blood (Donohugh 1996). Once in circulation eosinophils are recruited to sites of inflammation in tissues in a process mediated by eotaxins and IL-5 (Jacobsen et al. 2012). Activation of eosinophils leads to the production of cytotoxic cationic granule proteins, reactive oxidative species and cytokines including IFN-Y, IL-2, IL-4, IL-12, IL-5, IL-9 and IL-13 (Stone et al. 2011).

1.7.1.6. Dendritic cells

Dendritic cells (DCs) are professional antigen presenting cells that serve as sentinels of the immune system. They are formed from various cell lineages and are expressed in small numbers in most tissues throughout the body including skin, nose, lungs and stomach (Banchereau & Steinman 1998). They originate from hematopoietic bone marrow progenitor cells which develop into immature DCs. These immature cells are characterised by their high endocytic activity and low T-cell activation potential. Immature DCs constantly explore their immediate environment for pathogens that are mainly of viral or bacterial origin. This is achieved via the expression of PRRs such as toll like receptors (TLRs). These TLRs recognise specific chemical entities that are present on pathogens (Mellman 2013; Dalod et al. 2014).

Following exposure to danger signals including TLR ligands and proinflammatory signals such as LPS, TNF-α, or DAMPs such as HMGB1 or heat shock proteins, the process of maturation in immature DCs is initiated. During this process, the endocytotic ability of the cells is downregulated while the lysosomes and antigen processing components of the cell are activated, upregulating the peptide-MHC production also resulting in higher expression of costimulatory molecules such as CCR7, CCR5 and CCR1 and increased secretion of IL-12 (Rescigno et al. 1998; Han et al. 2009). Once matured DCs migrate to the T-cell affluent regions of the lymph nodes and initiate antigen specific memory or naïve T-cell responses. DCs capture and take up microbial antigens from the external environment and passage these antigens to naïve T-cells, which are present at low levels in the blood and migrate to the lymph nodes (Banchereau & Steinman 1998). DCs marshal the presence of pathogens to the adaptive immune system, which triggers a series of antigen-specific responses. This is achieved via the coordination of proteolytic apparatus present in the endosomal-lysosomal system, the cytosol and the endoplasmic reticulum (Cella et al. 1997). This helps to break down the pathogen derived proteins resulting in antigenic peptides which are processed and presented by MHC molecules. However, this presentation is not adequate to initiate a T-cell response on its own. For this, co-stimulation is required and it is provided mainly by CD40, CD80 and CD86 as well as other molecules. These are expressed on the antigen presenting cell surface and interact with ligands CD28 and CD40L (Mellman 2013; Hubo et al. 2013). Activation of naïve T-cells requires various signals from DCs. Signal I is regulated by MHC in complex with a peptide that has been processed from antigens and is recognised by specific T-cell receptors. Signal II, the costimulatory signal, is non-antigen specific but the presence of this signal is imperative for complete T-cell activation to occur (Kalinski 2009). It is mainly provided by the initiation of CD28 on the T-cell via ligation with CD80 and CD86 molecules on the DC. A third signal exists by the way of soluble factors such as the cytokines IL-12, IL-

15, IL-6 and TNF-α which also play a role in the activation and proliferation of naïve T-cells. A combination of these signals define the T-cell differentiation process (Kapsenberg 2003).

1.7.1.7. Natural killer cells

Natural killer cells are cytotoxic lymphocytes that play a critical role in the innate immune system, mainly against intracellular viruses and bacteria. They are defined by their ability to kill infected cells upon development without further differentiation and make up between 5-15% of mononuclear cells in the blood. Their development occurs mainly in the bone marrow from hematopoietic stem cells differentiating into lymphoid progenitors which further differentiate into NK-T progenitors (Leischner et al. 2015). Natural killer cells can be identified via the expression of CD56 and CD16, which plays a role in the recognition of antibody-coated cells, and the absence of the T-cell marker CD3 (Caligiuri 2008). The function of NK cells is to eliminate infected cells, including virally infected and tumorigenic cells, and produce the proinflammatory cytokine IFN-γ, activating macrophages to destroy phagocytosed microbes. NK cells are equipped with cytotoxic proteins stored within secretory lysosomes. The major cytotoxic proteins contained within these secretory lysosomes in NK cells are the granzymes and perforin (Kägi et al. 1994). Recognition of a target cell induces secretory lysosome exocytosis and the release of the cells cytotoxic contents. Perforin works to mediate the entry of granzymes into the cytoplasm of the target cell, once inside they cleave a number of intracellular targets including caspases, causing cell death via apoptosis, eliminating the stores of infected cells (Voskoboinik et al. 2015; Korey R. Demers, Morgans A. Reuter 2013).

NK cells are able to differentiate between infected and healthy cells via the interplay between signals generated from activating and inhibitory receptors. Activating NK cell receptors include CD16, NKG2D and the short-tailed members of the killer immunoglobulin like receptors (KIRs). These signal via the association with DAP10 allowing for Pi3-kinase

activation or DAP-12 containing immunotyrosine based activation motifs (ITAM) (Lanier 2008). Stimulation of these motifs leads to the downstream phosphorylation of signalling substrates. Inhibitory NK receptors contain long tail members of the KIR family along with LAIR-1 and KLRG-1 which signal via the cytoplasmic immunotyrosine based inhibitory motifs (ITIM) (Lanier 2008). Signalling from inhibitory receptors stimulates phosphatases to inhibit protein kinases. Interaction between NK cells and other cellular components involves a complex interplay between the signals originating from activating and inhibitory receptors (Pegram et al. 2011). Stimulation of the activating receptors induces the cellular killing profile of NK cells, while activation of inhibitory receptors impedes NK cell function preventing cellular destruction.

1.7.2. The adaptive immune system

The adaptive immune system, also known as the acquired immune system or more rarely the specific immune system, is a subset of the entire immune system that consists of highly specialised cells which are responsible for the destruction of invading pathogens and the toxic products they generate. Unlike innate immunity, the adaptive immune responses are specific to individual pathogens (Chaplin 2010). This feature is due to the antigen-specific receptors that are displayed on the surface of lymphocytes in the adaptive immune system. This differs from the innate immune system in that pathogen-specific receptors are already encoded in the germline of innate immune cells.

1.7.2.1. Cellular components

Adaptive immune responses are undertaken by white blood cells known as lymphocytes. These responses can be classified as antibody-mediated responses and cell-mediated responses, which are carried out via B-cells and T-cells respectively. Both of these classes of cells originate from the same hematopoietic stem cells and prior to their activation are morphologically identical.

1.7.2.2. B-Cells

B-cells and their associated antibodies are critical components of humoral immunity which serves to protect against a plethora of pathogens. They are identifiable via their specific expression of CD19 and differentiate into either long-lived memory cells or effector plasma cells to protect against pathogens via the secretion of antibodies. B-cells develop from hematopoietic stem cells within the bone marrow and are present in peripheral lymphoids. The humoral immune response is triggered via the binding of antigens to IgM and IgD on naïve B-cells. This activation leads to the proliferation and subsequent differentiation of these cells to yield antibody secreting plasma cells and memory B-cells. A marker of B-cell activation is the production of antibodies apart from IgM and IgD in a process known as isotype switching. As a humoral response mounts, the activated B-cells secrete IgE antibodies which bind to antigens with high affinity. IgG is the major antibody found in the blood and extracellular fluid, it plays an important role in the control of infection in various tissues. They have been detected in cases of drug hypersensitivity to therapeutics including piperacillin (Clark & Dalmasso 1982; Amali et al. 2017).

1.7.2.3. T-lymphocytes

T-cells are activated by the presence of a foreign antigen to then proliferate and differentiate into effector T-cells. These can be classified into two distinct categories; helper T-cells (CD4+)

and cytotoxic T-cells (CD8$^+$). These cells are the products of hematopoietic stem cell differentiation and relocate to the thymus from the bone marrow via the bloodstream. Once in the thymus these cells expand to produce a subset of cells known as thymocytes. Initially these cells do not express receptors for CD4 or CD8 and are therefore classified as double negative. These double negative cells undergo a process of TCR-β chain rearrangement to generate cells which are positive for both CD4 and CD8, defined as double positive cells. Next these double positive cells undertake a process of TCR-α chain rearrangement which results in the generation of CD4 or CD8 single positive cells which migrate from the thymus into circulation (Overgaard et al. 2015).

1.7.2.4. Cytotoxic T-cells

Cytotoxic (CD8$^+$) T-cells are crucial for the immune defence mechanisms against intracellular pathogens including viruses and bacteria. CD8$^+$ T-cells destroy the infected cell before microbes are able to proliferate and infect neighbouring cells. The infection of cells by intracellular pathogens results in the breakdown of foreign proteins through antigen processing. This leads to peptide fragments being presented to the T-cell receptor of CD8$^+$ T-cells via MHC class I.

Naïve CD8$^+$ T-cells only need a short exposure to antigenic peptide displayed by MHC to become activated and induce cellular division. Once activated CD8$^+$ cells initiate a process of programmed differentiation resulting in them becoming effector cytotoxic T-cells. These cells secrete the proinflammatory cytokines IFN-γ and TNF-α and effector molecules including granzymes, FasL, and perforin (Bell *et al.*, 2013).

Cytotoxic T-cells secrete the pore forming protein perforin, which undergoes polymerisation with the plasma membrane of the target cells resulting in the formation of transmembrane channels. The formation of these pores allows the granzymes, contained within the cytotoxic

T-cell, to enter the infected cell. Once inside these granzymes cleave the intracellular proteins, halting viral protein production which results in cellular death via apoptosis (Voskoboinik et al. 2015; Korey R. Demers, Morgans A. Reuter 2013).

Cellular killing can also be initiated by CD8^{+} T-cells via the FasL pathway which is upregulated by CD8^{+} T-cells post activation. The interaction between FasL expressed on the cellular surface of the CD8^{+} T-cell and the cell surface death receptor Fas, which is commonly expressed on target cells, results in the formation of the intracellular death signalling complex (DISC) (Kischkel et al. 1995; Rouvier et al. 1993). Activation of DISC results in the upregulation of cellular caspase signalling eventually leading to cell death via apoptosis (Yang et al. 2008).

The role of CD8^{+} T-cells has been implicated in a the hypersensitivity reactions to variety of drugs including carbamazepine (Ko et al. 2011; Lichtenfels et al. 2014), nevirapine (Keane et al. 2014) and abacavir (Chessman *et al.*, 2008; Bell *et al.*, 2013; Naisbitt *et al.*, 2015) which will be discussed in more detail later.

1.7.2.5. T-helper cells

CD4^{+} T-helper cells play a role in a variety of immune functions, including the activation of the innate immune system, B-cells, cytotoxic T-cells, non-immune cells and the suppression of immune mediated reactions. CD4^{+} T-cells play an important role in immunological memory T-cell responses and consequently a reduction in their cellular numbers increases the hosts susceptibility to a number of infectious diseases. The initial step of differentiation of naïve T-cells is the antigenic stimulation which occurs as a result of the interactions of the TCR of CD4 with the antigenic peptide MHC II complex presented by antigen presenting cells. This induces a network of downstream signalling pathways which will eventually result in naïve cell proliferation and subsequent differentiation into effector, memory or regulatory T-cells

(Zhu et al. 2010). This process is dependent on many factors including the presence of particular cytokines within the cellular environment, the types of APCs present as well as costimulatory molecules (Luckheeram et al. 2012). The distinct populations of differentiated CD4^{+} T-cells can be divided into two major groups Th1 and Th2 (Mosmann et al. 1986), while newer subclasses have been identified in recent years (Weaver 2009; Eyerich et al. 2009).

1.7.2.6. Th1 and Th2 helper cells

Th1 and Th2 cells can be characterised by the cytokines secreted in response to stimulation but also via the expression of cell surface markers. Th1 cells are considered to be proinflammatory and produce IFN-γ as a primary cytokine as well as lymphotoxin, IL-2 and in some cases TNF-α. Conversely Th2 cells are considered to be anti-inflammatory and are characterised by their secretion of IL-4, IL-5 and IL-13, coupled with their inability to produce IFN-γ and lymphotoxin (Zhu et al. 2010).

The cytokines IL-12 and IFN-γ are pivotal for the instigation of downstream signalling pathways involved in the production of Th1 cells. IL-12, produced by APCs following their activation, is able to activate natural killer cells subsequently leading to the generation of IFN-γ (Trinchieri et al. 2003). The differentiation of Th1 cells is dependent on various transcription factors working in coordination with each other. The main transcription factor involved in this process is T-bet, a member of the T-box family of transcription factors, which is induced in naïve CD4^{+} T-cells in response to both an antigen and IFN-γ (Kanhere et al. 2012). IFN-γ is also shown to promote activation of the transcription factor STAT1 which in turn promotes further expression of T-bet and the suppression of Th2 and Th17 cells, as well as further IFN-γ secretion (Luckheeram et al. 2012). This creates a positive feedback loop where IFN-γ secretion will result in further IFN-γ secretion downstream. Th1 responses are known to take place in retaliation to bacterial and viral infection.

Th2 cellular differentiation contrasts greatly from Th1 in that the cytokines IL-2 and IL-4 are required for the initiation of the pathway to generate these cells. IL-4 is produced by mast cells or eosinophils in response to helminths. Secretion of IL-4 results in the upregulation of the transcription factors STAT6 (Trinchieri et al. 2003) and GATA-binding protein GATA-3, the major regulating factor in the generation of Th2 cells (Kanhere et al. 2012). GATA3 is upregulated by STAT6 in response to IL-4 generation subsequently resulting in further IL-4 secretion which leads to an amplification of the Th2 response and subsequent inhibition of Th1 and 17 development.

Two further subgroups of T-helper cells have been recently discovered, these being Th17 and Th22 cells. They are characterised by their secretion of IL-17 and IL-22 respectively (Chen & O'Shea 2008; Eyerich et al. 2009).

The Th17 subset plays a key role in the killing of extracellular bacteria and fungi via the recruitment of neutrophils and the induction of inflammation. The differentiation of Th17 cells is mediated by the proinflammatory cytokines IL-1 and IL-6, which are secreted by dendritic cells in response to the presence of bacterial particles, along with IL-21 and IL-23. IL-1, IL-6 and IL-21 are thought to mediate the early stages of Th17 differentiation while IL-23 may be involved in promoting proliferation and overall maintenance of differentiated Th17 cells (Estelle et al. 2006). The key regulator of this process is the retinoic acid receptor related orphan receptor gamma-T (RORYT). The anti-inflammatory cytokine TGF-β also plays a pivotal role in this differentiation process. When secreted in the presence of IL-6, TGF-β causes an enhancement of the transcription factor STAT3 via the inhibition of suppressor of cytokine signalling 3 (SOCS3), a negative regulator of the STAT3 signalling pathway (Veldhoen et al. 2006; Manel et al. 2008). This inhibition results in the further activation of RORYT producing secretion of IL-17 and in some cases IL-22. Secreted IL-17 is primarily involved in the recruitment of neutrophils, thereby producing an overall inflammatory response. IL-22

however is produced in epithelial tissues and functions primarily to regulate the integrity of the epithelial barriers via the induction of repair mechanisms. However, IL-22 may also play a role in the inflammatory response by way of chemokine production promoting the migration of immune cells.

While IL-22 secretion is associated with Th17 cell activation in response to bacterial and fungal infection, a subset of CD4^{+} T-cells is known to exist, which indeed secrete IL-22, but not IL-17 (Fujita 2013). IL-22 demonstrates both proinflammatory and anti-inflammatory characteristics. Th22 cells originate from the stimulation of naïve T-cells in the presence of IL-6 and TNF-α in a process dependent on the aryl hydrocarbon receptor (AHR) (Bouchery et al. 2014). While immune cells are capable of IL-22 secretion, its receptor is restricted to non-hematopoietic cells such as epithelial cells, with high expression found in the skin, liver, intestine and kidneys. IL-22 is known to be involved in a variety of inflammatory skin diseases including psoriasis (Boniface et al. 2007), atopic dermatitis (Nograles et al. 2010) and contact dermatitis (Larsen et al. 2009) as well as recently being shown to play a key role in the hypersensitivity reactions to the β-lactam drug piperacillin (Sullivan et al. 2016).

Regulatory T-cells (Tregs) are a subset of CD4^{+} T-cells characterised by their expression of CTLA4, CD25 and FoxP3 which function in the suppression of the immune system following an immune response as well as playing a role in the maintenance of tolerance to self-antigens (Rudensky 2011). The development of Tregs is dependent on FoxP3 which is a member of the forkhead family of transcription factors and Treg cells are known to secrete the cytokines IL-10 and TGF-β which have a marked inhibitory effect on the proliferation and functions of T-cells thereby acting to control the immune response (Vignali et al. 2008). Tregs act to supress the immune response via the secretion of these inhibitory cytokines or via upregulation of the cell surface receptor CTLA4, a negative mediator of T-cell activation. Dysregulation of Treg cell function may result in a variety of autoimmune diseases including

type 1 diabetes, multiple sclerosis and psoriasis many of which are mediated by Th1 responses (Vojdani & Erde 2006). Impaired Treg function and number will result in a loss of the suppression abilities of the immune system which can lead to overstimulation of CD4$^+$ effector T-cells resulting in an unregulated overproduction of proinflammatory cytokines which have autoimmune effects (Rudensky 2011).

Further subsets of CD4$^+$ T-helper cells also exist including Th9 and follicular helper T-cells (Tfh). Their cytokine secreting profiles along with the key mediators in their cellular differentiation from naïve T-cells are shown in Figure 1.2.
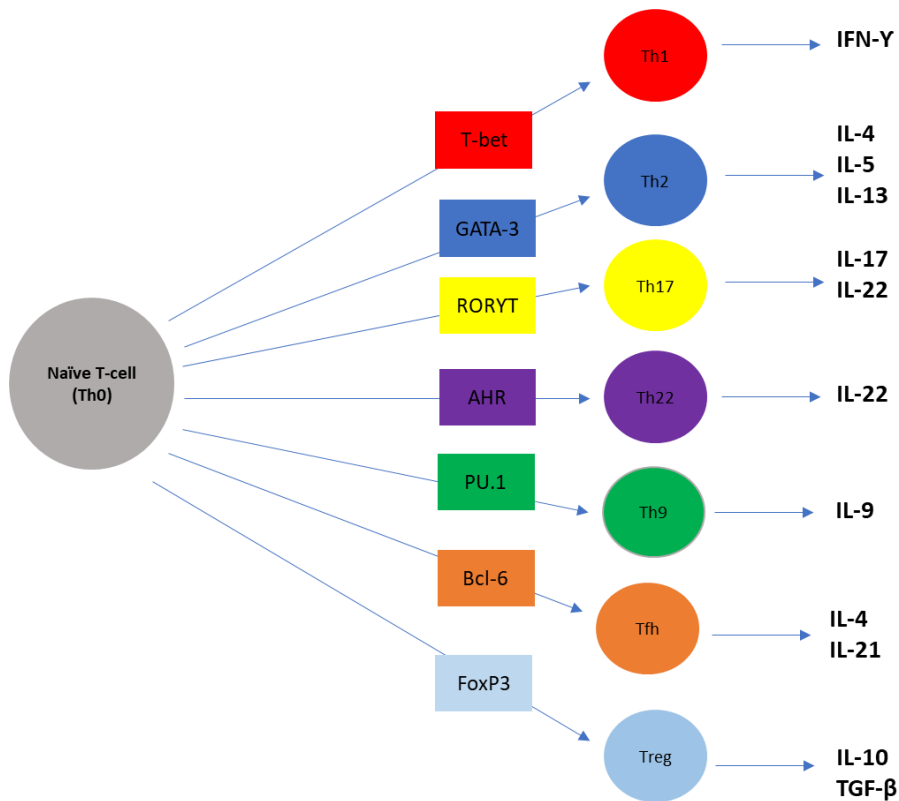
Figure 1.2. Maturation of naïve T-cells into T-helper cell subsets. The differentiation of naïve T-cells into multiple subsets of T-helper cells with the governing transcription factor for each primary pathway indicated, along with the primary cytokines secreted by each T-helper subset. T-bet (T-box transcription factor), GATA-3 (Anti-GABA transporter 3), RORYT (Retinoic acid receptor related orphan receptor gamma T), AHR (aryl hydrocarbon receptor, PU.1 (macrophage transcription factor), Bcl-6 (B-cell lymphoma 6), FoxP3 (forkhead box P3).

1.8. Antigenic processing and presentation

Antigen processing is a vital immunogenic procedure which is pivotal for the initiation of an immune response in T-cells. This mechanism exists on cell types including mononuclear phagocytes, B-cells and non-phagocytotic cells such as dendritic cells (Chesnut & Grey 1985). The pathways of antigen processing convert antigenic proteins that are either present in the cytosol or those that have been internalized from the extracellular environment into peptide fragments. These fragments are then loaded onto MHC molecules and subsequently presented to T-cells. Two general pathways exist for antigen processing.

Class I MHC pathway: MHC class I molecules primarily present antigen which have been manufactured within the antigen presenting cell. Such intracellular antigens are mainly of viral or bacterial origin whereby a virus enters the cell and escapes into the cytosol. Antigens may also be derived from microbes, internalized via phagosomes, which are capable damaging the phagocytic membrane forming pores allowing exit into the cytosol (Neefjes et al. 2011). These proteins undergo a process of digestion to yield peptides via proteolysis which takes place in large multiprotein enzyme complexes known as proteasomes (Leone et al. 2013). These newly generated peptides are transported into the cellular endoplasmic reticulum (ER) via a specialised transporter protein known as the transporter associated with antigenic presentation (TAP). This transporter is found in the membrane of the ER and is responsible for mediating the transport of peptides from the cytosol into the ER in an ATP dependent process (Blum et al. 2013). Within the ER, the TAP associates with the protein tapasin which has strong affinity for newly formed MHC class I molecules. Peptides that enter the ER via TAP along with peptides synthesized within the ER are cleaved to the correct size to allow binding to the MHC via the ER-resident amino peptidase (ERAP) (Leone et al. 2013). This allows for the binding of the peptide to the MHC class I which is bonded to TAP via tapasin (Blum et al. 2013). Once the peptide is bound the MHC it loses its affinity for tapasin

allowing it to escape the ER for cell surface presentation. The stable MHC class I molecules then move to the cell surface via the golgi apparatus via the formation of exocytic vesides. Peptide bound MHC class I is then expressed on the surface of the antigen presenting cell for subsequent interaction with CD8^{+} T-cells (Harding & Unanue 1990; Neefjes et al. 2011).

Class II MHC pathway: MHC class II antigen processing involves the manufacture of peptides from antigens that have been internalized via endocytosis. This processing pathway is only carried out by specialist APCs such as dendritic cells and macrophages. The extracellular antigen binds to the APC and is internalized via endocytosis, this is carried out via the expression on cell surface receptors that can recognise various microbial structures (Roche & Furuta 2015). Following internalization, the protein antigen is enveloped by vesicles known as endosomes. These proteins are cleaved enzymatically within endosomes and lysosomes by proteases such as cathepsins, producing peptides capable of binding to the MHC cleft (Villadangos et al. 1999). MHC class II molecules are generated within the ER via the correlation of individual α and β chains through binding of an invariant chain trimer which blocks the peptide binding site making it impossible for peptides to bind MHC class II within the ER (Broeke et al. 2013). The MHC is then transported to the cell surface via endosomal vesicles. Once inside the endosome the invariant chain is proteolytically degraded, thereby freeing the peptide binding cleft for the antigenic peptides (Robinson & Delvig 2002; Roche & Furuta 2015). Peptide bound MHC class II is then expressed on the antigen presenting cell surface where it is recognised by CD4^{+} T-cells.
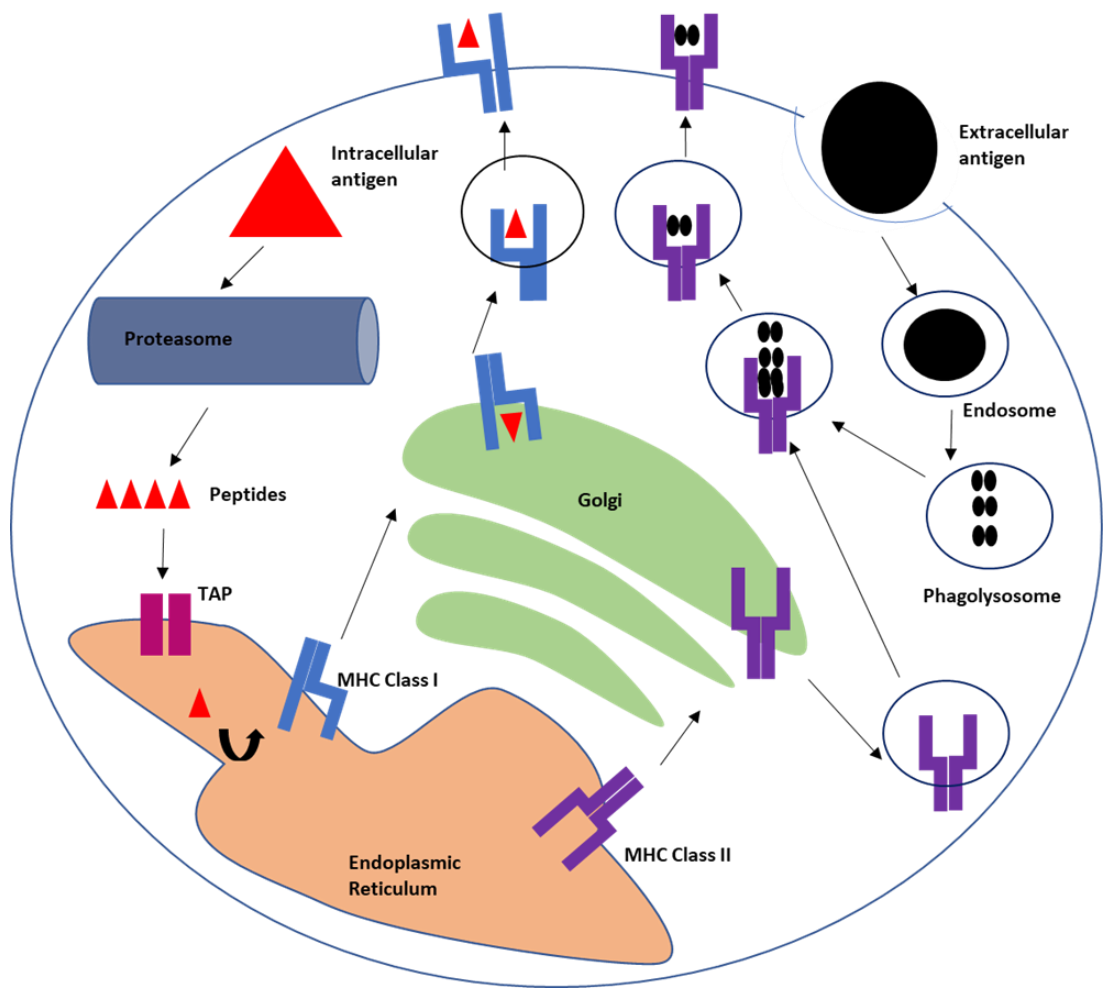
Figure 1.3. Antigen processing and presentation. Class I: Intracellular antigens are degraded in the proteasome into peptides containing around 9 amino acids. They are then transported into the endoplasmic reticulum by the transporter associated with antigen presentation where they bind to MHC class I molecules. Finally the MHC bound peptide is trafficked to the golgi apparatus where it is loaded into a vesicle and trafficked to the cell surface for recognition by T-cells. **Class II:** Extracellular antigens are ingested by phagocytosis and processed by endosomal enzymes. The class MHC II molecules are transported to the golgi then subsequently to the phagolysosome to allow for peptide loading. This MHC-peptide complex is then transported to the cell surface for display to T-cells.

1.9. Mechanisms of hypersensitivity reactions

1.9.1. Hapten hypothesis

The inception of the hapten hypothesis dates back to the 1930's to studies conducted by Landsteiner and Jacobs using chemically reactive compounds with a small molecular weight such as dinitrofluorobenzene (DNFB). They were able to sensitize guinea pigs to this compound and speculated that protein conjugation may be involved the observed immune response (Landsteiner & Jacobs 1936). Similarly, the hapten hypothesis proposes that small molecules such as drugs do not have immunogenic properties on their own and to initiate an immune response they must act as haptens. A hapten is defined as a small chemically reactive molecule (MW <1000 D) which is capable of undergoing a stable covalent binding process to a larger protein or peptide altering the side chain of the bound residue (Adam et al. 2011; Pavlos et al. 2015).

These haptenated proteins are processed by the antigen presenting cell, a process which results in the display of haptenized peptides by MHC class I or II molecules. This is recognised by T-cells as a foreign antigen and initiates a *de* novo immune response (Adam et al. 2011; Llano & Brander 2012). Most environmental haptens act as cutaneous allergens producing an allergic contact dermatitis (ACD) reaction on the skin. The most common haptens include urushiol, nickel, oxazolone, phosphorylcholine, p-phenylenediamine (Erkes & Selvan 2014). The immunogenicity of each hapten is dependent on many properties including how rapidly the hapten can bind, how quickly it can penetrate the skin and other factors such as electrophilicity, hydrophobicity and bioavailability (Erkes & Selvan 2014; Chipinda et al. 2011). A prime example of a hapten like drug is the beta lactam penicillin which is known to covalently bind to the lysine groups within cellular and serum proteins (Pichler 2002; Padovan et al. 1997).

Haptens may induce an immune response via stimulation of both the innate and adaptive immune system. Innate responses occur following the covalent binding of the hapten to the cells proteins which subsequently emit a danger signal thereby activating immune system components such as the upregulation of costimulatory CD40 (Sanderson et al. 2007). These hapten protein complexes may also be presented to T-cells by MHC as a hapten modified peptide which will trigger a complete immune response (Naisbitt et al. 2000; Pichler 2007).

However, most drugs are not capable of undergoing haptenation with a cellular protein on their own and require bioactivation via metabolism to become protein reactive (Williams et al. 2000; Castrejon et al. 2010). This is termed the prohapten concept and it highlights the fact that while many drugs are not chemically reactive themselves, they are able to be metabolized into reactive intermediates capable of eliciting an immune-mediated response (Castrejon et al. 2010) (Naisbitt et al. 2000; Pichler 2002). Therefore prohaptens are not protein reactive unless they have been metabolized to the electrophillic state (Erkes & Selvan 2014). A prime example of this is the antibiotic sulfamethoxazole (SMX) which becomes reactive via intracellular metabolism via CYP2C9 in the liver to sulfamethoxazole-hydroxylamine (SMX-NHOH) which can be converted to nitroso-sulfamethoxazole (SMX-NO) (Cribb & Spielberg 1992). SMX-NO is capable of binding covalently to cysteine residues on proteins and if the level of binding exceeds a certain threshold may cause toxicity. However it can also produce a neo-antigenic signal for specific T-cells eliciting an immune response (Sanderson et al. 2007).

1.9.2. Pharmacological interaction model

The ability of small drugs to evoke a T-cell response without covalently binding to a larger protein is in direct contrast with the hapten/prohapten model. This has led to the proposition of the pharmacological interaction (PI) model (Pichler 2002). This proposes that chemically inert drugs, which are incapable of binding covalently to proteins or peptides, can interact

directly with and bind to MHC molecules and/or the T-cell receptor (TCR) reversibly and in a non-covalent manner without the involvement of the antigen processing and presentation (Llano & Brander 2012; Pavlos et al. 2015; Adam et al. 2011; Pichler 2008).

Indeed it has been demonstrated with drugs such as carbamazepine and some of its metabolites that removal of the antigen processing pathway via aldehyde fixation maintains the ability to induce T-lymphocyte proliferation (Wu et al. 2006). As well as carbamazepine, drugs such as SMX, lidocaine and mepivacain have been shown to activate T-cells via this pathway (M P Zanni, von Greyerz, Schnyder, Wendland, et al. 1998; Zanni et al. 1999; Schnyder et al. 1997). Furthermore, T-cells which are activated via this mechaism are shown to respond raipdly to drug stimulation by way of increased calcium influx and T-cell downregulation when coincubated with these drugs, something which would take far longer if acting via a hapten mechanism (Zanni et al. 1998). Although it is now well established that drugs activate certain T-cells via a direct MHC-TCR binding interaction, the site and nature of the binding has not been defined. It is possible that drugs could interact primarily with the MHC molecules, MHC binding peptide or the TCR.

1.9.3. Altered peptide repertoire model

Neither the hapten or PI concept have ever been accepted as a full explanation of abacavir hypersensitivity syndrome in HLA-B*57:01 positive individuals. Abacavir undergoes extensive oxidative metabolism to generate a number of isomeric carboxylic acids, three of which are formed in the cytosol of APCs. The formation of these carboxylates takes place through a two-step oxidation process via a reactive aldehyde intermediate (Bell *et al.*, 2013). This reactive aldehyde binds to proteins to form conjugates, demonstrated *in vitro* using human serum albumin (HSA) and glutathione S-transferase Pi (GSTP) (Meng et al. 2014). However, this aldehyde or its protein conjugates have not been shown to activate T-cells (*unpublished data).* Furthermore no haptenated peptides by abacavir have ever been

detected, compounded by the fact that abacavir has been shown to elute unbound from peptides at the MHC (Illing et al. 2012). As the interactions of abacavir with HLA-B*57:01 take place in a non-covalent manner via van der waals forces, the PI model can be accepted as a model for activation of some abacavir clones. Indeed, it has been shown that abacavir can induce responses in T-cell clones in a period of minutes, suggesting direct interaction with surface MHCs (Adam et al. 2012). However, glutaraldehyde fixation of APCs significantly reduces the number of antigen specific T-cells when compared to unfixed APCs. It was also demonstrated that a significant reduction in abacavir presentation was apparent in the mutant cell line 721.220 which expresses HLA-B*57:01 but is deficient in tapasin, something not observed in 220.hTsn which is not deficient in tapasin (Chessman et al. 2008). In the MHC class I antigen presentation pathway endogenous peptide, ligands are synthesised in the cytoplasm by the process of proteolysis and subsequently imported into the endoplasmic reticulum by the transporter associated with antigen presentation (TAP), where the peptide loading is enhanced by the chaperone tapasin (Chessman et al. 2008). The loss of either TAP or tapasin results in impaired peptide loading and a loss of antigen presentation; however, the addition of exogenous peptide ligands restores the immune response, demonstrating that abacavir hypersensitivity reactions are dependent on the antigen presentation pathways, something which drugs interacting via the PI mechanism are known to bypass (Chessman et al. 2008). Indeed, T-cells have been shown to be activated by abacavir via two independent pathways (Bell *et al.*, 2013). Approximately 50% of abacavir-specific CD8^{+} T-cell clones were activated in the absence of APCs. While other abacavir clones required APCs and furthermore incubation of abacavir T-cell clones with APCs pulsed overnight with the drug was sufficient to induce a T-cell response in some clones (Bell *et al.*, 2013). Therefore, a number of clones from HLA-B*57:01[+] donors are activated via a different mechanism. In 2012 *Illing et al* demonstrated that incubation of antigen presenting cells with abacavir will gives rise to an alteration of the peptide repertoire that is presented to T-cells by HLA-

B*57:01. Using mass spectrometry, it was found that treatment with abacavir favoured peptides with small chain C-terminal amino acids including isoleucine and leucine, instead of the larger chain amino acids phenylalanine and tryptophan commonly detected in untreated cells. This was observed only at the C-terminal of the peptide and not been seen with any closely related alleles including HLA-B*57:03 and HLA-B*58:01. This incepted the hypothesis that abacavir modifies the conformation of the antigen binding cleft of HLA-B*57:01 reducing its size and allowing for the accommodation of smaller chain amino acids (Illing et al. 2012; Norcross et al. 2012; Ostrov et al. 2012). These altered peptides are subsequently presented to T-cells, which perceive them to be foreign. It is hypothesized that these altered peptide sequences are responsible for the activation of certain CD8^{+} T-cells in abacavir hypersensitive patients. As mentioned earlier, abacavir can also induce T-cell activation via direct binding with surface MHCs. These responses can take place in minutes therefore not allowing sufficient time for loading of a new peptide onto HLA-B*57:01 (Adam et al. 2012). Therefore, it is likely that direct binding of abacavir can alter the conformation of the existing bound peptide, mimicking that of a native peptide to a closely related allele, in a manner similar to allo-reactivity often observed in organ transplant rejection (Adam et al. 2014).
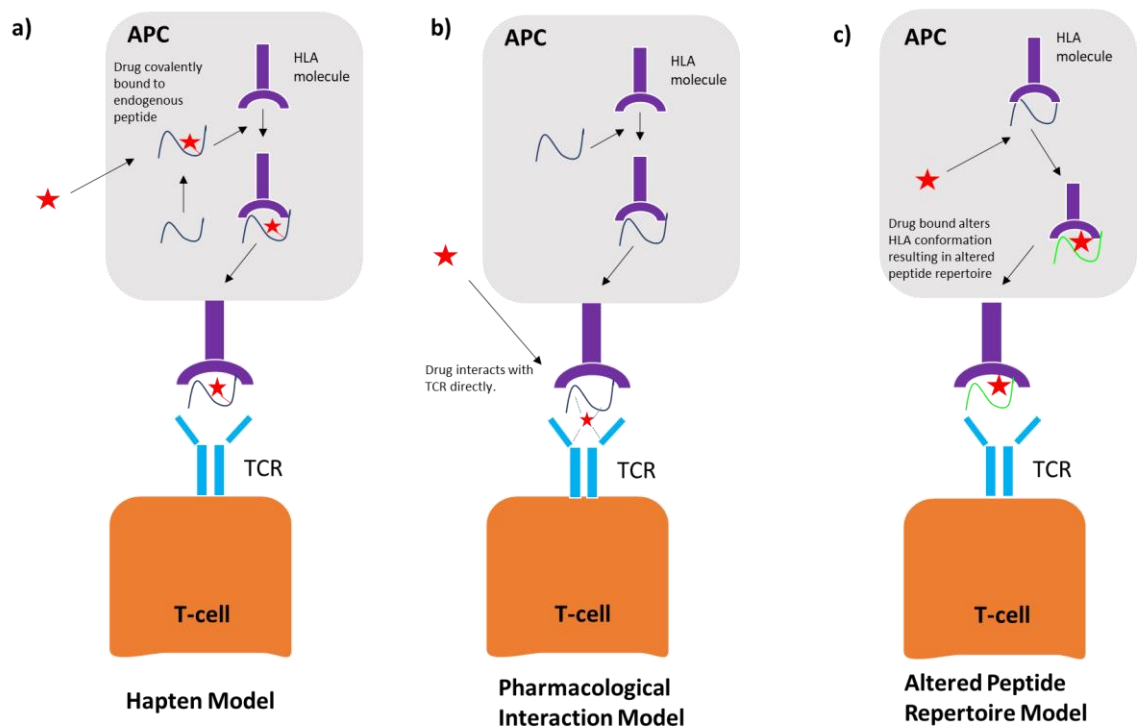
Figure 1.4. Mechanisms of drug/metabolite specific T-cell activation. a) Hapten model. A small molecule (drug or metabolite) binds covalently to a larger protein or peptide, these haptenated proteins are processed by the APC resulting in the display of haptenated peptides to T-cells. b) Pharmacological interaction model. Drugs can interact directly and bind with the TCR and some HLA-molecules without the need for antigen processing. c) Altered peptide repertoire model. The bound drug alters the shape and chemistry of the antigen binding cleft, leading to an accommodation of a range of new self-peptides not previously exposed to peptides.

1.9.4. The Danger Model

The danger model was first proposed in 1994 by Polly Matzinger. This model is built as a critique of the self vs non-self-model first proposed by Burnet in 1962. According to the self vs non-self-model, all foreign units (i.e. non-self) will be subjected to an immune response, while no response will be targeted against the hosts own entities (i.e. self). Contrary to this theory, the danger model proposes that cellular self-elements can initiate an immune response if they pose a threat such as cellular stress and autografts, while non-self-entities may be tolerated if they pose no danger to the host (Matzinger 1994; Matzinger 2002). According to this model the immune system gives more attention to potential danger signals than the presence of a foreign particle. This may indeed explain why exposure to a plethora of non-self-entities fails to evoke an immune response in the absence of cellular damage. Furthermore, this model may also explain how endogenous molecules can initiate immune mediated reactions (Li & Uetrecht 2010). Danger signals consist of molecules or molecular frameworks that are secreted by cells undergoing cellular stress or death. This causes the activation of APCs, normally in the resting state, which provide costimulatory signals even in the absence of a foreign antigen (Gallucci & Matzinger 2001).

It is thought that three immune signals are required for the induction of a complete immune response, but at least two are necessary for immune activation (Curtsinger et al. 1999). Signal 1 comprises the interaction between the MHC peptide complex and the TCR. Signal 2 represents the interactions between the co-stimulatory molecules expressed on the antigen presenting cell and the TCR along with the presence of the pro-inflammatory cytokines such as IL-2, TNF-α and IFN-γ which can induce the upregulation of co-stimulatory molecule expression. The presence of signal 1 without 2 is thought to lead to tolerance (Pirmohamed et al. 2002). Signal 2 is regulated via the release of exogenous PAMPs such as viral RNA, LPS

and peptidoglycan as well as endogenous DAMPs released from dead or damaged cells including heat shock proteins, IFN-α and IL-1β (Pradeu & Cooper 2012).

Signal 3 is derived from polarising cytokines that can interact directly on T-cells leading to Th1 or Th2 responses. Therefore, a drug could theoretically act as signal 1 via providing the source of the antigen and signals 2 and 3 by evoking cellular damage, thereby inducing the production of the aforementioned endogenous danger signals. Furthermore, some drugs have been known to cause damage to APCs such as DCs along with provoking necrotic cell death which combined with antigenic determinants may evoke T-cell activation (Pirmohamed et al. 2002; Curtsinger et al. 1999; Park et al. 2001).

Danger signalling has been detected with several drugs known to cause hypersensitivity reactions. This includes SMX and its metabolite SMX-NO which upregulate expression of the co-stimulatory molecule CD40 through covalent modification of intracellular proteins (Sanderson et al. 2007). Amoxicillin was shown to propel dendritic cells from hypersensitive patients to a mature phenotype, thereby inducing T-cell proliferation in a similar fashion to danger signals such as LPS (Rodriguez-Pena et al. 2006).

Abacavir was shown to evoke the redistribution of HSP70 in PBMCs isolated from abacavir hypersensitive patients when compared to naïve. Furthermore, the blocking of HSP70 itself and its cellular surface receptors CD14 and TLR2 was shown to completely blunt the observed redistribution of HSP70 (Martin et al. 2007). Abacavir has also been demonstrated to evoke the secretion of endogenous DAMPs such as IL-1β in inflammasomes that have been primed with exogenous PAMPs such as LPS *in vitro* (Toksoy et al. 2017). Inflammasome activation is a two-step procedure that first involves priming via stimulation of a TLR. It has been previously demonstrated that TLR8 can be activated by the HIV-1 virus leading to subsequent release of IL-1β (Guo et al. 2014). This incepts the theory that the presence of HIV-1 may

prime inflammasomes via TLR8 stimulation and the IL-1β release may be stimulated by treatment with abacavir (Toksoy et al. 2017).

1.10. Major Histocompatibility Complex

Major Histocompatibility Complex (MHC) class I and II proteins are essential components of the innate and adaptive immune system. Both proteins play a key role in the capture and subsequent presentation of peptides, on the surface of the antigen presenting cell, thereby allowing for their recognition by T-cells.

The human MHC locus is found on the short arm of chromosome 6 at the 6p21.3 position. Chromosome 6 is approximately 150-180Mb in size, with the MHC locus comprising of around 4Mb (genomic data). In humans, the MHC class I and II genes are known as Human Leukocyte Antigen (HLA) class I and II genes respectively.

HLA genes are closely linked with the MHC being inherited as a HLA haplotype from each parent by means of mendelian genetics. Strong linkage equilibrium exists between the antigens from different HLA loci present on a HLA haplotype.

The HLA system displays extreme polymorphism in humans, being the most polymorphic region in the genome. Variations in the amino acid residues at numerous locations throughout the HLA lead to subtle alterations in the shape of the peptide binding groove, thereby having a direct influence on the specificity of peptides bound to the HLA molecule.

MHC class I is present on all nucleated cells and can theoretically be expressed on all cell types except red blood cells (Hewitt 2003). Class I MHC includes HLA-A, HLA-B and HLA-C loci with bound peptides presented on the cellular surface of the antigen presenting cell for recognition by cytotoxic CD8^{+} T-cells. Class I MHCs are heterodimers of a single heavy chain integrated membrane protein and a β_2-microglobulin soluble protein. The extracellular component of the heavy chain is comprised of three domains; the α1, α2 and α3, while β_2m

comprises the fourth domain. Of these domains, the α1 and α2 constitute the peptide binding groove on the upper region of the class I molecule while α3 carries the transmembrane domain (Wieczorek et al. 2017). While not being membrane bound, β_2-microglobulin, plays a key role in the transport of newly synthesised MHC molecules to the cellular surface after peptide loading (Harding & Unanue 1990). The binding groove of MHC class I is closed at each end by a conserved tyrosine residues present in the structure. This tends to limit the length of peptide which can typically bind to the MHC to those of between 8 and 10 amino acids; however, it has been demonstrated in some instances that peptides are capable of protruding from the groove at the N-terminal region which can allow for accommodation of longer peptide sequences (Pymm et al. 2017). The C-terminus of these peptides typically resides in the F-pocket of the MHC (Illing et al. 2012).

Class II MHCs are expressed on professional antigen presenting cells such as macrophages, B-cells and especially dendritic cells. Class II MHCs are encoded by HLA-DR, HLA-DQ and HLA-DP loci, with bound peptides presented on the cellular surface for the recognition by CD4^{+} effector cells (Neefjes et al. 2011). While being structurally similar to class I, class II MHCs are composed of two separate membrane bound chains, α and β, to form the peptide binding groove. Class II MHCs therefore adopt a more open structure of the binding groove allowing for the accommodation of peptides between 13 and 25 amino acids in length with the N-terminus of these peptides typically residing in the P1 pocket of the MHC (Münz 2016).

The peptide binding groove incorporates peptides via the formation of hydrogen bonds between the side chains of the MHC and residues of the peptide. Also, interactions between the anchor residues of the peptide (P2, 5, 6 and Ω (C-terminal peptide) in MHC class I and P1, 4 and 9 in MHC class II) and specific binding grooves within the MHC molecule are important for the binding of the peptide (Wieczorek et al. 2017).

Class III MHC molecules include secreted proteins that display immune functions such as heat shock proteins and cytokines (TNF-α). Class III MHC does not exhibit the same function as class I and II but is located between them on the short arm of chromosome 6.
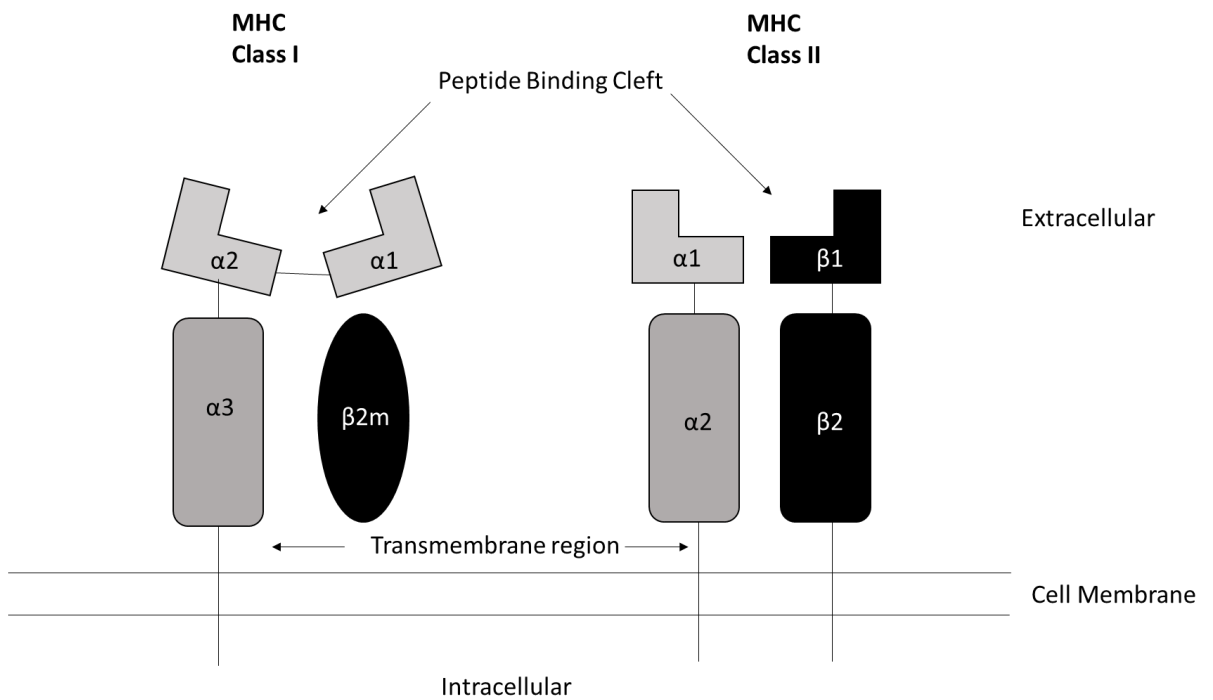
Figure 1.5. Class I and II MHC structure.

1.11. HLA-Nomenclature

The genes that encode the HLA-alleles are highly polymorphic and are situated on the short arm of chromosome 6 which contains more than 200 protein-encoding genes, many of which are related to the immune system.

The first HLA-antibody and antigen was discovered by Dausset via the observation of *in vitro* agglutination in serum taken from an agranulocytic individual when mixed with bone marrow from another individual (Dausset et al. 1952). HLA-A and B antigens were subsequently identified, followed by the discovery of the HLA-C loci in 1970 (Thorsby et al. 1970) and then class II alleles in 1978 (Albert et al. 1978). Serological techniques were originally used for the detection of HLA polymorphisms. This was achieved by the identification of epitopes present

on HLA molecules that evoked an antibody response (Tait 2011). The use of the aforementioned leukocyte agglutination and microlymphocytoxicity assays were employed to investigate this (Terasaki & McLelland 1964).

The advancement of gene sequencing techniques led to the development of assays that identified the full polymorphism of HLA-genes, something that serological techniques were limited in doing. This has allowed for the inception of a new method of nomenclature of HLA-alleles (Tait 2011; Torres & Moraes 2011). The new nomenclature involves a letter corresponding to the locus to which the allele is situated. The letter is succeeded by an asterix which indicates the use of sequencing techniques to identify the allele.

Each allele has a unique number corresponding to up to four sets of numbers that are divided by colons. The numbers preceding the first colon describe the type of allele which matches the serological antigen associated with an allotype. The next set of numbers following the colon describes the subtypes with numbers being assigned in the order to which DNA sequences have been determined. Alleles that are unique from others only by silent nucleotide substitutions within the coding sequence are discriminated by a third set of digits. A fourth set of numbers is assigned to alleles which differ only by sequence polymorphisms in the non-coding regions. Finally, a discretionary suffix may accompany the allele number in the form of a letter which is added to specify the alleles expression status (Marsh et al. 2010).

The list of suffixes is outlined below:

N= null allele

L= Low cell surface expression

S= Secreted allele but not present on the cell surface

C= Assigned to alleles that produce proteins present in cytoplasm but not on cell surface

A= Aberrant expression, where there is some doubt about protein expression

Q= Questionable expression

However, as of 2010 the suffix's A and C were no longer used to classify alleles (Torres & Moraes 2011).

HLA- B * 01: 01: 01: 01 N

Separator

Specific HLA-protein, amino acid differences

Polymorphism in non coding region

Gene identified on B locus

Allele group

Silent Mutation

Null

Figure 1.6. Nomenclature of HLA-alleles.

1.12. HLA-associations with adverse drug reactions

Many T-cell mediated ADRs have been associated with the carriage of HLA alleles in susceptible individuals to a variety of culprit drugs (Table 1.3). These HLA associations can include both class I and II allleles, with notable examples described below.

Culprit Drug	Adverse Drug Reaction	HLA-association	Ethnicity	Reference
Abacavir	HSS	HLA-B*57:01	Caucasian	(Mallal et al. 2002)
Carbamazepine	SJS/TEN	HLA-B*15:02	Han Chinese	(Chung et al. 2004) (Ozeki et al. 2011)
		HLA-A*31:01	Japanese	(McCormack et al.
	SJS/TEN, MPE		European	2011)
Allopurinol	SJS/TEN, DRESS	HLA-B*58:01	Han Chinese	(Hung et al. 2005)
Flucloxacillin	DILI	HLA-B*57:01	Caucasian	(Daly et al. 2009)
Dapsone	HSS	HLA-B*13:01	Chinese	(Zhang et al. 2013)
Lamotrigine	SJS/TEN	HLA-B*15:02	Han Chinese	(Man et al. 2007)
	HSS	HLA-A*31:01	Caucasian	(McCormack et al. 2012)
Phenytoin	SJS/TEN	HLA-B*15:02	Han Chinese	(Man et al. 2007)
Amoxicillin-Clavulanate	DILI	HLA-DRB1*15:01 HLA-DQB1*06:02	Caucasian	(Lucena et al. 2011)
Lumiracoxlib	DILI	HLA-DRB1*15:01	Caucasian	(Singer et al. 2010)
Ticlopidine	DILI	HLA-A*33:03	Japanese	(Hirata et al. 2008)
Nevirapine	DRESS	HLA-DRB1*01:01	Hispanic, African	(Martin et al. 2005)
		HLA-C*04:01	Malawian	(Carr et al. 2013)

Table 1.3. Examples of HLA restricted adverse drug reactions.

1.12.1. Carbamazepine

Carbamazepine is a sodium channel blocking agent commonly prescribed in the treatment of epilepsy and nerve pain such as trigeminal neuralgia. SJS and its associated disease TEN are implicated in some individuals undergoing treatment with this anticonvulsant. *Chung et al 2004* conducted a case control study in patients with carbamazepine induced SJS (44 patients in total), with 5 patients overlapping with TEN. These patients were compared against 101 controls who had been taking carbamazepine for at least 3 months with no adverse events (CBZ-tolerant). Genotyping for HLA alleles A, B and C along with DRB1 was carried out and it was found that the allele HLA-B*15:02 was present in all 44 of the individuals with CBZ-SJS. This allele was only present on 3 of the individuals from the CBZ-tolerant group of the study yielding an odds ratio, the measure of association between exposure and outcome, of 2504 (Chung et al. 2004). A follow up study by the same group confirmed the association between the risk allele HLA-B*15:02 and SJS/TEN reactions induced by carbamazepine; however, the induction of milder skin reactions such as macropapular eruption was found not to be associated with HLA-B*15:02 (Hung et al. 2006). Further studies also confirmed these findings indicating a strong association between the observed reactions and the carriage of this risk allele in the Han Chinese population (Locharernkul et al. 2008; Man et al. 2007). Indeed, prospective genotyping measures for the HLA-B*15:02 risk allele are now employed in Han Chinese populations prior to the prescription of carbamazepine and those testing positive are provided with alternative therapeutics such as lamotrigine (Phillips & Mallal 2011; Chen et al. 2011). However, studies on patients of European descent with carbamazepine induced SJS demonstrated no apparent association with HLA-B:15:02, once such suggestion for this may be the prevalence of another allele which may be protective of these reactions (Alfirevic et al. 2006). The prevalence of the HLA-B*15:02 risk allele within the Caucasian population is relatively low

(1-2%) when compared with the Han Chinese population (8%), suggesting that other alleles may be involved in the regulation of SJS/TEN reactions induced by carbamazepine.

Ozeki et al 2011 conducted a large GWAS within the Japanese population which indicated the presence of SNP's associated with carbamazepine induced ADRs. These SNP's were found to be situated on chromosome 6p21.33 including the HLA-A locus. Subsequent genotyping of single HLA-A alleles identified the presence of HLA-A*31:01 in around 60% of individuals that displayed carbamazepine-induced adverse drug reactions. This demonstrated HLA-A*31:01 as a risk factor for adverse drug reactions induced by carbamazepine yielding a sensitivity and specificity of 60% and 87.5% respectively (Ozeki et al. 2011). The association of adverse drug reactions, including maculopapular exanthema (MPE) and in some cases SJS/TEN, with carbamazepine and the carriage of HLA-A*31:01 in the Caucasian population has also been demonstrated (McCormack et al. 2011; Gidal 2011).

While the SJS/TEN reactions induced by carbamazepine in patients carrying the HLA-B*15:02 allele appears to be exclusive to Japanese populations, the association between ADRs and the HLA-A*31:01 allele has been observed in both Asian and European populations. However, the association between this allele and the observed ADRs is much weaker than that of HLA-B*15:02 which yields a sensitivity value of close to 100% (Kaniwa & Saito 2013). In a systematic review of published genotyping data, *Yip et al* in 2012 demonstrated an odds ratio of 113.4 for HLA-B*15:02 and carbamazepine induced SJS/TEN. These findings corresponded to a number needed to treat (NNT), the average number of patients wo needed to be treated to prevent one additional adverse outcome, value of 461 with regard to prospective genotyping for HLA-B*15:02 (Yip et al. 2012). Conversely the carriage of HLA-A*31:01 displayed significant association with various manifestations of carbamazepine hypersensitivity in multiple ethnicities providing an odds ratio of 9.5. This translates to a NNT value of between 47 and 67 patients, indicating a much lower number of individuals required

to treat in order to prevent one case of hypersensitivity (Yip et al. 2012). These findings suggested an effective use of HLA genotyping for the avoidance of carbamazepine hypersensitivity. Indeed, prospective genotyping for HLA-B*15:02 is now commonly undertaken in the Asian populations, however to date genotyping for HLA-A*31:01 has not yet been employed prior to carbamazepine therapy.

CD8$^+$ T-cells isolated from carbamazepine induced SJS/TEN patients proliferate and secrete cytokines following *in vitro* activation with carbamazepine. Furthermore, the TCR Vβ-11IGSY was identified to be prevalent in 84% of patients with SJS/TEN, while being absent in all tolerant patients. It was also shown that PBMCs primed from healthy volunteer's positive for the HLA-B*15:02 and TCR Vβ-11IGSY were able to display cytotoxicity in the presence of carbamazepine. These cytotoxic responses could subsequently be diminished via the addition of anti-TCR-Vβ-11 antibody indicating a pivotal role for the TCR in carbamazepine induced SJS/TEN (Ko et al. 2011) . It was next shown that CD8$^+$ T-cell responses induced by carbamazepine were independent of antigen processing machinery and involved a direct interaction of the drug with the HLA-B molecule (Wei, Chung, et al. 2012). *Lichtenfels et al* isolated T-cell clones from patients positive for the HLA-A*31:01, with indicative symptoms such as MPE. Subsequent phenotyping of these clones demonstrated the presence of both CD4$^+$ and CD8$^+$ T-cell clones, both of which evoked a cytotoxic effector function (Lichtenfels et al. 2014). While activation of CD8$^+$ T-cell clones was wholly dependent on the HLA-A*31:01 allele, shown by the blunting of the proliferative response in the presence of MHC Class I block, CD4$^+$ responses were only diminished in the presence of MHC Class II block. These findings led to the subsequent discovery of the involvement of a class II allele DRB1*04:04 in the CD4$^+$ mediated T-cell response. Indeed, strong linkage disequilibrium exists between DRB1*04:04 and HLA-A*31:01 indicating that a common haplotype may be an important factor in the multiclonal response to carbamazepine observed in Caucasians (Lichtenfels et

al. 2014).   While the HLA-A*31:01 allele has strong association with SJS/TEN in Japanese populations, such association is weak in Europeans. Conversely, the expression of HLA-A*31:01 in European populations has a strong association with the milder but still problematic reactions MPE and DRESS, not commonly observed in Japanese populations (Ozeki et al. 2011; McCormack et al. 2011). As mentioned previously, the class II allele DRB1*04:04 forms a common haplotype with HLA-A*31:01 in Caucasians. CD4+ mediated T-cell reactions to carbamazepine were restricted to the DRB1*04:04 allele, suggesting that in the Caucasian population CD4+ T-cell responses form the primary response to carbamazepine, hence the preferential manifestations of MPE and DRESS (Lichtenfels et al. 2014). Such common haplotype with HLA-DRB1*04:04 is not as frequent in Japanese populations, suggesting that responses to carbamazepine in HLA-A*31:01 individuals are primarily mediated by CD8+ T-cells, hence the manifestation of much more serious reactions i.e. SJS/TEN (Ozeki et al. 2011). Indeed, this suggests that the ethnicity of the individual seems to be pivotal for the manifestation of the cutaneous reactions to carbamazepine.

1.12.2. Allopurinol

Allopurinol is a xanthine oxidase inhibitor used for the treatment of hyperuricemia related diseases including gout, Lesch-Nyham syndrome and recurrent kidney stones (Wortmann 2002) . However, it is one of the most frequent causes of adverse drug reactions, contributing to approximately 5% of Severe Cutaneous Adverse Reactions (SCARs) (Roujeau et al. 1995; Hung et al. 2005). In 2005 *Hung et al* using genetic marker studies demonstrated the relationship between the observed reactions to allopurinol and the prevalence of the HLA-B*58:01 allele in the Han Chinese population. This allele was detected in 100% of patients exhibiting allopurinol induced SCARs but only in a small percentage of allopurinol tolerant patients (15%) (Hung et al. 2005). This association was subsequently detected to a more modest degree, in various other populations including Thailand, Japan, South Korea,

Australia and Europe (Lonjou et al. 2008; Tassaneeyakul et al. 2009; Kaniwa et al. 2008), indicating HLA-B*58:01 to be an effective marker for the adverse reactions. More recently, a study was undertaken to assess the validity of prospective screening for the HLA-B*58:01 allele prior to treatment in Taiwanese individuals displaying need for allopurinol therapy, that had not been previously exposed to the drug (Ko et al. 2015). From this it was identified that no patient who had tested negative for HLA-B*58:01 exhibited any symptoms of SCARs, leading to the conclusion that prospective genotyping for HLA-B*58:01 was capable of reducing the incidence of allopurinol induced SCARs in the Taiwanese population (Ko et al. 2015). The prevalence of the HLA-B*58:01 in the Asian populations is around 15-18% but much lower in Europeans accounting for 1-2% (Plumpton et al. 2017), therefore prospective genotyping for HLA-B*58:01 may prove to be a cost effective means in Asian countries, already demonstrated in Korea (Park, *et al.*, 2015) and Thailand (Saokaew et al. 2014), but due to the low prevalence in European populations it is unlikely that this method would be a cost effective procedure currently (Plumpton et al. 2017). Allopurinol is rapidly metabolized to oxypurinol *in vivo* with a plasma half-life of 1-2 hours, suggesting oxypurinol to be implicated in the induction of SCARs (Yun et al. 2013). Indeed, LTT results from allopurinol allergic patients demonstrate dose dependent T-cell activation in response to oxypurinol, but not allopurinol (Yun et al. 2013). Furthermore, T-cell lines generated to allopurinol and oxypurinol reacted immediately to the addition of either drug in an antigen processing independent manner. Docking studies suggested oxypurinol to bind HLA-B*58:01 with a higher affinity than allopurinol, suggesting oxypurinol is primary sensitizer in allopurinol allergic patients (Yun et al. 2014). Currently, the U.S Food and Drug administration (FDA) does not advise HLA-B*58:01 genotyping for allopurinol therapy; however, as the cost of effective genotyping continues to reduce, this may become a useful practice in the future.

1.12.3. Flucloxacillin

Flucloxacillin is a beta-lactam antibiotic belonging to the penicillin class, which is commonly used to treat a broad range of gram-positive bacterial infections such as skin and tissue infections, respiratory and urinary tract infections and diseases such as meningitis (Wing et al. 2017). Despite being generally well tolerated, flucloxacillin is associated with cholestatic liver injury affecting new users of the drug at a rate of 8.5 per 100,000 (Andrews & Daly 2008; Russmann et al. 2005). This can occur via interference with the bile flow through inhibition of bile formation and transport both into and out of hepatocytes as well as affecting the normal function of the bile ducts (Padda et al. 2012). 5'hydroxymethylflucloxacillin is the main active metabolite of flucloxacillin which is generated via the hydroxylation of the 5-methyl group of the isoxazole ring, achieved via the actions of the CYP3A4 enzyme (Thijssen 1979). Flucloxacillin does not display direct cytotoxicity on hepatocytes or biliary epithelial cells. However, conditioned media from cultured hepatocytes that were preincubated with flucloxacillin initiated a significant increase in lactate dehydrogenase, often released during tissue damage, in the biliary epithelial cells. Furthermore, this observed response was lost following inhibition of CYP3A4 metabolism and enhanced following CYP3A4 induction (Lakehal et al. 2001). Much like the parent drug, the flucloxacillin metabolites did not display direct toxicity. While these findings accounted for the mechanism of flucloxacillin injury, they did not explain why such reactions were found only in a small number of individuals.

In 2009 *Daly et al* conducted a GWAS study using over 800,000 markers in 51 cases of flucloxacillin-induced DILI. This study identified the association between flucloxacillin liver injury and the carriage of the HLA-B*57:01 allele, also heavily associated in hypersensitivity reactions to the antiretroviral drug abacavir (Daly et al. 2009; Mallal et al. 2002). Association with this allele implicates a role of T-cells in the adverse reaction. Indeed, flucloxacillin

specific T-cell responses were detected in PBMCs isolated from DILI patients via the ELIspot assay (Maria & Victorino 1997).

Monshi et al demonstrated the flucloxacillin-specific PBMC responses from patients with flucloxacillin-induced liver injury by way of IFN-γ secretion, with no such activation observed in tolerant individuals or drug naïve patients. Responsive T-cell clones obtained to patients were identified as CD4$^+$ and CD8$^+$. Furthermore, mass spectrometric analysis of albumin obtained from flucloxacillin-treated cell cultures revealed the presence of irreversibly bound haptens generated via the direct adduction of flucloxacillin. The CD8$^+$ responses were processing dependent and HLA-B*57:01 restricted. This indicates the role of the hapten model as a paradigm for T-cell mediated reactions to flucloxacillin. A strong correlation between the strength of flucloxacillin binding and the level of the proliferative response observed provides further supporting evidence (Monshi et al. 2013).

However, it was later identified that flucloxacillin was able to stimulate CD8$^+$ T-cells in two individual manners (Wuillemin et al. 2013). Indeed, T-cell clones generated to flucloxacillin from HLA-B*57:01$^+$ and HLA-B*57:01$^-$ drug naïve individuals were found to follow two distinct patterns of activation. It was found that the hapten mechanism of activation was observed primarily in HLA-B*57:01$^-$ individuals, while T-cells from those positive for the risk allele responded in a mechanism more consistent with the PI model. This was confirmed via the identification of immediate reactions and the presence of labile binding, which was easily removed by washing. Furthermore, these responses had no dependence on the antigen processing, suggesting direct interaction (Wuillemin et al. 2013). Activation via the hapten mechanism in this study was not restricted to HLA-B*57:01, as flucloxacillin pulsed APC responses were only observed in HLA-B*57:01$^-$ individuals. Given the presence of multiple binding sites on a protein, it is unlikely that the hapten mechanism will be restricted to a single allele based on the fact that after processing a plethora of potential drug bound

peptides would be generated, with the ability to be loaded onto many different HLA-alleles (Wuillemin et al. 2013). A recent study by *Yaseen et al* identified preferential activation of flucloxacillin via a hapten mechanism in T-cells generated from DILI patients positive for HLA-B*57:01. This was confirmed using APC pulsing assays, where T-cell clones were activated only by pulsed autologous HLA-B*57:01 APCs (Yaseen et al. 2015). Conversely, responses to soluble flucloxacillin were observed across a number of HLA-allele mismatched APCs. This suggests that HLA-B*57:01 patient responses to flucloxacillin are mediated via the hapten mechanism while T-cells generated from healthy donors are activated with the parent drug in an antigen processing independent mechanism, i.e. PI (Yaseen et al. 2015). This indicates the role of multiple mechanisms in driving T-cell activity towards flucloxacillin.

1.13. Abacavir

Abacavir ((1S,4R)-4-(2-amino-6-(cyclopropylamino)-9H-purin-9-yl)-2-cyclopentene-1-methanol) is an antiretroviral prodrug used for the treatment of the Human Immunodeficiency Virus (HIV). It belongs to the nucleoside reverse transcriptase inhibitor (NRTI) class of antiretroviral's, the other being non-nucleoside reverse transcriptase inhibitors (NNRTI's), with HIV treatment being most effective when abacavir is used in conjunction with other anti-retroviral agents such as lamivudine and zinovudine (Hervey & Perry 2000). The chemical formula of abacavir is $C_{14}H_{18}N_6O$ and the chemical structure consists of a cyclopentenyl moiety, a 2-amino purine moiety and a cyclopropyl moiety as shown in Figure 1.7.
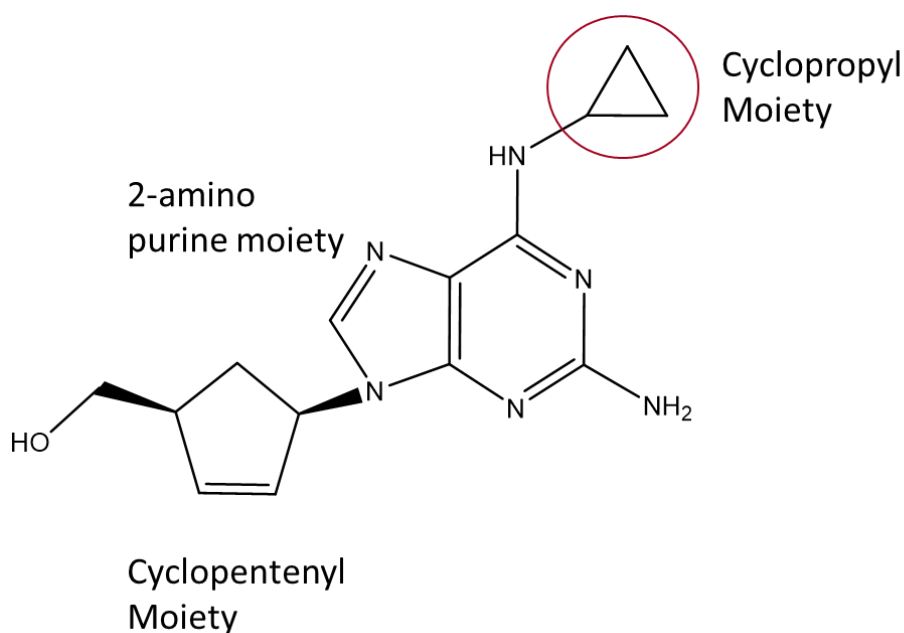
Figure 1.7. Chemical structure of abacavir

1.13.1. Mechanism of action

Abacavir is a carbocyclic nucleoside analogue which is metabolised into a 2'-deoxyguanosine nucleoside analogue. It is broken down in an anabolic process through a pathway not involving enzymes known to phosphorylate other NRTI drugs (Hervey & Perry 2000). In the primary metabolic pathway, abacavir is metabolised to abacavir 5'-monophosphate via the action of the stereospecific enzyme adenosine phosphotransferase (Barbarino et al. 2014; Faletto et al. 1997). This is followed by a deamination process to form carbovir 5'monophosphate via the action of an unknown cytosolic enzyme. It then undergoes further rounds of phosphorylation by cellular kinases to generate first carbovir di-phosphate and finally carbovir tri-phosphate (Barbarino et al. 2014; Hervey & Perry 2000; Faletto et al. 1997).

Carbovir monophosphate may be generated via another minor metabolic pathway (minor pathway) which accounts for less than 2% of the generated metabolite. In this pathway abacavir is converted to 6-amino carbovir, which can then be phosphorylated via adenosine

phosphotransferase generating 6-amino carbovir monophosphate. Next, via the action of adenosine monophosphate deaminase, it is converted to carbovir monophosphate. The minor metabolised product 6-amino carbovir can be deaminated to generate the metabolite carbovir and next via the action of AMP deaminase and 5'-nucleoside inosine phosphotransferase respectively the generated metabolites are converted to carbovir monophosphate, which are subsequently phosphorylated to yield carbovir triphosphate (Faletto et al. 1997) (Figure 1.8).
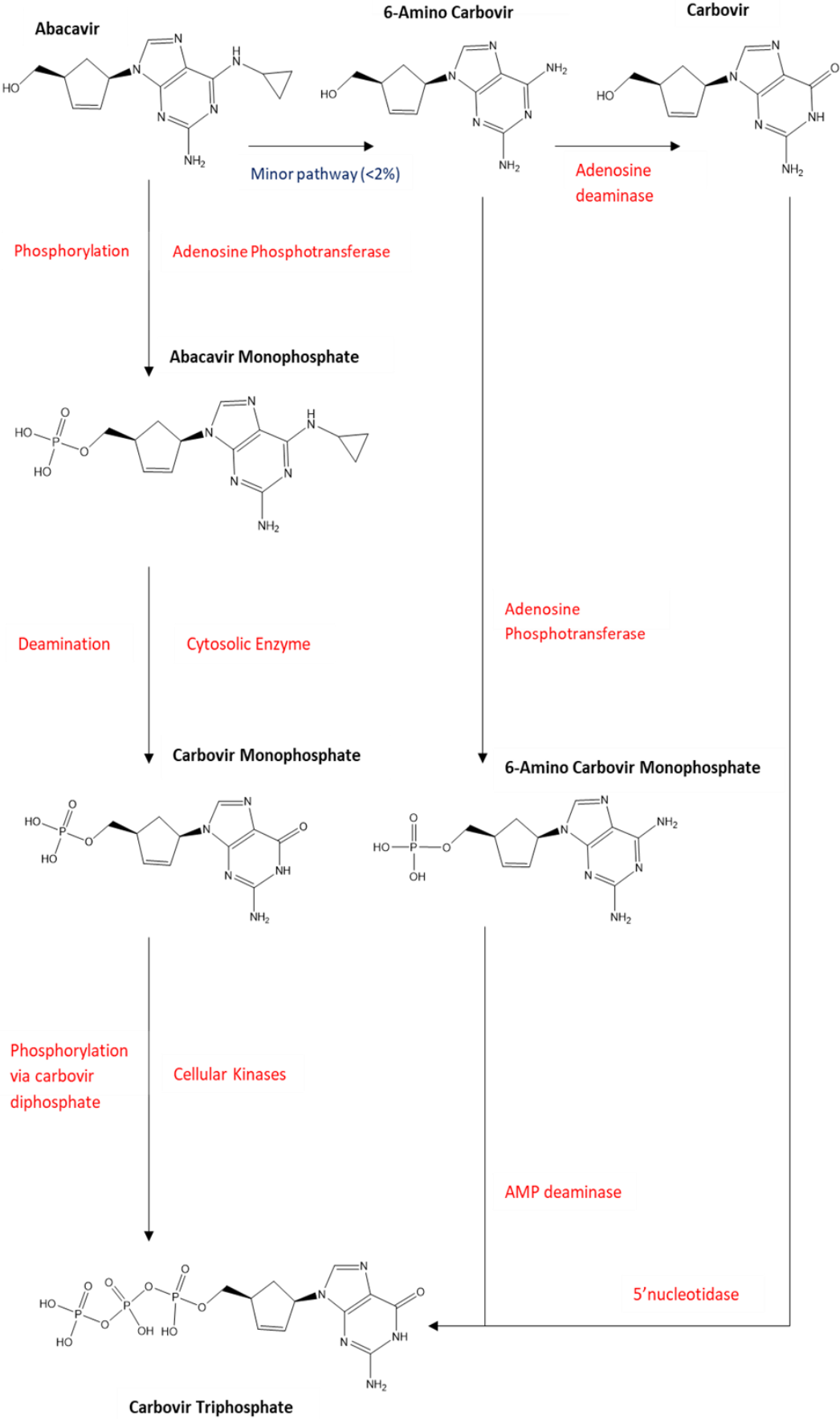
Figure 1.8. Intracellular phosphorylation of abacavir via multiple pathways to generate carbovir triphosphate which blocks viral replication

HIV is a single stranded RNA virus which undergoes the process of reverse transcription to generate double stranded viral DNA. This process is dependent on the enzyme reverse transcriptase, specific to HIV. The viral DNA is then integrated into the host's genome and, via mechanisms using the host's machinery, used to produce viral offspring.

As previously mentioned, abacavir is metabolised to carbovir triphosphate, which then competes with the endogenous nucleotide 2'deoxyguanosine triphosphate (dGTP) for integration into the nucleic acid chain at the active site (Hervey & Perry 2000). Carbovir triphosphate lacks the 3'-OH structure which is required for the 5' to 3' phosphodiester linkage. When incorporated into the viral DNA strand, carbovir triphosphate inhibits the addition of new bases which in turn blocks further strand elongation, leading to a premature halt in viral DNA synthesis resulting in chain termination, thereby resulting in a cessation of viral replication (Martin & Kroetz 2013).

Abacavir is rapidly absorbed following oral administration and demonstrates around an 83% bioavailability. On average following a 300mg dose twice a day abacavir's plasma concentration (C_{max}) ranges from 0.64 to 4.38 mg/L which is usually reached around 40 minutes to 1 hour after ingestion. The area under the concentration time curve (AUC 0-12 hours) after a single oral dose of 300mg in a fasted individual is on average 6.02 ± 1.73 mg/L/hr, although it should be noted that food does not significantly alter the absorption of abacavir.

The volume of distribution of abacavir is 0.86 ± 0.15 L/kg following an intravenous administration. The protein binding of the drug is approximately 50% and is not dependent on concentration. The clearance is determined as 0.8 ± 0.24 L/hr/kg which was representative of an HIV infected adult receiving a single IV dose of 150mg.

Abacavir is metabolised by enzymes in the liver including alcohol dehydrogenase and possesses a mean elimination half-life of 1.54 ± 0.63 hours This hepatic metabolism generates a reactive aldehyde, which readily isomerizes to be converted to carboxylic acids (Walsh et al. 2002). The reactive aldehyde is capable of adduction reactions with the N-terminal valine of haemoglobin via a Schiff base formation (McDowell *et al.*, 1999; Walsh, Reese and Thurmond, 2002; Charneira *et al.*, 2011; Bell *et al.*, 2013; Meng *et al.*, 2014). Approximately 1.2% is excreted in the urine as abacavir, while 30% is excreted as the 5'carboxylic acid metabolite and a further 36% as the 5'guanosine metabolite. Furthermore 16% of the dose is excreted in the faeces and 15% is excreted in the urine as unknown metabolites.

1.13.2. Abacavir-induced hypersensitivity

Hypersensitivity reactions to abacavir are CD8^{+} T-cell mediated and take place in 5-8% of patients treated with the drug (Lucas et al. 2015). This syndrome is restricted to those who are positive for the HLA-B*57:01 allele which consequently has led to the inception of prospective genotyping of patients for this risk allele prior to abacavir prescription (Mallal et al, 2008).

These hypersensitivity reactions generally occur within the first 6 weeks of commencing treatment with abacavir with a median time to onset being 11 days (Mallal et al. 2008), (Hetherington et al. 2001). Symptoms include fever, rash, GI and respiratory symptoms as well as constitutional symptoms such as weight loss, all of which become more severe with continued dosing. Of these symptoms the most frequently reported were a combination of fever, rash and fatigue as well as GI symptoms such as nausea, vomiting and diarrhoea, while respiratory symptoms such as pharyngitis and coughs were much less common (Symonds et al. 2002). Following onset of such symptoms the cessation and discontinuation of abacavir therapy is imperative, leading to a reversal of symptoms (Mallal et al. 2008). Any subsequent

rechallenge following a HSR with abacavir is contraindicated and can produce far more serious reactions such as hypotension within a few hours which can be life threatening (Mallal et al. 2008; Hetherington et al. 2001; Mallal et al. 2002).

Such symptoms of abacavir hypersensitivity can be difficult to detect as they are non-specific and often indistinguishable from symptoms of infections, reactions to other drugs and symptoms of inflammatory disease (Mallal et al. 2008).

In 2002 *Mallal et al* conducted a study using MHC region typing in 200 HIV patients that had been exposed to abacavir. Of these 200 patients, abacavir hypersensitivity was identified in 18 patients while 167 patients had gone 6 weeks or more of abacavir treatment without developing any symptoms of hypersensitivity, this group was defined as abacavir tolerant. From the 18 abacavir hypersensitive patients, 14 tested positive for the HLA-B*57:01 allele (78%) which was also present in 4 of the 167 abacavir tolerant patients (2%) (Mallal et al. 2002). From this they concluded that the withholding of abacavir in patients positive for this allele would diminish the frequency of hypersensitivity reactions (Mallal et al. 2002). These finding were mirrored in a 2002 retrospective, case control study conducted by *Hetherington et al.* HLA-B*57:01 was present in 39 of the 84 abacavir hypersensitive patients (46%) and 4 of the 113 control patients (4%) (Hetherington et al. 2002). This group concluded that the retrospective genotyping should not be used to diagnose a hypersensitivity reaction due to the dangers of rechallenging with abacavir but instead recommended the potential of prospective genotyping (Hetherington et al. 2002).

The PREDICT-1 study conducted by *Hughes et al* in 2008 was a fully powered, randomized, blinded, prospective study designed to assess the clinical relevance of HLA-B*57:01 screening, with a view to reducing hypersensitivity reactions to abacavir in HIV-positive patients. Subjects were randomised into an abacavir containing treatment regime with or without prospective screening for HLA-B*57:01. Those in the prospective screening group

who tested positive for this risk allele were excluded from the treatment regime, while close hypersensitivity monitoring was carried out in the non-screening group (Hughes et al. 2008). A reduction from 7.3% to 3.6% in clinically suspected abacavir hypersensitivity reactions was observed in the genetic screening group compared with the non-genetic screening group. This laid down a marker for the effectiveness of prospective genotyping for HLA-B*57:01 prior to commencement of abacavir therapy (Hughes et al. 2008). This study was continued by *Mallal et al* who carried out a double blinded, prospective, randomized study which encompassed 1956 patients from 19 different countries, accounting for different ethnicities. Patients were randomly assigned to a prospective screening group with those who were HLA-B*57:01 positive excluded from the trial and a standard of care treatment with abacavir group without the prospective genotyping (Mallal et al. 2008). Epicutaneous patch testing was performed for the purposes of clinically diagnosing a hypersensitivity reaction. Prospective screening eradicated hypersensitivity reactions to abacavir with 0% of the patients in the prospective group experiencing a hypersensitivity reaction while 2.7% of patients in the control group experienced a clinically diagnosed hypersensitivity reaction (Mallal et al. 2008). This yielded a negative predictive value of 100% and a positive predictive value of 47.9% (Mallal et al. 2008). This demonstrated the ability of prospective genotyping and other pharmacological tests to be used as a means of preventing adverse effects of a therapeutic.

The cost effectiveness of prospective genotyping for the HLA-B*57:01 risk allele prior to commencing abacavir therapy has been demonstrated. *Hughes et al* conducted a study in 2004 where patients with and without abacavir hypersensitivity were identified and genotyped for HLA-B*57:01. Alongside this a cost effectiveness analysis was undertaken to assess the cost of testing and the cost of treating abacavir hypersensitivity as well as the cost and selection of alternate treatment regimens (Hughes et al. 2004). In this study 46% of

patients who had suffered abacavir hypersensitivity were HLA-B*57:01 positive while 10% of patients in the control group were also positive for this allele. Furthermore the cost effectiveness model in the study demonstrated testing for HLA-B*57:01 to be of beneficence over not testing due to being less expensive than treating hypersensitivity reactions (Hughes et al. 2004). This was continued by *Schackman et al* using a simulated cohort of patients commencing HIV therapy with an aim to assessing the cost effectiveness of treatment with abacavir and tenofovir with prospective HLA-B*57:01 genotyping (Schackman et al. 2008). Testing for HLA-B*57:01 generated a cost effectiveness ratio of $36,700/QALY when compared with no testing. However prospective genotyping in tenofovir therapy actually increased the cost of therapy with no obvious improvements in the quality adjusted life expectancy and cost more than an abacavir treatment regime with prospective genotyping (Schackman et al. 2008). Therefore, it was concluded that prospective HLA-B*57:01 genotyping is a cost-effective means of preventing hypersensitivity reactions to abacavir in patients. In July 2008 the FDA issued a boxed warning on abacavir and abacavir containing medications strongly advising patients to seek screening for HLA-B*57:01 allele prior to commencing abacavir therapy.

The generation of responsive T-cell clones to abacavir *in vitro* from drug naïve healthy donors positive for the HLA-B*57:01 allele has been widely demonstrated (Chessman *et al.*, 2008; Adam *et al.*, 2012; Bell *et al.*, 2013; Naisbitt *et al.*, 2015). Furthermore responses in abacavir specific T-cell clones are not observed when co-incubated with antigen presenting cells expressing closely related alleles such as HLA-B*57:02 (114 Asp-Asn, 116 Ser-Tyr, 156 Leu-Arg), HLA-B*57:03 (114 Asp-Asn, 116 Ser-Tyr) or HLA-B*58:01 (45 Met-Thr, 46 Ala-Glu, 97 Val-Arg, 103 Val-Leu) indicating that abacavir binding is highly specific to HLA-B*57:01 with particular sensitivity in the F-pocket region of the allele namely residue Serine 116 (Ostrov et al. 2012; Illing et al. 2012; Chessman et al. 2008).

Unmodified abacavir binds to HLA-B*57:01 in a non-covalent manner across the bottom of the antigen binding cleft and protruding into the F-pocket where the carboxy terminal amino acid tryptophan usually anchors peptides bound to HLA-B*57:01 (Ostrov et al. 2012; Illing et al. 2012; Norcross et al. 2012). Abacavir binds specifically to HLA-B*57:01 and induces an alteration in the shape and chemistry of the antigen binding cleft consequently altering the repertoire of endogenous peptides that can bind to HLA-B*57:01 (Ostrov et al. 2012; Illing et al. 2012; Norcross et al. 2012). Using peptide elution studies *Illing et al* demonstrated a change in the repertoire of self-peptides in the presence of abacavir. C1R-B *57:01 cells comprise a fully functional B-cell line transfected to express HLA-B*57:01, which can act as professional APCs. These cells were treated in the presence and absence of abacavir and the peptides eluted from the antigen presenting cells were subsequently analysed via mass spectrometry. It was observed that up to 25% of the total peptides eluted from the HLA-B*57:01 in the presence of abacavir were novel self-peptides not detected in abacavirs absence (Illing et al. 2012). The prevalence of larger amino acids phenylalanine and tryptophan was severely diminished at the PΩ position (C-terminus) of the peptide corresponding to the F-pocket region of the MHC. The decrease in these amino acids was replaced with a significant increase in the smaller side chain amino acids leucine and isoleucine at the same position, while an increase in valine prevalence was also observed however the change was not significant in this study. This mass shift in amino acid prevalence was only observed in the PΩ position and nowhere else on the peptide chain (Illing et al. 2012). Furthermore, these findings were not mirrored in closely related alleles of HLA-B*57:01 including HLA-B*57:03 or HLA-B*58:01, nor were there any differences in the prevalence of the small side chain amino acids at the P2 (B-pocket) position between abacavir-treated and untreated cells (Illing et al. 2012).

Norcross et al demonstrated the alteration of self-peptides from the typical peptides containing C-terminal tryptophan, phenylalanine and tyrosine residues common to treated and untreated samples alike. However, peptides observed only in abacavir-treated cells displayed a far higher prevalence of the smaller amino acids isoleucine and leucine at the C-terminal position. Furthermore, two synthesized peptides containing C-terminal isoleucine and leucine residues demonstrated strong affinity binding interactions within HLA-B*57:01 in the presence of abacavir. Importantly, similar observations were not detected with flucloxacillin bound to HLA-B*57:01 (Norcross et al. 2012).

The binding affinity of peptides was also tested by *Ostrov et al* using positional scanning combinatorial peptide libraries in both the presence and absence of abacavir. Again, in the absence of abacavir a stronger preference for binding HLA-B*57:01 was shown in peptides with C-terminal tryptophan and phenylalanine. However, in the presence of abacavir an increased affinity was detected in *de novo* peptides containing C-terminal smaller chain amino acid residues valine, alanine and isoleucine all of which displayed an increase in prevalence of between 5 and 8 fold compared to untreated cells (Ostrov et al. 2012). Individual synthesized peptides with respective C-terminal valine (pep-V) and tryptophan (pep-W) were generated. HLA binding studies demonstrated that pep-V required abacavir in a dose dependent manner in order to bind to HLA-B*57:01 with sufficient affinity while no significant binding effect of abacavir was observed for pep-W binding (Ostrov et al. 2012).

As previously mentioned, abacavir consists of a cyclopentenyl moiety, a 2-amino purine moiety and a cyclopropyl moiety. It has been demonstrated that the cyclopropyl moiety of abacavir plays a key role in the interactions with HLA-B*57:01. This moiety extends towards and protrudes into the F-pocket, leading to interactions that reduce the size of the MHC peptide binding cleft accounting for the preference of smaller chain amino acids such as leucine and isoleucine (Illing et al. 2012). These findings are consistent with previous studies

where it was shown that endogenous peptides extracted from HLA-B*57:01 cells treated with abacavir contained alternate peptide sequences compared to untreated cells, which were shown to be predominantly leucine and isoleucine. Taken together these studies provide a strong case for abacavir interactions within HLA-B*57:01 demonstrating a possible unique manner of T-cell activation relying on the presentation of altered self-peptides to T-cells. Patients are generally tolerant to these peptides as they are never exposed to them in the context of HLA-B*57:01. However, presentation of these altered self-peptides by HLA-B*57:01 can be mistaken for a foreign entity by CD8^{+} T-cells, leading to an immune reaction (Ostrov et al. 2012; Norcross et al. 2012; Illing et al. 2012; Llano & Brander 2012). It is also possible that T-cells may be activated by presentation of an existing HLA-B*57:01 binding peptide, but in an altered conformation (Figure 1.9) (Illing et al. 2013).

Despite the 100% NPV with abacavir hypersensitivity reactions, only 55% of individuals that are positive for HLA-B*57:01 will develop a hypersensitivity reaction upon exposure to abacavir (Lucas et al. 2015; Mallal et al. 2008). Indeed, abacavir-specific T-cells are detectable in the circulating blood of HLA-B*57:01 donors who have never been exposed to the drug (Adam et al. 2012; Schnyder et al. 2013). Using patch testing, S*chnyder et al* 2013, demonstrated only patients with previous confirmed hypersensitivity reactions to abacavir produced skin reactions on exposure to abacavir, while those without prior abacavir exposure, both HIV patients and healthy donors, yielded negative tests (Schnyder et al. 2013). These findings suggest previous abacavir hypersensitivity to be a pre-requisite for a skin reaction to the drug. Furthermore, the onset of hypersensitivity reaction symptoms has been shown in some cases to occur as early as 36 hours post first exposure to the drug, compared to the typical onset time of around 3-6 weeks. This has led to the proposition that abacavir may activate memory T-cells present from a previous immunogenic episode via cross reactivity. This specifies that HLA-B*57:01 restricted CD8^{+} memory T-cells previously

primed to a pathogen specific epitope may cross recognise a self-peptide that has been presented by HLA-B*57:01 in the presence of abacavir, thereby initiating a rapid immune response (Lucas et al. 2015). This mirrors the model of heterologous immunity's role in graft and transplant rejection caused by cross reactivity between viral specific memory T-cells and mismatched HLA molecules (Amir et al. 2010).

Indeed, it has been recently demonstrated that structural similarity between viral peptides and self-peptides presented by HLA-B*57:01 in the presence of abacavir exists (Yerly et al. 2017). In this study, the crystal structure of the abacavir self-peptide VTTDIQVKV was complexed to abacavir and HLA-B*57:01. The authors detected solvent accessible side chains protruding for recognition by T-cells. This self-peptide corresponded to the human transcription elongation factor SPT5 isoform A 976-984 which has previously been shown to stimulate T-cells from patients with abacavir hypersensitivity syndrome (Yerly et al. 2017). Using BLAST search three more peptides were identified with a sequence homology to SPT5a of between 40 and 80%. These three peptides corresponded to the HIV-1 virus or the HSV1 or 1/2 virus. TCR transfected jurakat cells were treated with these viral peptides and peptide VTQQAQVRL and T-cell activation was observed in the absence of abacavir. This peptide sequence corresponded to the Human Simplex Virus 1/2 and when complexed within HLA-B*57:01 demonstrated a similar binding conformation to peptide VTTDIQVKV, indicating similar interactions with T-cells. However the T-cell response with this peptide was only observed in transfectants expressing one particular TCR (BeS-B7) indicating tha these cross reactive memory responses may be exclusive to a small sub population of CD8⁺ T-cells (Yerly et al. 2017).
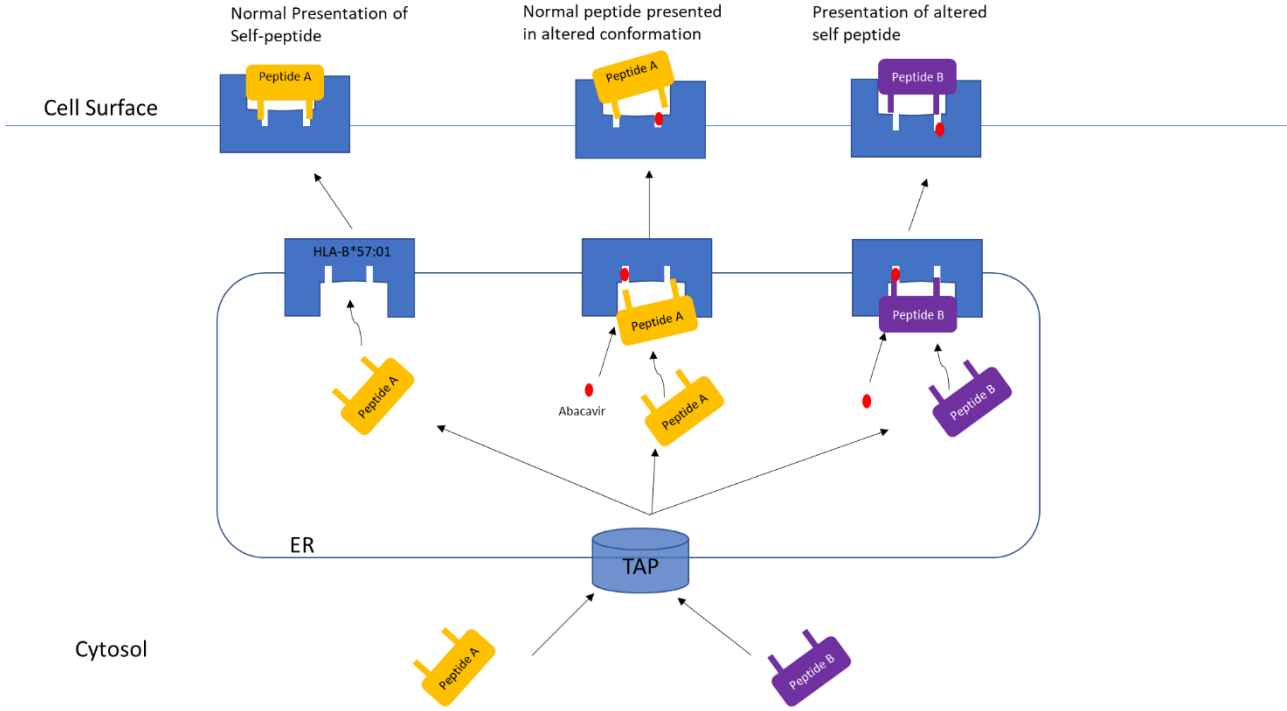
Figure 1.9. Formation of HLA-B*57:01 abacavir-peptide complexes possessing immunogenic properties. Adapted from *Illing et al 2013.*

1.14. Aims and objectives of thesis

Despite it being well established that hypersensitivity reactions observed to abacavir are exclusive to the carriage of the MHC class I allele HLA-B*57:01 (Mallal et al. 2008), the underlying mechanisms of abacavir hypersensitivity reactions remain unclear. Indeed, *Illing et al* and others have demonstrated the shift in the prevalence of peptides presented to T-cells in the presence of abacavir (Illing et al. 2012; Ostrov et al. 2012; Norcross et al. 2012). Prospective genotyping is employed for the carriage of HLA-B*57:01 in patients prior to treatment with abacavir, with those positive for the risk allele excluded from abacavir therapy. It has been demonstrated that modification to the 6-aminocyclopropyl moiety of abacavir is capable of diminishing the unwanted T-cell activation observed with abacavir, while retaining the antiviral activity of the compound (Naisbitt et al. 2015).

Thus, the aims of this thesis were

- To investigate the further modifications to the 6-amino cyclopropyl moiety of abacavir on T-cell responses and the antiviral potency of the compound.

- Using a panel of abacavir analogues as molecular probes, explore the binding and interactions of the compounds within HLA-B*57:01 and its relationship with T-cell activity.

- To investigate the effects of the abacavir substituted analogues on the peptide repertoire displayed on the antigen presenting cell surface.

- To evaluate if the unique self-peptides eluted from HLA-B*57:01 in the presence of abacavir are capable of stimulating a T-cell response in the presence and absence of the drug.

Chapter 2. Generation of abacavir-specific CD8$^+$ T-cell clones from a panel of HLA-B*57:01 drug naïve donors.

2.1 Introduction

Abacavir is a prodrug which when converted to its metabolite carbovir inhibits viral chain replication via halting the reverse transcription of the viral RNA. However, exposure to this potent antiviral therapeutic is accompanied by the risk of severe hypersensitivity reactions observed exclusively in individuals carrying the risk allele HLA-B*57:01 (Mallal et al. 2002; Martin et al. 2004; Mallal et al. 2008). Due to the high prevalence of this risk allele, primarily in the Caucasian population, and the 100% NPV, genetic screening for HLA-B*57:01 is routinely carried out in HIV patients prior to the commencement of abacavir therapy, with those testing positive HLA-B*57:01 prescribed an alternate therapy regimen (Mallal et al. 2008).

Abacavir is known to cause the secretion of proinflammatory cytokines including IFN-γ and TNF-α from immune cells. While these responses have been detected in PBMCs from abacavir hypersensitive patients (Almeida et al. 2008) it is difficult to detect this response using PBMCS from drug naïve individuals exposed to abacavir *in vitro*. This is mainly due to the large pool of cells encompassed by PBMCs in healthy donors all of which have different characteristics, making it difficult to obtain a distinctive result which can be individually attributed to a defined cell population.

For this reason, the generation of abacavir-induced T-cell lines from healthy donor PBMCs followed by cloning provides an effective mechanism to generate functional T-cells responsive to abacavir, for mechanistic studies, without the additional complication of handling the HIV virus. The procedure of T-cell cloning is carried out using a technique known as serial dilution which is a relatively simple and cost-effective process, utilising T-cells primary growth factor IL-2, with the only notable draw back being the time consumption of the procedure.

Drug specific T-cells have been generated to a plethora of therapeutics known to be associated with adverse reactions including carbamazepine (Wu et al. 2006; Lichtenfels et al. 2014), lamotrigine (Naisbitt et al. 2003), sulfamethoxazole (Castrejon et al. 2010), dapsone and dapsone nitroso (Alzahrani et al. 2017), flucloxacillin and amoxicillin (Yaseen et al. 2015) among others.

In the case of abacavir, the generation of drug specific T-cell clones has been widely demonstrated (Chessman *et al.*, 2008; Bell *et al.*, 2013; Adam *et al.*, 2014; Naisbitt *et al.*, 2015). All responsive clones generated to abacavir identify as CD8^{+} accounting for the Th1 response commonly observed, which are characterised by the secretion of the proinflammatory cytokines such as IFN-γ. Utilisation of studies with T-cell clones allows for the quick and concise analysis of T-cell characteristics including phenotype, cytokine secretion and mechanistic studies such as the ability to be activated by abacavir in the presence and absence of antigen presenting cells.

Abacavir is hypothesised to interact with HLA-B*57:01 by way of non-covalent binding. Abacavir can bind directly to MHC peptide complexes to activate T-cells via a PI mechanism (Adam *et al.*, 2012; Bell *et al.*, 2013). However, abacavir also induces a change in the shape and chemistry of the peptide binding groove, namely in the F-pocket region. Such change results in the accommodation of altered self-peptides, with a new repertoire carrying smaller chain anchors at the C-terminal region for presentation to T-cells. These abacavir induced self-peptides are perceived as foreign by T-cells, presumably also resulting in a CD8^{+} mediated immune response (Illing et al. 2012; Norcross et al. 2012; Ostrov et al. 2012).

In this chapter, we explore the ability to generate abacavir-responsive T-cells from a panel of healthy, drug naïve donor's positive for HLA-B*57:01. Some of the generated T-cell clones were then further analysed for cellular phenotype and mechanistic studies to examine the reactivity of the clones along with underlying mechanism of activation by abacavir.

2.2 Aims

The aim of this chapter is to generate abacavir-specific T-cell clones from healthy drug-naïve donors positive for the HLA-B*57:01 risk allele. These generated clones will be subjected to further functional analysis for their cellular phenotype, mechanisms of T-cell activation and cytokines secretion properties.

2.3 Methods

2.3.1 Materials

Abacavir was received as a gift from GlaxoSmithKline (GSK). Human AB serum and foetal bovine serum were obtained from Innovative Research Class A (Michigan, USA) and Invitrogen (Paisley, UK) respectively. Interleukin-2 (IL-2) was purchased from Peprotech (London, UK). Multisort bead separation kits were supplied by Miltenyi Biotec (Surrey, UK). Antibodies for staining were purchased from BD Biosciences (Oxford, UK). ELIspot kits including the coating and detection antibodies, strepdavidan alkaline phosphate conjugate and BCIP/NBT substrates were purchased from Mabtech (Stockholm, Sweden). Other reagents were purchased from Sigma-Aldrich (Dorset-UK) unless otherwise stated.

2.3.2 Cell culture medium

Cell culture medium for T-cells (R9) is composed of RPMI supplemented with 10% human AB serum, HEPES (25mM), penicillin (1000 U/mL), streptomycin (0.1mg/mL), L-glutamine (2mM) and transferrin (25μg/mL).

EBV transformed B-cells were cultured in F1 medium composed of RPMI supplemented with 10% foetal bovine serum, HEPES (25mM), penicillin (1000 U/mL), streptomycin (0.1mg/mL) and L-glutamine (2mM).

2.3.3. Isolation of peripheral blood mononuclear cells (PBMCs)

PBMCs were isolated from blood collected in heparinised vacuette 9mL tubes. The blood (25mL) was slowly layered on top of 25mL of lymphoprep and centrifuged at 2000 rpm at 25°C with acceleration set to 4 and the brake set to 0. The buffy coat layer was transferred to a fresh 50mL tube using a Pasteur pipette. The PBMCs were washed a further two times

using HBSS to remove any remaining lymphoprep solution and the pellet was resuspended in 30mL of R9 medium.

The PBMC suspension (10µL) was diluted in an equal volume of trypan blue and cells were counted using a Neubauer haemocytometer under a Leica DME microscope (Leica Microsystems, Milton Keynes). Cell viability was measured by trypan blue exclusion and the percentage viability of the cells was assessed as follows: percentage viability = viable number of cells/ total number of cells x 100.
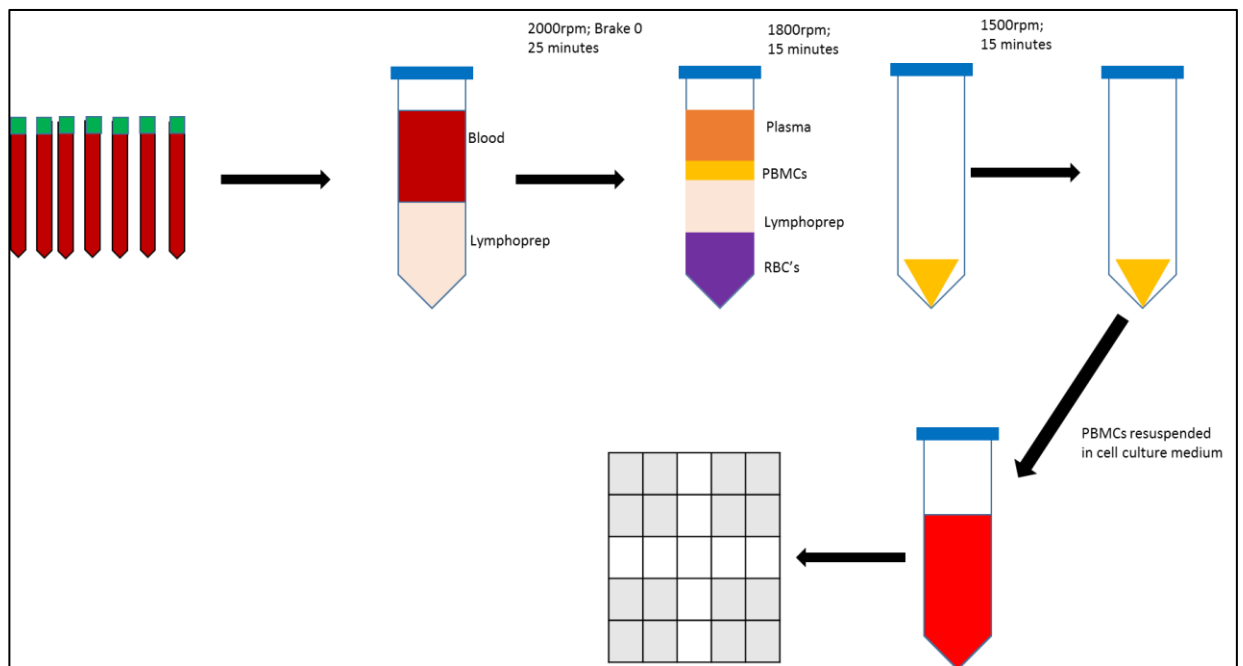
Figure 2.1 Isolation of PBMCs from whole blood patient samples via density centrifugation.

2.3.4 EBV generation

Epstein-Barr virus transformed B-cell lines (EBVs) were produced from the PBMCs of cohort donors. Virus producing B95.8 cells were centrifuged at 1500 rpm for 10 minutes and 9mL of the supernatant was aspirated and filtered over donor PBMCs ($5x10^6$). Cyclosporin A (CSA) (1µg/mL) was added and cells were incubated overnight (37^OC; 5% CO_2). Cells were then centrifuged and resuspended in F1 medium + CSA and transferred to a 24 well plate to a maximum of 2mL. These were incubated for 3 weeks being fed with F1 medium + CSA (1µg/mL) twice a week to prevent growth of non-immortalised EBV infected B-cells. Once sufficient growth of EBVs had taken place, cells were transferred to a 25mL flask and fed twice a week with F1 media alone. These cells were used as a ready supply of immortalised autologous antigen presenting cells.

2.3.5 Generation of abacavir-responsive T-cells.

HLA-B*57:01 positive donors were selected from our cell cohort containing PBMCs from 1200 genotyped healthy donors. The cohort derives largely from the Liverpool student population; thus it is extremely unlikely that any donor has been exposed to abacavir. Ethical approval for the study was obtained from the local research ethics committee and each donor underwent a consenting process prior to blood donation. For studies in this thesis, a total of five donors were utilized. Donors 1-4 were used for the generations of abacavir-specific T-cell clones, while donor 5 was used for the naïve T-cell priming assay, described in chapter 4. PBMCs from each donor were incubated in the presence of abacavir (35µM) in R9 medium for a period of 14 days. On days 6 and 9 cells were fed with R9 medium containing IL-2 to preserve the abacavir driven expansion of T-cells. On day 14, CD8$^+$ T-cells were positively selected using MultiSort kits (Miltenyi Biotec, Surrey UK) and T-cell clones were generated via means of serial dilution.

CD8^{+} T-cells were seeded at a concentration of 0.3/1/3 cells/ well (96 well U-bottomed plate) and stimulated with allogenic PBMC feeder cells (5x10^{4}/well) and the mitogen phytohaemagglutin (PHA; 5µg/mL) in R9 medium containing IL-2 (2µL/mL). Cells were fed every 2 days with R9 medium containing IL-2 (2µL/mL) and well growing clones were transferred to a new 96 well plate and expanded across 4 wells. On day 14 clones were restimulated and further expanded for a further 28 days.

Donor	Donor ID	HLA-A	HLA-B	HLA-C	HLA-DRB1	HLA-DRBQ1
1	0617	A*01:01:01G A*32:01:01G	B*57:01:01G B*57:01:01G	C*06:02:01G C*06:02:01G	DRB1*07:01:01G DRB1*07:01:01G	DQB1*03:03:02G DQB1*03:03:02G
2	0957	A*02:01:01G A*11:01:01G	B*07:05:01G B*57:01:01G	C*06:27 C*07:02:01G	DRB1*15:01:01G DRB1*15:02:01	DQB1*06:01:01G DQB1*06:01:01G
3	0158	A*01:01:01 A*01:01:01	B*07:TDVB B*57:01:01G	C*06:DDAR C*07:02	DRB1*01:01:01 DRB1*15:01:01	DQB1*05:01:01 DQB1*06:02:01
4	0622	A*02:01:01G A*03:01:01G	B*44:02:01G B*57:01:01G	C*05:01:01G C*06:02:01G	DRB1*04:01:01 DRB1*07:01:01G	DQB1*03:01:01G DQB1*03:03:02G
5	021	A*02:01:01G A*11:01:01G	B*07:EH B*57:01:01G	C*06:27 C*07:02	DRB1*15:01:01 DRB1*15:02:01	DQB1*06:01 DQB1*06:01

Table 2.1. HLA-allele typing of five healthy drug naïve donors. Yellow denotes positive expression of the HLA-B*57:01 risk allele for hypersensitivity reactions to abacavir.

2.3.6. Testing clones for antigen specificity

Approximately four weeks after beginning the serial dilutions abacavir-specificity was measured by assessing cell proliferation in the presence of the drug. Abacavir induced proliferation was measured by culturing T-cell clones (5x10^{4}/50µL) with irradiated autologous EBVs (1x10^{4}/50µL) in the presence and absence of an optimal concentration of abacavir (35µM). Following 48-hour incubation, tritiated thymidine (0.5µCi) was added and proliferation was assessed 16 hours later via scintillation counting. The proliferative response of T-cell clones is expressed as counts per minute (cpm). A stimulation index is obtained by dividing the average cpm of the drug treated wells by the average of the control wells. T-cell

clones with a proliferative stimulation index of 2 or greater were picked and expanded by mitogen restimulation in cell culture media containing irradiated allogenic PBMCs ($5x10^5$ cells/well), IL-2 (5µL/mL) and PHA (10µg/mL) for further analysis.

2.3.7. Confirmation of antigen specificity via ELIspot Assay

ELIspot plates were activated with 15µL of 35% EtOH and washed 5 times with dH_2O. The plates were then coated with 100µL/well of interferon gamma capture (IFN-γ) antibody (15µg/mL) and incubated overnight at 4^OC. The following day, wells were washed 5 times with sterile PBS and then blocked with 250µL of R9 medium at room temperature for a period of 30 minutes to prevent non-specific binding. Drug specific T-cell clones ($5x10^4$/50µL) were added to each well along with autologous EBVs ($1x10^4$/ 50µL). Cells were then cultured in the presence or absence of abacavir (35µM, 100µL) for a period of 48 hours at 37^OC; 5% CO_2. Following a 48 hour incubation period, cells were discarded and the plates were washed 5 times with 250µL PBS. Biotin labelled detection antibody was diluted 1µg/mL in PBS containing 0.5% FBS and 100µL/well was added to the plate, which was then incubated for 2 hours at room temperature. Following this incubaton period the detection antibody was discarded and the plate washed with PBS (250µL/well). Streptavidin-ALP diluted to 1µg/mL in PBS containing 0.5% FBS was added to the plate at 100µL/well and the plate was incubated at room temperature for 1 hour. Next, wells were again washed with PBS and 100 µL of filtered BCIP/NBT substrate was added to each well for a period of 20 minutes in the dark at room temperature. Wells were then washed under running cold water to stop the reaction and the plate was left to dry overnight then counted using an AID ELIspot reader (Cadama Medical, Stourbridge, UK).

2.3.8. CD4/CD8 cellular phenotyping via flow cytometry

Flow cytometry was used to investigate the cell surface phenotype and function of T-cell clones. This was primarily used to assess if T-cells expressed CD4 or CD8 markers. T-cells (50µL) were transferred to a FACs tube and 1.5µL of CD4 (FITC) and CD8 (PE) antibody was added to each tube and incubated at 4^OC for 20 minutes in the dark. Following incubation, 500µL of FACs buffer was added to each tube and cells were centrifuged at 1500rpm, 4^OC for a period of 5 minutes. Supernatant was then discarded and cells were resuspended in 200µL FACs buffer. Phenotyping on clones was performed using BD FACSCanto II flow cytometer (CD4-FITC) and (CD8-PE).

2.3.9. Dose and antigen presenting cell dependency of abacavir-specific CD8$^+$ T-cell clones.

The dependence on antigen presenting cells for activation of abacavir-specific CD8$^+$ T-cell clones was analysed by conducting dose response assays to abacavir in the presence and absence of autologous EBVs. Abacavir-specific CD8$^+$ T-cell clones were incubated in the presence of abacavir at concentrations of 0-35µM in the presence and absence of autologous APCs for a period of 48 hours (37^OC; 5% CO_2). Activation of T-cells was quantified using the IFN-γ ELIspot assay.

2.3.10 Abacavir Pulsing of APCs

Autologous EBVs (functioning as APCs) were pulsed with abacavir (35µM) (37^OC; 5% CO_2) for a period of 1, 4 and 16 hours to assess processing dependency and kinetics. Following incubation, EBVs were washed three times in R9 medium. The cells were then irradiated and cultured with T-cell clones ($5x10^4$/ 50µL). No further drug was added and T-cell responses were measured using IFN-γ ELIspot as described in section 2.3.7. Soluble abacavir (35µM) was used as a positive control.

2.3.11 Analysis of cytokine secretion from abacavir-specific CD8^{+} T-cell clones.

The cytokine secretive profiles of abacavir clones was assessed using the ELIspot assay for various cytokines including; IFN-γ, IL-5, IL-10, IL-13, IL-17, IL-22 and effector molecules granzyme B, perforin and FasL. T-cell clones were incubated ($5x10^4$/ 50µL) with autologous APCs ($1x10^4$/ 50µL) in the presence and absence of abacavir (35µM). Cytokine secretion was measured using the respective detection antibodies according to the manufacturer's instructions and plates were counted using AID-ELIspot reader.

2.3.12. TCRV$_\beta$ analysis of T-cell responsive clones.

TCR V$_\beta$ expression analysis of individual T-cell clones was conducted using IOTest® beta mark (Beckman Coulter, Indianapolis, USA). This test allows for the multi-parametic analysis of TCR V$_\beta$ expression in human T-cells via the use of FITC and PE conjugated antibodies. . Each antibody was capable of detecting three individual TCR V$_\beta$ (FITC, PE, FITC/PE), meaning the TCR V$_\beta$ detection kit could detect a total of twenty four TCRs. A total of eight tubes was required per clone tested. Cellular suspension (50µL) was transferred to each tube and TCR V$_\beta$ antibodies (A-H) (5µL) were added individually to the respective eight tubes. Cells were incubated in the presence of the antibodies for 20 minutes in the dark at room temperature. Next, cells were washed and resuspended in 200µL of FACs buffer before being analysed using BD FACSCanto II flow cytometer.

2.3.13 Statistical analysis.

For comparison between control and test values in proliferation assays the Mann-Whitney test was used.

2.4. Results

2.4.1 Generation of abacavir-specific T-cell clones

From a total of 2279 clones tested across the four donors utilized (donors 1-4), 101 were found to proliferate in the presence of abacavir yielding a stimulation index (SI) value of 2 or greater. A varied number of responsive clones was found across the four donors in this study with the percentage of responsive clones ranging from as low as 0.4% in donor 2 to 12.5% in donor 4 (Table 2.2). Figures 2.2-2.4 show the proliferative response in all clones incubated in the presence of abacavir across the four donors.
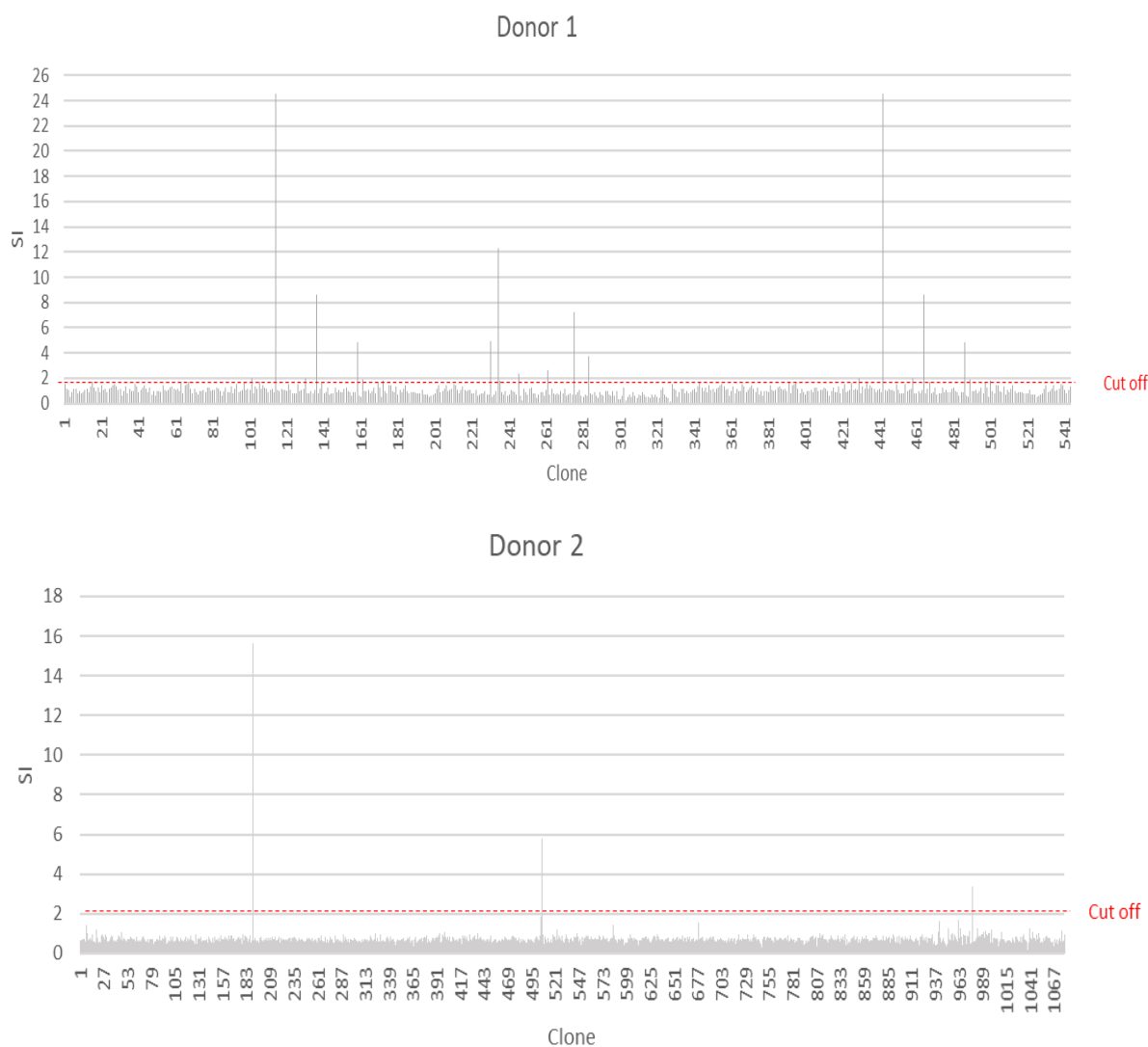
Figure 2.2. Antigen specificity of T-cell clones to abacavir (Donor 1, HLA-0617 and Donor 2, HLA-0957, both genotyped as HLA-B*57:01 positive. T-cell clones (5×10^4/50µL) were co-incubated with autologous APCs (1×10^4/50µL) in the presence and absence of abacavir (35µM) in a U-bottomed 96 well microplate. Cells were incubated for 48h (37°C; 5% CO_2). Tritiated thymidine was then added for an additional 16h incubation. T-cell proliferation was assessed using scintillation counting. Clones with a stimulation index (SI) of 2 or greater were considered positive and were expanded for further study.

84
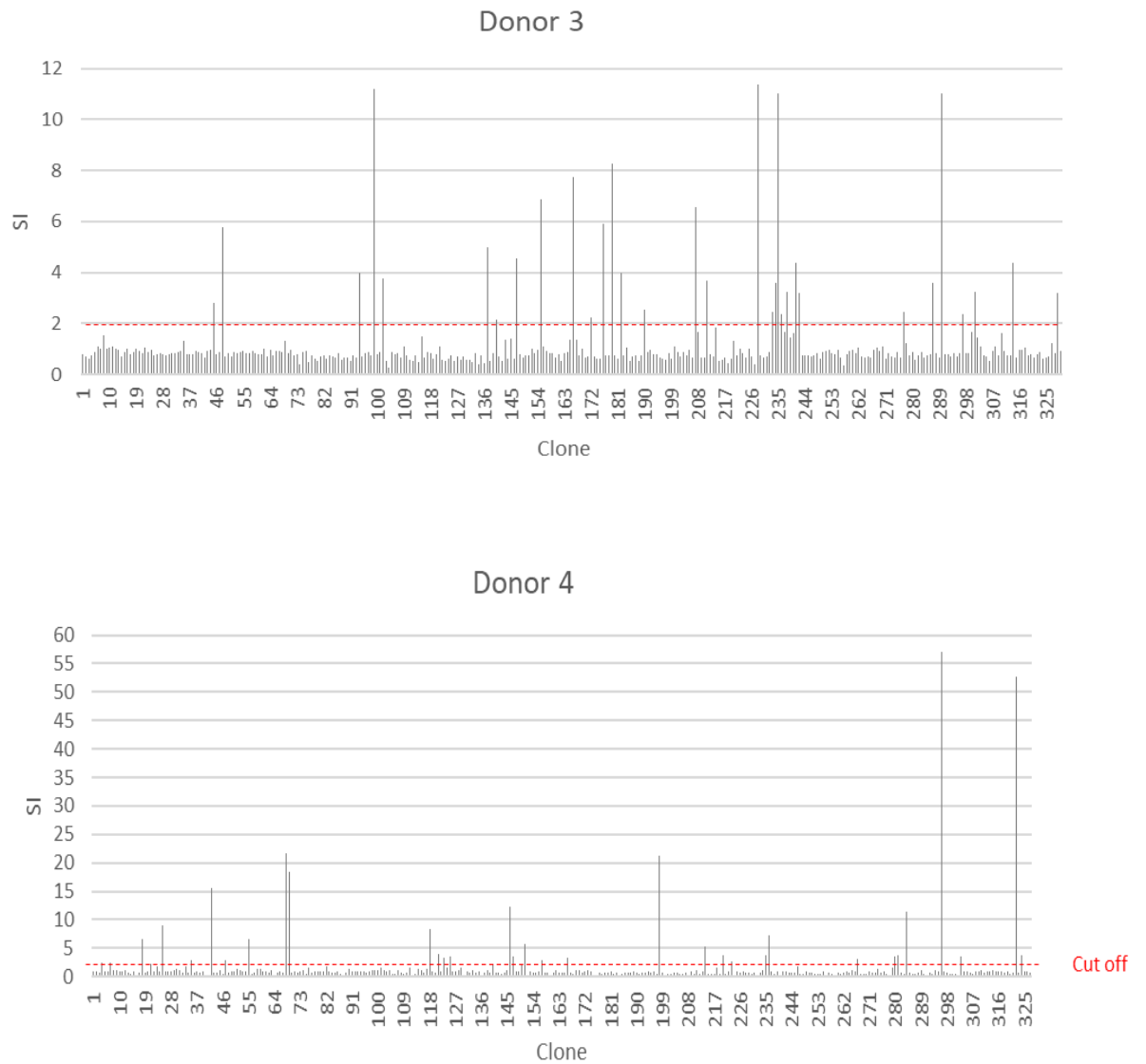
Donor 3

Donor 4

Figure 2.3. Antigen specificity of T-cell clones to abacavir (Donor 3, HVN-158 and Donor 4, HLA-0622, both genotyped as HLA-B*57:01 positive. T-cell clones (5×10^4/50µL) were co-incubated with autologous APCs (1×10^4/ 50µL) in the presence and absence of abacavir (35µM) in a U-bottomed 96 well microplate. Cells were incubated for 48h (37°C; 5% CO_2). Tritiated thymidine was then added for an additional 16h incubation. T-cell proliferation was assessed using scintillation counting. Clones with a stimulation index (SI) of 2 or greater were considered positive and were expanded for further study.

Donor	Donor 1	Donor 2	Donor 3	Donor 4	Total
Clones Tested	544	1078	320	327	2279
Responsive on initial test	26	4	30	41	101
Percentage of responsive	4.8%	0.4%	9.4%	12.5%	4.47%

Table 2.2. Responsive clones generated from four HLA-B*57:01 positive donors.
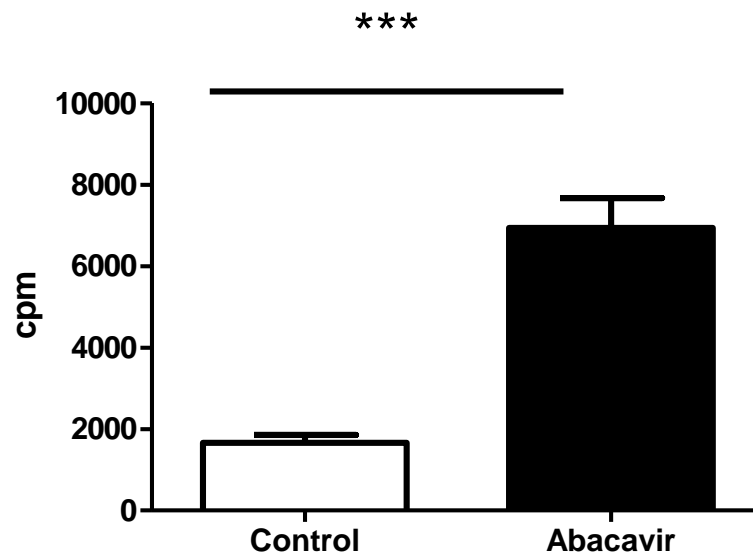
Figure 2.4. T-cell response of abacavir-specific clones. Average proliferative response of T-cell clones incubated from four HLA-B*57:01 donors with abacavir (35µM). Cell culture media (Control) was used as a negative control. Data shown as mean of all responsive clones vs control ± SEM. * *P<0.05*, ** *P<0.01*, *** *P<0.001*.

2.4.2 Confirmation of antigen specificity of abacavir-specific T-cell clones

Clones which generated a proliferative response corresponding to an SI of 2 or greater were subjected to mitogen driven expansion for a period of 2 weeks to allow for cellular growth. Following this restimulation period clones were further tested to confirm their antigen specificity to abacavir. Due to its enhanced sensitivity over the proliferation assay for CD8$^+$ T-cell clones, the secretion of IFN-γ was used as a readout for this stage by utilisation of the ELIspot assay as described in section 2.3.7. Following incubation of abacavir with clones and EBVs for 48 hours, the ELIspot plate was developed via the separate additions of detection antibody and streptavidin conjugate followed by BCIP/NBT substrate. The precipitation of the substrate manifests as spots at the sites of IFN-γ secretion, allowing for the quantification of T-cell activity. Lack of observed IFN-γ secretion in a particular T-cell clone at the second test indicates a false positive result was obtained at the proliferation readout stage or that the clone has lost antigen specificity to abacavir. All clones failing to produce a cytokine secretive response were subsequently destroyed. From the 101 clones obtained to abacavir at the first testing stage, 52 displayed distinct IFN-γ secretion in the presence of abacavir at the 2nd testing stage. Figures 2.5-2.8 show the IFN-γ secretion from abacavir T-cell clones incubated in the presence and absence of the drug. All responsive T-cell clones were maintained in cell culture and used for further experiments.
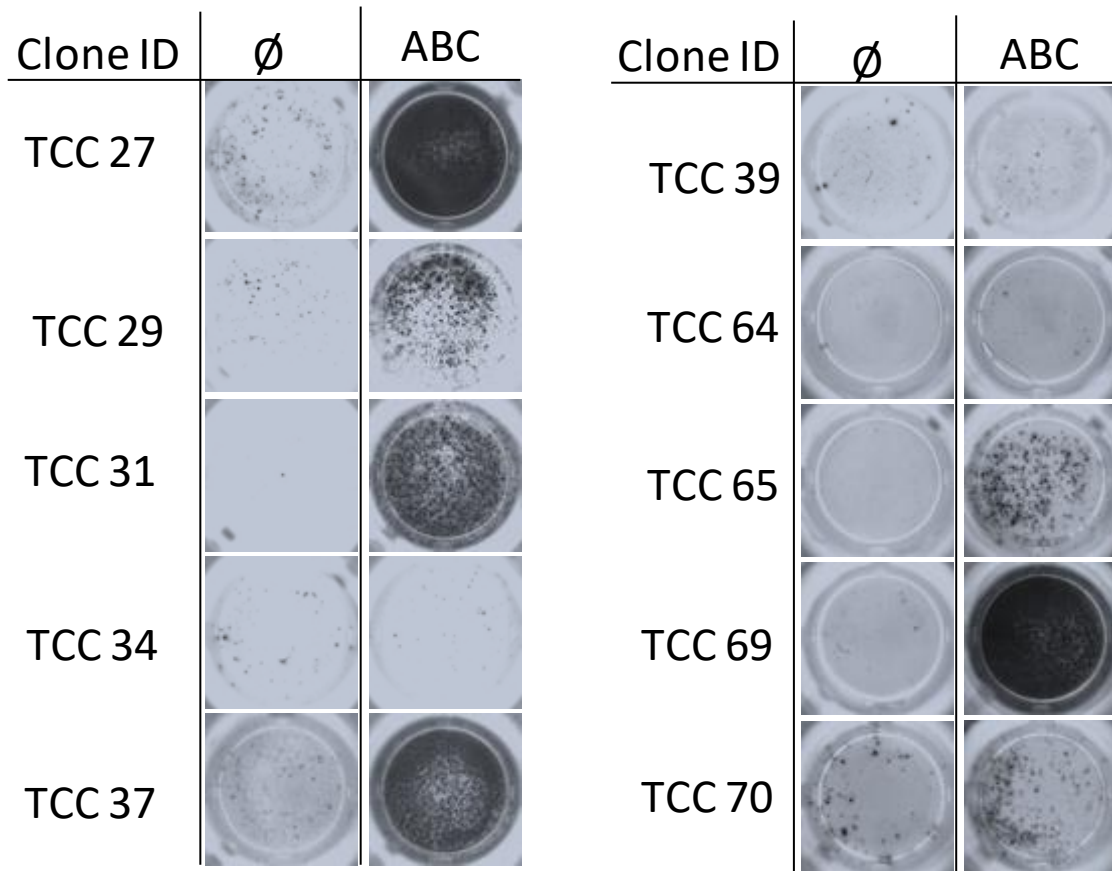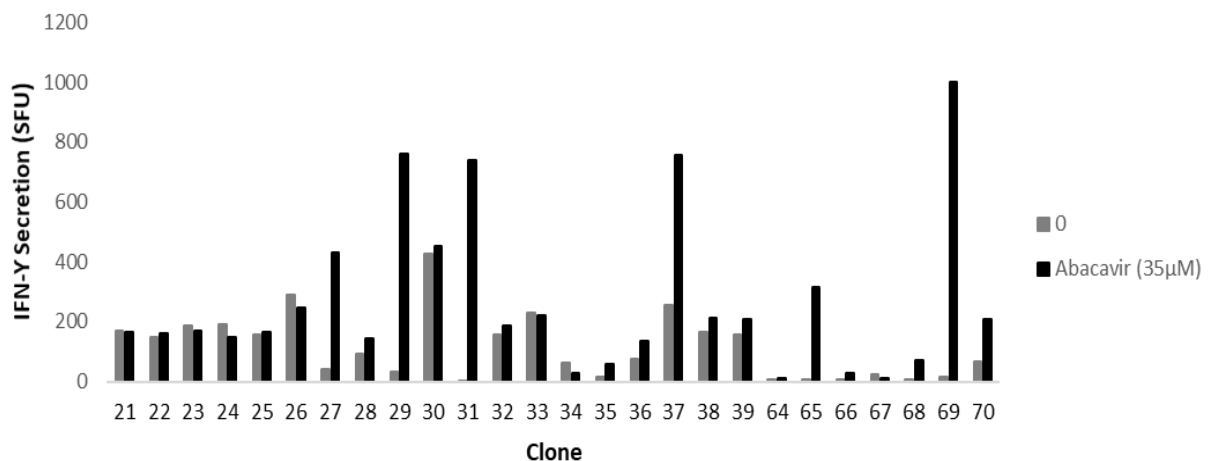
Figure 2.5. Confirmation of antigen specificity of T-cell clones from Donor 1 (HLA-0617). a) ELIspot well images from a panel of representative clones tested for secretion of IFN-Y. b) Secretion of IFN-γ from all T-cell clones to Donor 1. Grey bars denote cells incubated with R9 medium and black bars denote cells incubated with abacavir for 48h. ELIspot plates were coated with human IFN-γ antibody and incubated at 4°C overnight. T-cell clones (5×10^{4}/50μL) were co-incubated with APCs (1×10^{4}/50μL) in the presence and absence of abacavir (35μM) for 48h (37°C; 5% CO_2). The ELIspot plate was then developed according to the manufactures protocol and counted using ELIspot AID reader.
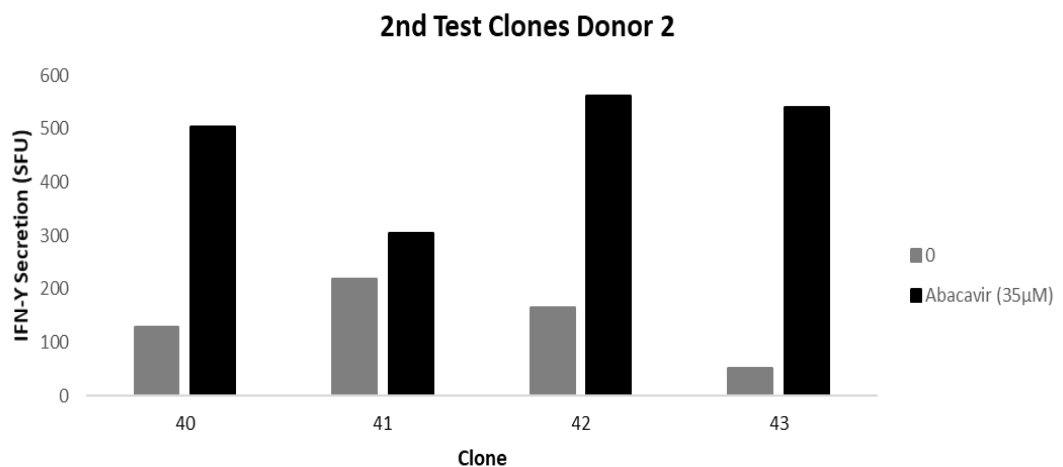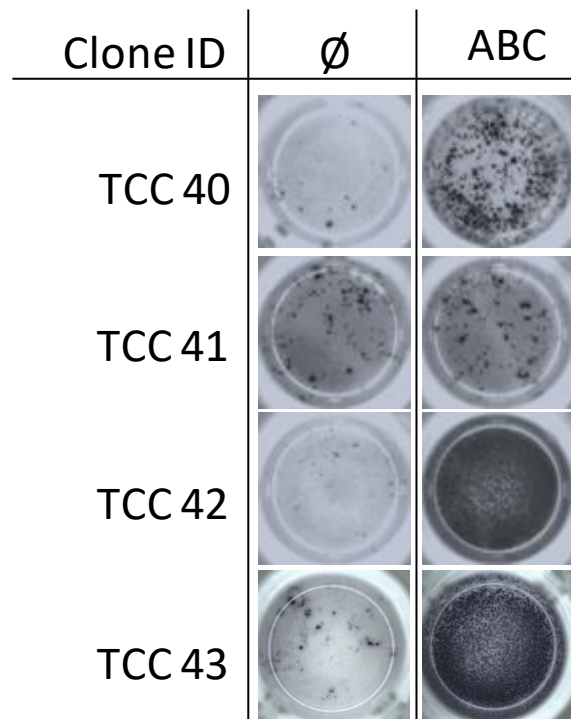
Figure 2.6. Confirmation of antigen specificity of T-cell clones from Donor 2 (HLA-0957). a) ELIspot well images from a panel of representative clones tested for secretion of IFN-γ. b) Secretion of IFN-γ from all T-cell clones to Donor 2. Grey bars denote cells incubated with R9 medium and black bars denote cells incubated with abacavir for 48h. ELIspot plates were coated with human IFN-γ antibody and incubated at 4°C overnight. T-cell clones (5×10^{4}/50μL) were co-incubated with APCs (1×10^{4}/50μL) in the presence and absence of abacavir (35μM) for 48h (37°C; 5% CO_2). The ELIspot plate was then developed according to the manufacturers protocol and counted using ELIspot AID reader.

2nd Test Donor 3
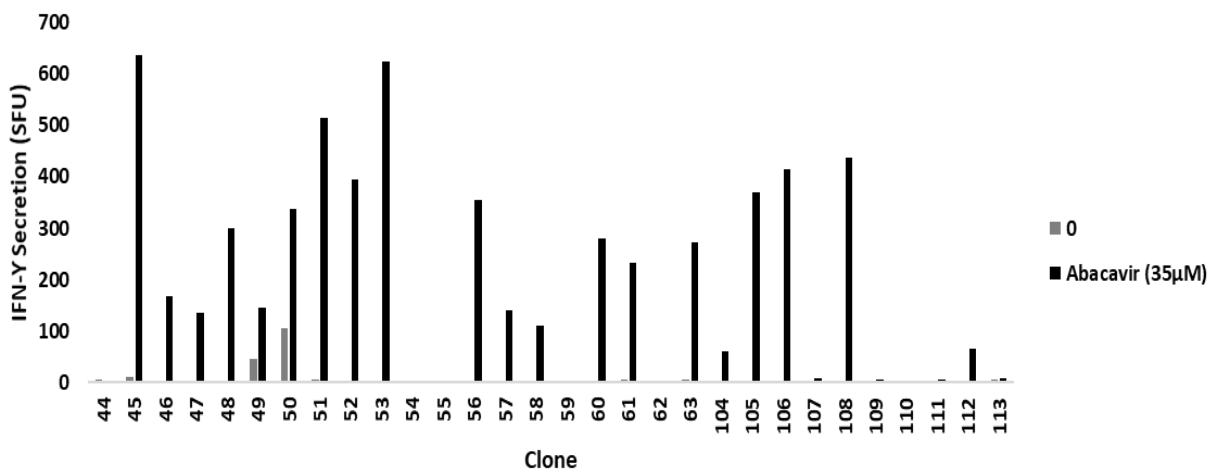
Figure 2.7. Confirmation of antigen specificity of T-cell clones from Donor 3 (HVN-158). a) ELIspot well images from a panel of representative clones tested for secretion of IFN-γ. b) Secretion of IFN-γ from all T-cell clones to Donor 3. Grey bars denote cells incubated with R9 medium and black bars denote cells incubated with abacavir for 48h. ELIspot plates were coated with human IFN-γ antibody and incubated at 4°C overnight. T-cell clones ($5x10^{4}$/ 50μL) were co-incubated with APCs ($1x10^{4}$/ 50μL) in the presence and absence of abacavir (35μM) for 48h (37°C; 5% CO_2). The ELIspot plate was then developed according to the manufacturers protocol and counted using ELIspot AID reader.

Clone ID	Ø	ABC	Clone ID	Ø	ABC
TCC 71			TCC 92		
TCC 73			TCC 97		
TCC 79			TCC 99		
TCC 81			TCC 119		
TCC 86			TCC 121		

2nd Test Donor 4

Figure 2.8. Confirmation of antigen specificity of T-cell clones from Donor 4 (HLA-0622). a) ELIspot well images from a panel of representative clones tested for secretion of IFN-γ. b) Secretion of IFN-γ from all T-cell clones to Donor 4. Grey bars denote cells incubated with R9 medium and black bars denote cells incubated with abacavir for 48h. ELIspot plates were coated with human IFN-γ antibody and incubated at 4°C overnight. T-cell clones ($5x10^{4}$/50µL) were co-incubated with APCs ($1x10^{4}$/50µL) in the presence and absence of abacavir (35µM) for 48h (37°C; 5% CO_2). The ELIspot plate was then developed according to the manufacturers protocol and counted using ELIspot AID reader.

2.4.3 T-cell phenotyping

Abacavir-responsive T-cell clones were analysed for surface receptor expression of CD4 and CD8. T-cell clones (50µL) were co-incubated with CD4-FITC and CD8-PE antibodies then analysed via flow cytometry using BD FACSCanto II flow cytometer. All abacavir-responsive T-cell clones generated from the four HLA-B*57:01 positive donors were phenotyped as CD8 (Figure 2.9 shows the representative analysis for donor 1 CD4/CD8 phenotyping).
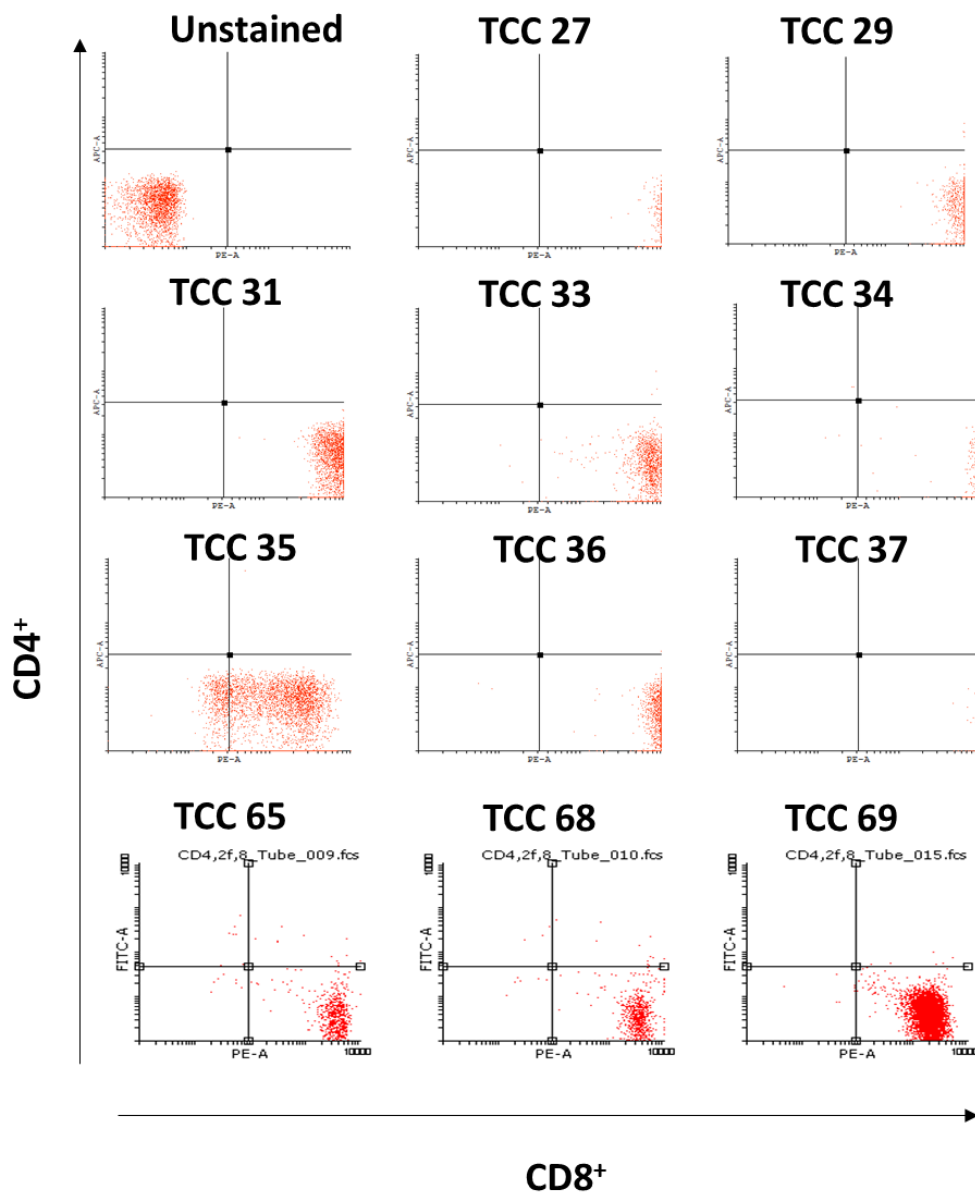
Figure 2.9. Cell phenotyping for expression of CD4 and CD8 on the surface of abacavir-specific T-cell clones. Cells (50µL) were stained with antibodies CD4-FITC and CD8-PE and incubated for 20 minutes at 4°C. Cells were then washed and flow cytometry used to analyse cellular phenotype (BD FACSCANTO II)

2.4.4 Dose-and antigen presenting cell-dependency for activation of abacavir-specific CD8+ T-cell clones

The activation of abacavir-specific CD8+ T-cell clones was assessed in the presence and absence of APCs using IFN-γ secretion as a primary readout. A total of nine abacavir clones from the HLA-B*57:01 positive donors were selected and tested at concentrations of abacavir ranging up to 35μM. Cytokine secretion was observed in abacavir-specific T-cell clones in both the presence and absence of APCs. The T-cell activation of nine representative abacavir clones tested is shown in Figures 2.10-2.12. It was observed that in the case of some clones (TCC 27) minimal difference exists in T-cell activation between clones incubated in the presence of APCs and those incubated without APCs. In most of the clones tested, despite T-cell activation occurring in the absence of APCs there is an enhanced activation observed in the presence of APCs. Some T-cell clones demonstrated no activation at all when incubated with abacavir in the absence of APCs (TCC 40 and 41) indicating the reliance on antigen processing and presentation for T-cell activation. It can also be observed that for most abacavir clones which are activated in the absence of APCs that as the concentration of the drug decreases the requirement of APCs for T-cell activation becomes apparent i.e. TCC 42 ceases to respond in the absence of APCs at 0.9μM and TCC 63 at 1.25μM.
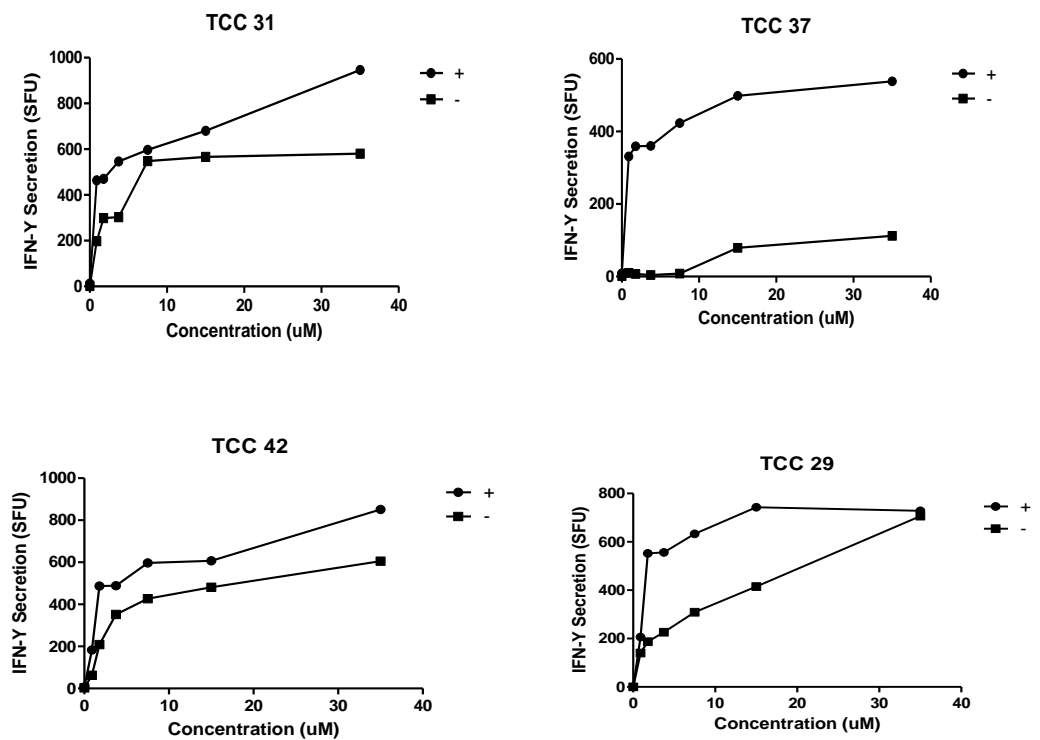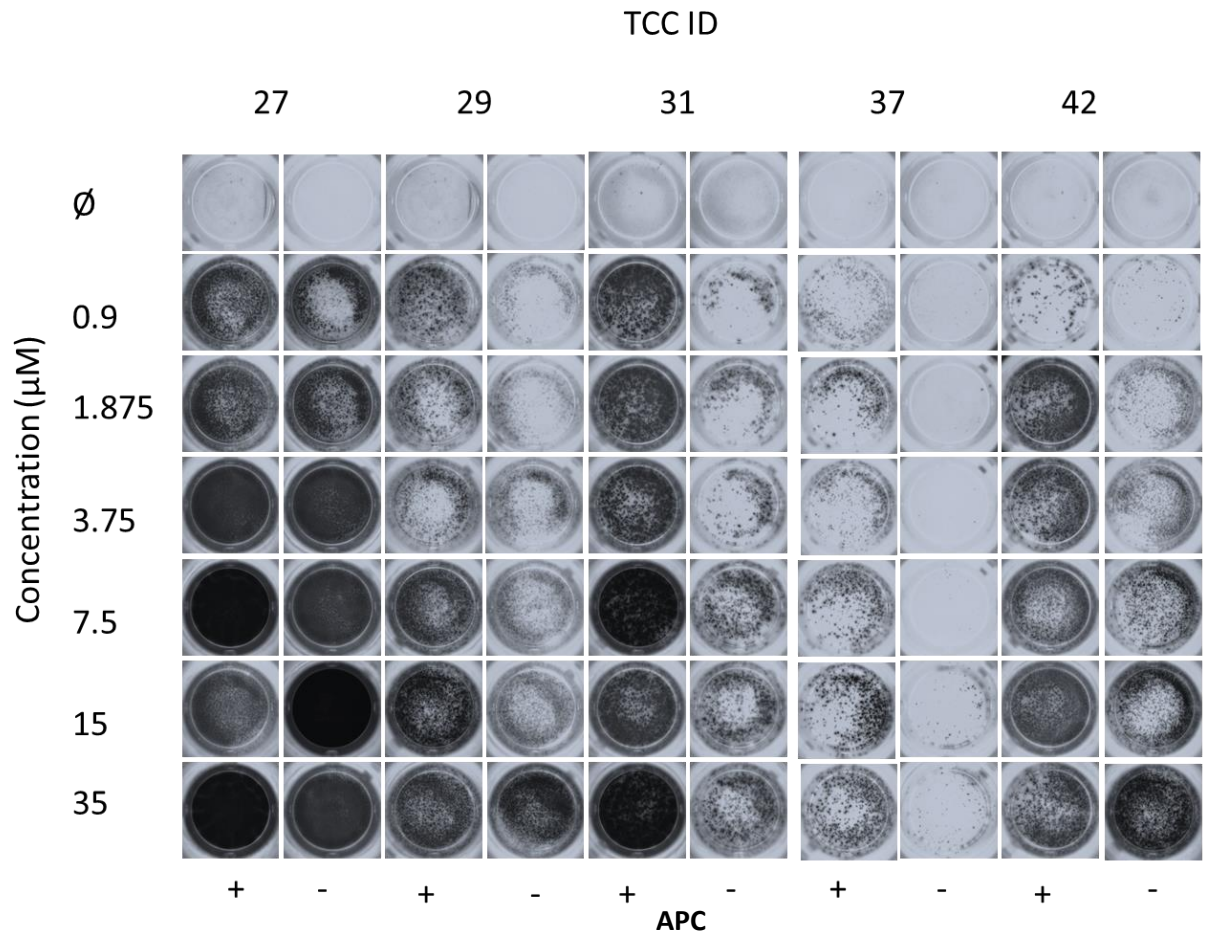
Figure 2.10. Dose-and antigen-presenting cell dependency of abacavir responsive T-cell clones. T-cell clones were incubated +/- autologous APCs in the presence of abacavir (ABC 0-35µM) for 48 hours (37°C; 5% CO_2). ELIspot plates were developed following manufacturer's instructions and plates were read using AID ELIspot reader.
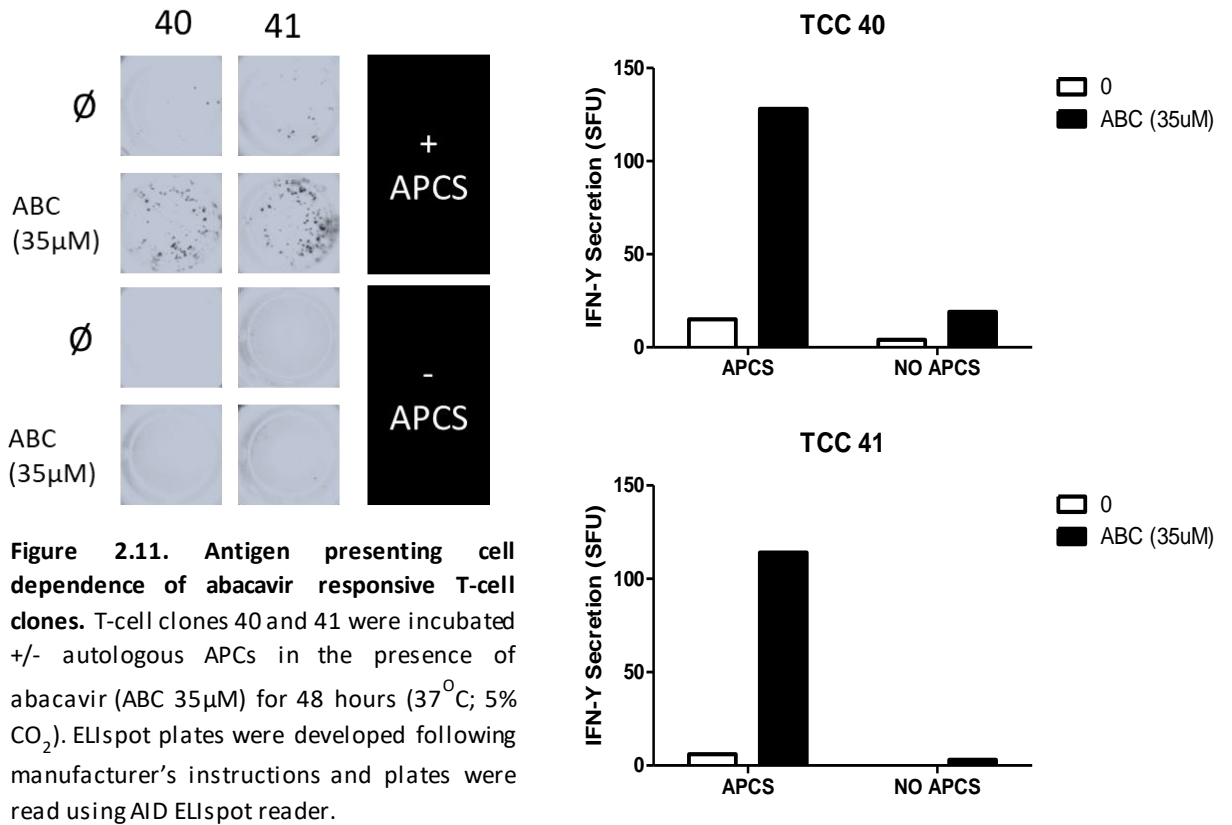
Figure 2.11. Antigen presenting cell dependence of abacavir responsive T-cell clones. T-cell clones 40 and 41 were incubated +/- autologous APCs in the presence of abacavir (ABC 35μM) for 48 hours (37°C; 5% CO_2). ELISpot plates were developed following manufacturer's instructions and plates were read using AID ELISpot reader.
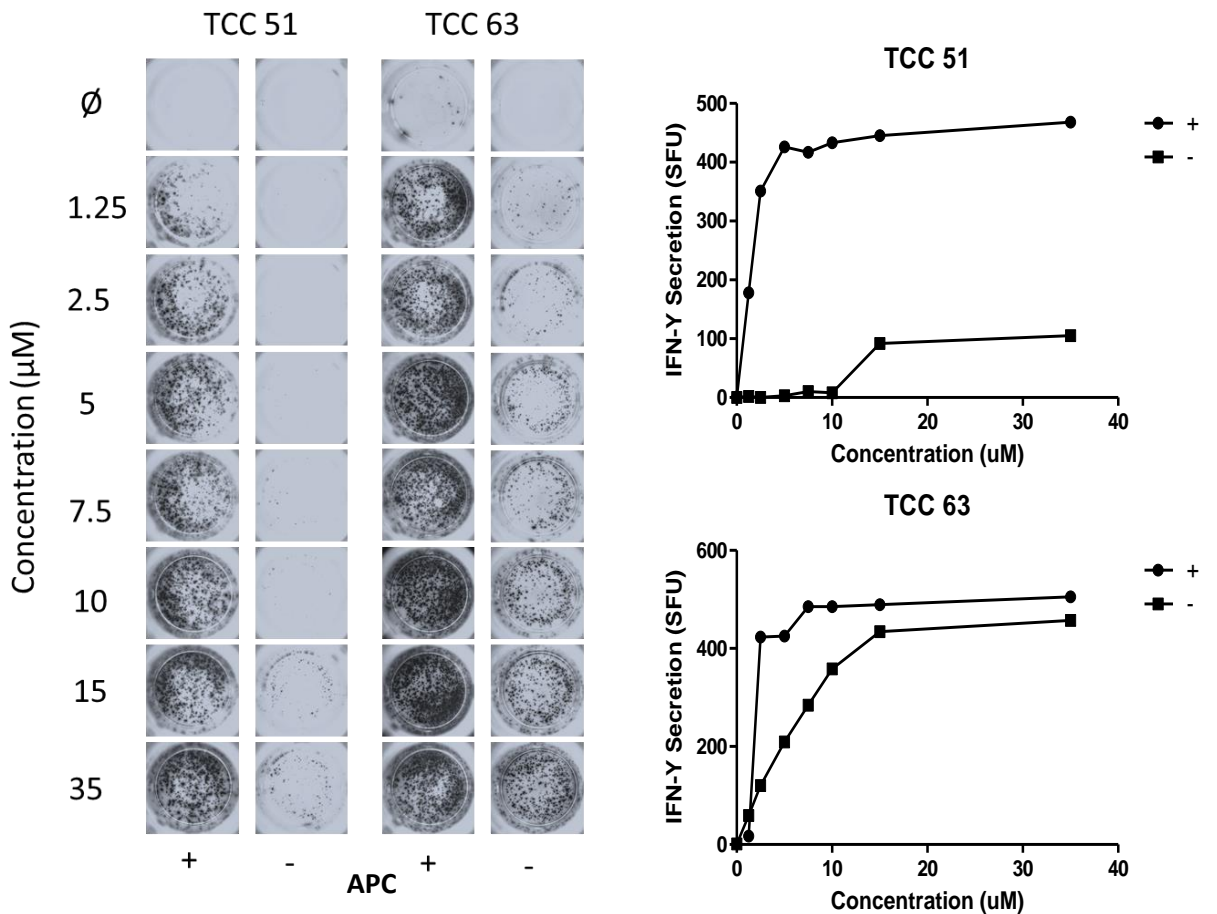
Figure 2.12. Antigen presenting cell dependence of abacavir responsive T-cell clones. T-cell clones 51 and 63 were incubated +/- autologous APCs in the presence of abacavir (ABC 0-35μM) for 48 hours (37°C; 5% CO_2). ELISpot plates were developed following manufacturer's instructions and plates were read using AID ELISpot reader.

2.4.5 Activation of abacavir-specific clones with drug pulsed antigen presenting cells.

Ten representative abacavir-specific T-cell clones were used to ascertain the principal pathway of T-cell activation employed by the clones. Autologous APCs were incubated with abacavir (35µM) for periods of 1 hour, 4 hours and 16 hours. Following incubation, the cells were washed three times and irradiated prior to co-incubation with T-cell clones (5×10^4/ 50µL). The T-cell response was measured by IFN-γ secretion using the ELIspot assay. T-cell clones incubated with autologous APCs in the presence of soluble abacavir (35µM) were used as a positive control.

All clones produced strong IFN-γ secretion in the presence of soluble abacavir at the optimal concentration of 35µM. With exception of clone 121, all abacavir-specific T-cell clones produced a response to drug pulsed APCs for a time period of 16 hours. Clones which evoked T-cell activation to the pulsed APCs are presumed to interact via the altered peptide repertoire mechanism while those which were pulse negative interact via the PI mechanism. However, many clones produced T-cell activation to APCs pulsed for the shorter time periods of 4 hours and 1 hour. This indicates the likely employment of both the altered peptide and PI mechanism as these time points are not sufficient for the antigen processing to take place fully, thereby suggesting direct interaction with surface MHC peptide complexes.

a)

b)

Figure 2.13. Activation of abacavir-specific T-cell clones with pulsed APCs. a) Representative well images from ELIspot of T-cell clones incubated with APCs pulsed for 1h, 4h or 16h in the presence and absence of abacavir (35µM). b) Graphs displaying IFN-γ secretion from four of the ten representative clones pulsed for 1h, 4h and 16h. Ten representative abacavir responsive CD8^{+} T-cell clones from three HLA-B*57:01 donors were used. Autologous APCs were pulsed with abacavir (35µM) overnight (37[O]C; 5% CO_2). The following day cells were washed three times to remove unbound drug and T-cell clones (5x10^{4}/50µL) were co-incubated with irradiated autologous APCs (1x10^{4}/50µL). The T-cell response was measured via IFN-γ secretion. APCs pulsed with R9 medium alone (mock pulsed) were used as a negative control and soluble abacavir (35µM) was used as a positive control.

2.4.6 Cytokine secretion panel of CD8+ abacavir-responsive T-cell clones

The cytokine secretion profiles of abacavir-specific clones was assessed using ELIspot assay for various cytokines including; IFN-Y, IL-5, IL-10, IL-13, IL-17, IL-22 and the effector molecules granzyme B, perforin and FasL. Six abacavir clones were selected and incubated ($5x10^4$/ 50μL) with autologous APCs ($1x10^4$/ 50μL) in the presence of abacavir (35μM). Cytokine secretion was measured using the respective detection antibodies according to the manufacturer's instructions.

Figure 2.14 shows the cytokine secretion profiles from the six abacavir-specific clones. Secretion of proinflammatory cytokines IFN-γ and IL-13 was observed across all six of the clones tested along with granzyme B. Secretion of IL-5 was observed in low levels in one of the clones. No secretion of the anti-inflammatory cytokine IL-10 was observed in any clones in response to abacavir. Similarly, no Th17 or Th22 cytokines were detected. Secretion of the effector molecules FasL and perforin was detected in some of the clones in response to abacavir stimulation but not others indicating the differing mechanisms of T-cell activation employed across the clones.
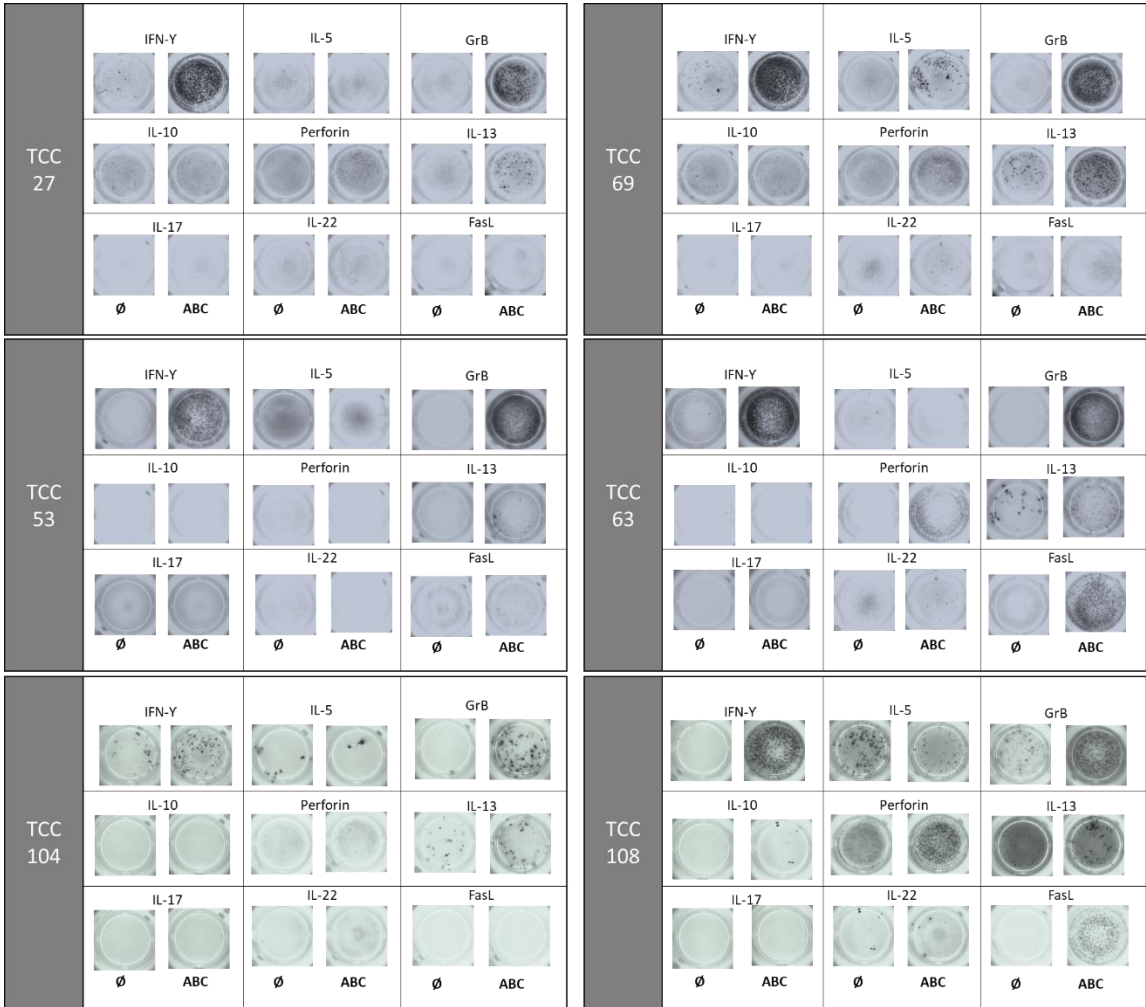
Figure 2.14. Abacavir-specific cytokine activity of CD8^{+} T-cell clones. ELIspot well images from six representative abacavir-responsive T-cell clones incubated in the presence and absence of abacavir (37^OC; 5% CO_2). T-cell activation was measured via the ELIspot assay for the respective cytokines.

2.4.7. TCRV$_\beta$ analysis of T-cell responsive clones.

To investigate the TCR expression of abacavir-specific T-cell clones, V$_\beta$ analysis was carried out on a panel of 29 abacavir responsive T-cell clones. As shown in figure 2.15 a varied TCR expression employed across the T-cell clones tested, with 24% of clones expressing a TCR V$_\beta$ undetectable by the TCR kit. This indicates the expression of a rare TCR out with the 85% encompassed by the antibodies.

a)

b)
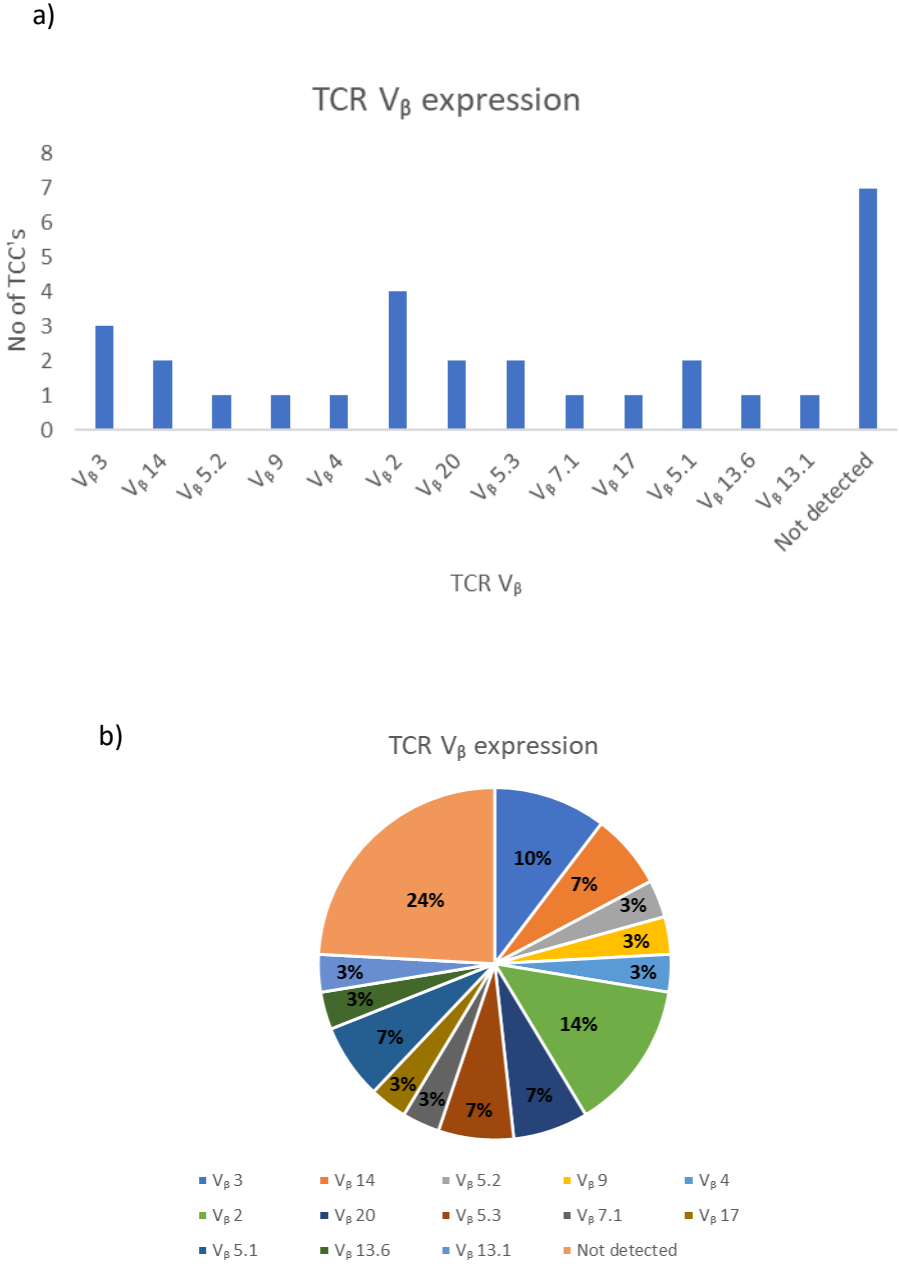
Figure 2.15. Comparison of TCR V$_\beta$ expression across the abacavir-responsive T-cell clones. a) Bar chart and b) Pie chart displaying the varied expression of TCR V$_\beta$ expression across abacavir-responsive T-cell clones.

2.5 Discussion

Hypersensitivity reactions to abacavir are observed exclusively in individuals carrying the HLA-B*57:01 risk allele, this association yields a NPV of 100% and a PPV of 48-55% (Mallal et al. 2008). Abacavir-specific CD8^{+} T-cell responses can be assessed via the use of lymphocytes isolated from healthy drug naïve volunteers positive for HLA-B*57:01. It has been demonstrated in various studies that abacavir-responsive T-cell clones from healthy, drug naïve individuals can be generated (Bell *et al.*, 2013; Adam *et al.*, 2014; Naisbitt *et al.*, 2015). Abacavir binds non-covalently with HLA-B*57:01 altering the shape and chemistry of the peptide binding groove, specifically in the F-pocket region. This leads to the accommodation of an altered repertoire of self-peptides displayed on the antigen presenting cells surface, specifically with smaller C-terminal anchors. It is hypothesised that the presentation of these altered peptides on the surface for recognition by T-cells evokes an immunological response due to their perception as foreign antigens by the T-cells (Illing et al. 2012; Ostrov et al. 2012; Norcross et al. 2012). Studies to ascertain the mechanisms of T-cell activation in response to abacavir can be carried out comparatively easily on abacavir clones relative to PBMCs, which encompass many cells of varying characteristics, making it difficult to attribute a function to a particular cell type.

The aim of this chapter was to generate abacavir-responsive CD8^{+} T-cell clones from four HLA-B*57:01 positive healthy donors that had not been previously exposed to the drug, for use throughout this thesis. A panel of these responsive clones were subjected to further testing for cellular phenotype, dose-dependency along with antigen processing dependency and cytokine secretion profile.

A total of 2279 clones tested for abacavir-specificity across the four donors, 101 were found to proliferate in response to abacavir on first testing. This yielded an overall percentage of responsive clones of 4.6%, which is lower than in previous studies (Naisbitt et al. 2015);

however, this value is skewed by the exceptionally low number of clones generated from donor 2 (0.4%). As shown in Table 2.2, the percentage yield of responsive clones displayed considerable variation between donors with some yielding a responsive clone value of as high as 12% while others were lower (0.4-4.5%). It would be intriguing to find out whether this represents a difference in T-cell receptor precursor frequency. If so, this might influence susceptibility to abacavir hypersensitivity. Antigen specificity on first test responsive clones was confirmed via the use of IFN-γ secretion as a readout due to the superiority of the ELIspot assay over proliferation for CD8$^+$ T-cell clones. All clones displaying a proliferation SI>2 were subjected to an ELIspot assay to analyse the secretion of the proinflammatory cytokine IFN-γ as a test for antigen specificity in response to abacavir. All clones demonstrating a distinct increase in IFN-γ secretion when co-incubated with abacavir compared to control were maintained in cell culture while those displaying no significant difference between untreated and abacavir treated were identified as false positives and were removed from cell culture. From the 101 abacavir clones responsive on first testing, 52 were found to secrete IFN-γ in response to co-incubation with abacavir. All 52 of these T-cell clones were phenotyped as CD8$^+$, consistent with all previous findings in abacavir-responsive T-cell clones (Chessman *et al.*, 2008; Bell *et al.*, 2013; Adam *et al.*, 2014; Naisbitt *et al.*, 2015).

Dose-response analysis of selected abacavir clones indicated a variation in T-cell reactivity to decreasing concentrations of abacavir even in the presence of APCs. Some T-cell clones responded to abacavir at exceptionally low concentrations (<1μM) e.g. TCC 27, while others displayed limited activation at concentrations below the optimal (35μM), TCC 40. Similarly, the activation profile of T-cells in response to abacavir was varied across the different T-cells, which were shown to be activated both in the presence and absence of APCs (Figures 2.10-2.12). Some T-cell clones displayed strong T-cell activation in both the presence and absence of APCs, even at low concentrations of abacavir. However other clones required abacavir and

professional APCs for activation. Of note, all clones express surface class I molecules. The dependence on professional antigen presenting cells for T-cell activation was observed in many abacavir clones as the concentration of the drug decreased. Despite activation of T-cells in the absence of APCs in many clones the T-cell response was much lower than in the presence of APCs suggesting the ability of these clones to utilize both APC dependent and independent activation pathways in response to abacavir. Antigen presenting cell pulsing assays were employed to further assess the mechanism of T-cell activation within a panel of abacavir-responsive T-cell clones. Optimal pulsing time was 16h to allow for abacavir binding to endogenous HLA-B*57:01, protein processing and subsequent loading of the MHC binding peptides and finally their transport to the cellular surface. Pulsing assays yield negative results for drugs which activate cells via the PI mechanism (Martin P. Zanni et al. 1998; Pichler 2002a; Pichler 2008; Wu et al. 2006). Thus, it is likely that pulse positive abacavir-specific clones are activated via the altered peptide repertoire concept. Some abacavir clones displayed a diminished response when 16-hour abacavir pulsed APCs were compared with co-incubation with soluble abacavir. Furthermore, a small number of clones produced a T-cell response to APCs pulsed with abacavir for reduced periods of time (1 hour and 4 hours) indicating the self-presenting ability of these clones as well as direct interaction with surface MHC molecules (Adam *et al.*, 2012; Bell *et al.*, 2013). Collectively, these data demonstrate the capability of abacavir-responsive T-cell clones to utilize activation pathways which are both processing dependent and independent. Across the abacavir clones tested, the secretion of the proinflammatory cytokines IFN-γ and IL-13 along with granzyme B was detected at high levels in all clones, while no secretion of IL-10, IL-17 and IL-22 was detected. Secretion of IL-5 was observed in one abacavir clone at relatively low levels. Secretion of the effector molecule perforin and expression of FasL was varied across the abacavir-specific T-cell clones tested. In two clones expression of FasL was accompanied by secretion of perforin, while in 2 other clones lack of FasL expression and perforin secretion was detected. However,

in clones 27 and 69 perforin secretion was detected at low levels but expression of FasL could not be observed, indicating the use of other mechanisms for perforin secretion. Consistent with previous findings the TCR V_β repertoire across the abacavir-responsive T-cell clones tested displayed strong variation between the clones (Bell *et al.*, 2013). Notably, a large percentage of abacavir-responsive T-cell clones (24%) expressed a rare TCR not included in the range detectable by the TCR V_β antibody kit. The variability between abacavir clones suggests the existence of a heterologous population of abacavir-specific CD8+ T-cell with unique characteristics.

The data presented in this chapter demonstrates that it is possible to generate abacavir-specific CD8+ T-cell clones from healthy drug naïve volunteer's positive for the HLA-B*57:01 allele. These clones can be activated via two pathways that utilise the binding of abacavir to endogenous HLA-B*57:01 in an antigen processing dependent manner (Chessman et al. 2008) and also via direct interaction with surface MHC molecules (Bell *et al.*, 2013). Cytokine secretion data further demonstrates the variability in response observed in abacavir clones to stimulation by the drug. Taken together these data indicate the differing characteristics of T-cell clones generated from healthy donors by way of activation pathways and the responses observed to abacavir exposure. This illustrates the existence of a heterogenous pool of T-cells with varying characteristics, presenting important implications for drug safety analysis.

Chapter 3- Development of novel abacavir analogues that do not bind to HLA-B*57:01 or activate CD8⁺ T-cells through modification of the 6-amino cyclopropyl group.

3.1 Introduction

The association between the prevalence of HLA risk alleles and hypersensitivity reactions to several different therapeutic agents has been widely documented. This includes severe cutaneous reactions such as SJS/TEN in patients expressing the HLA-B*15:02 allele with the anti-epileptic drug carbamazepine (Chung et al. 2004), as well as with the xanthine oxidase inhibitor allopurinol in patients expressing HLA-B*58:01 (Hung et al. 2005). However, the most widely recognised association between hypersensitivity reactions and the expression of HLA risk alleles are the reactions experienced exclusively in patients carrying HLA-B*57:01 with the antiretroviral drug abacavir. These reactions yield a 100% NPV and a PPV of 48% with HLA-B*57:01 (Mallal et al. 2008; Mallal et al. 2002; Martin et al. 2004; Hetherington et al. 2002).

Abacavir binds to HLA-B*57:01 in a non-covalent manner, the interactions within the peptide binding groove result in a reduction in the prevalence of larger C-terminal anchors such as tryptophan and phenylalanine, accompanied by an increase in the smaller C-terminal anchors such as valine, leucine and isoleucine (Illing et al. 2012; Ostrov et al. 2012; Norcross et al. 2012). These findings led to the inception of the hypothesis that the binding of abacavir to HLA-B*57:01 induces changes in the shape and chemistry of the F-pocket of the peptide binding groove, reducing its size, consequently altering the repertoire of peptides accommodated on the surface of the MHC molecules for presentation to T-cells. As these unique self-peptides are not observed in the absence of abacavir they are perceived as foreign by CD8^{+} T-cells, meaning an immune reaction is initiated (Ostrov et al. 2012; Illing et al. 2012).

The generation of abacavir-specific CD8^{+} T-cell clones from drug naïve healthy donors positive for the HLA-B*57:01 allele has been widely demonstrated (Chessman *et al.*, 2008; Adam *et al.*, 2012; Bell *et al.*, 2013; Naisbitt *et al.*, 2015). Furthermore abacavir is

hypothesised to activate T-cell clones via two autonomous pathways where activation of the T-cells is dependent on the antigen processing and subsequent display of peptides by the MHC, and another where the drug is capable of interacting with the MHC T-cell receptor (Bell *et al.*, 2013). The need for the antigen processing was demonstrated elegantly by *Chessman et al*, via the eradication of the class I restricted pathway in antigen presenting cells which was sufficient to abrogate T-cell responses to abacavir (Chessman et al. 2008). *Bell et al 2013*, demonstrated the need for the antigen processing pathways in the generation of an abacavir-specific response in T-cell clones. It was found that up to 50% of clones were activated by antigen presenting cells pulsed for 16 hours in the presence of abacavir, but not by APCs pulsed for 1 hour only. Additionally, abacavir was detected intracellularly in APCs pulsed for the 16 hour period, leading to the conclusion that abacavir is rapidly taken up and remains present in the APC for the whole 16 hours. Furthermore, these responses were abrogated following removal of the antigen processing pathways via glutaraldehyde fixation, indicating the imperative role for MHC processing and presentation (Chessman et al. 2008). However, this pathway accounts for approximately 50% of all abacavir-responsive CD8^{+} T-cell clones, other clones were found to activate the proliferation of T-cell clones in the absence of antigen presenting cells or with glutaraldehyde fixed APC, indicating that abacavir may activate T-cell clones via a direct interaction with the surface MHC (Adam *et al.*, 2012; Bell *et al.*, 2013).

The 6-amino cyclopropyl group of abacavir is imperative for the binding and interaction with HLA-B*57:01. The cyclopentyl and cyclopurine moieties nestle in the D and E pockets of HLA-B*57:01 respectively, while the cyclopropyl moiety extends into the F-pocket of HLA-B*57:01 inducing a conformational change in the peptide binding groove, reducing its size and thereby accounting for the preferred accommodation of the smaller chain amino acids mentioned earlier (Illing et al. 2012). This conformational change within the peptide binding

groove of HLA-B*57:01 may allow still for the binding of normal peptides observed in abacavirs absence, however the presence of abacavir within HLA-B*57:01 will result in the display of peptides in an altered conformation to the one in abacavirs absence, which can be sufficient to trigger a T-cell response (Illing et al. 2013). The metabolite of abacavir, carbovir, which lacks the cyclopropyl moiety (Figure 3.1) is known to be devoid of immune responses in CD8^{+} T-cells, indicating a specific role for the 6-amino cyclopropyl moiety interacting within the F-pocket of the HLA-B*57:01 (Chessman et al. 2008).
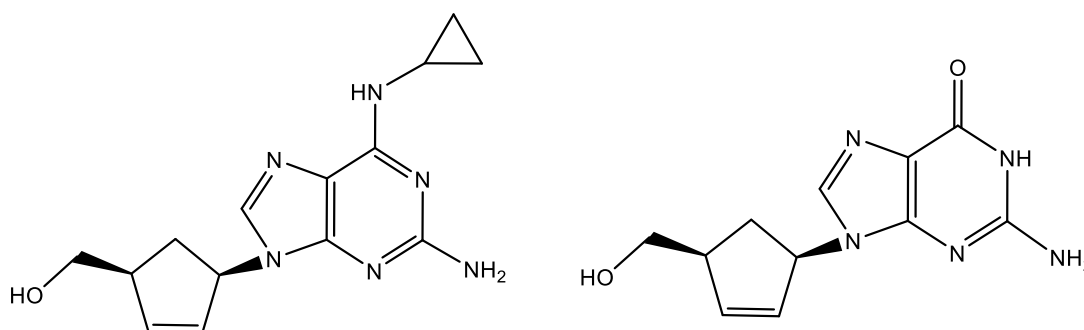
Figure 3.1. Chemical Structure of abacavir and its metabolite carbovir

Therefore, the theory that modifications to the cyclopropyl moiety of the compound could abolish the undesired T-cell activation observed with abacavir but retain the favoured antiviral activity was presented as a promising avenue for research.

Indeed, this concept was explored by *Naisbitt et al 2015* via the construction and synthesis of sixteen abacavir analogues, all of which contained substitutions at the 6-amino position of the compound, in place of the cyclopropyl group. From this sixteen, two analogues were identified that were devoid of T-cell activation when co-incubated with abacavir-responsive T-cell clones. Both analogues contained *N*-linked branched chains of three carbon atoms; analogue **15** (isopropyl) and analogue **16** (methyl-isopropyl). Additionally, both retained some antiviral activity as well as possessing reasonable *in vitro* cytotoxicity profiles.

Molecular modelling studies revealed unfavourable binding conformations of compounds **15** and **16** within the F-pocket of HLA-B*57:01. Docking of these compounds within the antigen binding cleft resulted in the presence of unfavourable steric clashes between the functional groups of the analogues and the HLA-binding peptide, as well as amino acid residues within the F-pocket. The presence of these clashes indicate a hindrance in the binding capabilities of the two analogues within the F-pocket, meaning a change in the repertoire of self-peptides could not be induced resulting in a failure to activate T-cells (Naisbitt et al. 2015). Indeed, when docked into HLA-B*57:01 following the same procedure no such clashes were apparent between the cyclopropyl group of abacavir and the HLA-binding peptide or amino acid residues. This was also true for analogue **17** (propyl) which displayed clear activation of abacavir T-cell clones (Naisbitt et al. 2015). This study not only established the potential for generation of structural analogues of abacavir which can maintain antiviral activity and be deficient in the unwanted T-cell responses, but also gave a greater insight into the HLA-B*57:01 binding characteristics of the compounds and the relationship between HLA-B*57:01 binding and the activation of T-cells.

Using this concept, another fourteen abacavir analogues were synthesised with further modifications to the 6-amino cyclopropyl moiety. These analogues were constructed around the azetidine ring group which has previously been demonstrated to maintain a favourable antiviral profile similar to abacavir (Daluge *et al.*, 1997). These compounds were synthesised firstly to be examined as potential replacements for abacavir in a therapeutic setting based on their respective antiviral activity and T-cell activation profiles. Secondarily, these compounds were also utilized as molecular probes to explore the binding characteristics within HLA-B*57:01. Furthermore, peptide elution studies were carried out to investigate the effect of the 6-amino cyclopropyl group substitutions on the observed repertoire of peptides, given the obvious alterations seen with abacavir (Illing et al. 2012).

Using these procedures, we have developed a paradigm for the generation of safer antiviral agents by gaining a greater understanding into the interactions of compounds within HLA-B*57:01 and its relationship with the repertoire of self-peptides presented on the surface of the antigen presenting cells for recognition by T-cells (Figure 3.2).
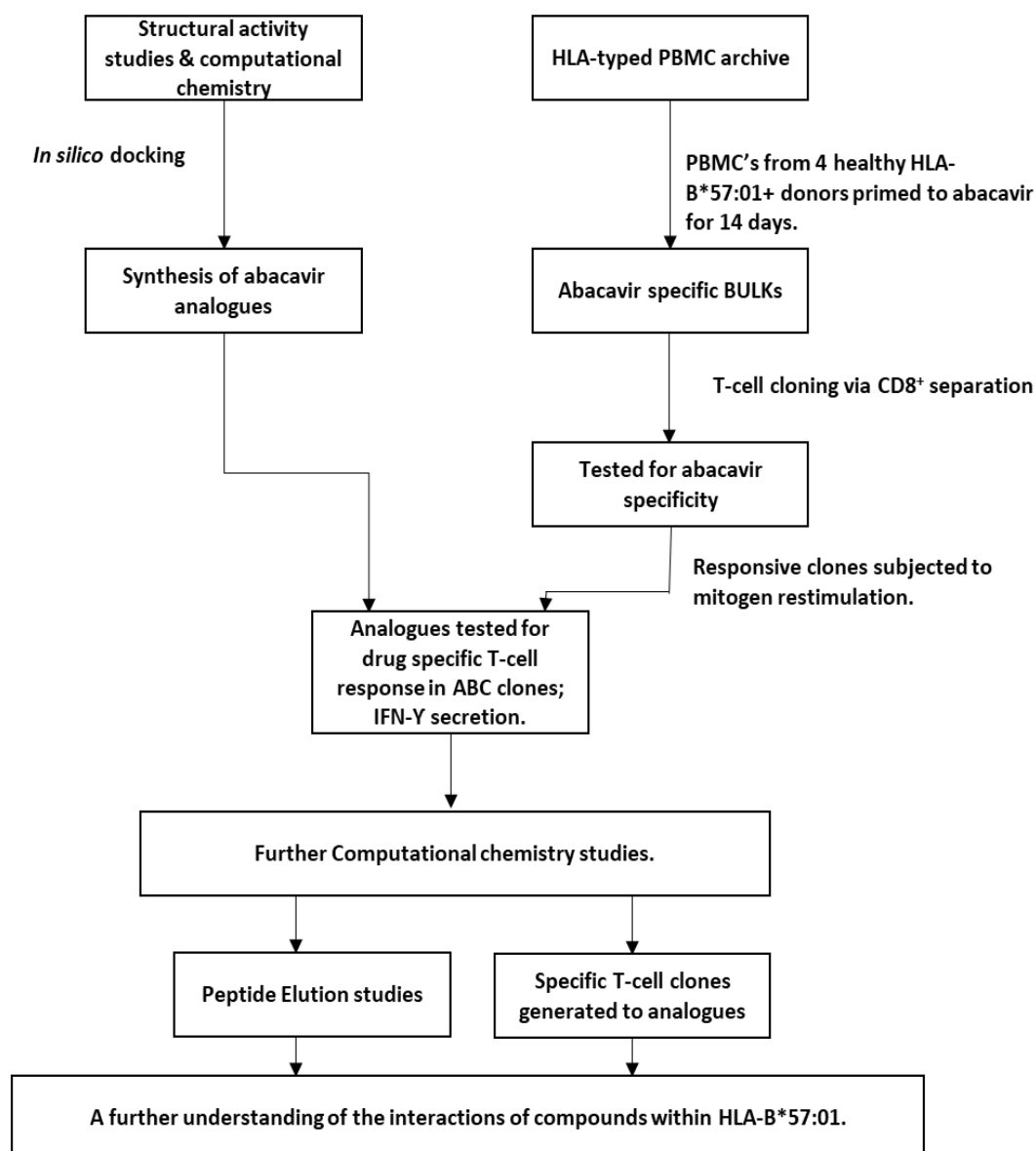
Figure 3.2. Experimental design and structure of abacavir substituted analogues.
Schematic representation of experimental procedure for design and use of abacavir analogues as molecular probes for greater understanding of the interactions within HLA-B*57:01.

3.2. Aims.

In this chapter we aimed to develop a new series of abacavir analogues constructed around cyclic amine derivatives, namely the azetidine ring structure. These analogues were screened to investigate their T-cell activation capabilities, as well as their antiviral potency and safety profiles. Once a select number of promising analogues were identified, their interactions within HLA-B*57:01 was further examined via molecular modelling. Furthermore, the effect of these compounds on the repertoire of peptides presented to T-cells by HLA-B*57:01 was examined and compared to the peptide repertoires in untreated and abacavir treated cells. Finally, the safety of these promising analogues was confirmed via the generation of T-cell clones specific to the respective abacavir substituted analogues. Taken together, the studies in this chapter will help develop a tool for providing a greater understanding into the relationship between the T-cell activation profile and the binding interactions of the compounds within HLA-B*57:01.

3.3. Methods

3.3.1. Materials

Abacavir was received as a gift from GlaxoSmithKline (GSK). Human AB serum and foetal bovine serum (FBS) were obtained from Innovative Research (Michigan, USA) and Invitrogen (Paisley, UK), respectively. Interleukin-2 (IL-2) was purchased from Peprotech (London, UK). Multisort bead separation kits were supplied by Miltenyi Biotec (Surrey, UK). Antibodies for staining were purchased from BD Biosciences (Oxford, UK). ELIspot kits including the coating and detection antibodies, streptavidin alkaline phosphate conjugate and BCIP/NBT substrates were purchased from Mabtech (Stockholm, Sweden). Other reagents were purchased from Sigma-Aldrich (Dorset, UK) unless otherwise stated.

3.3.2. Synthesis of abacavir substituted analogues

The initial part of the project involved the synthesis of a stock sample of key intermediate **1** (Figure 3.3.). Compound 1 (150.00 mg, 564.55 µmol, 1.00 *eq*), azetidine (2.00 *eq*) and N, N-diisopropylethylamine (145.92 mg, 1.13 mmol, 2.00 *eq*) were taken up into a microwave tube in isopropyl alcohol (2.00 mL). The sealed tube was heated at 70 °C for 2 hours under microwave. LCMS showed that the starting material was consumed completely. The mixture was concentrated in vacuum to yield the crude product. The crude product was then purified by prep TLC purification to yield the respective analogues as described in detail in Appendix section 1. Analogue synthesis was performed by Professor Paul O'Neill (Department of Chemistry at the University of Liverpool).
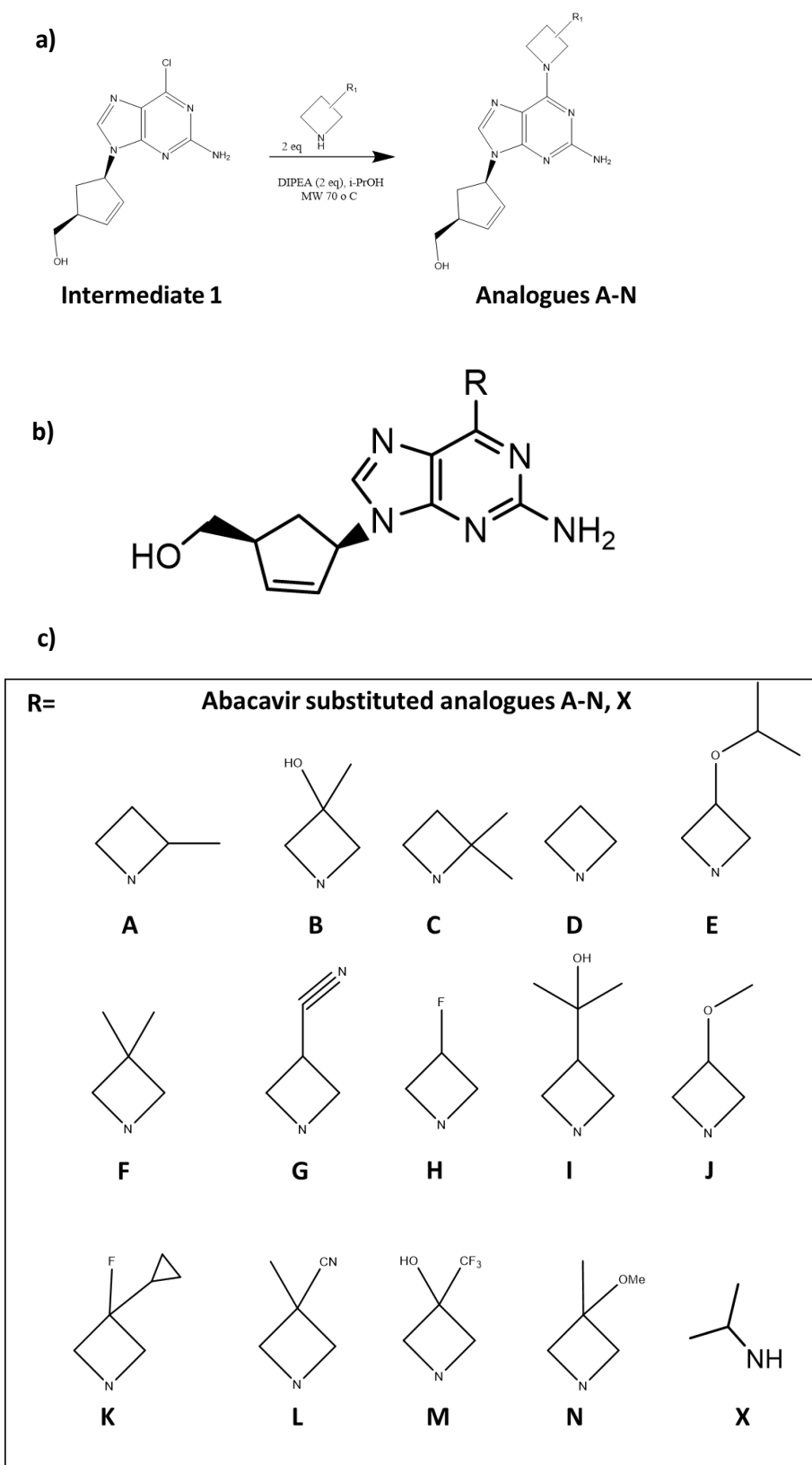
Figure 3.3. Abacavir analogues. a) Generalized procedure for the synthesis of the abacavir analogues A-N. b) Structure of abacavir with the 6-amino cyclopropyl functional group replaced with R. c) Functional groups of the abacavir analogues **A-N** and **X.**

3.3.3. Cell culture media.

Cell culture medium for T-cells (R9) is composed of RPMI supplemented with 10% human AB serum, HEPES (25mM), penicillin (1000 U/mL), streptomycin (0.1mg/mL), L-glutamine (2mM) and transferrin (25µg/mL).

EBV transformed B-cells were cultured in F1 medium composed of RPMI supplemented with 10% foetal bovine serum, HEPES (25mM), penicillin (1000 U/mL), streptomycin (0.1mg/mL) and L-glutamine (2mM).

3.3.4. Generation of abacavir-specific T-cell clones

CD8$^+$ T-cell cloning was carried out as described in detail in section 2.3.5. Briefly; PBMCs from HLA-B*57:01 positive donors were selected from an established HLA-typed healthy donor cohort. PBMCs from each donor were incubated in the presence of abacavir (35µM) in R9 medium for a period of 14 days. On days 6 and 9 cells were fed with cell culture medium containing IL-2 (2µL/mL) to preserve the abacavir driven expansion of T-cells. On day 14, CD8$^+$ T-cells were positively selected using MultiSort kits (Miltenyi Biotec, Surrey UK) and T-cell clones were generated via serial dilution. CD8$^+$ T-cells were seeded at a concentration of 0.3/1/3 cells/ well (96 well U-bottomed plate) and stimulated with allogeneic PBMC feeder cells and PHA (5µg/mL) in R9 medium containing IL-2 (2µL/mL). Cells were fed every 2 days with R9 medium containing IL-2 (2µL/mL) and well growing clones were transferred to a new 96 well plate and expanded across 4 wells. On day 14 clones were restimulated and further expanded for 28 days.

3.3.5. Testing for drug antigen specificity

Approximately four weeks after beginning the serial dilutions, abacavir-specificity was measured by assessing cell proliferation in the presence of the drug. Abacavir-induced

proliferation was measured by culturing T-cell clones ($5x10^4$/50µL) with irradiated autologous EBVs ($1x10^4$/50µL) and abacavir (35µM) (total volume 200µL/96 well U-bottomed plate). Following 48 hour incubation, tritiated thymidine (0.5µCi) was added to each well and proliferation was assessed 16 hours later via scintillation counting. The proliferative response of the T-cell clones was expressed as radioactive counts per minute (cpm). T-cell clones with a proliferative stimulation index (SI) of 2 or greater were picked and expanded by mitogen driven restimulation in R9 medium containing irradiated PBMCs ($5x10^5$ cells/well), IL-2 (5µL/mL) and PHA (10µg/mL) for further analysis.

The antigen specificity of the abacavir-responsive T-cell clones were confirmed by analysing IFN-γ secretion in response to abacavir using the ELIspot assay described in detail in section 2.3.7. All clones displaying a significant increase in IFN-γ secretion in response to abacavir were maintained in cell culture for use in further experiments.

3.3.6. Antiviral activity and cytotoxicity of abacavir analogues.

3.3.6.1. Antiviral activity

Human T-cell lymphotropic virus-I carrying human cell line (MT-4) cells are a human cell line with high sensitivity to the HIV-1 virus, making them ideal candidates for the analysis of antiviral activity (Gyuris et al. 1992).

MT-4 cells were co-incubated with HIV-1 IIIB cells for a period of 1 hour. Following this incubation period, the infected cells were seeded in a 96 well plate containing serially diluted compounds (highest concentration 500µM; 8 concentrations, 4 fold serial dilutions in duplicate) and incubated for a period of 5 days with virus and cell controls as a comparator. Following incubation, cell viability was measured via luminescence using CellTiter-Glo reagent. The antiviral activity of the compounds was measured based on the protection of virus induced cytopathic effect at each concentration normalised by the virus control.

The antiviral activity of a compound was calculated as shown below:

Activity (%) = (Raw data$_{compound}$-Average$_{Virus Control}$)/(Average$_{Cell Control}$ -Average$_{Virus Control}$)*100

EC$_{50}$ values were calculated according to dose response curves generated using GraphPad Prism software version 5.01. These experiments were conducted by the WuXi App Tech company in Shanghai.

3.3.6.2. Cytotoxicity

The cytotoxicity of the analogues was assessed using the same parameters as described in the antiviral testing, excluding the virus control.

The compounds cellular toxicity was calculated as shown below:

Viability (%) = (Raw data$_{compound}$)/(Average$_{Cell Control}$)*100.

CC$_{50}$ values were calculated according to dose response curves generated using GraphPad Prism software version 5.01.

3.3.7. Inhibition of T-cell and B-cell proliferation with abacavir analogues.

To ascertain the direct effect of the analogues on cellular proliferation, the analogues and abacavir were cultured in the presence of EBV transformed B-cells or PBMCs at concentrations of 0-250µM. In the case of B-cells, the analogues were co-incubated for a period of 48 hours then tritiated thymidine was added directly to the cells for a further 16 hours. Cells were then harvested onto a printed filter mat and radioactive incorporation was assessed via scintillation counting on a microBeta counter. In the case of PBMCs, cells were co-incubated with the compounds for a period of 72 hours before PHA (10µg/mL) was added to promote the proliferation of viable cells. Following a further 24-hour incubation, tritiated thymidine was added directly onto the cells for a further period of 16 hours. Cells were then

harvested and radioactive incorporation was measured as described above. IC_{50} values were calculated using SigmaPlot software 13.0.

3.3.8. CD8+ T-cell activity of abacavir analogues

To measure the effect of modifying the 6-amino cyclpropyl group of abacavir with regards to the activation of abacavir-specific T-cells, T-cell clones ($5x10^4$/50μL) were incubated with autologous EBVs ($1x10^4$/50μL) in the presence or absence of the abacavir analogues (10, 20, 50μM) (total volume 200μL/96 well U-bottomed plate) for a period of 48 hours and IFN-γ secretion was assessed via ELIspot (described in detail in section 2.3.7). Abacavir was used as a positive control. The HLA-B*57:01 mediated CD8+ T-cell responses to the abacavir analogues was tested in six abacavir-responsive T-cell clones from four healthy drug naïve donors expressing the HLA-B*57:01 risk allele.

3.3.9. HLA-B*57:01 molecular modelling

Molecular modelling was carried out under the supervision of Dr Neil Berry in the Department of Chemistry at the University of Liverpool. Ligands were prepared for docking in Spartan'08 (wavefunction inc. Irvine, California, USA: 1991-2009). A native SMA ligand was exported from the protein data bank (PDB), code 3UPR (Ostrov et al. 2012). For each analogue, the cyclopropyl group of abacavir was replaced. Merk molecular force field minimization calculations were performed with all atoms frozen except newly added substitutions. For docking studies GOLD 5.1 (CCDC Software Limited, Cambridge, UK) was used to examine the potential binding poses of the abacavir analogues within the F-pocket of HLA-B*57:01. Figures of abacavir analogue binding conformations within HLA-B*57:01 were produced using PYMOL software version 2.5.

3.3.10. MHC purification and peptide elution

CIR.B*57:01 cells (Chessman et al. 2008) were grown to high confluency in the presence or absence of 35µM abacavir/analogue for a minimum of 4 days, prior to washing in PBS, pelleting and snap freezing in liquid nitrogen. Cell pellets of $4\text{-}5\text{x}10^8$ cells were lysed by mechanical and detergent based lysis, the lysates cleared by ultracentrifugation, and MHC class I complexes isolated by immunoaffinity purification using solid-phase bound pan class I antibody w632 as described previously (Dudek et al. 2012). Complexes were dissociated using 10 % acetic acid and fractionated by Reversed Phase High Performance Liquid Chromatography (RP-HPLC) on a 4.6mm internal diameter x 100mm monolithic reversed-phase C18 HPLC column (Chromolith SpeedROD; Merck Millipore) using an ÄKTAmicro HPLC (GE Healthcare) system. Peptides were loaded at 1mL/min onto the column in 98% Buffer A (0.1% trifluoroacetic acid) and 2% Buffer B (80% acetonitrile, 0.1% trifluoroacetic acid), and bound material eluted by running a gradient of buffer B at 2ml/min of 2-15% over 0.25 minutes, 15-30% over 4 minutes, 30-40% over 8 minutes, 40-45% buffer B over 10 min, with collection of 500µL fractions. Fractions were vacuum concentrated and reconstituted in 0.1% formic acid.

3.3.11. MS analysis

Reconstituted fractions were analysed by liquid chromatography-tandem mass spectrometry (LC-MS/MS) via a data dependent acquisition strategy using a NanoUltra cHiPLC system (Eksigent) coupled to an SCIEX 5600+ TripleTOF mass spectrometer equipped with a Nanospray III ion source. Samples were loaded onto a pre-equilibrated cHiPLC trap column (3 µm, ChromXP C18CL, 120 Å, 0.5 mm x 200 µm), at 5µL/min in 0.1% formic acid, 2% acetonitrile, and separated over a cHiPLC column (3 µm, ChromXP C18CL, 120 Å, 15 cm x 75 µm) using a linear gradient of 2-35% Buffer B (80% acetonitrile, 0.1% formic acid)/Buffer

A(0.1% formic acid) over 75 minutes at a flow rate of 300nL/min. Data acquisition occurred with the following instrument parameters: ion spray voltage, 2,400 V; curtain gas, 30 l/min; ion source gas, 20 l/min; and interface heater temperature, 150 °C. MS/MS switch criteria selected the top 20 ions meeting the following criteria per cycle: m/z >200 amu, charge state of +2 to +5, intensity >40 counts per second. After two selections for fragmentation, ions were ignored for 30 seconds. For assignment MS/MS spectra were searched against the human proteome (UniProt/Swiss-Prot v2016_04) using ProteinPilot software (version 5.0, SCIEX). Peptide elution studies and analysis via mass spectrometry were carried out by Dr Patricia Illing in the Department of Biochemistry and Molecular Biology at Monash University in Melbourne Australia.

3.3.12. Generation of CD8+ T-cell clones to a panel of abacavir substituted analogues

Cloning to abacavir 6-amino substituted analogues was carried out using the same method described in section 3.3.4 for abacavir, with PBMCs being primed to respective analogues **G**, **H**, **J** and **X** with these compounds being used for first testing in place of abacavir. These compounds were selected based on their respective inductions of IFN-γ secretion in abacavir-responsive T-cell clones, with **G** and **X** representing non-activating analogues and **H** and **J** comprising activating analogues.

3.3.13. Confirmation of antigen specificity and cross reactivity of CD8+ T-cell clones to abacavir analogues

Clones specific to abacavir analogues were tested for IFN-γ secretion using ELIspot assay. Briefly; T-cell clones ($5x10^4$/well) along with autologous EBVs ($1x10^4$/well) were incubated in the presence or absence of respective analogues (35µM) with cell culture medium as a negative control for 48 hours (37°C; 5% CO_2). Abacavir (35µM) was used to assess cross-reactivity of T-cell clones and PHA (10µg/mL) was used as a positive control where required.

3.3.14. Statistical Analysis

For comparison between control and test values in proliferation assays the Mann-Whitney test was used. Two-way ANOVA was used for comparison between abacavir and the analogue values.

3.4. Results.

3.4.1. Synthesis of abacavir analogues.

Fourteen abacavir substituted analogues were synthesised in good yields and high analytical purity for both pharmacological and immunological experiments. NMR, LCMS and accurate mass and yield values are described in appendix section 2. Azetidine substituted analogues were classified by letters **A-N**. The isopropyl substituted analogue (Naisbitt et al. 2015) was reclassified as analogue **X** to be used as a comparator in assays. The relative structures are shown in Figure 3.3.

3.4.2. Generation of abacavir-specific CD8$^+$ T-cell clones

T-cell clones specific to abacavir were generated using serial dilution assays. From a total of 2279 clones tested across four HLA-B*57:01 positive donors, 101 were found to proliferate in the presence of abacavir on first testing, (Control, 1665 ± 188.5 cpm: abacavir 35µM, 6940 ± 729 cpm; P< 0.0001) (Section 2.4.1).

Due to receiving the fourteen abacavir analogues in batches, at different times, a total of 15 abacavir clones from the four HLA-B*57:01 positive donors were used. T-cell clones possess limited life in cell culture, often present issues when thawed and can lose antigen specificity over time, meaning a broad range of abacavir-responsive T-cell clones were used. Each analogue was tested to a total of six abacavir clones across the four healthy, drug naïve donors expressing HLA-B*57:01. All clones responsive in second test were phenotyped as

CD8+ (Section 2.4.3). The abacavir-responsive T-cell clones used for assays in this chapter are displayed in Table 3.1 with their corresponding donor. Results for T-cell specificity assays of these abacavir clones and subsequent phenotyping data is discussed in detail in section 2.4.

Donor 1: HLA-0617	Donor 2: HLA-0957	Donor 3: HVN-0158	Donor 4: HLA-0622
TCC 27	TCC 40	TCC 51	TCC 78
TCC 70	TCC 42	TCC 56	TCC 79
TCC 3 *		TCC 60	TCC 86
TCC 20 *		TCC 63	TCC 100
			TCC 103

Table 3.1 Panel of abacavir-responsive T-cell clones used for assays in this chapter

* Clones generated to abacavir + natural peptide 15, these clones demonstrated a strong response to abacavir and were incorporated into T-cell analogue assays. Second test data and phenotyping for these clones is found in chapter 5.

3.4.3. Antiviral activity of 6-amino substituted abacavir analogues

The antiviral activity of the fourteen abacavir analogues was ascertained using cell viability assays carried out by the WuXi App Tech company in Shanghai. The antiviral activity of the analogues was measured on the basis that HIV kills MT-4 cells, thereby cellular survival was an indication of antiviral activity, presented as EC_{50}. The cytotoxicity of the analogues in MT-4 cells was also determined using the same process but without viral infection of the MT-4 cells prior to incubation with the analogues, cytotoxicity values are presented as CC_{50}.

Consistent with previous findings, abacavir demonstrated potent antiviral properties (EC_{50} 2.05µM) and a relatively favourable cytotoxicity profile (CC_{50} 42.4µM). Across the fourteen abacavir substituted analogues a diverse range of antiviral potency was observed with some analogues possessing antiviral potency to a similar degree as abacavir (**D** and **H**), while others

displayed no antiviral activity within the range of concentrations used (**E**, **F**, **I** and **N**).

Replacement of the cyclopropyl moiety of abacavir with an azetidine ring (**D**) maintains the antiviral profile of the compound (EC_{50} 2.979μM). Furthermore, the addition of a fluoro group to the azetidine ring at the 3-position of the ring (**H**) retains the antiviral activity of the compound (EC_{50} 2.456μM). Also, both analogues **D** and **H** possessed more favourable cytotoxicity in MT-4 cells than abacavir. Antiviral activity (EC_{50}), cytotoxicity (CC_{50}) and SI (CC_{50}/EC_{50}) are presented in Table 3.2. Compounds with no antiviral activity or cytotoxcity are presented as >500μM.

Compound ID	Unit	Antiviral activity (EC50)	Cytotoxicity (CC50)	SI (CC50/EC50)
Abacavir	μM	2.05	42.44	20.7
Analogue A	μM	16.68	>500	>29.98
Analogue B	μM	59.09	>500	>8.46
Analogue C	μM	30.08	263.2	8.75
Analogue D	μM	2.979	160	53.71
Analogue E	μM	>500	>500	ND
Analogue F	μM	>500	>500	ND
Analogue G	μM	38.55	>500	>12.97
Analogue H	μM	2.456	234.3	95.4
Analogue I	μM	>500	>500	ND
Analogue J	μM	85.76	>500	>5.83
Analogue K	μM	33.59	467.7	13.92
Analogue L	μM	411.4	>500	>1.21
Analogue M	μM	33.67	343	ND
Analogue N	μM	>500	>500	18.14

Table 3.2. Antiviral activity and cytotoxicity values for 14 abacavir analogues (A-N) with abacavir as a comparator. Antiviral activity and cytotoxicity was measured in MT-4 cells and values are presented as EC_{50} and CC_{50} respectively.

3.4.4. Inhibition of T-cell and B-cell proliferation by abacavir and the abacavir substituted analogues.

To assess cytotoxic profiles, abacavir and the fourteen substituted analogues were incubated with PBMCs and EBV transformed B-cells at concentrations of 0, 10, 25, 50, 75, 100 and 250μM for periods of 72 and 48 hours, respectively. Proliferation was measured using ^{3}H thymidine incorporation. Abacavir (PBMC 66.7μM IC_{50} EBV 102.3μM) inhibited proliferation of both T-cells and B-cells in a concentration dependent manner (Figure 3.5). Similar IC_{50} values were found for analogues **D** (PBMC 61μM; EBV 220μM) and **H** (PBMC 71μM; EBV 175μM) while all other analogues suppressed proliferation of T-cells and B-cells at much higher concentrations, with many failing to generate 50% inhibition of proliferation within the range of concentrations used (**I**, **L** and **N**).

Compound	Inhibition of mitogen driven PBMC proliferation IC50 (μM).	Inhibition of B-cell proliferation IC50 (μM).
Abacavir	66.7	102.3
Analogue A	112	222.7
Analogue B	>250	>250
Analogue C	78	>250
Analogue D	61	220
Analogue E	102	245
Analogue F	98	>250
Analogue G	141	227
Analogue H	71.5	175
Analogue I	>250	>250
Analogue J	112	>250
Analogue K	239	>250
Analogue L	>250	>250
Analogue M	123	241
Analogue N	>250	>250

Table 3.3. Inhibition of T-cell and B-cell proliferation in PBMC's and EBV transformed B-cells respectively. Inhibition presented as IC_{50} in μM calculated using non-linear regression. Analogues which failed to react 50% inhibition within concentration range used presented as >250.

a)

b)
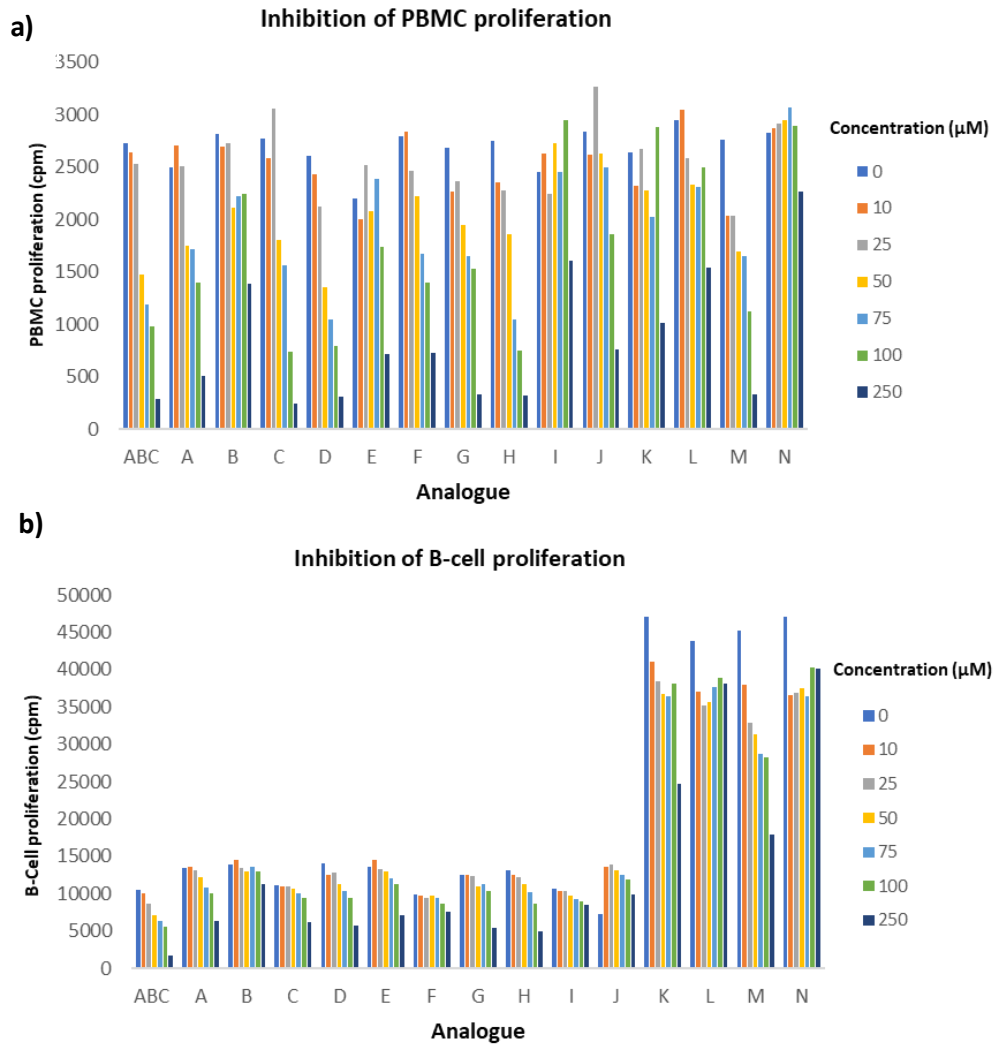
Figure 3.5. Inhibition of T-cell and B-cell proliferation in PBMC's and EBV transformed B-cells respectively. Graphical representation of inhibition of a) PBMC proliferation and b) B-cell proliferation in the presence of abacavir (ABC) and analogues A-N at concentrations of 0-250μM.

3.4.5. CD8$^+$ T-cell activity of abacavir analogues.

All abacavir substituted analogues (**A**-**N**) contained azetidine linked groups in place of the 6-amino cyclopropyl moiety while analogue **X** (isopropyl amino) from a previous series of analogues (Naisbitt et al. 2015) was also incorporated into this assay as a comparator. To assess the effect of these substitutions on CD8$^+$ T-cell activity, six abacavir clones from four HLA-B*57:01 positive donors were co-incubated with autologous APCs in the presence of these fifteen abacavir analogues for 48 hours. Little to no T-cell proliferation was observed in abacavir-specific clones co-incubated with ten of the substituted analogues. Slight activation was detected with analogue **D** at 50µM, with only analogue **J** inducing significant T-cell proliferation within the concentration range studied (Figure 3.6).
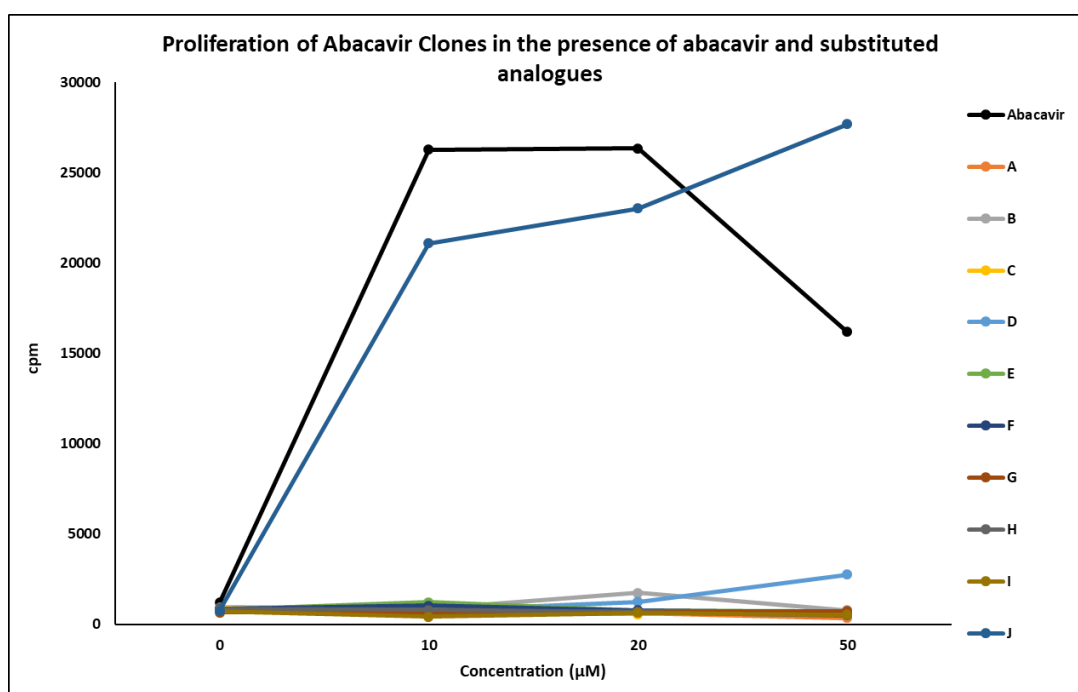
Figure 3.6. T-cell proliferation induced by co-incubation with abacavir analogues at concentrations of 10, 20 and 50µM. Abacavir (black) was used at the same concentrations as a comparator.

Based on these findings, IFN-γ ELIspot was used to measure T-cell responses in abacavir clones due to its enhanced sensitivity over proliferation. A varied response was observed across all fifteen abacavir analogues. The first five analogues (**A-E**), with the exception of **B** (azetidine methyl 3-ol) and **E** (azetidine isopropyl), evoked T-cell responses in the clones to some degree.

The second five analogues (**F-J**) demonstrated a reduced T-cell activation profile in the T-cell clones compared to abacavir, except for analogue **J** (azetidine methoxy). Limited T-cell activity was observed in analogues **F**, **G** and **I** while **J** displayed a strong activation profile in the abacavir clones which was similar to the IFN-γ secretion levels observed for abacavir itself. Interestingly, analogue **H** (azetidine fluoro) induced no T-cell activity at concentrations of 10 and 20μM, however the higher concentration of 50μM resulted in a strong CD8^{+} T-cell response (Figure 3.7).

Analogue **K** (cyclopropyl-fluoro azetidine) activated some T-cell clones while analogues **L-N** completely lacked any T-cell activity in all abacavir-responsive T-cell clones. In concordance with findings from *Naisbitt et al 2015*, analogue **X**, again did not evoke T-cell activation in all abacavir-specific CD8^{+} T-cell clones.

Based on their respective structures, antiviral activity and T-cell activation profiles, these findings presented analogues **D**, **G, H**, **J**, **M** and **X** as candidates to take forward for further experiments. Analogues **D** and **J** represent the compounds with strong potential to induce cross-reactivity with abacavir-responsive T-cell clones, while **M** and **X** comprised those with no ability to activate abacavir specific T-cell clones. Analogue **H** was selected for further analysis based on the fact that T-cells were only activated by this analogue at higher concentrations.
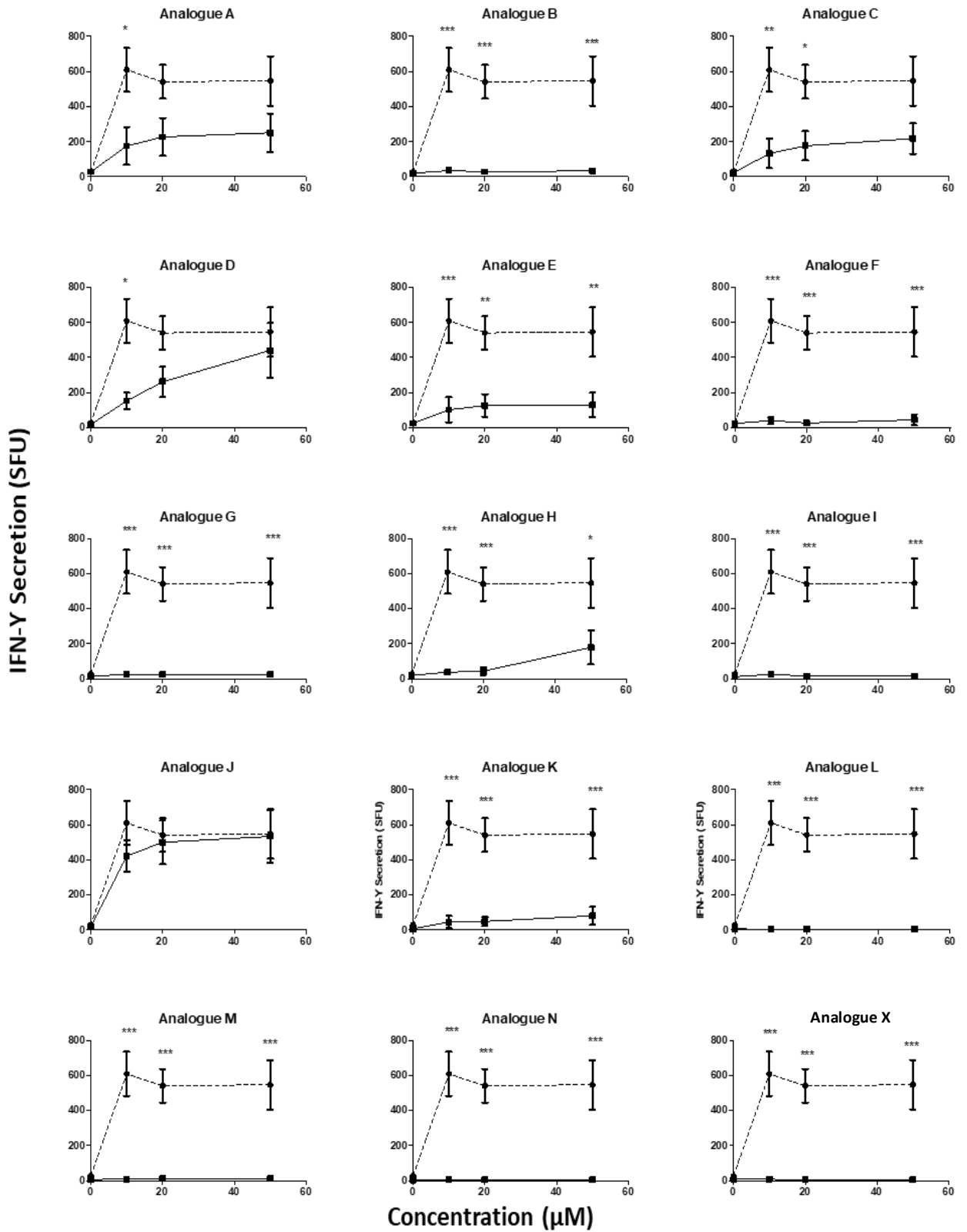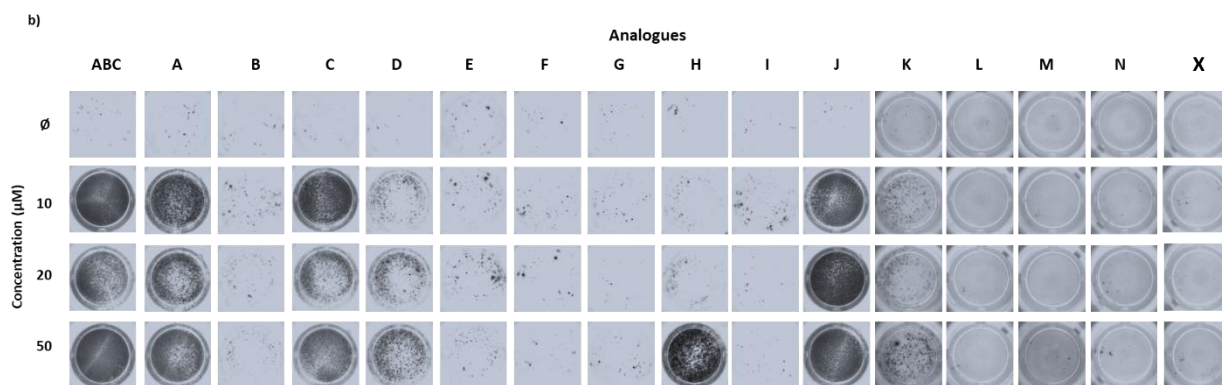
Figure 3.7. CD8^{+} T-cell activity of abacavir analogues. a) Mean IFN-γ secretion from six abacavir-responsive T-cell clones incubated in the presence of the 14 abacavir analogues (solid line) at concentrations of 0, 10, 20 and 50μM. Analogue **X** from *Naisbitt et al* was also tested against the six clones as a comparator. The mean abacavir response across six clones (dotted line) was used as a comparator. Comparison of abacavir and analogue values were analysed using Two Way ANOVA, * $P<0.05$, ** $P<0.01$, *** $P<0.001$. b) Eli-spot well images from 1 representative abacavir clone incubated in the presence of abacavir analogues **A-N**, analogue X and abacavir (ABC) as a comparator.

3.4.6. Molecular modelling of abacavir analogues within HLA-B*57:01.

We sought to assess the binding characteristics of the selected abacavir analogues within the F-pocket of HLA-B*57:01 and this relationship with T-cell activation. A molecular docking protocol was developed which replicated the crystal structure of the binding conformation of abacavir within the F-pocket of HLA-B*57:01. Using this protocol, the binding orientations of the analogues **D**, **G**, **H, M** and **X** were predicted within the F-pocket. Analogues were expected to bind in a similar fashion to abacavir with the cyclopurine moiety of the compound forming hydrogen bonds with the amino acid residues Asp-114, Ser-116 and Ile-124. The conserved binding structure of abacavir suggests that modifications to the cyclopropyl moiety may produce steric clashes between the functional group of the compound and the HLA binding peptide, and in some cases residues of HLA-B*57:01.

The binding pose employed by abacavir displays no overlapping in the atomic radii of the cyclopropyl group and that of the HLA-binding peptide, nor the Tyr-123 residue of HLA-B*57:01. Clear protrusion of the cyclopropyl moiety of abacavir deep into the F-pocket region

is observed with no apparent steric clashes between the functional group and the HLA-binding peptide, nor with residues within the F-pocket (Figure 3.8). This indicates a favourable binding pose of abacavir within HLA-B*57:01 to allow for strong interactions to induce a conformational change in the F-pocket that will result in the accommodation of altered self-peptides to be presented to T-cells. However, despite binding HLA-B*57:01 in a similar conformation to abacavir, the isopropyl functional group analogue **X** produces steric clashes with the Val-9 residue of the HLA-binding peptide as well as the Tyr-123 residue of HLA-B*57:01. This is demonstrated by the overlapping atomic radii of analogue **X**'s functional group and amino acid residues. The prevalence of such clashes demonstrates a hindrance in the binding of the compound within HLA-B*57:01, resulting in a lack of T-cell activity in abacavir clones (Figure 3.8).

Analogues **D** and **H**, with the ability to induce T-cell activity, assume a favourable binding orientation within HLA-B*57:01 indicated by the absence of clashes between the respective functional groups and the amino acid residues of the peptide or within HLA-B*57:01. Analogue **D** in particular adopts a binding conformation very similar to that of abacavir, unsurprisingly eliciting T-cell activation (Figure 3.8). Analogue **H** however, binds within HLA-B*57:01 in an altered manner to abacavir and analogue **D** with the guanosine portion of the compound inverted, suggesting this analogue to bind in an unconventional manner, which may explain why T-cells were activated by this analogue only at the higher concentrations.

Conversely, the addition of a nitrile group at the 3-position of the azetidine ring (**G**), eradicated all T-cell responses observed in the ELIspot assay. When docked into HLA-B*57:01 again a non-conventional binding conformation was observed, which, unlike with **H**, resulted in the presence of steric clashes between the azetidine ring and the Val-9 residue of the HLA-binding peptide. Similarly, analogue **M** did not activate abacavir-specific T-cells in the ELIspot assay, while adopting a binding orientation in HLA-B*57:01 which resulted in the clashing

between the branched fluoride functional group and residues on the HLA-binding peptide (Figure 3.8). This is unsurprising based on previous results with branched chain functional groups within HLA-B*57:01. Collectively these data suggest that the binding conformations adopted by analogues which are known to evoke a T-cell response yield no unfavourable clashes within the peptide binding groove thereby allowing for the accommodation of altered self-peptides not observed in the absence of abacavir. The presence of such unfavourable steric clashes between the functional groups of the non-activating abacavir analogues and pep-V suggest that the binding of these analogues would hinder the presentation of this peptide. This would likely result in the presentation of other peptides or this peptide in an altered conformation. Both of these situations would yield the presentation of peptides distinct from those observed in the presence of abacavir, which may lead to the loss of cross-reactivity with abacavir-specific CD8^{+} T-cell clones.

a)   **i)**   **Abacavir**
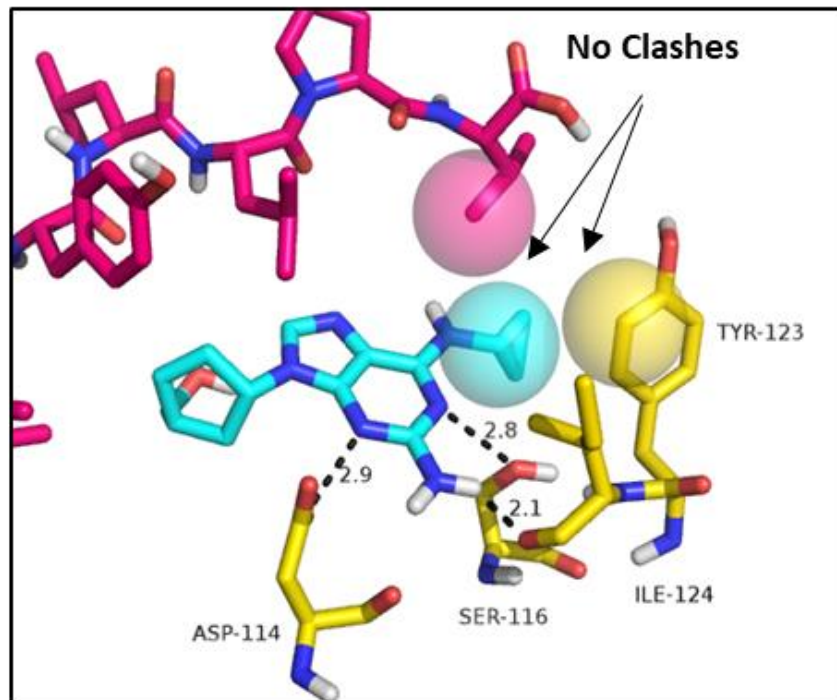
ii)   **Analogue X**
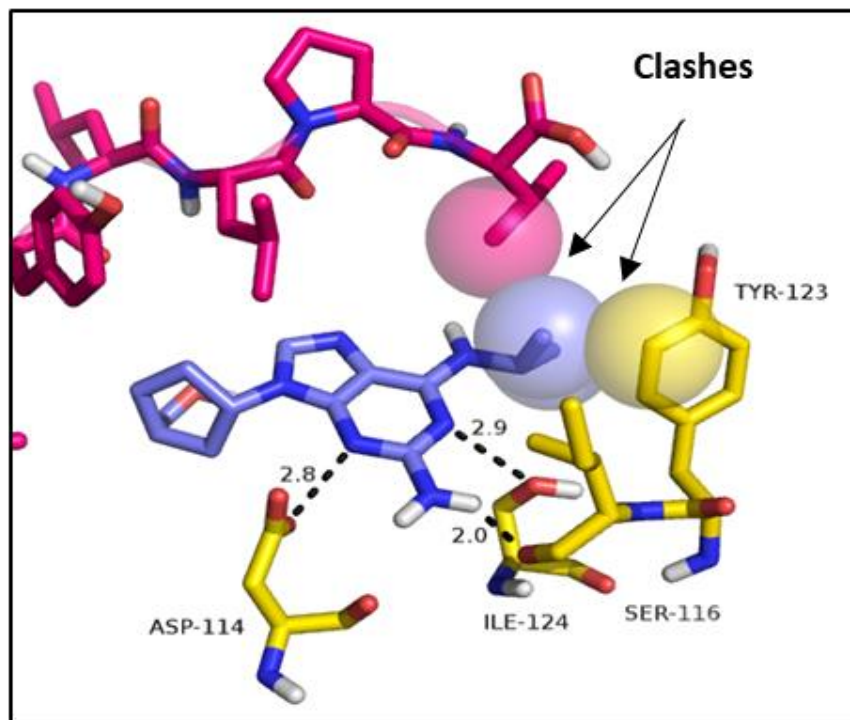
b)   **i)   Analogue D**
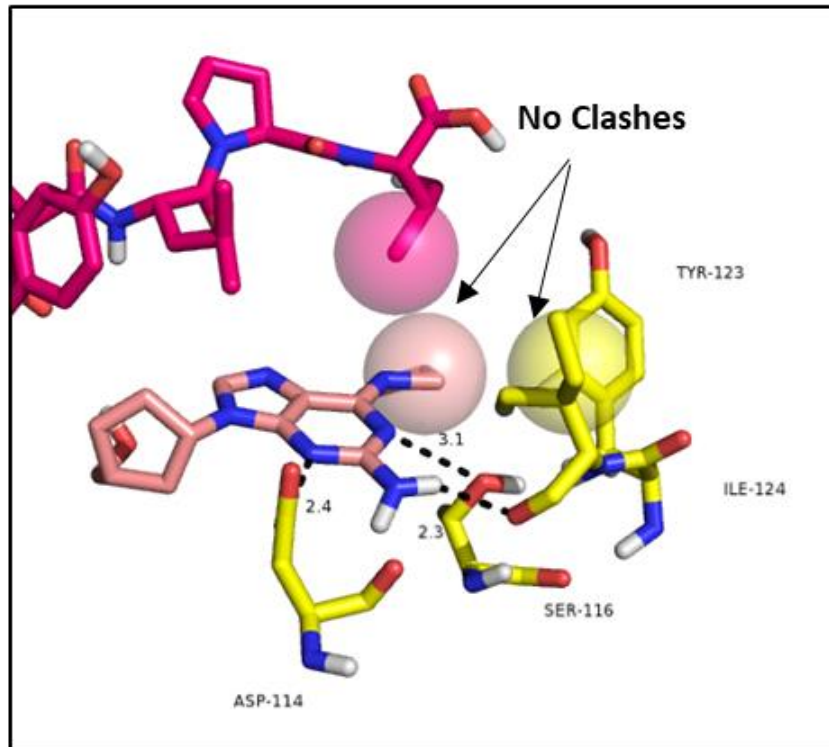
ii)   Analogue G
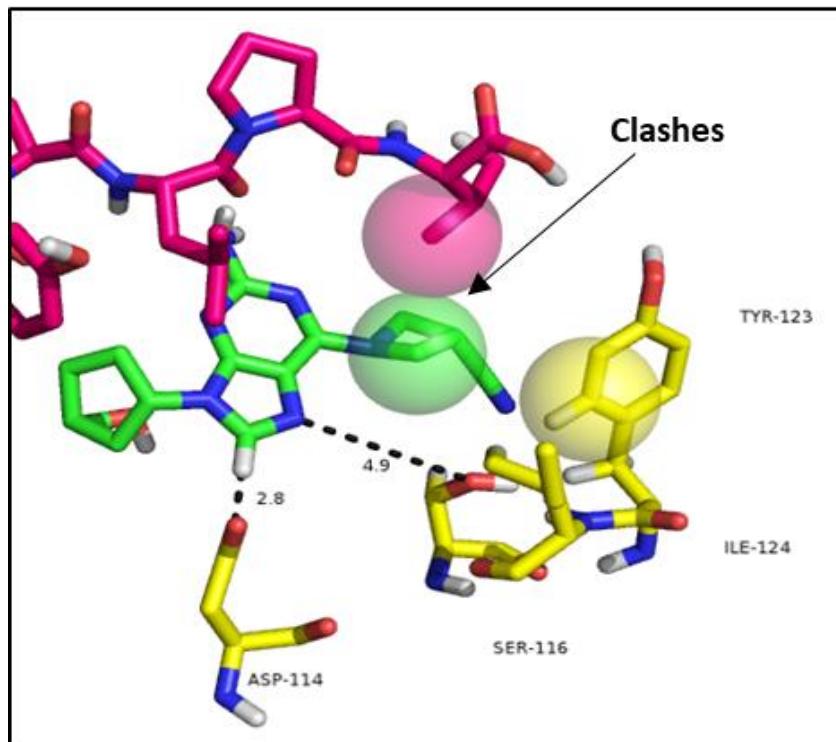
iii) Analogue H
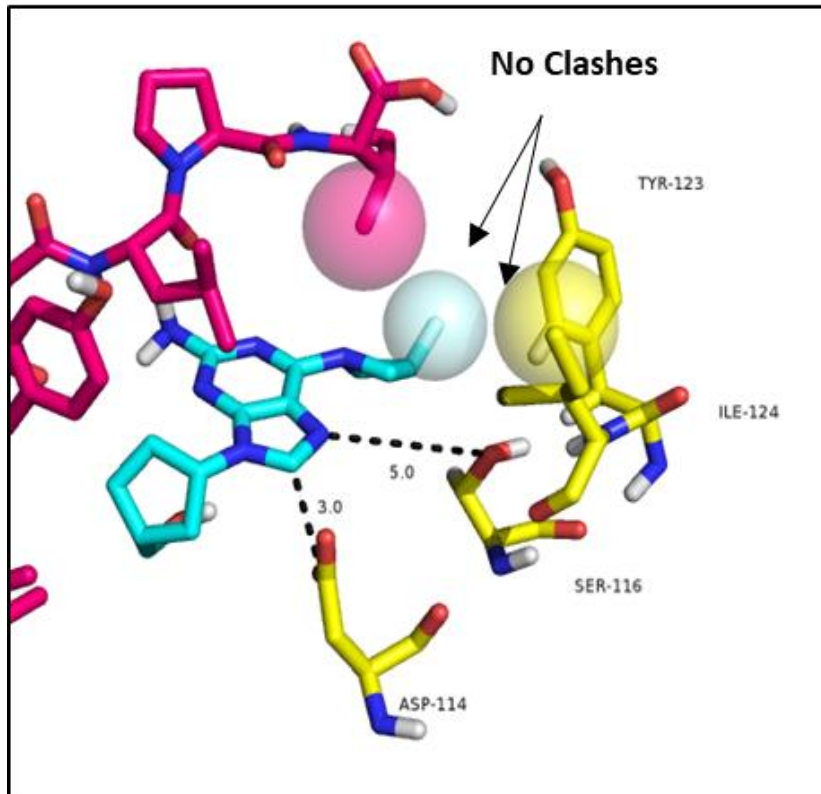
iv) Analogue M
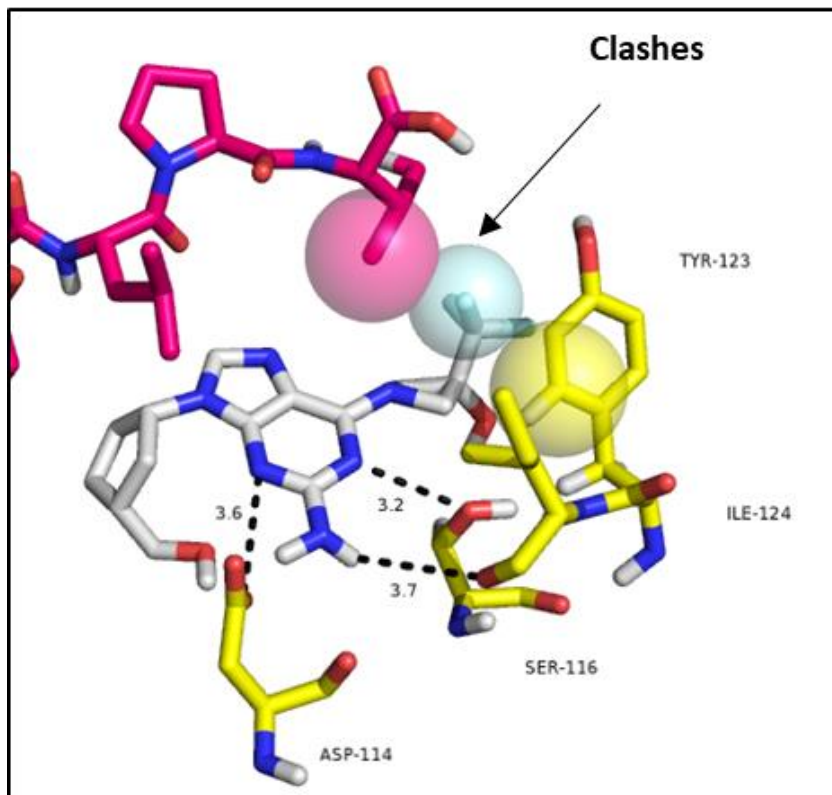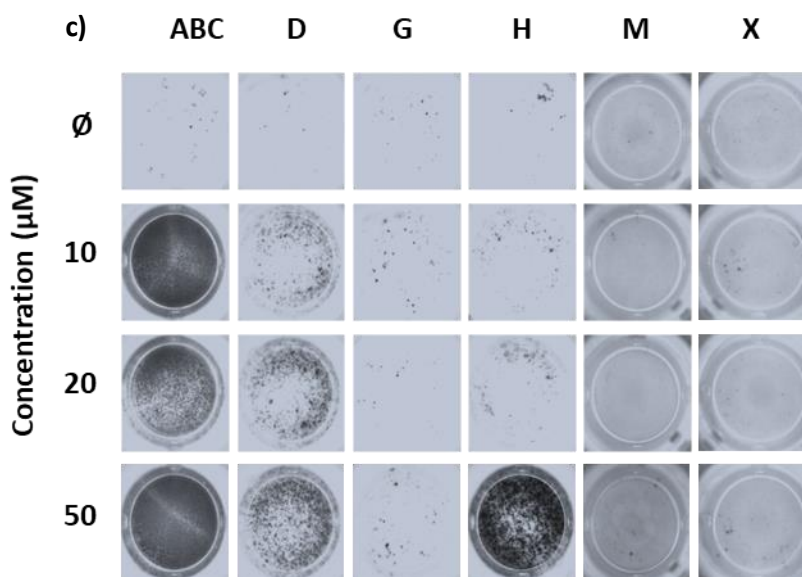
Figure 3.8. Direct comparison of the CD8^{+} T-cell activity of abacavir substituted analogues and the binding orientations within the F-pocket of HLA-B*57:01. a) Crystal structure of HLA-B*57:01 (PDB:3UPR) represented with the peptide, abacavir and analogue **X** coloured as pink, cyan and blue sticks respectively. i) Crystal structure binding orientation of abacavir. Stick representation of the peptide, pep-v (HSITYLLPV) shown in pink with the chemical structure of abacavir in cyan. Key amino acid residues which bind abacavir are shown as yellow sticks. All non-polar hydrogen atoms removed. Key hydrogen bond interactions shown as black dashes. Spheres used to illustrate the atomic radii of the atoms in the cyclopropyl group of abacavir, peptide molecule and Tyr-123 amino acid. ii) Docking solution of analogue **X** (isopropyl) in the F-pocket of HLA-B*57:01. b) Docking solution of analogues i) **D** (azetidine), ii) **G** (azetidine-3-carbonitrile), iii) **H** (azetidine-fluoro) and iv) **M** (azetidine-trifluoromethyl) in the F-pocket of HLA-B*57:01. Stick representation of the peptide, pep-v (HSITYLLPV) shown in pink. Amino acid protein residues shown as yellow sticks, with key hydrogen bond interactions shown as black dashes. All non-polar hydrogen atoms removed. Spheres used to illustrate the atomic radii of the atoms in the functional group of the analogue, peptide and Tyr-123 amino acids. c) Representative ELIspot images from wells containing abacavir and analogues **D**, **G**, **H**, **M** and **X**.

3.4.7. Peptide elution from HLA-B*57:01 expressing APCs in the presence of a panel of abacavir analogues.

To investigate the effect of the abacavir analogues on the peptide repertoire presented by HLA-B*57:01 to T-cells, peptide elution studies were carried out on C1R.B*57:01 cells incubated in the presence and absence of abacavir (35µM) or the abacavir analogues (35µM). Reconstituted peptide fractions were analysed by liquid chromatography-tandem mass spectrometry (LC-MS/MS). Peptide fractions analysed from C1R.B*57:01 cells incubated with abacavir demonstrated a strong shift toward the prevalence of peptides containing the smaller chain amino acids, isoleucine and valine, at the P9 position. Initially all peptides eluted from HLA-B*57:01 were analysed in the presence of the four substituted abacavir analogues (**D, H, M** and **X**) and the shift in prevalence of individual amino acids was compared to untreated and abacavir treated cells. Incubation with abacavir results in the significant enrichment of isoleucine and leucine at the C-terminal of the peptides. Furthermore, at the Ω-2 position a significant decrease in prevalence of arginine and lysine was observed. Both these amino acids are known to stabilise the interactions of the peptide with the Asp-114 amino acid, which in this case is blocked by the binding of abacavir. When analysed at the global level, taking all peptides into consideration, no apparent shift was observed in the prevalence of the smaller amino acids when cells were incubated with the abacavir analogues. We next analysed if any shift in amino acid prevalence was evident if peptides that were eluted in the absence of abacavir (untreated) were filtered out and removed from consideration. Upon removal of these peptides, a broad shift in some amino acids was observed in the presence of some of the analogues. In the presence of analogue **X,** an increase in 9-12 mer ligands terminating in amino acids methionine and alanine was observed, while little to no prevalence of amino acids isoleucine, leucine or valine was detected. Similarly, analogue **M** produced no apparent shift in the prevalence of the small chain amino acids at the C-terminal, displaying an overall similarity with the constitutive

ligands at the C-terminal position (untreated) (Figure 3.9). Conversely, the T-cell stimulating abacavir analogue **D**, when analysed in the absence of peptides prevalent in untreated cells, yielded an augmentation of isoleucine at the C-terminal of the peptide, although to a lesser extent than what was observed in abacavir treated cells along with increase in prevalence of methionine. Again, reduction of the amino acids arginine and lysine was observed at the Ω-2 position indicating analogue **D** to possess a similar binding profile within HLA-B*57:01 to abacavir. Incubation with analogue **H** also generated an increase in the prevalence of C-terminal isoleucine (Figure 3.9). Similar enrichment of isoleucine and methionine was observed in cells incubated with analogue **H** with the increase in isoleucine being less than the observed prevalence in the presence of abacavir, which may explain why analogue **H** only activated abacavir clones at higher concentrations. Indeed, the peptides eluted from HLA-B*57:01 in the presence of analogues **D** and **H** demonstrate significant overlap with peptides detected in the presence of abacavir (Figure 3.9).
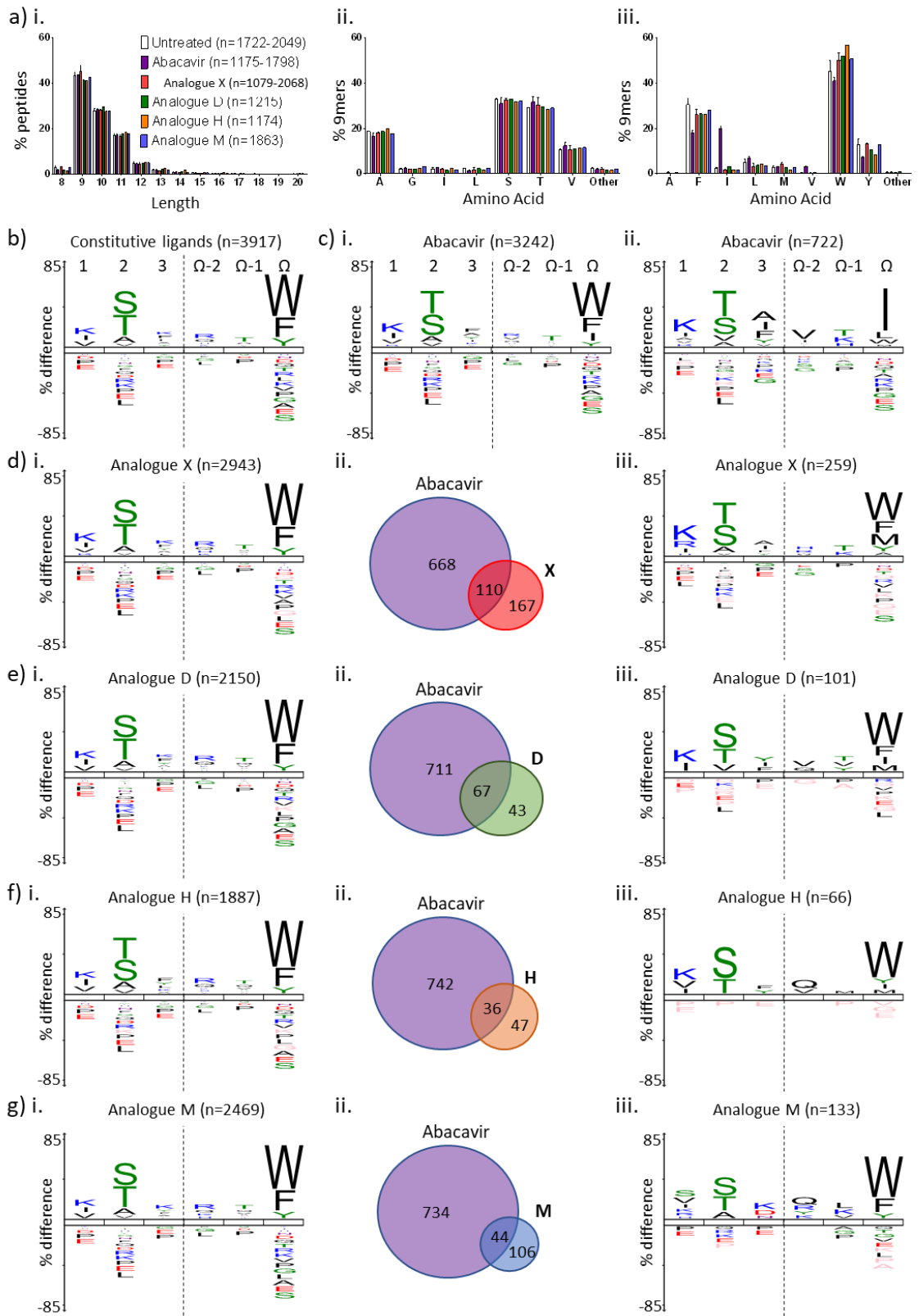
Figure 3.9. Comparison of amino acid prevalence in peptides eluted from HLA-B*57:01 in the presence of abacavir and analogues D, G, H, M and X .a) Length (**i**) and primary anchor characteristics (**ii**. Position 2, **iii**. C-terminal) of HLA-B*57:01 ligands isolated from CIR.B*57:01 grown in the absence of drug treatment, or in the presence of 35μM Abacavir (black) or analogues **X** (red), **D** (green), **H** (orange) or **M** (blue). Analyses are based on non-redundant peptide identifications (by sequence, modifications not considered) per data set made at a confidence greater than that for a 5% false discovery rate (FDR) and filtered for ligands of endogenous HLA molecules of parental CIR cells. Anchor residue preferences are shown for 9mers and are depicted as the proportion of peptides that possess specific amino acids at position 2 (**ii**) and the C-terminus (**iii**). Data shown is the mean (+/- SD) of triplicate experiments for untreated and abacavir treated cells, duplicate experiments for analogue **X**, and single experiments for the remaining analogues. **b)** IceLogo for P1 to P3 and PΩ-2 to PΩ of 9-12mer peptides in the constitutive repertoire of HLA-B*57:01. **c)** Enrichment logo for 9-12mer HLA-B*57:01 ligands detected in the presence of abacavir in this study either **i.** unfiltered or **ii.** filtered for constitutive ligands (i.e. potential neo-epitopes). **d), e), f)** and **g)** show **i.** Icelogos for 9-12mer HLA-B*57:01 ligands detected in the presence of analogues **X, D, H** and **M, ii.** Venn diagrams showing the numbers of potential neo-epitopes identified in both abacavir and analogue treatments and iii. IceLogos for 9-12mer neo-epitopes identified. IceLogos were generated using Icelogo software (Colaert, N. et al. Nature Methods 6, 786-787 (2009)) utilising the human swiss-prot proteome as the reference set. Letter height corresponds to % difference in frequency of the amino acid compared to presence in the human proteome.

3.4.8. Generation of responsive CD8⁺ T-cell clones to a selection of abacavir analogues.

3.4.8.1. Analogue G

From a total of 568 clones tested to analogue **G** across 2 donors, 5 responsive clones were generated. As previously mentioned all clones generated from serial dilutions, following mitogen restimulation for a two-week period, were subjected to a second test by means of IFN-γ ELIspot to confirm their specificity to the drug in question. Clones generated to the analogues were tested in this way to the respective analogue (35µM), abacavir (35µM) (to assess the cross reactivity of the clones) and PHA (10µg/mL) (used as a positive control). Across the two HLA-B*57:01 positive donors a very small number of clones proliferated in response to stimulation by analogue **G**. Five clones from each donor with the highest SI values, some of which were less than 2, were expanded for further testing. All were phenotyped as CD8⁺ (Figure 3.10)

No T-cell clones to analogue **G** produced significant IFN-γ secretion in response to co-incubation with analogue **G** or abacavir. However, IFN-γ secretion was observed in clones stimulated with the positive control PHA, indicating the ability to secrete the proinflammatory cytokine, but not in response to abacavir or analogue **G**. These results were consistent across both donors tested (Figure 3.10).

a) i)

Analogue G			
Donor	Donor 1	Donor 4	Total
Clones Tested	287	281	568
Responsive on initial test	2	3	5
Percentage responsive	0.7%	1%	0.9%

ii)
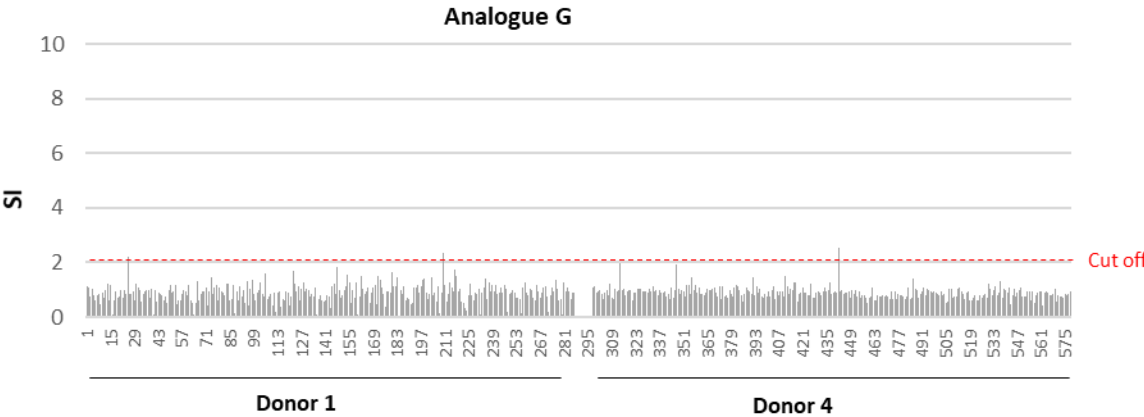
Figure 3.10. Generation of specific T-cell clones to analogue G from 2 healthy HLA-B*57:01 drug naïve donors. a) i) Table and ii) bar chart displaying number of responsive clones generated to analogue G from donors 1 and 4. b) Second testing of a panel of picked and expanded clones to analogue G incubated in the presence of abacavir (35μM) and analogue G (35μM). R9 medium and PHA (10μg/mL) were used as negative and positive controls respectively. c) Representative phenotyping of picked clones to analogue G (CD4-FITC/CD8-PE).

3.4.8.2. Analogue H

From a total of 514 clones to analogue H across 2 healthy HLA-B*57:01 drug naïve donors, 24 responsive clones proliferated in the presence of analogue H on first testing (Control, 1926 ± 451.4 cpm: analogue H 35μM, 6094 ± 1216 cpm; $P < 0.01$). All clones were phenotyped as CD8+ (Figure 3.11).

a) i)

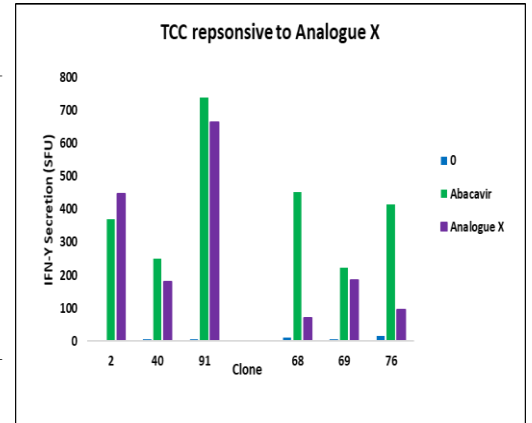| Analogue H			
Donor	Donor 1	Donor 4	Total
Clones Tested	322	192	514
Responsive on initial test	16	8	24
Percentage responsive	4.96%	4.16%	4.67%

ii)
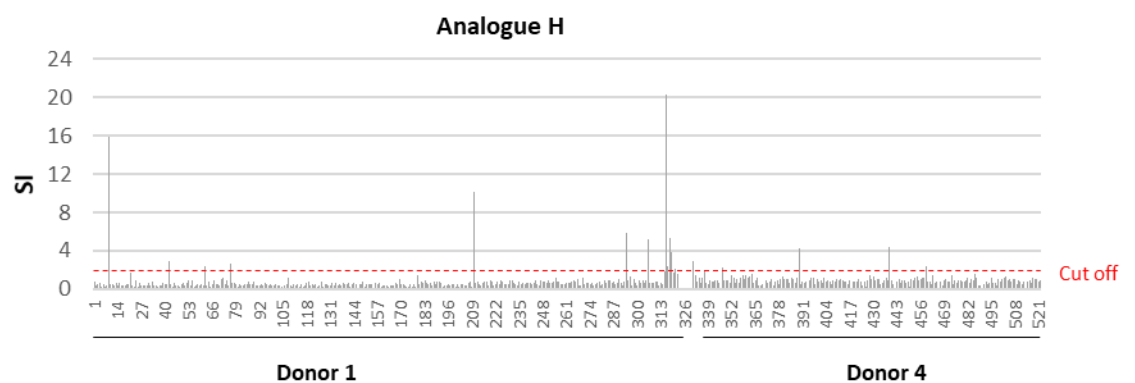
b)
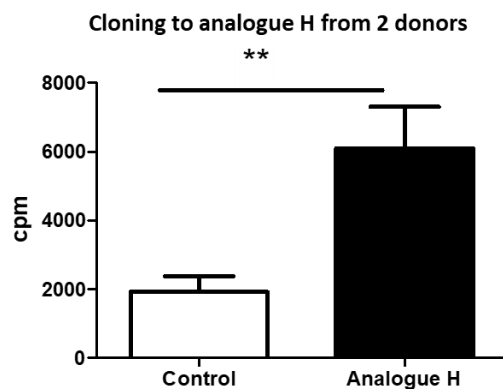
Figure 3.11. Generation of T-cell clones with specificity for analogue H from 2 HLA-B*57:01 donors. a) i) Table and ii) bar chart displaying number of responsive clones generated to analogue **H** from donors 1 and 4. b) Comparison of mean cpm values from all responsive clones to Analogue **H**. Control (0), Analogue **H** (35μM). Mann Whitney test used for comparison between control and drug treated values. Data shown as mean of all responsive clones vs control ± SEM *P<0.05, **P<0.01, *** P<0.001

Responsive clones were generated to analogue **H** across both the HLA-B*57:01 donors that were capable of evoking a CD8$^+$ T-cell response when incubated in the presence of the analogue. Furthermore, these clones also demonstrated a strong cross-reactivity profile when incubated in the presence of abacavir (Figures 3.12-3.13). Next, the ability of these clones to respond at concentrations lower than 50µM, the concentration at which abacavir clones responded to analogue **H**, was examined. All responsive clones to analogue **H** demonstrated a strong T-cell response to the analogue at concentrations 5-35µM. Furthermore, with the exception of clone 5, all clones specific to analogue **H** demonstrated strong cross reactivity with abacavir at low concentrations (Figure 3.12-3.13). Cross reactivity was detected at concentrations of abacavir as low as 5µM in some cases and displayed similar activation in a dose-dependent manner as observed with analogue **H** stimulation.
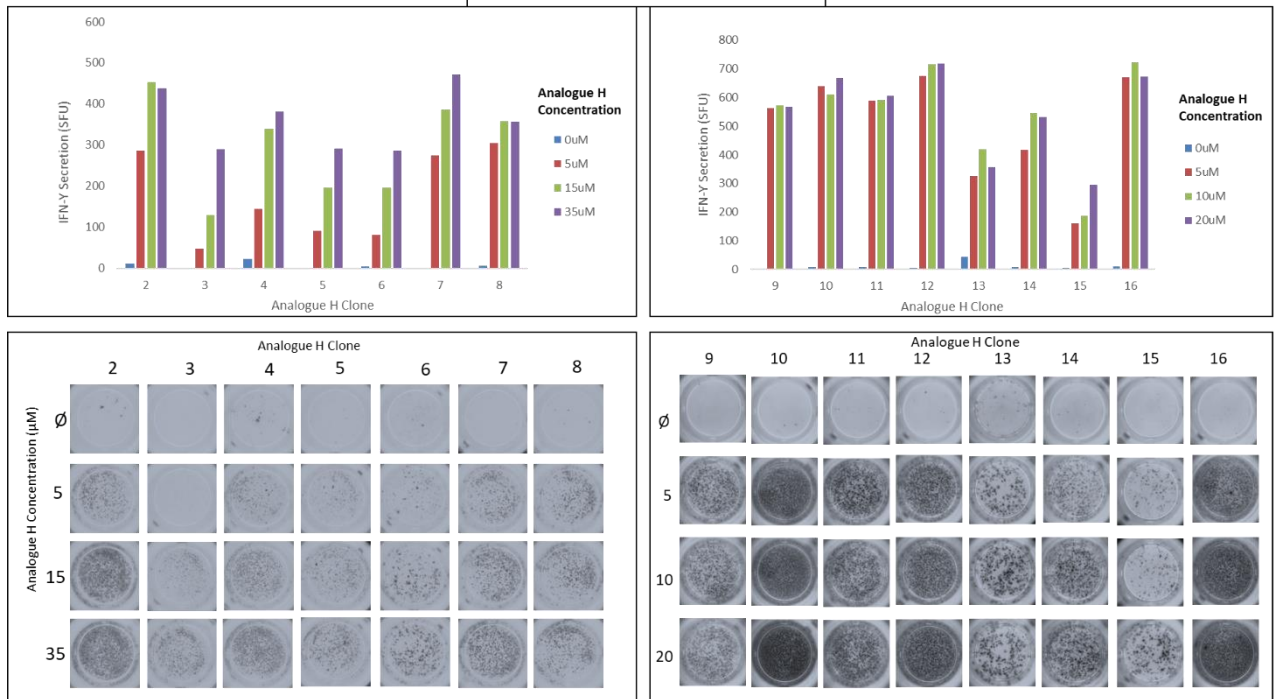
a) i)
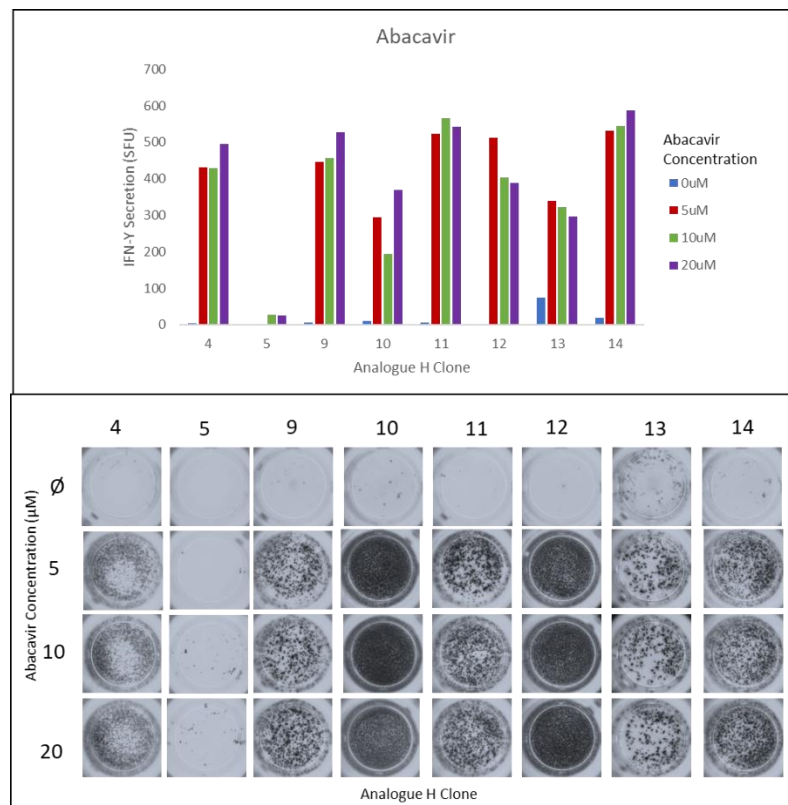
Figure 3.12. T-cell activity and cross reactivity of analogue H clones from donor 1. T-cell activation of clones specific to analogue **H** incubated in the presence of i) analogue **H** (5-35µM) and ii) abacavir (5-20µM).
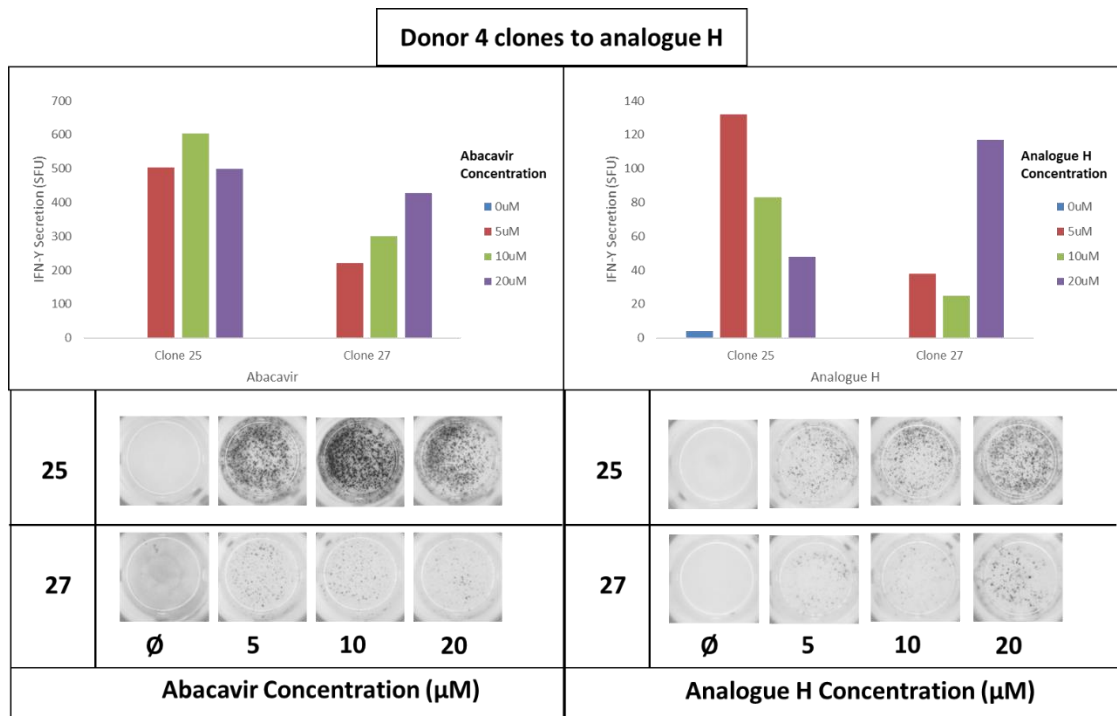
Figure 3.13. T-cell activity and cross reactivity of analogue H clones from donor 4. T-cell activation of clones specific to analogue **H** incubated in the presence of i) analogue **H** (5-35µM) and ii) abacavir (5-20µM).
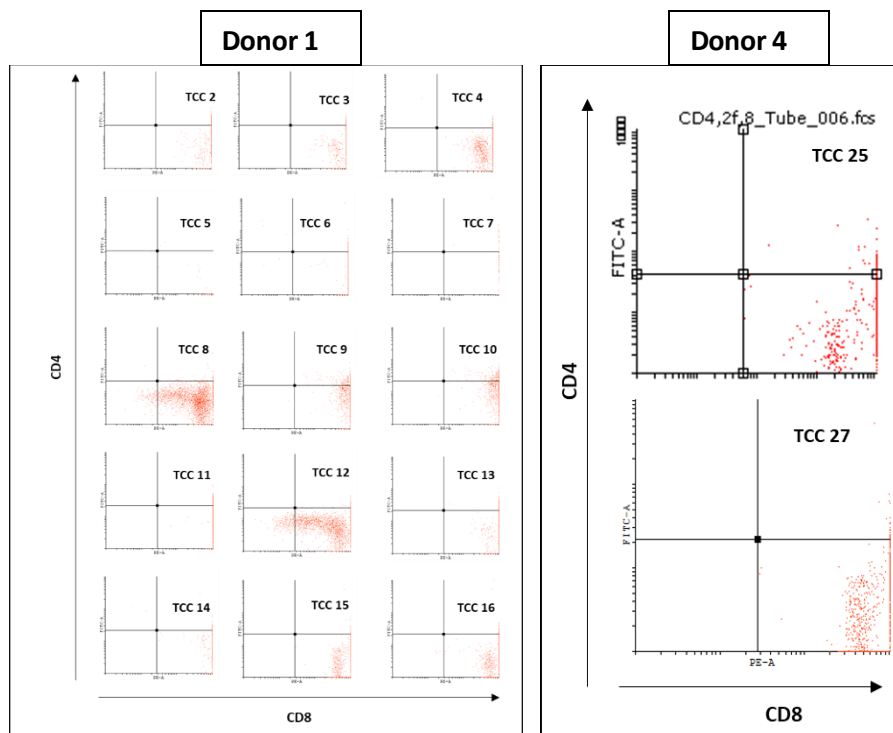
Figure 3.14. Representative phenotyping of responsive clones to analogue **H** from donors 1 and 4 (CD4-FITC/CD8-PE).

3.4.9. Analogues X and J

Due to the high number of responsive clones generated from each analogue a panel of representative clones from each donor were selected per analogue to undergo subsequent phenotyping and further experiments to test for antigen specificity.

3.4.9.1. Analogue X

From a total of 401 tested clones to analogue **X** across 2 healthy drug naïve donors expressing HLA-B*57:01, 99 were found to proliferate in the presence of the analogue on first testing, with some yielding SI values >50. (Control, 2824 ± 449.8 cpm: analogue **X** 35µM, 24050 ± 2574 cpm; $P < 0.0001$) (Figure 3.15).

A strong T-cell response was observed in clones generated from donor 1 incubated in the presence of analogue **X**. Cross reactivity to abacavir was also demonstrated (Figure 3.16). Clones generated from donor 4 presented a strong cross reactivity in the presence of abacavir; however, they only responded weakly to analogue **X**. T-cell activation was observed in differing magnitudes across the three responsive clones tested (Figure 3.16). All clones were phenotyped as CD8$^+$ (Figure 3.17).

a) i)

Analogue X			
Donor	**Donor 1**	**Donor 4**	**Total**
Clones Tested	216	185	401
Responsive on initial test	85	17	99
Percentage responsive	37.9%	9.2%	24.7%

ii)
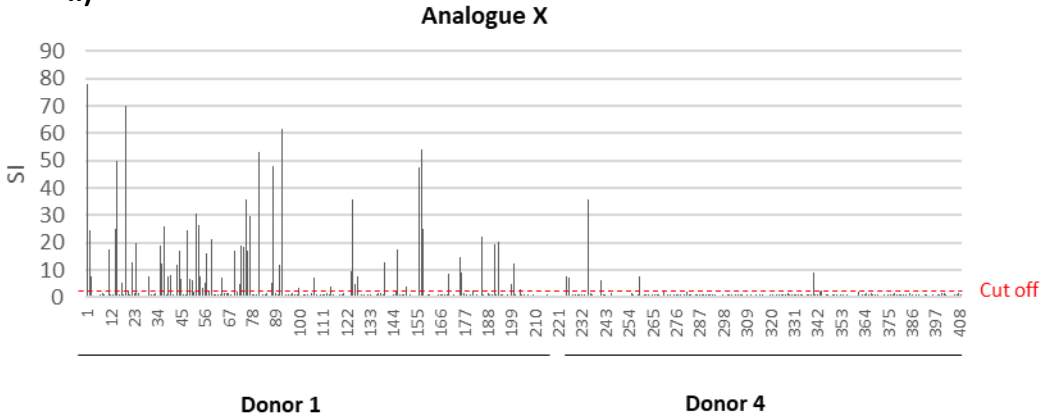
b)
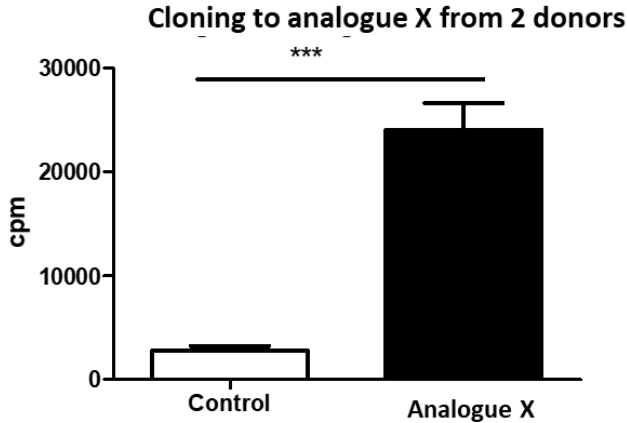
Figure 3.15. Generation of specific T-cell clones to analogue X from 2 HLA-B*57:01 donors. a) i) Table and ii) bar chart displaying number of responsive clones generated to analogue **X** from donors 1 and 4. b) Comparison of mean cpm values from all responsive clones to analogue **X**. Control (0), Analogue **X** (35µM). Data shown as mean of all responsive clones vs control ± SEM. Mann Whitney test used for comparison between control and drug treated values, *P<0.05, **P<0.01, *** P<0.001
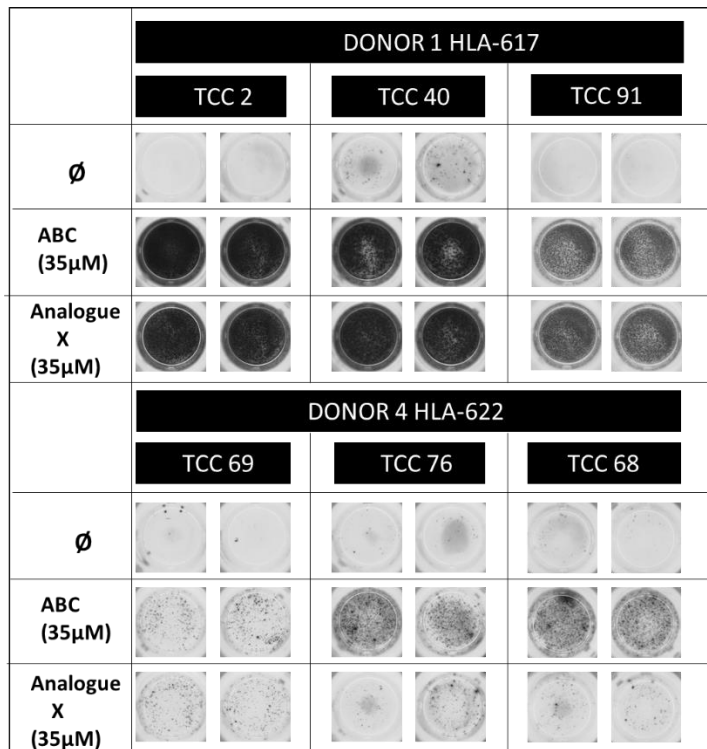
Figure 3.16. T-cell activity and cross reactivity of analogue X clones from donor 1 and 4. T-cell activation of clones specific to analogue **X** incubated in the presence of abacavir (35µM) and analogue **X** (35µM).
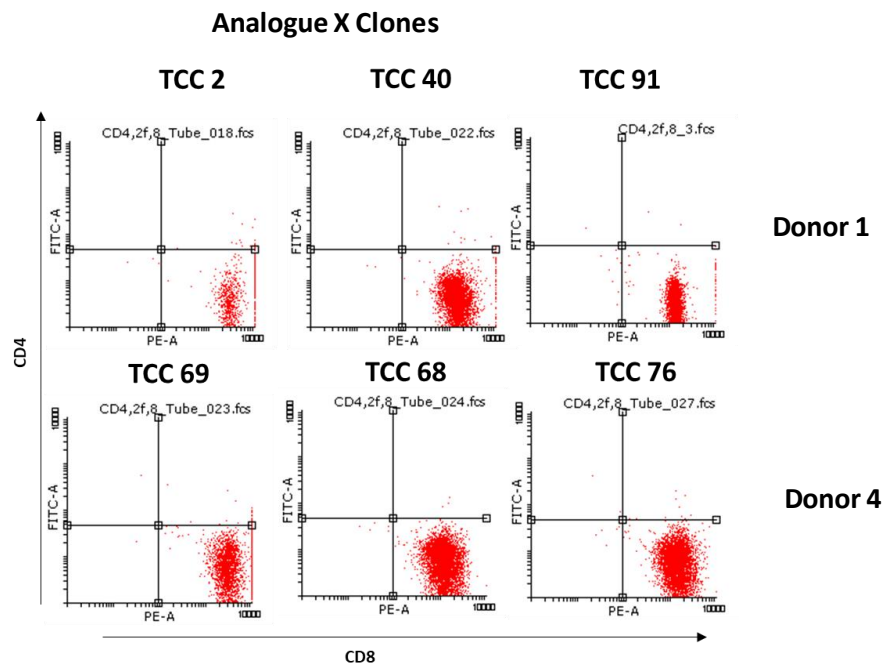
Analogue X Clones

Figure 3.17. Representative phenotyping of picked clones to analogue **X** from donors 1 and 4 (CD4-FITC/CD8-PE).

3.4.9.2. Analogue J

From a total of 282 tested clones to analogue **J** across 2 healthy drug naïve donors positive for the HLA-B*57:01 allele, 95 proliferated in the presence of the analogue on first testing some yielding SI values >100 (Control, 1799 ± 150.9 cpm: analogue **J** 35µM, 24860 ± 2533 cpm; *P*< 0.0001) (Figure 3.18).

Clones generated to analogue J presented an enhanced T-cell response when re-challenged with the analogue, while also demonstrating strong cross reactivity properties with abacavir. These findings were consistent across the two donors, although again clones generated from donor 1 were more reactive than donor 4 (Figure 3.19). However, the difference in IFN-γ secretion was far more modest between donors with analogue **J** than what was observed with analogue **X**. IFN-γ secretion from clones generated from donor 1 was immeasurable due to limitations with the ELIspot counting software and were assigned arbitrary values of 1000 SFU. All clones were phenotyped as CD8+ (Figure 3.19).

a)

Analogue J			
Donor	**Donor 1**	**Donor 4**	**Total**
Clones Tested	138	144	282
Responsive on initial test	66	29	95
Percentage responsive	47.8%	20.1%	33.7%

ii)

Analogue J

b)

Cloning to analogue J from 2 donors
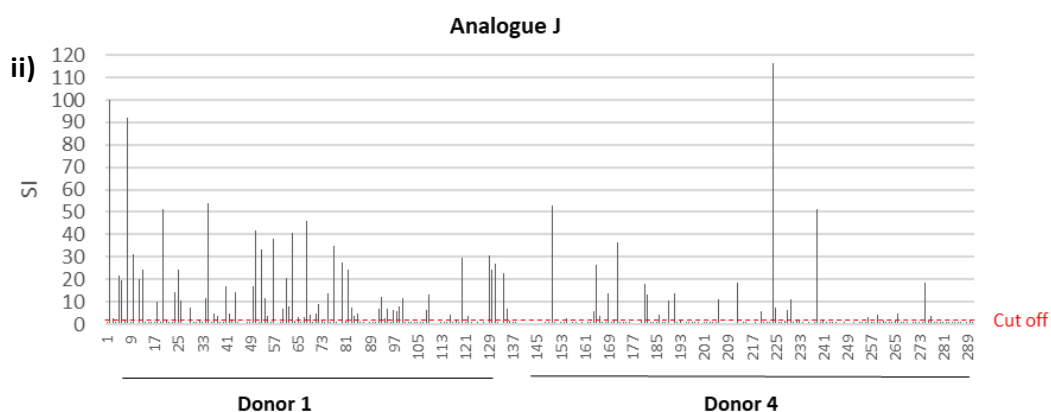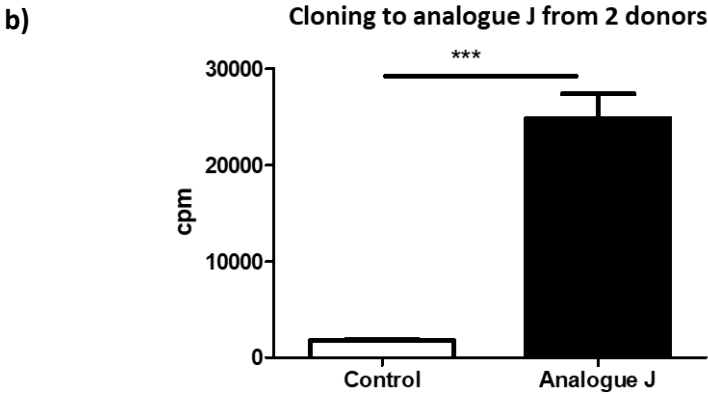
Figure 3.18. Generation of specific T-cell clones to analogue J from 2 HLA-B*57:01 donors. a) i) Table and ii) bar chart displaying number of responsive clones generated to analogue J from donors 1 and 4. b) Comparison of mean cpm values from all responsive clones to analogue J. Control (0), analogue J (35µM). Data shown as mean of all responsive clones vs control ± SEM Mann Whitney test used for comparison between control and drug treated values, *P<0.05, **P<0.01, *** P<0.001

a)
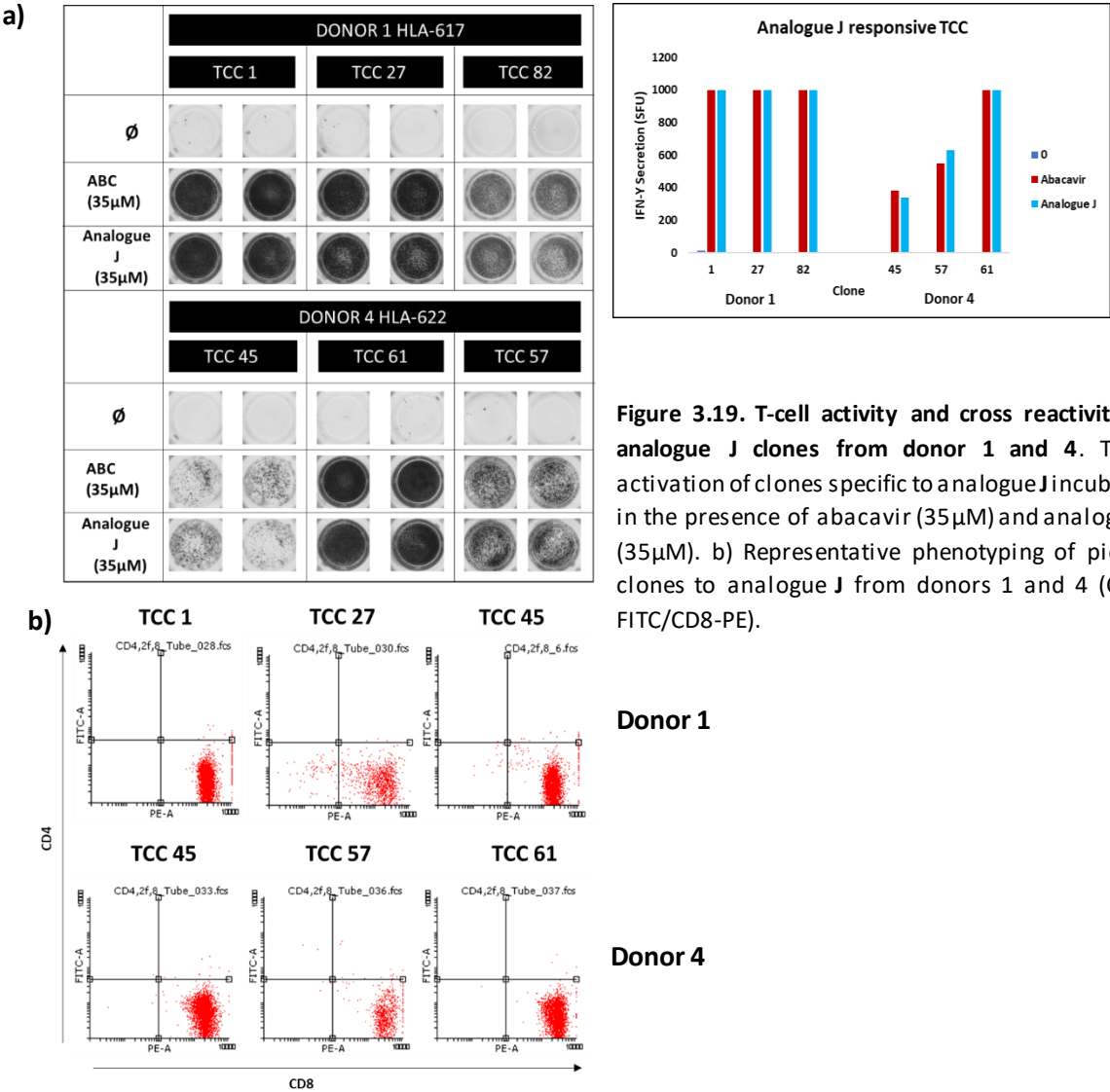
Figure 3.19. T-cell activity and cross reactivity of analogue J clones from donor 1 and 4. T-cell activation of clones specific to analogue J incubated in the presence of abacavir (35µM) and analogue J (35µM). b) Representative phenotyping of picked clones to analogue J from donors 1 and 4 (CD4-FITC/CD8-PE).

b)

3.5. Discussion

Hypersensitivity reactions to abacavir take place in 4-8% of individuals receiving the drug as a component of antiretroviral therapy (Mallal et al. 2008). Genotyping studies are now commonly employed to screen individuals for the HLA-B*57:01 risk allele as a safety measure prior to the commencement of abacavir therapy, with those testing positive excluded from the regimen.

The ability of abacavir to interact non-covalently within HLA-B*57:01 and induce a change in the repertoire of peptides displayed to T-cells on the surface of antigen presenting cells has been demonstrated (Ostrov et al. 2012; Illing et al. 2012; Norcross et al. 2012). Indeed, a distinct shift in the prevalence of peptides containing smaller amino acids including leucine, isoleucine and valine at the C-terminal of the peptide was discovered, while a marked reduction in the larger chain amino acids at the same position was also observed. Abacavir is thought to be responsible for this alteration in these self-peptides presented via its interactions within the F-pocket of HLA-B*57:01. These interactions induce a conformational change in the peptide binding groove via a reduction in the size of the F-pocket which accounts for accommodation of the smaller amino acids. It is also speculated that this alteration in the conformation of the peptide binding groove may still allow for the accommodation of peptides observed in the absence of abacavir, but in an altered conformation (Illing et al. 2013). As T-cells only display tolerance to the peptides which they are exposed to during their development in the thymus, exposure to these previously unseen peptides would be perceived as foreign epitopes and therefore initiate a CD8^{+} T-cell response (Illing et al. 2013; Illing et al. 2012). *Chessman et al.,* elegantly demonstrated the requirement for antigen processing and presentation pathways in abacavir-mediated CD8^{+} T-cell responses (Chessman et al. 2008), while the presence of another independent mechanism via direct interaction with the MHC T-cell receptor has also been reported (Bell

et al., 2013). Indeed, clones that utilise both mechanisms of T-cell activation were incorporated into this study.

Here we investigated the possibility of generating safer alternative compounds to abacavir via the modification of the 6-amino cyclopropyl moiety, demonstrated to be imperative for the interaction within HLA-B*57:01 to alter the peptide repertoire. For this study fourteen abacavir analogues were synthesised around the azetidine ring group, a stable structure allowing for the construction of further substituted analogues (Figure 3.4.) (Daluge *et al.*, 1997; Faletto *et al.*, 1997).

Replacement of the cyclopropyl moiety with structural variants around the azetidine group revealed differential effects on both antiviral and T-cell activity of the compounds. Replacement with the azetidine ring alone, while having an equivalent antiviral potency to abacavir, resulted in the activation of CD8$^+$ T-cells in all abacavir clones tested, while addition of a nitrile group at the 3-position of the azetidine ring was sufficient to abrogate the T-cell response. Similar to previous results the addition of branched chains again resulted in the loss of T-cell responses (Naisbitt et al. 2015), however this was only observed when added to the 3-position of the azetidine ring (**B**, **F, I** and **M**) not at the 1-position (**A** and **C**). Interestingly, the addition of a fluoride group at the 3-position of the azetidine ring (**H**) resulted in a T-cell response in abacavir-specific clones only at the higher concentration of 50μM, while possessing equipotent antiviral activity to abacavir (EC$_{50}$ 2.456μM).

While many compounds lacking the propensity to induce T-cell activity retained antiviral activity, none were as active as abacavir itself. Based on these findings, our next strategy was to employ a selection of these analogues as molecular probes to gain a greater understanding of their binding and interactions within HLA-B*57:01 and its relationship with T-cell activation. From the T-cell non-activating analogues, **G** and **M** were selected along with analogue **X** from the series of abacavir analogues published by *Naisbitt et al 2015*. Analogues

G and **M** were unable to stimulate T-cell activity in abacavir clones, whilst also having reduced cytotoxicity compared to abacavir in all cell lines. However, the antiviral profile of these analogues (EC_{50} 38.55 and 33.67µM respectively) was around 15-fold lower than abacavir (EC_{50} 2.05µM). Co-incubation with analogue **X** again failed to stimulate T-cell activity in the ELIspot assay. While the analogue retained antiviral activity it was to a lower level than abacavir (Naisbitt et al. 2015).

Molecular modelling of the analogues revealed a distinct relationship between the binding of the compounds within HLA-B*57:01 and the ability to activate of CD8^{+} T-cells. Analogues **G**, **M** and **X**, all incapable of promoting T-cell responses, bound HLA-B*57:01 in a manner that yielded the presence of unfavourable steric clashes between the functional groups of the compounds and the amino acid residues of both the HLA-binding peptide and residues within the F-pocket itself such as the Tyr-123. No such clashes were observed with the analogues capable of activating T-cells (**D** and **H**) or abacavir itself (Figure 3.8). The presence of these clashes particularly with the HLA-binding peptide in the presence of the non-activating analogues indicates their inability to bind HLA-B*57:01 and form a complex with HLA-binding peptide (pep-v). Conversely analogues **D** and **H** demonstrated a binding pose within HLA-B*57:01 with sufficient affinity to induce conformational changes within the F-pocket allowing for the presentation of the altered self-peptides identified by *Illing et al (2012), Norcross et al (2012) and Ostrov et al (2012)*. This indicates the potential for using molecular modelling as a screening tool to study the binding of compounds within HLA proteins to investigate their effect on T-cell activation. However, as only one HLA-binding peptide (pep-V) was employed for this analysis, future studies must consider the incorporation of a wider range of HLA-binding peptides, terminating in a broader range of amino acids, as well in alternate conformations as uncovered by recent studies, to uncover whether a similar relationship exists (Illing et al. 2013).

To investigate the effect of the abacavir analogues on the self-peptides presented to T-cells on the surface of the antigen presenting cell, peptide elution studies from HLA-B*57:01 were conducted and analysed via mass spectrometry. Analogue **X** underwent peptide elution assays in triplicate due to its availability in high quantities. Analogues **D**, **H** and **M** were available in much lower quantities and therefore around 10mg of each was used for these experiments allowing for the assay to be carried out in singlet. Peptide elution studies were not conducted on analogue **G** due to limited quantities of the compound available.

Consistent with previous findings, co-incubation with abacavir induced strong enrichment of small chain amino acids isoleucine and leucine at the C-terminal of the peptide (Illing et al. 2012; Norcross et al. 2012; Ostrov et al. 2012). A decrease in the prevalence of arginine and lysine at the Ω-2 position was noted in the presence of abacavir, which is thought to be caused by the blocking of interactions between constitutive peptides and the Asp-114 amino acid by the binding of abacavir. When all peptides eluted from HLA-B*57:01 were taken into consideration for analysis in the presence of the individual analogues, no significant change was observed in the prevalence of the small amino acids at the C-terminal position when compared to untreated cells (Figure 3.9 a)). However, removal of peptides eluted from untreated cells from consideration revealed a shift in the prevalence of amino acid isoleucine at the C-terminal position in the presence of analogues **D** and **H**, both known to have T-cell activating capabilities. No such increase was observed in the presence of the analogues that lacked the ability to activate T-cells (**M** and **X**). Of the peptides eluted in the presence of analogue **D**, 67 displayed overlap with those eluted from HLA-B*57:01 in the presence of abacavir both in this study and previous studies (Illing et al. 2012) while 43 were peptides unique to the analogue. This overlap was again observed in the presence of analogue **H** however to a lesser degree than **D**, 36 peptides observed with abacavir and 47 unique to analogue **H**, which may explain why T-cell activation was observed in analogue **H** only at

higher concentrations. While overlap of the peptides observed in the presence of abacavir was seen with analogues **X** and **M**, most terminated with a larger amino acid residue such as methionine, phenylalanine or tryptophan which would not typically be accommodated by an altered conformation of the peptide binding groove. Enrichment of C-terminal alanine was observed in the presence of analogue **X**, some of which overlapped with alanine terminating peptides detected in the presence of abacavir. These studies demonstrate that the introduction of branched chains to the functional group of abacavir by way of isopropyl (**X**) or trifluoromethyl (**M**) is sufficient to abrogate the cross-reactivity in abacavir-responsive T-cell clones. Introduction of these functional groups results in a reduction in the binding affinity of the compound within HLA-B*57:01 resulting in an inability to induce the presentation of an altered peptide repertoire to T-cells. On the other hand, the introduction of the azetidine ring alone or an azetidine linked fluoride group resulted in a degree of T-cell activation. These analogues bind with sufficient affinity to induce an alteration in the peptide repertoire presented to T-cells by HLA-B*57:01. The degree of T-cell activation in the presence of these analogues was for the most part less than abacavir, which is likely due to the lower number of peptides eluted with the C-terminal isoleucine when compared to abacavir.

The CD8$^+$ mediated T-cell activity in the presence of the abacavir analogues was observed in memory T-cells with specificity to abacavir, thereby indicating a cross reactivity profile of the clones. We next sought to confirm the safety of the abacavir analogues via the generation of analogue specific memory T-cells from PBMCs of the same HLA-B*57:01$^+$ donors, which had not been previously examined. T-cell cloning was carried out with four separate analogues, two with a T-cell activation profile (**H** and **J**) and two unable to activate T-cells (**G** and **X**). No specific clones were generated to analogue **G** across the two HLA-B*57:01 positive donors.

This confirms the addition of an azetidine linked nitrile group does not activate T-cells *in vitro* and would be unlikely to if administered to patients.

Unsurprisingly, cloning to the analogues that possessed T-cell activation properties (**H** and **J**) in abacavir clones, yielded a plethora of analogue specific T-cell clones that displayed strong T-cell activation in response to the respective analogues and also abacavir itself. These responses were observed at lower concentrations of both the analogue and abacavir, consistent with previous observations with abacavir-specific clones (Bell *et al.*, 2013; Naisbitt *et al.*, 2015) (Figure 3.12-3.13).

Importantly, cloning to analogue **X**, to our surprise, yielded an abundance of responsive clones with strong T-cell activity to both analogue **X** and abacavir in donor 1 (HLA-0617). Similar results were observed in donor 4 (HLA-0622), with some clones displaying enhanced responses to abacavir than analogue **X**. It was interesting to find such responsive clones primed to analogue **X** based on their lack of T-cell activity in abacavir clones in studies conducted both in this chapter and previous studies (Naisbitt et al. 2015). As previously mentioned, abacavir induced an increase in HLA-B*57:01 peptide ligands terminating in isoleucine (Illing et al. 2012; Norcross et al. 2012; Ostrov et al. 2012). However, unlike analogues **D** or **H**, analogue **X** induces an enrichment of 9-12 mer peptides terminating in the amino acid alanine (Figure 3.9) while 110 of the peptides eluted from HLA-B*57:01 in the presence of this analogue are also prevalent in the presence of abacavir. Given that alanine terminating peptides constitute a smaller part of the observed abacavir induced repertoire it was not surprising that cross-reactivity was absent with abacavir specific T-cell clones in the presence of analogue **X**. In contrast, clones raised to analogue **X** were cross-reactive to abacavir, suggesting that the outgrown specificities fall within the abacavir repertoire. Indeed, the successful generation of analogue **X**-abacavir-reactive T-cell clones when priming to analogue **X** is consistent with a limited repertoire perturbation which seems to partially

overlap with the abacavir induced repertoire. Indeed, HLA-modelling of analogue **X** with an alanine terminating peptide would likely not yield clashes with the isopropyl group, warranting further study. As these results were unexpected, they indicate the importance of using of T-cell cloning in the assessment of the safety profile of a drug such as abacavir.

These studies demonstrate the ability to generate compounds which are devoid of the ability to induce T-cell activation but retain some antiviral activity via the modification of the 6-amino cyclopropyl moiety of abacavir. Furthermore, the use of a panel of these compounds as molecular probes provided considerable insight into the relationship between the binding of a compound within HLA-B*57:01 and the observed T-cell response. We also acknowledge the initially surprising findings in clones generated specifically to analogues with no T-cell activating properties with abacavir clones such as analogue **X**, where we saw considerable activation in response to this compound and abacavir itself. Taken together the findings in this chapter demonstrate the importance of a holistic approach to the design, manufacture and subsequent testing of a compound for efficacy and safety (Figure 3.2), employing the use of *in vitro* and *in silico* methods to further our own understanding of drug immune receptor binding.

Chapter 4 – An investigation into the impact of drug chirality on the induction of abacavir-specific CD8+ T-cell activity.

4.1 Introduction

The interaction of abacavir within the antigen binding cleft of HLA-B*57:01 is postulated to induce alterations in the shape and chemistry of the peptide binding motif. This causes a reduction in size of the F-pocket, allowing for the accommodation of smaller C-terminal anchors such as valine, leucine and isoleucine compared to the more conventional larger chain amino acids phenylalanine and tryptophan (Illing et al. 2012; Ostrov et al. 2012; Norcross et al. 2012). *Naisbitt et al 2015* elegantly generated pharmacologically active analogues of abacavir devoid of T-cell activation properties, via the introduction of N-linked branched carbon chains. Subsequent molecular modelling revealed unfavourable binding characteristics of these analogues within the antigen binding cleft of HLA-B*57:01, characterised by the presence of steric clashes between the analogues functional groups, the HLA-binding peptide, and amino acids within the F-pocket (Naisbitt et al. 2015).

This concept was further explored in chapter 3. Fourteen new abacavir analogues were constructed around variants of the azetidine ring, a stable chemical structure allowing for analogue synthesis but also displaying favourable antiviral activity (Daluge *et al.*, 1997). Although, some azetidine derivatives did not activate T-cells, these compounds did not possess the same antiviral activity as abacavir. Conversely, some compounds exhibited strong antiviral activity, but interacted with HLA-B*57:01 evoking T-cell responses. These data led us to synthesize additional of further chemical structures to further probe the drug binding HLA-B*57:01 interaction.

Chirality is the property of an object which is non-superimposable with its mirror image, with compounds of this nature often referred to as stereoisomers or enantiomers. While these compounds show an identical arrangement of bonds connecting their atoms, the relative orientation of these atoms in space differs greatly.

Mirror Image
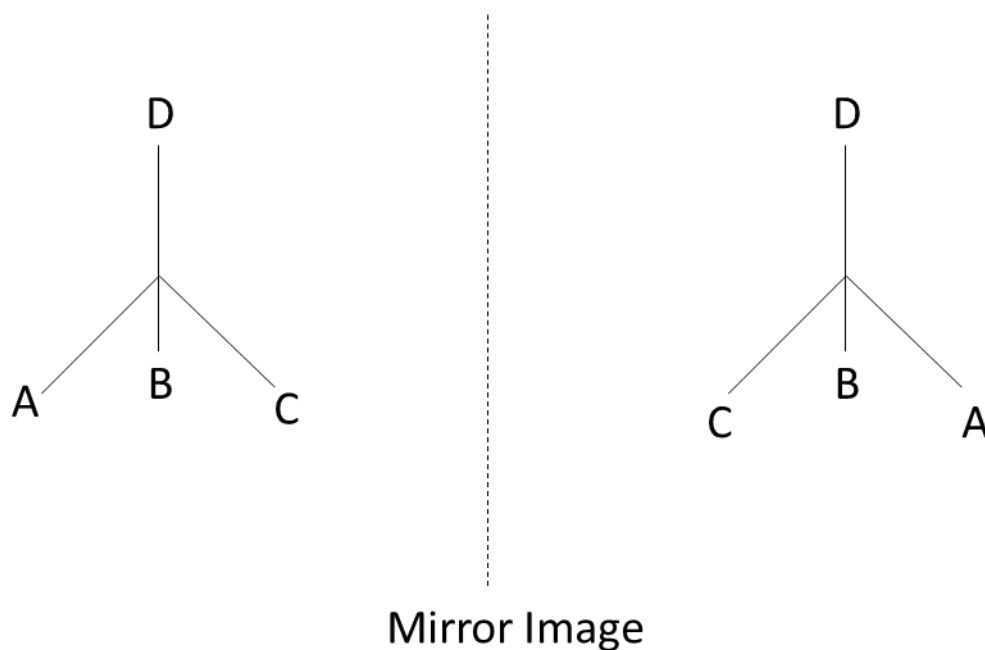
Figure 4.1 Chiral variants of a chemical structure.

With respect to their biological activity, enantiomers differ at both the quantitative and qualitative levels. Enantiomers may possess a plethora of biological properties in one conformation while being biologically inactive in the other. These differences can arise from differential interaction of the enantiomers with their given receptors, but also due to different pharmacokinetic effects such as protein binding, metabolism and transport (Nguyen et al. 2006; Triggle 1997).

In basic terms, for a drug to interact with a receptor its functional components must interact with the corresponding regions of the drug binding site. As can be seen in Figure 4.2, while one enantiomer is able to interact with corresponding sites on a receptor, the alternative enantiomer is not, due to the inappropriate alignment of the corresponding binding groups, inevitably leading to loss of the drugs action.
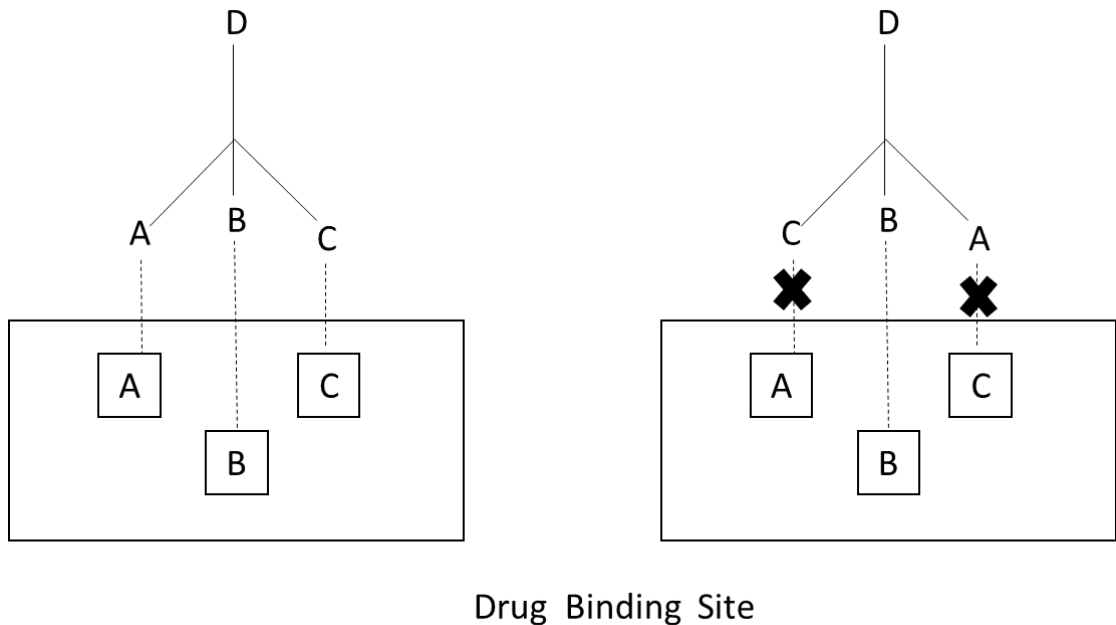
Drug Binding Site

Figure 4.2 Interaction between 2 enantiomers of a chiral drug and its binding site. *(Adapted from McConathy and Owens 2003).*

The enantiomeric specific side or toxic effects of drugs is well documented, the most infamous relating to treatment with the antiemetic sedative drug thalidomide, commonly prescribed in the 1960's to pregnant women as a treatment for morning sickness. Treatment with this drug resulted in serious birth defects in the offspring, associated with severe limb bud abnormalities and teratogenesis, a prime example of a type G ADR. It was found that while the R-stereoisomer of thalidomide was responsible for the sedative effects, the S-stereoisomer accounted for the induction of the severe birth defects observed (Chamberlain et al. 2014; Cuthbert et al. 1962). However, due the racemic nature of thalidomide in solution, allowing for the spontaneous conversion between the 2 enantiomeric variants, the generation of a stable stereoisoform of the drug was not possible (Vargesson 2015).

A relationship between a compounds potency and its chiral state has been demonstrated across a variety of drugs. The antidepressant drug citalopram functions via the antagonistic

block of serotonin reuptake, however the S conformation displays a pharmacological potency of around 30 times greater than the R counterpart (Koldsø et al. 2010).
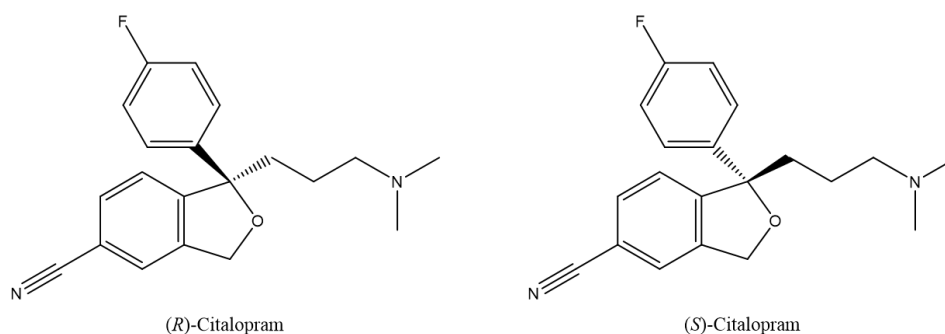
Figure 4.3. R and S conformations of citalopram.

Similarly, calcium channel antagonists such as verapamil also demonstrate enantiomeric specific pharmacological potency. Verapamil's vasodilatory properties are 10-20 times more potent in the S conformation (Satoh et al. 1980; Echizen et al. 1988). However, verapamil displays useful properties as a therapeutic agent in cancer chemotherapy, this requires use at high concentrations which are often associated with cardiotoxicity. Thus, for this medication it is the R isomer of verapamil which exhibits far lower cardiotoxicity than the S isoform, indicating differing uses for the same drug based on its chiral state (Nguyen et al. 2006; Satoh et al. 1980; Echizen et al. 1988).

The stereoisomerism of a compound has a bearing on its pharmacological action; however, this is not always a consequence of receptor binding and may be down to other pharmacological properties such as metabolism or toxicity (Triggle 1997; Nguyen et al. 2006).

The antidepressant fluoxetine displays similar levels of potency in the R and S conformations in the setting of its primary pharmacological actions; however, these enantiomers undergo different routes of metabolism (Cârcu-Dobrin et al. 2017). As such, the plasma levels of R-fluoxetine are less variable than the S isoform. R-fluoxetine and its metabolites inhibit CYP2D6 to a greater degree than S-fluoxetine and in Phase II studies the R isoform of the

drug at high concentrations resulted in prolonged cardiac repolarization leading to arrhythmia, something not observed in the S conformation (DeVane & Boulton 2002).

Other examples of enantiomeric specific pharmacology include the local anaesthetic bupivacaine which in the R isoform exhibits a systemic toxicity 50% more frequently than the S isoform. Cardiotoxicity caused by direct actions of the drug on the myocardium is the most common ADR (Huang et al. 1998). Additionally, ketamine in the S and R conformations differ in both pharmacokinetic and pharmacodynamic properties. The S stereoisomer of the drug is around 3 times more potent at its desired pharmacological target than its R counterpart. However, the S isoform is known to be a primary contributor to direct stimulation of cardiovascular tissues and has a much greater clearance rate than the R isoform, indicating the presence of enantiomeric-selective hepatic metabolism (Muller et al. 2016; Zeilhofer et al. 1992; Nau & Strichartz 2002). Similar enantiomeric specific adverse effects exist with the bronchodilator drug albuterol. R-albuterol exerts bronchodilatory and anti-inflammatory effects including the inhibition of T-cell proliferation as well as the impediment of goblet cell hyperplasia and mucus occlusion of the airways (Henderson et al. 2005), although these effects can be negated in the presence of the S-isoform (Baramki et al. 2002). Conversely, the S-enantiomer of albuterol firstly exerts bronchodilatory actions to a far lesser degree than the R isomer, but is also associated with proinflammatory actions such as the secretion of IgE induced histamine and IL-4, something completely absent with the R-isoform (Cho et al. 2001; Henderson et al. 2005).

In 2005 *Naisbitt et al* carried out studies using the oral anticoagulant phenindione which is associated with hypersensitivity reactions in up to 3% of patients. Drug-responsive T-cell clones generated specifically to phenindione produced proliferative responses when incubated in the presence of the drug. Of the four drug-responsive T-cell clones, three proliferated in response to the S stereoisomer of the alternate anticoagulant agent warfarin

and interestingly, one clone responded to warfarin in its R conformation. These data indicate that the enantiomeric-specific activation of T-cells by drugs is possible in hypersensitive patients (Naisbitt et al. 2005). Therefore, the use of chiral variants of the same structure presents as an interesting concept for investigating the safety of abacavir analogues in T-cell assays.

One obvious drawback of the T-cell cloning assay for the screening of a compounds safety, with regard to T-cell activation, is the time period required to concisely carry out the assay. On average T-cell cloning to a compound takes 6-8 weeks to fully generate responsive T-cell clones, which can lead to various issues with cells being in culture for such long periods of time. Also, if cell growth during cloning is low, restimulation with PBMC feeder cells requires a minimum of two weeks before cells can be tested. Therefore the exploration of other assays for the screening of compounds in a more timely manner is at the forefront of research. One such assay is the dendritic cell (DC) T-cell priming assay developed (Faulkner et al. 2012) and further optimised (Faulkner et al. 2016) to detect drug-specific responses from naïve T-cells co-incubated with autologous dendritic cells and a drug for a period of 8-14 days before restimulation with the drug and fresh DCs. Drug-specific T-cell responses can then be quantified using a variety of readouts. This assay demonstrated robust responses to a variety of drugs including SMX-NO, piperacillin, carbamazepine and the reactive species Bandrowski's base. However, no responses were detected with abacavir (Faulkner et al. 2016). Further refinement of the T-cell priming assay has been undertaken in recent years to consider responses from individual wells rather than a mean response across all wells, this is known as the T-cell multi-well assay (T-MWA). Therefore, use of this assay was undertaken to examine individual responses in naïve T-cells isolated from healthy drug naïve donors expressing the HLA-B*57:01 allele co-incubated with abacavir and DCs for 14 days. Should responses be found, abacavir substituted analogues could be incorporated into the assay to

provide a screening protocol in a much reduced period of time compared to conventional T-

cell cloning.

4.2 Aims

In this chapter, we further investigated the ability to remove the undesirable CD8^{+} T-cell stimulatory capacity of abacavir in HLA-B*57:01 positive individuals, while retaining the antiviral potency of the drug. For these studies, four further abacavir analogues were synthesised with substitutions in place of the 6-amino cyclopropyl moiety of the compound, consisting of structural variations around the open ring form of azetidine. Of these four newly synthesised analogues, two were structural enantiomers of the same compound. We investigated the safety of these compounds by analysing their T-cell induction abilities, along with their cellular toxicity profiles and antiviral activity. Again, using the four analogues as molecular probes and an enantiomer of abacavir, we aimed to investigate the binding of the compounds within the antigen binding cleft of HLA-B*57:01 and its relationship with the induction of T-cell activity. Finally, we examined the use of the T-cell multi-well assay for the screening of abacavir-induced T-cell responses.

4.3 Methods

4.3.1 Materials

Abacavir was received as a gift from GlaxoSmithKline (GSK). Human AB serum and foetal bovine serum were obtained from Innovative Research (Michigan, USA) and Invitrogen (Paisley, UK), respectively. Interleukin-2 (IL-2) was purchased from Peprotech (London, UK). Multisort bead separation kits were supplied by Miltenyi Biotec (Surrey, UK). Antibodies for staining were purchased from BD Biosciences (Oxford, UK). ELISpot kits including the coating and detection antibodies, streptavidin alkaline phosphate conjugate and BCIP/NBT substrates were purchased from Mabtech (Stockholm, Sweden). Other reagents were purchased from Sigma-Aldrich (Dorset-UK) unless otherwise stated.

4.3.2 Cell Culture Medium

Cell culture medium for T-cells (R9) is composed of RPMI supplemented with 10% human AB serum, HEPES (25mM), penicillin (1000 U/mL), streptomycin (0.1mg/mL), L-glutamine (2mM) and transferrin (25μg/mL).

EBV transformed B-cells were cultured in F1 medium composed of RPMI supplemented with 10% foetal bovine serum, HEPES (25mM), penicillin (1000 U/mL), streptomycin (0.1mg/mL) and L-glutamine (2mM).

4.3.3. Generation of abacavir responsive T-cells.

CD8$^+$ T-cell cloning was carried out as described in detail in section 2.3.5 using PBMCs from HLA-B*57:01 positive donors selected from our established HLA-typed healthy donor cohort.

4.3.4 Testing clones for antigen specificity

Approximately four weeks after beginning the serial dilutions abacavir-specificity was measured by assessing cell proliferation in the presence of the drug as described in section 2.3.6. Following two-week mitogen expansion of responsive abacavir clones, the antigen specificity to abacavir was confirmed via analysis of IFN-γ secretion in response to the drug using the ELIspot assay as described in section 2.3.7.

4.3.5 Synthesis of abacavir analogues

The initial part of the project involved the synthesis of a stock sample of compound **1** (Figure 3.1). With 2g of this chiral compound in hand, synthesis of the four target molecules (O-R) was completed (Appendix section 3).

Compound 1 (564.55 μmol, 1.00 *eq*), amine (2.00 *eq*) and N, N-diisopropylethylamine (145.92mg, 1.13 mmol, 2.00 *eq*) were taken up into a microwave tube in isopropyl alcohol (2.00mL). The sealed tube was heated at 70 °C for 2 hours under microwave. MS showed that the starting material was consumed completely. The mixture was concentrated in vacuum to give crude product.

Due to structural irregularities in MS data (appendix chapter 3), analogue O was removed from further assays.

Intermediate 1   **Analogues O-R**
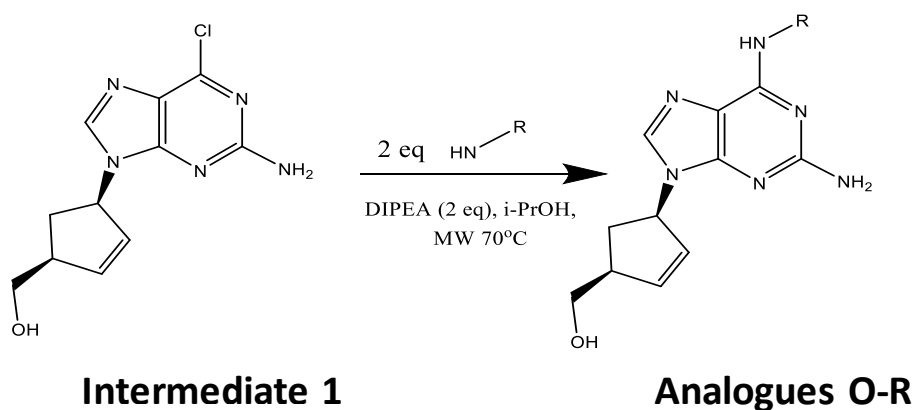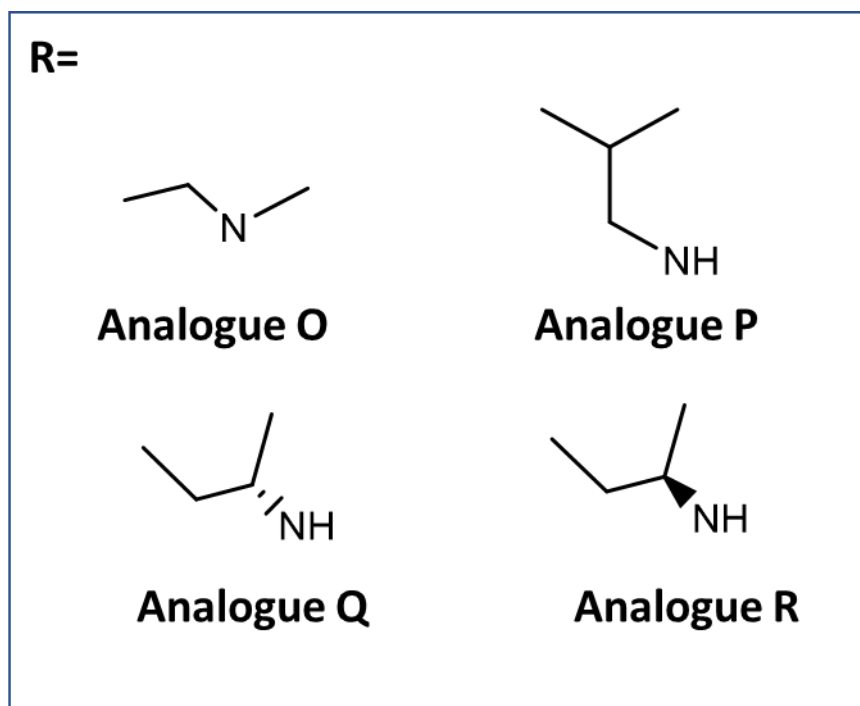
Figure 4.4. Synthesis and structures of abacavir analogues O-R.

4.3.6 Inhibition of T-cell and B-cell proliferation

To ascertain the effect of the compounds on cellular proliferation, the abacavir analogues were cultured in the presence of EBV transformed B-cells or PBMCs at concentrations of 0-250μM, with abacavir as a comparator as described in section 3.3.7.

4.3.7 CD8+ T-cell activity of abacavir analogues

To measure the effect of modifying the 6-amino cyclopropyl group of abacavir with regards to T-cell induction, T-cell clones ($5x10^4$/50μL) were incubated with autologous EBVs ($1x10^4$/50μL) in the presence or absence of the three abacavir substituted analogues (10, 20, 50μM) (total volume 200μL/96 well U-bottomed plate) for a period of 48 hours and IFN-γ secretion was assessed via ELIspot as described in detail in section 2.3.7.

The activity of some analogues in T-cell clones was also assessed using the proliferation assay. T-cell clones ($5x10^4/50\mu L$) were cultured in a 96 well U-bottomed plate in the presence of irradiated autologous EBVs ($1x10^4/50\mu L$) in the presence of abacavir or the substituted analogues at varying concentrations for a period of 72 hours ($37^{\circ}C$; 5% CO_2) (total volume $200\mu L$/96 well U-bottomed plate). Cells incubated with R9 medium alone were used as a negative control. Tritiated thymidine ($0.5\mu Ci$/well) was added for the final 16 hours. Cells were next harvested onto a filter mat and T-cell proliferation was assessed via scintillation as described in section 2.3.6.

4.3.9 HLA-B*57:01 molecular modelling

The binding conformations of the four abacavir analogues were modelled within HLA-B*57:01 using the same protocol as described in section 3.3.9.

4.3.10 Antiviral activity and cytotoxicity of abacavir analogues

4.3.10.1 Antiviral activity

Analysis of the antiviral activity of the abacavir analogues was conducted using HIV-1 IIIB infected MT-4 cells by the WuXi App Tech company in Shanghai as described in section 3.3.6.1.

4.3.10.2 Cytotoxicity

The cytotoxicity of the analogues was assessed as described in section 3.3.6.2.

4.3.11 Magnetic bead separation of naïve T-cells.

CD14$^+$ cells were isolated via positive selection from the total PBMC population using magnetic beads and columns according to the manufacturer's instructions (Miltenyi Biotech, Surrey-UK). For isolation of naïve T-cells, a pan negative T-cell separation was performed on

the non-CD14$^+$ fraction of the cells, using anti-T-cell antibody cocktail. CD3$^+$ T-cells, obtained via negative selection, were then subjected to positive selection for Treg (CD25$^+$) and memory T-cells (CD45RO) with naïve T-cells being obtained via negative selection (CD3$^+$, CD25$^-$, CD45RO$^-$, CD45RA$^+$).

4.3.12 T-cell multi-well priming assay

PBMCs from two healthy, abacavir naïve, HLA-B*57:01 positive donors (HVN-021 and HVN-158, Table 2.1) were isolated via density centrifugation as described in section 2.3.3 and cells were sorted via magnetic bead separation as described in section 4.3.14. For the generation of dendritic cells, CD14$^+$ cells were isolated via positive selection and grown for 7 days in the presence of GM-CSF (800U/mL) and IL-4 (800U/mL). Dendritic cells were matured overnight in the presence of LPS (1µg/mL) and TNF-α (50ng/mL) prior to use. Mature dendritic cells (8x10^3 cells/well) were co-cultured in a 96-well plate with naïve or memory T-cell (2x10^4 cells/well) in the presence of abacavir (35µM). Cells were incubated for a period of 12-14 days with R9 medium used as a negative control. Following incubation, cells were washed three times and stimulated with abacavir (35µM) for a further 2 days. Cells were then tested for abacavir-specific T-cell activation using proliferation as a readout via ^{3}H thymidine incorporation (Section 4.3.9). The cpm values of the R9 wells were averaged and each individual well cpm of abacavir treated cells was divided by this value to yield an SI. SI values of 1.5-.1.9, 2.0-3.9 and 4 and above were considered low, moderate and high responses respectively.
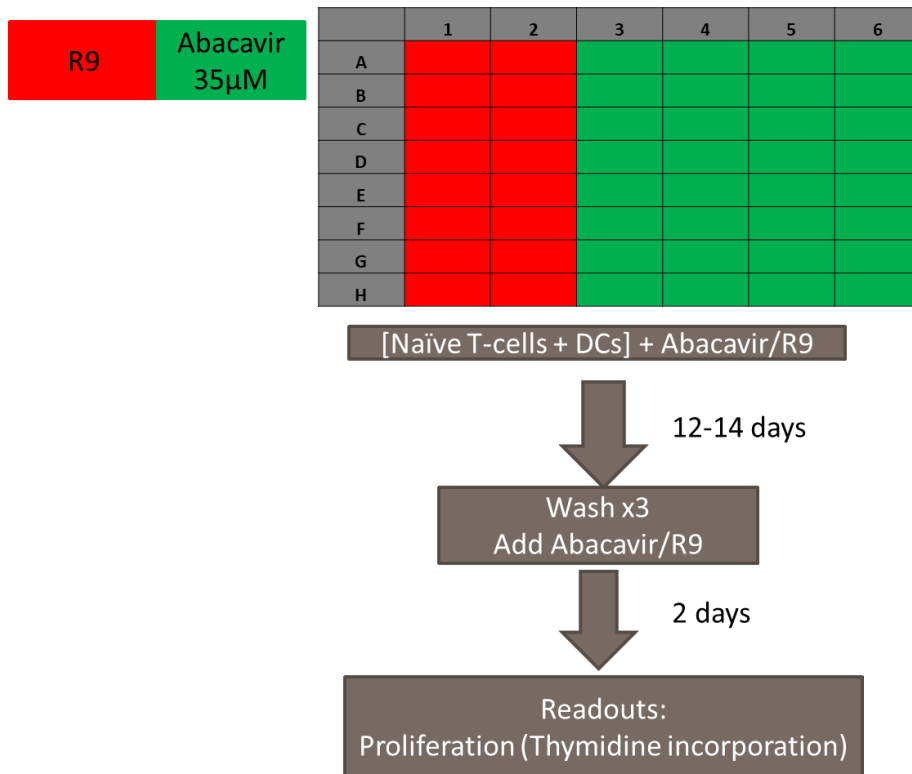
Figure 4.5. Schematic of T-cell multi-well priming assay. Isolated naïve T-cells are co-incubated with DCs in the presence or absence of abacavir for 12-14 days. Next cells are washed three times and fresh abacavir or R9 medium was added for a further 2 days. Finally ^{3}H thymidine was added for a further 16 hours and cellular proliferation was assessed.

4.3.13 Statistical analysis

For comparison between control and test values in proliferation assays the Mann-Whitney test was used. Two way ANOVA was used for comparison between mean abacavir and analogue values in ELIspot assays.

4.4. Results

4.4.1 Generation of abacavir-specific T-cell clones

From a total of 2279 seeded cells across four HLA-B*57:01 positive donors, 101 were found to proliferate in the presence of abacavir on first testing, (Control, 1665 ± 188.5 cpm: abacavir 35µM, 6940 ± 729 cpm; P< 0.0001). Comparison of average cpm, confirmation of antigen specificity and subsequent cellular phenotyping is presented and discussed in chapter 2. The abacavir responsive T-cell clones used in this chapter are outlined in Table 4.1.

Donor 1: HLA-0617	Donor 3: HVN-0158	Donor 4: HLA-0622
TCC 27	TCC 51	TCC 79
TCC 70	TCC 60	TCC 86
TCC 3 *	TCC 65	TCC 100
TCC 20 *		TCC 105

Table 4.1 Abacavir responsive CD8+ T-cell clones from three HLA-B*57:01 positive donors used in this chapter. * Clones generated to abacavir + natural peptide 15, these clones demonstrated a strong response to abacavir and were incorporated into T-cell analogue assays. Second test data and phenotyping for these clones is found in chapter 5.

4.4.3 Inhibition of T-cell and B-cell proliferation by abacavir and abacavir analogues

To investigate if the abacavir analogues inhibited lymphocyte proliferation via direct toxic effects, PBMCs and EBV-transformed B-cells (1×10^5/well) were incubated in the presence of the analogues at concentrations of 0-250μM, with abacavir used as a comparator. T-cell and B-cell proliferation was inhibited by abacavir in a dose-dependent manner, generating respective IC_{50}'s of 66.7μM and 94.6μM (Table 4.2). Analogue **P** demonstrated a dose-dependent inhibition of B-cell and T-cell proliferation yielding IC_{50}'s of 91.8μM in PBMCs, 157μM in B-cells. Co-incubation with analogue **Q** resulted in inhibition of proliferation at higher concentrations than with abacavir in both T-cells (IC_{50} 162μM) and B-cells (IC_{50} 129μM). Furthermore, analogue **R** inhibited proliferation of T-cells with an IC_{50} of 93μM while inhibition of proliferation in B-cells in the presence of **R** was not detected within the range of concentrations used ($IC_{50} > 250$μM) (Table 4.2).
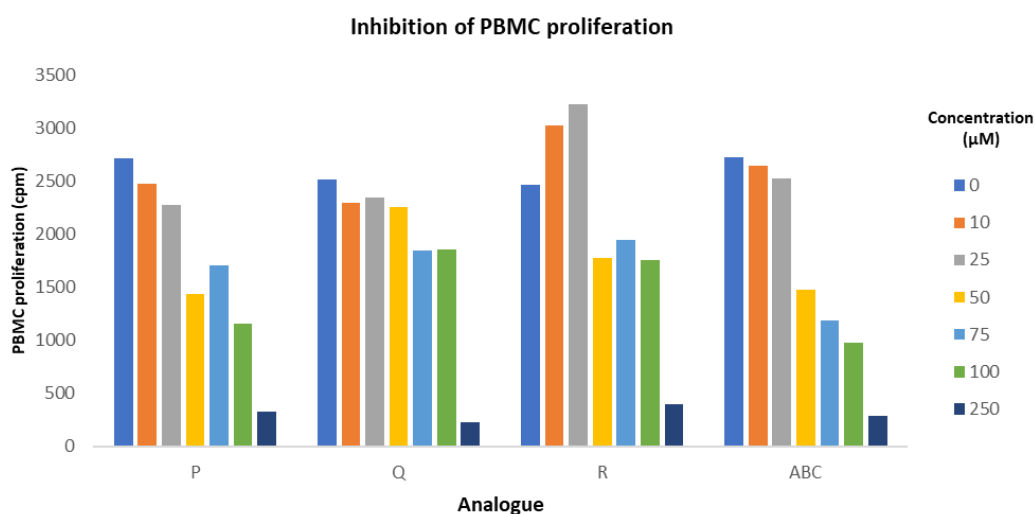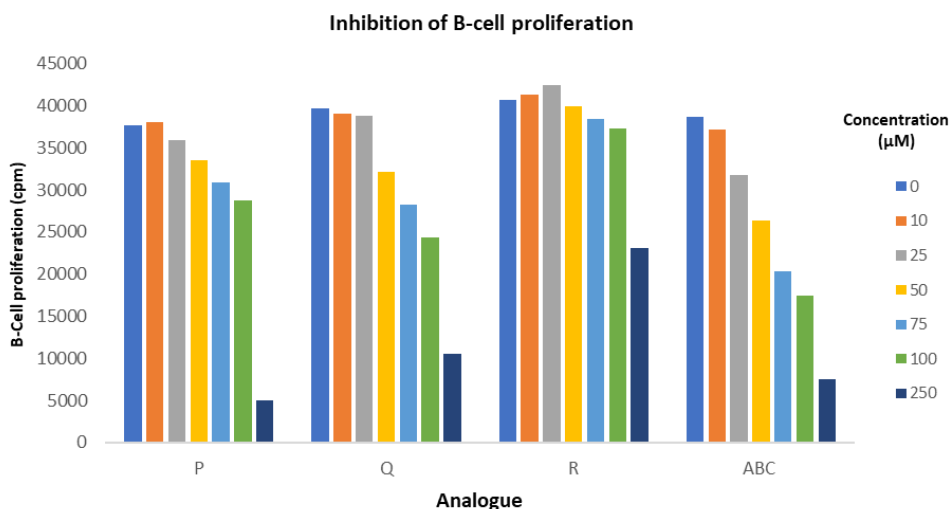
Figure 4.6. Cellular toxicity of abacavir analogues. Inhibition of proliferation of a) PBMCs and b) B-cells incubated in the presence of abacavir analogues at concentrations of 0, 10, 25, 50, 75, 100 and 250 μM. In the case of B-cells, the analogues were co-incubated for a period of 48 hours then tritiated thymidine was added directly to the cells for a further 16 hours. Cells were then harvested onto a printed filter mat and radioactive incorporation was assessed via scintillation counting on a microBeta counter. In the case of PBMCs, cells were co-incubated with the compounds for a period of 72 hours before PHA was added to promote the proliferation of viable cells. Following a further 24-hour incubation, tritiated thymidine was added directly onto the cells for a further period of 16 hours. Cells were then harvested and radioactive incorporation was measured as described above.

Compound ID	Inhibition of mitogen driven PBMC proliferation IC50 (μM).	Inhibition of B-cell proliferation IC50 (μM).
Abacavir	66.7	94.6
Analogue P	91.8	157
Analogue Q	162	129
Analogue R	93	>250

Table 4.2. Inhibition of T-cell and B-cell proliferation in the presence of abacavir and the analogues.

4.4.4 Effect of abacavir analogues on the activation of abacavir-specific CD8⁺ T-cells

The effect on CD8⁺ T-cell activation by the abacavir analogues was investigated using secretion of the proinflammatory cytokine IFN-γ as a readout due to its superiority over cell proliferation. Six abacavir-specific T-cell clones were co-incubated with the analogues in the presence of autologous APCs at concentrations of 0, 10, 20 and 50μM. Mean IFN-γ secretion of the six clones tested was compared with mean secretion across the same six clones in the presence of abacavir. Analogue **P** (isobutyl amino) induced strong activation of two abacavir clones with lesser activation observed in the other four (Figure 4.7). The effect of enantiomeric modification of the functional group of the abacavir analogues was explored with two compounds. Interestingly, the chirality of the functional groups had a pivotal role on the T-cell activation profile of the abacavir analogues. Analogue **Q** (S-$_{sec}$-butyl amino) activated CD8⁺ T-cell clones in a dose-dependent manner, in some cases to a higher degree than abacavir. Conversely, analogue **R** (R-$_{sec}$-butyl amino) displayed no activation of abacavir-specific T-cell clones, demonstrating enantiomeric-dependent activation of CD8⁺ T-cells.
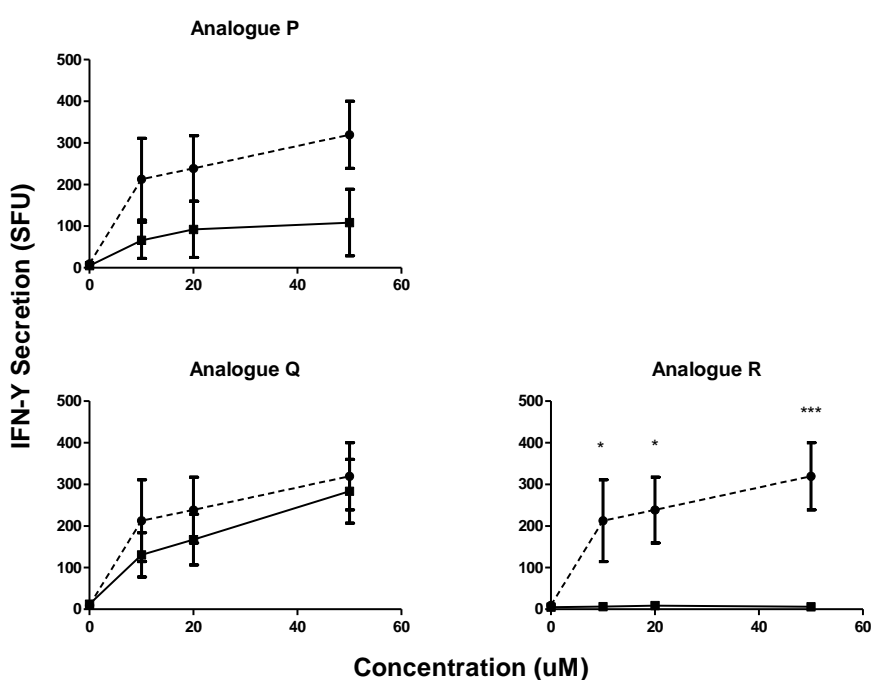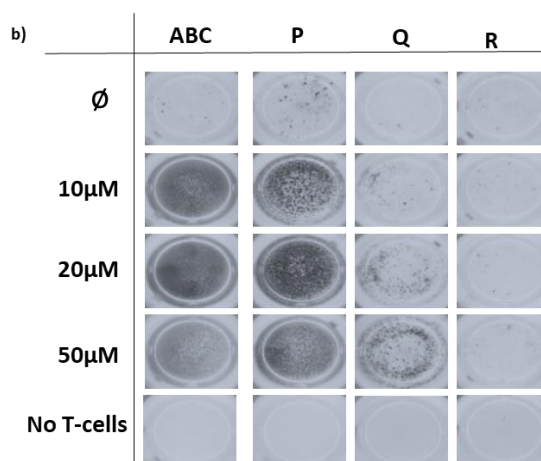
Figure 4.7 Direct comparison of the CD8^{+} T-cell activity of abacavir analogues a) Mean IFN-γ secretion from six abacavir-responsive T-cell clones incubated in the presence of analogues **P**, **Q** and **R** at concentrations of 0, 10, 20 and 50μM (Solid line). Mean IFN-γ secretion from the same six abacavir clones (dotted line) used as a comparator. Error bars ± S.E.M, comparison of abacavir and analogue values analysed using Two Way ANOVA, * $P<0.05$, ** $P<0.01$, *** $P<0.001$. b) ELIspot well images from one representative abacavir responsive T-cell clone incubated in the presence of analogues **P**, **Q** and **R** at concentrations of 0, 10, 20 and 50μM. Abacavir (ABC) at the same concentrations was used as a comparator.

4.4.5 Antiviral activity and Cytotoxicity of abacavir analogues.

The antiviral activity and cytotoxicity of the abacavir analogues was ascertained using the cytopathic effect assay (CPE) in HIV-IIIB infected MT-4 cells. Cellular viability was measured in MT-4 cells co-incubated with the respective analogues with virus control as comparator via luminescence using Cell-titer Glo reagent. This procedure was conducted on the basis that cellular death is instigated in MT-4 cells by HIV-IIIB infection, therefore cellular survival in the presence of a compound is a marker of antiviral activity. Cellular cytotoxicity was determined via the same methods but using MT-4 cells without prior viral infection. Antiviral activity and cytotoxicity of the analogues with was calculated using GraphPad Prism software and are displayed as EC_{50} and CC_{50}, respectively (Table 4.3).

With the exception of analogue **P** (EC_{50} 56.72μM), no analogues possessed detectable antiviral activity in MT-4 cells (EC_{50} >500μM) in comparison with abacavir, which exhibited potent antiviral activity properties (EC_{50} 7.626μM). The cellular cytotoxicity induced by the analogues is also displayed in Table 4.3. Abacavir analogues possess a cytotoxicity profile of between 2 and 6-fold lower than abacavir, revealing the diminished toxicity profile of analogues obtained via modifications to the 6-amino cyclopropyl moiety.

Compound ID	R1	Antiviral activity EC_{50} (μM)	Cytotoxicity CC_{50} (μM)	SI ($CC50/EC_{50}$)
Abacavir	Cyclopropyl	7.626	60.94	7.99
Analogue P	Isobutyl amino	56.720	241.60	4.26
Analogue Q	S-*sec*-butyl amino	>500	150.30	N/A
Analogue R	R-*sec*-butyl amino	>500	342.50	N/A

Table 4.3. Antiviral activity and cytotoxicity of abacavir and analogues measured in MT-4 cells.

4.4.6 Enantiomeric specific T-cell activation of abacavir and abacavir analogues.

Structurally, analogues **Q** and **R** differ only in the chirality of their functional group (sec-butyl amino) substituted in place of the 6-amino cyclopropyl group of abacavir. Analogue **Q** adopts the *S* conformation of the functional group while analogue R exists in the *R* conformation. Despite differing only in the chirality of their functional groups, analogues **Q** and **R** displayed polar effects on their respective abilities to induce T-cell activation. Analogue **Q** (S-$_{sec}$-butyl amino) exhibited a dose-dependent T-cell activation profile when co-incubated with abacavir-specific T-cell clones indicating strong cross reactivity. Conversely, analogue **R** (R-$_{sec}$-butyl amino) was not found to activate the same T-cell clones. Figure 4.8 shows the T-cell activation abilities of both analogues **Q** and **R** in six representative abacavir clones. All six abacavir clones were activated by analogue **Q**, whilst no difference in IFN-γ secretion was observed in the T-cell clones co-incubated with analogue **R** compared to control (Figure 4.8).
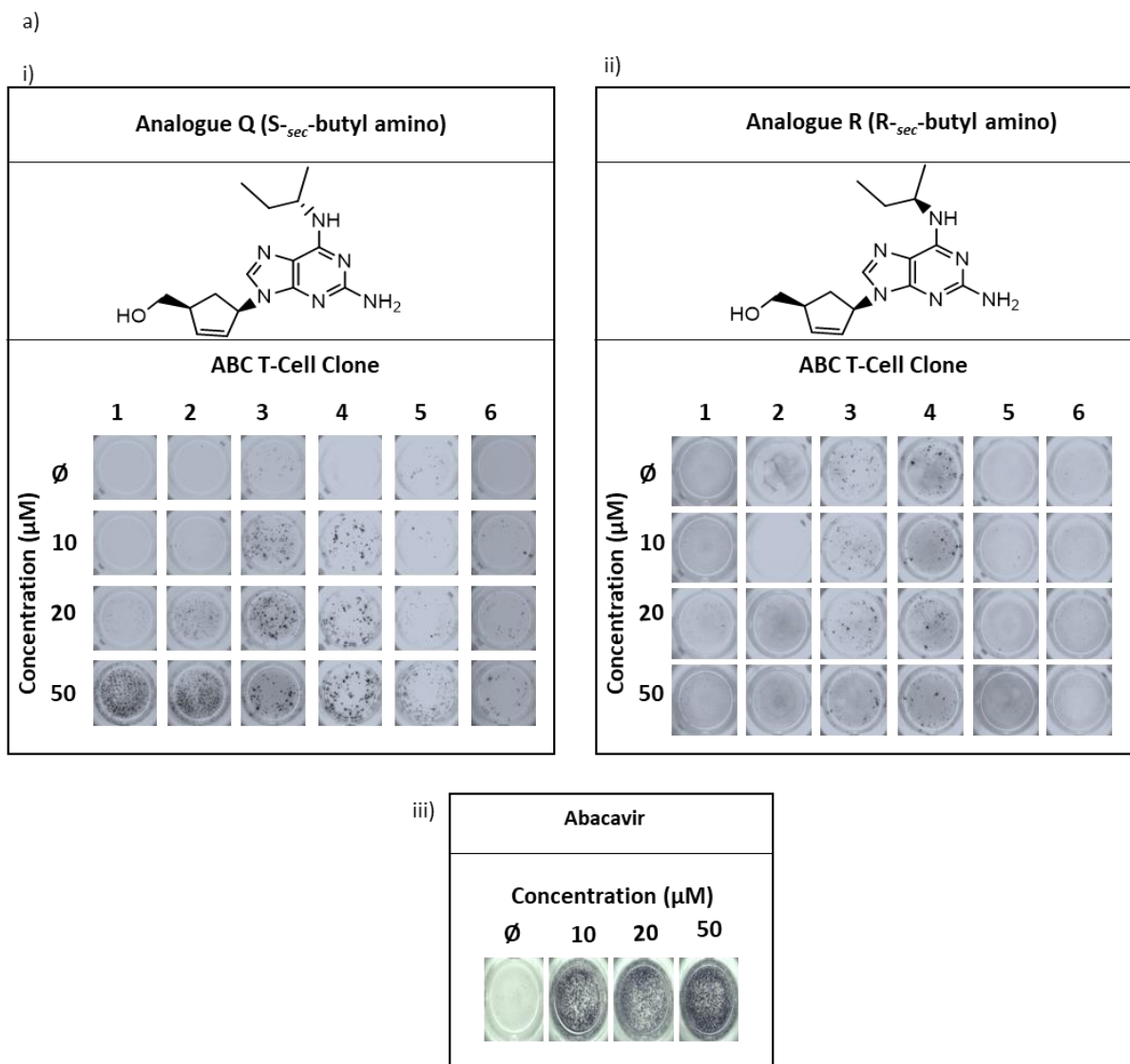
Figure 4.8. Direct comparison of the CD8$^+$ T-cell activity between enantiomer analogues Q and R. a) Structure of compounds and IFN-γ secretion from six abacavir responsive T-cell clones incubated in the presence of analogues i) **Q** and ii) **R**. Representative IFN-γ ELIspot images of six individual abacavir responsive CD8$^+$ T-cell clones incubated in the presence of analogues **Q** or **R**, at concentrations of 0,10,20 and 50μM. iii) Abacavir incubated in the presence of one representative clone, at the same concentrations, is shown as a comparator.

4.4.7 HLA-B*57:01 molecular modelling of abacavir analogues.

The same docking protocol from chapter 3 was used for analysis of the predicted binding poses of analogues **P-R**, which were subsequently compared to abacavir. All analogues were predicted to bind in a similar fashion to abacavir with the guanosine component of the molecule forming hydrogen bonds with Asp-114, Ser-116 and Ile-124 amino acids. From Figure 4.8 it can be seen that T-cell activating analogues **P** and **Q** bind within the HLA-B*57:01 antigen binding cleft in a similar conformation to abacavir which results in the absence of steric clashes between the compounds functional groups and the HLA-binding peptide, or the amino acids within the F-pocket. This indicates a favourable binding conformation adopted by these compounds within HLA-B*57:01 allowing for interactions to initiate a T-cell response. Conversely, analogue **R** is predicted to bind to HLA-B*57:01 in such a manner that inhibits the activation of T-cells. This is characterised by the increased distance between the guanosine portion of these compounds and the amino acids within HLA-B*57:01 when compared to abacavir and the activating analogues. Therefore, binding of this analogue within the F-pocket of HLA-B*57:01 unsurprisingly yielded the presence of steric clashes between their respective functional groups and the residues of the HLA-binding peptide (pep-V). As mentioned in chapter 3, the overlap of atomic radii within each compound with that of the HLA-binding peptide or amino acids within HLA-B*57:01 results in an unfavourable binding conformation of the compounds within HLA-B*57:01 which would not favour the docking of pep-V, likely leading to the binding of other distinct peptides. This results in a loss of T-cell activity, indicated by the lack of IFN-γ secretion with analogue **R**.
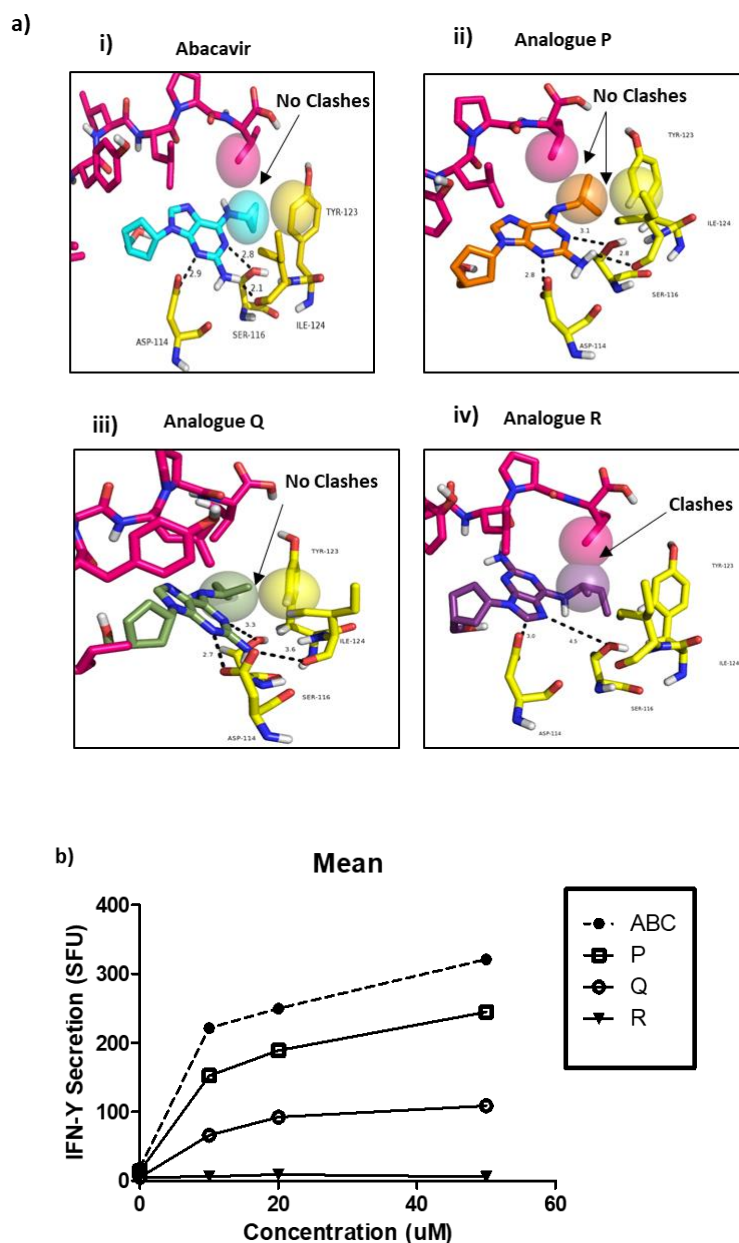
Figure 4.9. Direct comparison of the CD8^{+} T-cell activity of abacavir analogues and the binding orientations within the F-pocket of HLA-B*57:01. a) Crystal structure of HLA-B*57:01 (PDB:3UPR) represented with the HLA-binding peptide and compounds. i) Crystal structure and binding orientations of abacavir, stick representation of pep-V (HSITYLLPV; pink) and the chemical structure of abacavir (cyan). Key amino acid residues which bind abacavir are shown as yellow sticks. Non-polar hydrogen atoms have been removed. Key H bond interactions are shown as black dashes. Spheres are used to illustrate the atomic radii of the atoms in the cyclopropyl group of abacavir, peptide molecule and Tyr-123 amino acid. Docking solution of analogues ii) **P** (isobutyl amino), iii) **Q** (S-$_{sec}$-butyl amino) and iv) **R** (R-$_{sec}$-butyl amino) in the F-pocket of HLA-B*57:01. Stick representation of the peptide, pep-v (HSITYLLPV) shown in pink. Amino acid protein residues shown as yellow sticks, with key hydrogen bond interactions shown as black dashes. All non-polar hydrogen atoms removed. Spheres used to illustrate the atomic radii of the atoms in the functional group of the analogue, peptide and amino acids Tyr-123. b) Mean IFN-γ secretion from six abacavir responsive T-cell clones incubated in the presence of analogues **P**, **Q** and **R** at concentrations of 0, 10, 20 and 50μM. Abacavir (ABC) (dotted line) used as a comparator.

4.4.8 Effect of chirality on abacavir-induced CD8+ mediated T-cell responses

The chiral modification of abacavir at the cyclopentyl moiety has a dramatic effect on the ability of a compound to activate T-cells. Abacavir can induce CD8+ T-cell activation in a dose-dependent manner as observed by IFN-γ secretion and in some cases proliferation. Such activation was completely abrogated with the enantiomeric modification of the cyclopentyl moiety of the compound. No T-cell proliferation or IFN-γ secretion was observed using T-cells incubated in the presence of the **1R, 4S** abacavir enantiomer compared to abacavir in its native form (Figure 4.10). Molecular modelling of **1R, 4S** abacavir within HLA-B*57:01 demonstrates an altered binding conformation within the antigen binding cleft. The distance between the contact points within the 2-amino purine motif of the compound and the amino acids Asp-114, Ser-116 and Ile-124 is much greater with the **1R, 4S** enantiomer when compared to abacavir in its native form. This increase in distance of the contacts results in an altered binding conformation of the compound, which clashes with the Val-9 residue of the HLA-binding peptide. The large distance between the compound and the amino acids within HLA-B*57:01 diminishes the interactions with the amino acids within the F-pocket. This inhibits the induction of conformational changes in the shape of the binding motif, resulting in no accommodation of smaller C-terminal anchors. This consequently results in the loss of CD8+ T-cell activation (Figure 4.10).
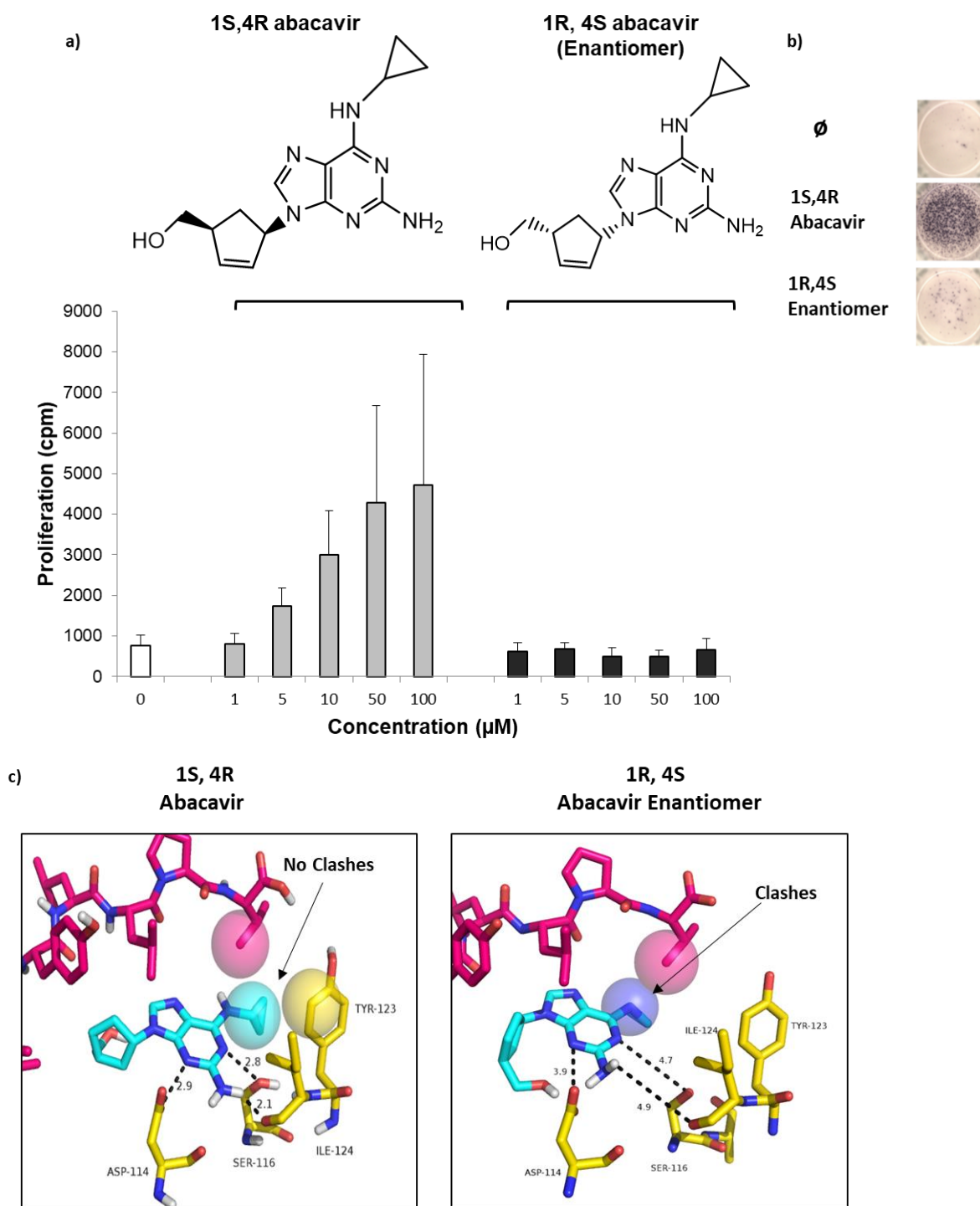
Figure 4.10. Direct comparison of abacavir and the 1R,4S enantiomer effects on CD8^{+} T-cell activation and binding within the F-pocket of HLA-B*57:01. a) Abacavir responsive T-cell clones were cultured in the presence of abacavir and the **1R, 4S** abacavir enantiomer at concentrations of 1, 5, 10, 50 and 100μM for 48 hours. Following the incubation period, tritiated [³H] thymidine was added and cells were incubated for a further 16 hours. Proliferation was measured via scintillation counting. b) Representative ELIspot images from wells containing abacavir and **1R, 4S** abacavir both at 50μM. c) Docking solution of abacavir (**1S,4R**) and abacavir enantiomer (**1R,4S**) in the F-pocket of HLA-B*57:01. Stick representation of the peptide, pep-V (HSITYLLPV) shown in pink. Amino acid protein residues shown as yellow sticks, with key hydrogen bond interactions shown as black dashes. All non-polar hydrogen atoms removed. Spheres used to illustrate the atomic radii of the atoms in the functional group of the compounds.

4.4.9. Incorporation of naïve T-cells from healthy drug naïve HLA-B*57:01[+] donors into the T-cell multi-well assay.

Using a T-MWA, the effect of naïve T-cell priming by abacavir was assessed in two HLA-B*57:01 positive drug naive donors (HVN-021 and HVN-158), genotyping data shown in Table 2.1. The assay was repeated using nitroso-sulfamethoxazole (SMX-NO) as a comparator. Between 40-80% of wells primed to SMX-NO responded when restimulated with the same drug antigen, yielding SI values as high as 60 in some wells in the case of HVN-021. While not being as responsive as HVN-021, naïve T-cells from HVN-158 demonstrated a moderate to high activation profile in response to SMX-NO generating SI values of up to 8. However, abacavir demonstrated little to no activation of naïve T-cells in either donor. HVN-021 displayed modest activation in the multi-well priming assay yielding SI values of up to 2. However, based on the low SI values observed in other wells and the complete lack of responsive T-cells in HVN-158 it is likely that these results were false positives (Figure 4.12).

HVN-021

Naïve Cells									
Abacavir (35uM)					SMX-NO (40uM)				
0.1	0.5	0.7	0.1		4.5	2.1	2.4	11.6	8.0
0.2	2.4	0.2	2.5		0.3	1.4	1.8	3.2	15.8
1.3	0.1	0.2	0.2		2.1	10.2	3.0	3.0	53.2
0.1	0.4	0.3	0.6		22.7	0.5	30.0	14.2	3.0
0.1	0.1	2.2	0.3		0.6	0.7	11.5	17.1	2.8
0.0	0.3	0.4	1.6		3.2	0.9	3.7	4.7	5.2
0.7	0.8	0.2	0.3		62.4	4.3	27.5	6.9	1.2
0.6	0.3	0.7	0.2		5.8	2.2	2.0	5.7	1.3

Response	SI
Low	1.5-1.9
Moderate	2-3.9
High	4+
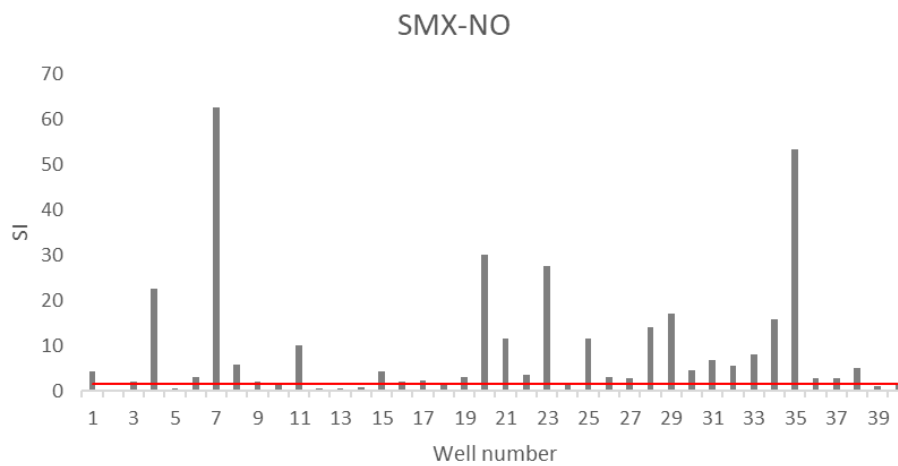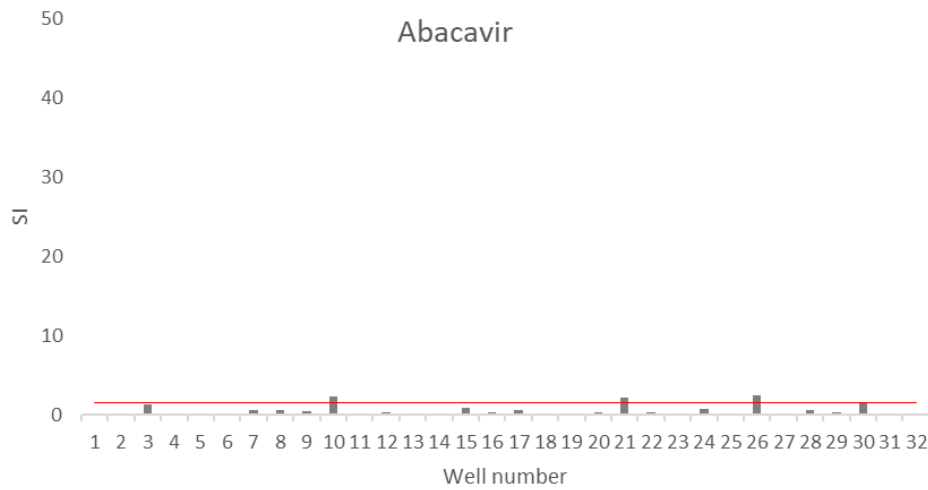
Figure 4.11. Naïve T-cell priming assay. Naïve T-cells isolated from PBMCs from HLA-B*57:01 positive, drug naïve, donor HVN-021 were co-incubated with abacavir and SMX-NO for a period of 14 days then rechallenged with the respective drugs. Activation of T-cells was measured via cellular proliferation, individual wells cpm were normalised against average cpm for control wells. SI values plotted to individual wells with SI values of 1.5-1.9 constituting low response, 2-3.9 moderate response and 4+ high response (*Faulkner et al 2016*). SI values plotted in bar chart with 1.5 cut off shown by red line.

HVN-158

Naïve Cells								
Abacavir (35uM)					SMX-NO (40uM)			
0.46	0.10	0.47	0.07		1.8	8.9	6.2	3.9
0.03	0.02	0.31	0.08		4.1	4.8	2.0	4.0
0.86	0.06	0.04	0.04		1.7	1.4	2.0	3.7
0.12	0.04	0.13	0.03		7.9	0.9	3.2	1.0
0.16	0.03	0.07	0.03		2.8	3.2	1.1	0.8
0.17	0.10	0.18	0.04		0.1	0.3	0.4	4.3
0.05	0.12	0.07	0.12		1.4	0.7	2.3	0.8
0.06	0.25	0.05	0.02		0.1	2.3	0.6	0.6

Response	SI
Low	1.5-1.9
Moderate	2-3.9
High	4+
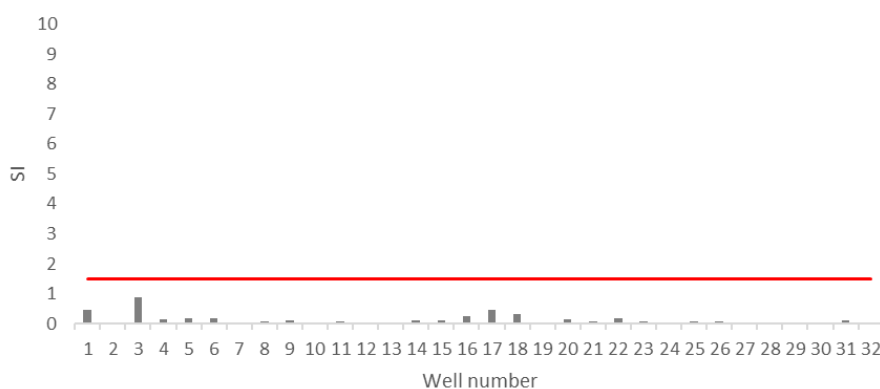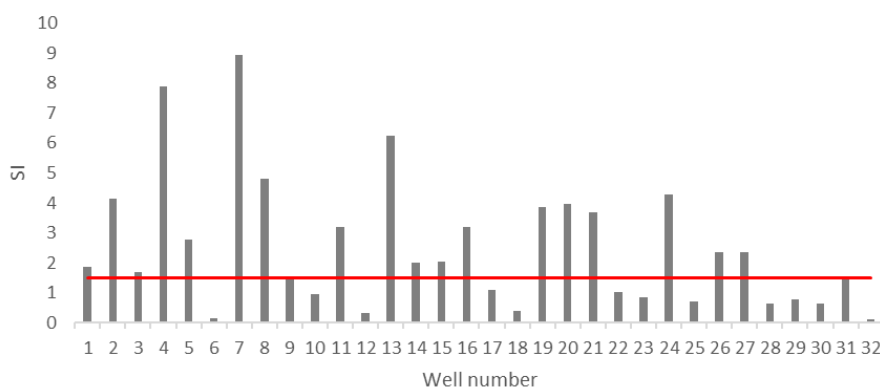
Figure 4.12. Naïve T-cell multi-well dendritic priming assay. Naïve T-cells isolated from PBMCs from HLA-B*57:01 positive, drug naïve, donor HVN-158 were co-incubated with abacavir and SMX-NO for a period of 14 days then rechallenged with the respective drugs. Activation of T-cells was measured via cellular proliferation, individual wells cpm were normalised against average cpm for control wells. SI values plotted to individual wells with SI values of 1.5-1.9 constituting low response, 2-3.9 moderate response and 4+ high response (*Faulkner et al 2016*). SI values plotted in bar chart with 1.5 cut off shown by red line.

4.5 Discussion

The concept of eradicating the cytotoxic T-cell response observed in response to abacavir in HLA-B*57:01 positive individuals via the generation of 6-amino substituted analogues was explored in detail in chapter 3 and in previous studies (Naisbitt et al. 2015). Continuing from these studies, a further four abacavir substituted analogues were synthesised, this time constructed around the open form of the azetidine ring, with two of these compounds being enantiomers of the same structure, (R-$_{sec}$-butyl amino) and (S-$_{sec}$-butyl amino) in order to investigate the ill-defined role of chirality on T-cell activation (Naisbitt et al. 2005).

All abacavir substituted analogues used in this study demonstrated a reduced cytotoxicity profile when compared with abacavir in range of cells (Tables 4.2 and 4.3), suggesting that substitution of the 6-amino cyclopropyl moiety of the compound does not significantly increase cellular toxicity (Naisbitt et al. 2015).

Introduction of the isobutyl amino group (analogue **P**) activated T-cell clones in a similar manner to abacavir. All six abacavir responsive T-cell clones were activated by analogue **P**, with two producing strong IFN-γ secretion while the other four demonstrated more modest cytokine secretion. The introduction of the isobutyl amino group was employed to further analyse the introduction of branched chained functional groups, which was explored by *Naisbitt et al* in 2015. The compound did not activate abacavir-specific T-cell clones. A further structural analysis indicates the similar binding of analogue **P** to abacavir, therefore a T-cell response was to be expected (Figure 4.9). Molecular modelling of analogue **P** revealed it to adopt to a similar binding conformation to abacavir (Figure 4.9) indicating favourable binding affinity to form a complex with the HLA-binding peptide to induce a T-cell response.

Analogues **Q** and **R** substitute the 6-amino cyclopropyl moiety of abacavir with the sec-butyl amino group in *S* and *R* conformations, respectively. Co-incubation of these compounds with

abacavir responsive CD8^{+} T-cell clones resulted in opposing effects on T-cell activation. Analogue Q (S-$_{sec}$-butyl amino) was a strong inducer of T-cell activation while analogue **R** (R-$_{sec}$-butyl amino) did not activate any CD8^{+} T-cell clones (Figure 4.8). Molecular modelling revealed the unique binding poses adopted by the chiral compounds within the F-pocket of HLA-B*57:01's antigen binding cleft (Figure 4.9). Analogue **Q** docked in a similar manner to abacavir, resulting in absence of steric clashes between the compound and the HLA-binding peptide (pep-V) or amino acids within the antigen binding cleft. This indicates a favourable binding posture of the compound within HLA-B*57:01 allowing for the induction of changes in shape and chemistry of the peptide binding groove ultimately leading to T-cell activation (Illing et al. 2012). Conversely, the docking conformation adopted by analogue **R** differs greatly from that of analogue **Q** and abacavir. The distance between the 2-amino purine moiety of the compound and the amino acids within HLA-B*57:01 is increased which indicates a lack of interaction within the peptide binding groove. Subsequently, binding of the compound leads to the presence of unfavourable clashes between the functional group of analogue **R** and the Val-9 residue of the HLA-binding peptide. The presence of such clashes demonstrates the inability of analogue **R** to bind to HLA-B*57:01 with sufficient affinity to allow for the presentation of an altered peptide repertoire on the antigen presenting cell surface for recognition by CD8^{+} T-cells, resulting in a lack of immune activation (Illing et al. 2012; Ostrov et al. 2012; Norcross et al. 2012). The cytotoxicity levels of analogues **Q** and **R** also differ based on their chirality (Tables 4.2 and 4.3), however in both cases antiviral activity of the analogues could not be detected within the range of concentrations used, indicating that the sec-butyl amino group is an unsuitable for replacement at the 6-amino cyclopropyl region of abacavir.

Next, we sought to assess whether the chiral modification of abacavir would remove the T-cell mediated reactions observed, via the use of a previously synthesised abacavir

enantiomer. In the standard state, **1S 4R**, abacavir is associated with severe hypersensitivity reactions mediated by CD8⁺ T-cells which secrete the proinflammatory cytokine IFN-γ. However, the chiral modification at the cyclopentyl moiety of the structure generated a stable compound lacking the propensity to activate T-cells by way of both IFN-γ secretion and proliferation (Figure 4.9). Unfortunately this compound was found to be pharmacologically inactive due to the enantioselective nature of the enzyme adenosine phosphotransferase (Faletto et al. 1997) meaning the enantiomer (**1R, 4S**) possessed no antiviral activity. Nevertheless, this enantiomeric modification was located at the cyclopentyl region of the compound which interacts with the D-pocket of HLA-B*57:01, indicating that modifications elsewhere in the structure of abacavir can prevent the protrusion of the cyclopropyl moiety into the F-pocket, thereby eliminating the T-cell mediated reactions observed to the drug.

Molecular modelling of the abacavir enantiomer within the F-pocket of HLA-B*57:01 revealed an altered binding pose of the compound when compared with abacavir in its natural form (Figure 4.10). The increased distance between the amino acid residues within the antigen binding cleft and the 2-amino purine portion of the abacavir analogue revealed a distinct lack of binding potential within HLA-B*57:01. This would impair the ability of the analogue to interact within HLA-B*5701 to induce the docking of pep-V. This would lead to the binding of other distinct peptides likely resulting in the loss of T-cell activity.

The naïve T-cell priming assay has been developed as a reproducible assay which is able to detect T-cell specific responses in non-hypersensitive individuals to a range of drugs including flucloxacillin, piperacillin, carbamazepine and the reactive species Bandrowski's base with the most notable being SMX-NO (Faulkner et al. 2016; Naisbitt et al. 2001; Naisbitt et al. 2002). Using the T-MWA, SMX-NO displayed strong activation of naïve T-cells from two donors positive for the HLA-B*57:01 risk allele yielding a percentage of responsive wells of

between 40 and 80% consistent with previous findings (Faulkner et al. 2012). Abacavir was incorporated into this study to ascertain if this model could be used as a diagnostic tool for abacavir hypersensitivity reactions *in vitro* which may allow for the quicker screening of abacavir substituted analogues in place of the conventional T-cell cloning assay. Naïve T-cells isolated from healthy drug naïve HLA-B*57:01 positive donors incubated in the presence of abacavir did not produce significant T-cell activation when rechallenged with the drug. Across the two donors abacavir yielded an overall percentage of responsive wells of 6% compared with the 64% value of responsive wells of cells incubated with SMX-NO. The use of this assay was also employed to further investigate the findings obtained by *Lucas et al 2015* which suggested the presence of pre-existing abacavir responsive memory CD8$^+$ T-cells. It was hypothesised that memory T-cells primed previously from an immunological event to a currently unknown antigen, possibly of viral origin were present in drug naïve individuals, accounting for hypersensitivity reactions observed upon first exposure to the drug, the inability of abacavir to activate naïve T-cells in these assays supports this conclusion (Lucas et al. 2015).

Taken together the data in this chapter demonstrates the important bearing that the chiral state of a compound has on its various functional properties. While chirality is already known to be pivotal in the pharmacological properties of a wide range of drugs, including antidepressants (McConathy & Owens 2003; Koldsø et al. 2010), asthmatics (Nowak et al. 2006) and drugs to treat hypertension (Satoh et al. 1980) its influence on T-cell activation was not widely explored. We were unable to fully investigate the different effects of the enantiomer analogues **Q** and **R** as neither displayed antiviral activity within the concentration range used. However, the chiral modification of these compounds functional group resulted in a change in the cytotoxicity of the compounds, with the R conformation displaying lower cellular toxicity in two of the three cell lines similar to findings observed with other

therapeutics. Importantly, we uncovered that T-cell activation by compounds is enantiomer specific, which had only been demonstrated by a small number of studies to date (Naisbitt et al. 2005). Indeed, given the high frequency of the HLA-B*57:01 risk allele in the Caucasian populations, associated with abacavir hypersensitivity reactions the enantiomeric dependence of abacavir-specific memory T-cells demonstrates an interesting concept for future study given the notoriety of abacavir hypersensitivity reactions.

Chapter 5- Activation of abacavir-specific CD8⁺ T-cell clones by a HLA-B*57:01 binding self-peptide in both the natural and amidated form.

5.1. Introduction.

Hypersensitivity reactions in response to abacavir occur exclusively in individuals carrying the MHC class I allele HLA-B*57:01 (Mallal et al. 2002). The association between this risk allele and the observed hypersensitivity reactions yields a 100% NPV, while having a PPV of around 55% (Mallal et al. 2008; Lucas et al. 2015).

Neither the hapten/prohapten or the PI models have sufficiently explained activation of T-cells and subsequent induction of hypersensitivity reactions to abacavir. The hapten model seems an unlikely concept for activation of T-cells by abacavir since the aldehyde metabolite, capable of forming covalent adducts, does not activate human T-cells *(unpublished data, Bell et al)*. Furthermore, abacavir has been demonstrated to elute unbound from peptides at HLA-B*57:01 demonstrating the interactions to be in a non-covalent manner (Illing et al. 2012). While the PI model accounts for activation of around 50% of abacavir-specific T-cell clones, it does not explain the full story (Bell *et al.*, 2013). *Chessman et al 2008* and *Bell et al 2013* both demonstrated the need for antigen processing for the activation of T-cells in response to abacavir. Firstly, abacavir-specific T-cell clones were activated only by 16-hour abacavir pulsed without the presence of soluble drug, but not in those pulsed for a shorter duration (1 hour). Furthermore these responses were abolished when antigen processing was inhibited via glutaraldehyde fixation, demonstrating the need for antigen processing and presentation on the surface of MHC-class I in some abacavir clones (Chessman *et al.*, 2008; Bell *et al.*, 2013).

In 2012, three separate studies were carried out focussing solely on another mechanism of T-cell activation by abacavir, the altered peptide repertoire model (Illing et al. 2012; Ostrov et al. 2012; Norcross et al. 2012). Proteomic studies discovered that up to 25% of the peptides eluted from HLA-B*57:01 in the presence of abacavir were unique self-peptides not detected in the absence of the drug. Furthermore, most of these new peptides contained

small C-terminal anchor residues such as valine, leucine and isoleucine compared to the more traditional larger chain C-terminal amino acids, phenylalanine and tryptophan commonly observed with the peptides eluted in abacavirs absence (Ostrov et al. 2012; Norcross et al. 2012; Illing et al. 2012). This led to the theory that treatment with abacavir in HLA-B*57:01 positive individuals resulted in a change in the shape and chemistry of the peptide binding groove of HLA-B*57:01, thereby allowing for the accommodation of peptides with smaller C-terminal anchors for presentation on the surface of the antigen presenting cell. Therefore, as T-cells are tolerant of peptides they are exposed to during development in the thymus, recognition of this altered peptide repertoire would be perceived as a foreign antigen and thereby a T-cell-mediated immune response would be initiated (Illing et al. 2012).

In chapter 3 we demonstrated via work with our collaborators in the Purcell Laboratory (Monash University, Melbourne) the shift in peptide prevalence in the presence of not only abacavir but to two abacavir analogues both of which evoked CD8+ mediated T-cell responses in abacavir-responsive T-cell clones. However, to date, the peptide sequences that induce T-cell activity after exposure to abacavir have not been fully defined. Obtaining clear results from T-cell assays examining the effect of abacavir-induced self-peptides on T-cell activation can prove difficult as these peptides are only thought to activate T-cells in the presence of abacavir. Therefore, it is difficult to distinguish a T-cell response to the peptides in the presence of abacavir from the response to abacavir alone using established readouts such as cytokine secretion and T-cell proliferation, as the same peptides will load onto HLA-B*57:01 naturally within the APC.

Studies analysing the T-cell mediated responses to abacavir-specific peptides have been relatively sparse. In 2015 *Lucas et al* suggested the presence of pre-existing memory T-cells primed to a previous immunogenic event which were able to cross-react with abacavir-

induced self-peptides, perhaps accounting for the hypersensitivity reactions observed to abacavir upon first exposure in some individuals (Lucas et al. 2015). In 2017 *Yerly et al* characterised the peptides specifically recognised by abacavir-responsive TCRs. This utilised abacavir and the crystal structure of the immunogenic self-peptide VTTDIQVKV, which possessed side chains exhibiting solvent exposure, indicating this peptide to be a potential motif for T-cell recognition. Basic Local Alignment Search Tool (BLAST) searches identified three viral peptide sequences originating from Human Immunodeficiency Virus (HIV) and Herpes Simplex Virus (HSV) that displayed structural similarity with VTTDIQVKV. Furthermore, one of these viral peptide sequences evoked a response in T-cell transfectants in the absence of abacavir, however this response was only observed in transfectants expressing one particular TCR (Yerly et al. 2017). Subsequent comparison with abacavir displayed similarity with the original peptide VTTDIQVKV, particularly in the contact regions with the TCR. These data suggest the ability of T-cells to cross-recognise and react with viral peptides, however, this characteristic is likely restricted to a small subset of T-cells (Yerly et al. 2017).

Previously, a panel of 120 unique 9-mer self-peptides, eluted from HLA-B*57:01 in the presence of abacavir, were imported to our research laboratory from the Purcell Laboratory (Monash University, Melbourne). These peptides were tested by Dr Mohammad Alhaidiri to analyse their ability to induce a CD8$^+$ T-cell response. Using C1R (HLA-deficient, TAP expressing, B-cell line transfected with HLA-B*57:01) and T2 (B-cell line transfected with HLA-B*57:01, TAP deficient) cells it was discovered that one peptide from the panel of 120 (peptide 15, NTVELRVKI) induced T-cell responses in both the presence or absence of abacavir. However, subsequent analysis via mass spectrometry identified the presence of C-terminal amide groups. Repetition of the experiments using peptides in their natural form, without C-terminal amidation, indicated no T-cell activation in the absence of abacavir.

However, T-cell activation was observed in a limited number of abacavir-specific T-cell clones in the presence of the drug (Figure 5.1-5.3). This data may suggest the activation of CD8$^+$ T-cells is evoked by an abacavir-induced self-peptide. Unfortunately, due to the difficulty distinguishing T-cell activation to abacavir in the presence or absence of the peptide with these assays, this was not confirmed.
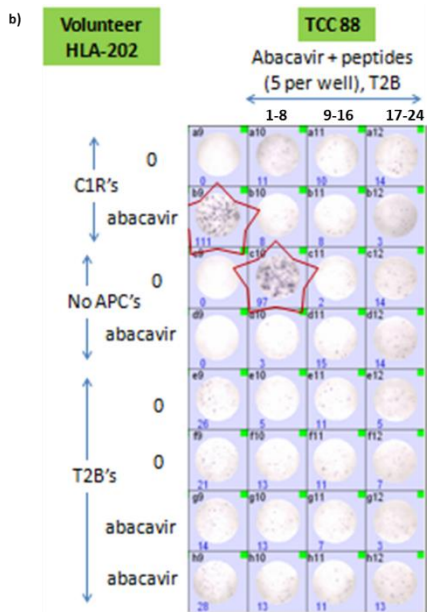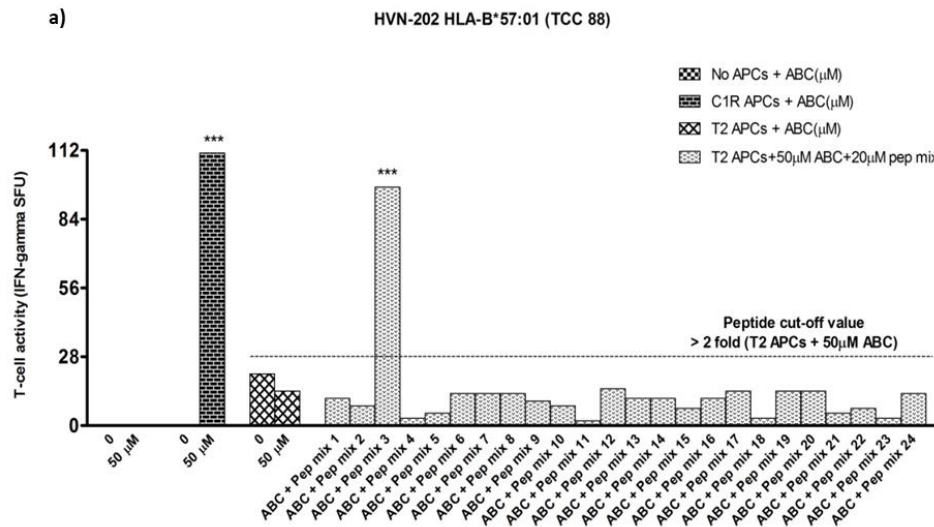
Figure 5.1. T-cell responses prompted by abacavir-induced self-peptide mixes. a) Abacavir-responsive T-cell clones incubated with T2 APCs and a mixture of up to 5 abacavir-self peptides per well (1-24) in the presence or absence of abacavir. T-cells were co-incubated with T2 APCs ± abacavir in the absence of peptides as a negative control. T-cells were also co-incubated with C1R APCs ± abacavir as a positive control. b) IFN-γ ELIspot well images of T-cell clones co-incubated with C1R and T2 APCs ± abacavir in the presence or absence of abacavir-induced self-peptide mixes (up to 5/well).

HVN-202 HLA-B*57:01 (TCC 88)
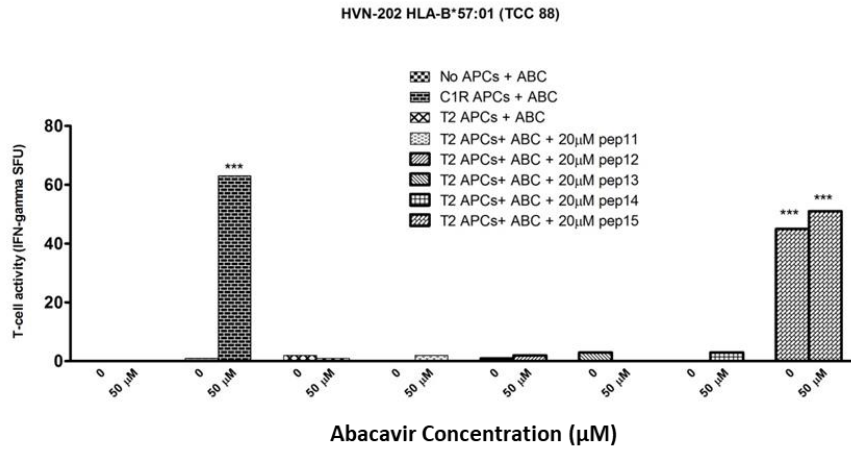
Figure 5.2. T-cell responses to a panel of individual abacavir-induced self-peptides in the presence/absence of abacavir. Abacavir-responsive T-cell clones were co-incubated with T2 APCs ± abacavir in the presence of abacavir-induced self-peptides 11-15. T-cells were co-incubated with C1R APCs ± abacavir as a positive control and with no APCs as a negative control.

HLA-B*57:01⁺ Donor
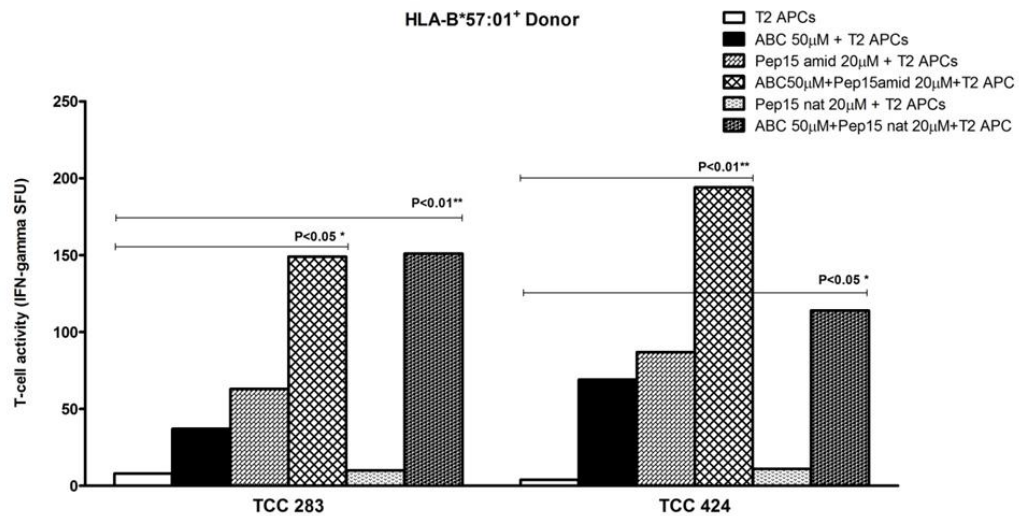
- N.B. Test of Two-way ANOVA used to analyze the graph

Figure 5.3. Activation of T-cells by abacavir-induced self-peptide 15 in natural and amidated form in the presence or absence of abacavir. Abacavir-responsive T-cell clones were co-incubated with T2 APCs ± abacavir in the presence of abacavir-induced self-peptide 15 in the natural and amidated form (20µM). T-cell activity was measured by means of IFN-γ secretion (SFU).

Therefore, we aimed to continue the T-cell work with peptide 15 and dissect the responses between the peptide in its natural and amidated form, via subjecting T-cells to a wider range of assays to assess the magnitude of T-cell activation induced by this abacavir-specific HLA-B*57:01 binding peptide.

5.2. Aims.

The aims of this chapter were to further analyse the abacavir-induced self-peptide 15 (NTVELRVKI) in both its natural and amidated form to further dissect the effect on T-cell activation in the presence or absence of abacavir. Furthermore, T-cells were subjected to a range of assays to investigate the actions of the peptides on T-cell activation. Finally, T-cell cloning was conducted to peptide 15 in both the natural and amidated form and responsive clones were subjected to mechanistic studies to explore dose- and antigen presenting cell-dependency and cellular phenotype for comparison with abacavir-specific T-cell clones.

5.3. Methods.

5.3.1. Materials.

Abacavir was received as a gift from GlaxoSmithKline (GSK). Human AB serum and foetal bovine serum were obtained from Innovative Research (Michigan, USA) and Invitrogen (Paisley, UK), respectively. Interleukin-2 (IL-2) was purchased from Peprotech (London, UK). Multisort bead separation kits were supplied by Miltenyi Biotec (Surrey, UK). Antibodies for staining were purchased from BD Biosciences (Oxford, UK). ELIspot kits including the coating and detection antibodies, streptavidin alkaline phosphate conjugate and BCIP/NBT substrates were purchased from Mabtech (Stockholm, Sweden). Other reagents were purchased from Sigma-Aldrich (Dorset-UK) unless otherwise stated.

5.3.2. Cell culture medium.

R9 medium for T-cells (R9) is composed of RPMI supplemented with 10% human AB serum, HEPES (25mM), penicillin (1000 U/mL), streptomycin (0.1mg/mL), L-glutamine (2mM) and transferrin (25μg/mL).

EBV transformed B-cells were cultured in F1 medium composed of RPMI supplemented with 10% foetal bovine serum, HEPES (25mM), penicillin (1000 U/mL), streptomycin (0.1mg/mL) and L-glutamine (2mM).

5.3.3. Maintaining C1R and T2 cells.

Cells from the class I deficient lymphoblastoid cell line, C1R and T2 were transfected with HLA-B*57:01 to be used in functional assays. C1R-B*57:01 cells comprise a fully functional B-cell line transfected to express HLA-B*57:01. T2-B*57:01 cells are a B-cell line transfected to express HLA-B*57:01 but the transporter associated with antigen processing (TAP) has been knocked out, meaning T2 cells antigen processing capabilities are severely diminished.

Both cell lines were maintained in F1 medium supplemented as described in section 5.3.2. C1R-B*57:01 cells were further supplemented with geneticin (500µg/mL) (Thermo-Fischer Scientific, Massachusetts, USA).

5.3.4. Generation of abacavir-specific T-cell clones.

5.3.4.1. T-cell cloning.

CD8+ T-cell cloning to abacavir was carried out in four HLA-B*57:01+ drug-naïve donors (donors 1-4) as described in detail in section 2.3.5.

5.3.4.2. Testing clones for antigen specificity.

Approximately four weeks after beginning the serial dilutions, abacavir-specificity was measured by assessing cell proliferation in the presence of the drug. This was conducted as described in section 2.3.6. The antigen specificity of the abacavir clones was confirmed using the IFN-γ ELIspot as described in section 2.3.7.

5.3.5. Activation of abacavir-specific T-cell clones by peptide 15 in natural and amidated form.

Abacavir-responsive T-cells ($5x10^4$/ 50µL) were co-incubated with C1R and T2 cells ($1x10^4$/ 50µL) in the presence or absence of abacavir for 48 hours (37^OC; 5% CO_2). T-cell clones were also co-incubated with T2 cells and peptide 15 in the natural and amidated forms (25µM) both individually, and in the presence or absence of abacavir (varying concentrations dependent on the T-cell clone used). T-cell responses were measured using the IFN-γ ELIspot assay.

5.3.6. Dose dependency of T-cell activation by abacavir with peptide 15 in natural form.

Abacavir-responsive T-cells ($5x10^4$/ 50μL) were co-incubated with autologous EBVs ($1x10^4$/ 50μL) and abacavir (0.1-30μM) in the presence or absence of natural peptide 15 (25μM) for 48 hours (37^OC; 5% CO_2). T-cell activation was quantified using the IFN-γ ELIspot assay.

5.3.7. Dose dependency of CD8$^+$ T-cell activation in in response to increasing concentrations of peptide 15 in natural and amidated form.

Abacavir-specific T-cell clones ($5x10^4$/ 50μL) were co-incubated with T2 cells ($1x10^4$/ 50μL) in the presence or absence of abacavir (35μM) at increasing concentrations of peptide 15 in both the natural and amidated form (10-50μM) for a period of 48 hours (37^OC; 5% CO_2). T-cell clones co-incubated with C1R APCs ($1x10^4$/ 50μL) in the presence or absence of abacavir were used as positive controls. T-cell activation was measured using cytokine secretion as a readout via the IFN-γ ELIspot assay.

5.3.8. Antigen presenting cell pulsing assays with peptide 15 in natural form.

Antigen presenting cells (C1R-B*57:01 and T2B*57:01) were incubated overnight with natural peptide 15 (25μM) in the presence or absence of abacavir (35μM). Cells pulsed overnight in R9 medium alone were used as a negative control and cells co-incubated with soluble abacavir were used as a positive control. Following pulsing, the APCs were washed three times in R9 medium and diluted to a cellular concentration of $2x10^5$/mL. The pulsed APCs were then co-incubated with abacavir-responsive CD8$^+$ T-cell clones ($5x10^4$/ 50μL) for a period of 48 hours (37^OC; 5% CO_2). Results were quantified using IFN-γ ELIspot.

5.3.9. T-cell responses to abacavir and/or peptide 15 pulsed EBVs prior washed with citrate phosphate buffer.

Elution of MHC bound peptides was carried out using a protocol established by *Burkhart et al. 2002.* Briefly, autologous EBVs were washed three times with PBS and resuspended in 0.5mL of cold citrate-phosphate buffer (0.131M citric acid/0.066M Na_2HPO_4, pH 3.0 containing 1% BSA) for 2 minutes at 4^OC. Next, the pH was neutralised with an excess of R9 medium and the cells were washed three times in R9 medium and diluted to a concentration of $1x10^6$/mL. EBVs were then pulsed with the natural peptide 15 in the presence or absence of abacavir for 16 hours (37^OC; 5% CO_2). Following pulsing, the EBVs were washed three times in cell culture media and co-incubated ($1x10^4$/ 50µL) with abacavir-specific T-cell clones ($5x10^4$/ 50µL). A pulsing experiment was carried out in parallel EBVs incubated in HBSS instead of citrate-phosphate buffer as a comparator. The T-cell activation in response to pulsed APCs was quantified using secretion of IFN-γ as a readout via the ELIspot assay.

5.3.10. T-cell responses to natural peptide 15 in the presence of glutaraldehyde-fixed APCs.

Autologous EBVs ($2x10^6$ cells/mL) were resuspended in 1mL of HBSS buffer. Glutaraldehyde (25%, 1µL) was added to the cells for 30 seconds, followed by the addition of 1mL of glycine (1M) for a further 45 seconds. EBVs were then washed three times and resuspended in R9 medium to a concentration of $2x10^5$ cells/mL. Abacavir-specific T-cell clones ($5x10^4$/ 50µL) were then co-incubated with the glutaraldehyde fixed EBVs ($1x10^4$/ 50µL) and natural peptide 15 (25µM) in the presence or absence of abacavir for 48 hours (37^OC; 5% CO_2). T-cells co-incubated with non-fixed EBVs in the presence or absence of abacavir were used as a positive control and T-cell activation was quantified using IFN-γ secretion by means of the ELIspot assay.

5.3.11. Generation of responsive T-cell clones to the natural form of peptide 15 in the presence of abacavir.

PBMCs isolated from one HLA-B*57:01 positive donor (Donor 1; HLA-0617) were incubated in the presence of abacavir (35μM) and natural peptide 15 (25μM) in R9 medium for a period of 14 days. On days 6 and 9 cells were fed with R9 medium containing IL-2 (200 IU/mL) to preserve the antigen driven expansion of T-cells. On day 14, CD8$^+$ T-cells were positively selected using MultiSort kits (Miltenyi Biotec, Surrey UK) and T-cell clones were generated via serial dilution as described in section 2.3.5.

5.3.11.1. Testing clones for antigen specificity.

Approximately four weeks after beginning the serial dilutions, T-cell specificity to abacavir + natural peptide 15 was measured by assessing cell proliferation in the presence of the drug and peptide. Proliferation was measured by culturing T-cell clones (5x10^4/ 50μL) with irradiated autologous EBVs (1x10^4/50μL) in the presence of abacavir (35μM) + natural peptide 15 (25μM). Following 48 hour incubation, tritiated thymidine (0.5μCi) was added and proliferation was assessed 16 hours later via scintillation counting. The proliferative response of T-cell clones was expressed as radioactive counts per minute (cpm). T-cell clones with a stimulation index of 2 or greater were picked and expanded by mitogen restimulation in cell culture media containing irradiated PBMCs (5x10^5 cells/well), IL-2 (5μL/mL) and PHA (10μg/mL) for further analysis.

5.3.11.2. Confirmation of antigen specificity of abacavir + natural peptide 15-responsive T-cell clones.

T-cell clones were tested to confirm their specificity to abacavir + natural peptide 15 via co-incubation (5x10^4/50μL) with autologous EBVs (1x10^4/50μL) in the presence or absence of abacavir (35μM) + natural peptide 15 (25μM) with R9 medium as a negative control. ELIspot

plates were developed according to the manufacturer's instructions and counted using an ELIspot AID reader. All clones displaying a significant difference in IFN-γ secretion between control and abacavir + natural peptide 15 treated cells were maintained in cell culture for use in further experiments.

5.3.12. Generation of responsive T-cell clones to amidated peptide 15.

CD8$^+$ T-cell cloning to amidated peptide was carried out as described in section 5.3.11 with the amidated form of peptide 15 (25µM) used as the primary antigen for initial proliferation assays, and subsequent confirmation of antigen specificity was provided via ELIspot.

5.3.13. Statistical analysis

For comparison between control and test values in the proliferation assays the Mann-Whitney test was used. Comparison between control and test values in the ELIspot assays (when available) was carried out using the students two sample t-test.

5.4. Results.

5.4.1. Generation of abacavir-specific T-cell clones.

T-cell clones specific to abacavir were generated using serial dilution assays. From a total of 2279 clones tested across four HLA-B*57:01 positive donors, 101 proliferated in the presence of abacavir on first testing, (0, 1665 ± 188.5 cpm: Abacavir 35μM, 6940 ± 729 cpm; $P<$ 0.0001). Results for T-cell specificity assays of abacavir clones and subsequent phenotyping data is discussed in detail in section 2.1. The abacavir-responsive T-cell clones used for assays in this chapter are displayed in Table 5.1 with their corresponding donor.

Donor 1: HLA-0617	Donor 2: HLA-0957	Donor 3: HVN-0158	Donor 4: HLA-0622
TCC 27	TCC 40	TCC 63	TCC 71
TCC 70	TCC 42	TCC 104	TCC 73
	TCC 43	TCC 105	TCC 86
		TCC 106	TCC 100
		TCC 108	TCC 103

Table 5.1 Abacavir-responsive CD8+ T-cell clones from four HLA-B*57:01 positive donors discussed in this chapter.

5.4.2. Activation of abacavir-specific T-cell clones with peptide 15 in natural and amidated form.

To investigate the effects of the abacavir-induced self-peptide 15 in both the natural and amidated form, three CD8$^+$ T-cell clones were selected and incubated with C1R and T2 APCs with the respective peptides in the presence or absence of abacavir. As T-cell clones 42 and 43 responded strongly in the absence of APCs at the optimal concentration of abacavir (35μM), a dose titration assay was carried out prior to the study (data not shown). T-cell clones 42 and 43 were found to rely on APCs for activation at concentrations of 0.1μM and 1μM respectively (data not shown). Clone 40 was not activated at 35μM in the absence of APCs and was therefore used at this concentration throughout.

In the presence of T2 APCs, T-cell activation in response to abacavir was not observed with clone 40, and was diminished when compared to C1R APCs in clones 42 and 43 (Figure 5.4). Addition of peptide 15 in the natural form did, in some clones, result in enhanced T-cell responses in the presence of abacavir, but no T-cell activation was observed to the peptides in the absence of abacavir. The amidated form of peptide 15 induced T-cell responses in the clones in the presence of abacavir, while moderate T-cell activation was also observed in the absence of abacavir. However, these findings (particularly with the natural peptide), were not reproducible on repeated testing, nor were they observed with other T-cell clones as it proved difficult to distinguish the response to abacavir in the presence of the peptides from the response observed to abacavir alone (Figure 5.5), leading to exploration of alternate assays for further investigation of peptide 15.
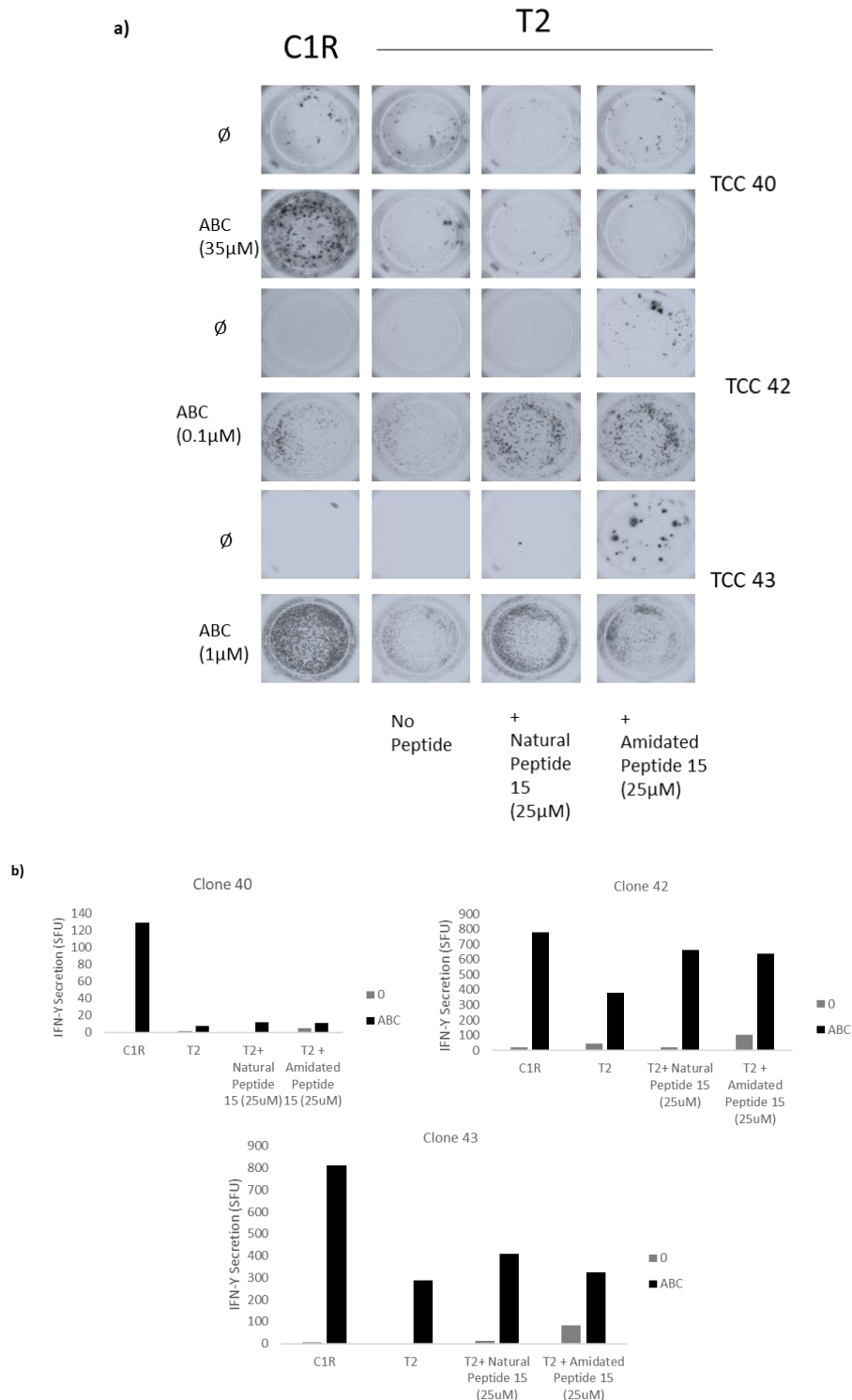
Figure 5.4. Induction of T-cell activity in abacavir-responsive clones by peptide 15 in natural and amidated form. Abacavir (ABC)-responsive CD8^{+} T-cell clones were co-incubated with T2 APCs ± abacavir in the presence or absence of peptide 15 in the natural or amidated form (25µM). T-cells incubated with T2 APCs with no peptide were used as a negative control and T-cells co-incubated with C1R APCs ± abacavir were used as a positive control. (ABC used at different concentrations/clone depending on the concentration for the clones dependence on APCs).
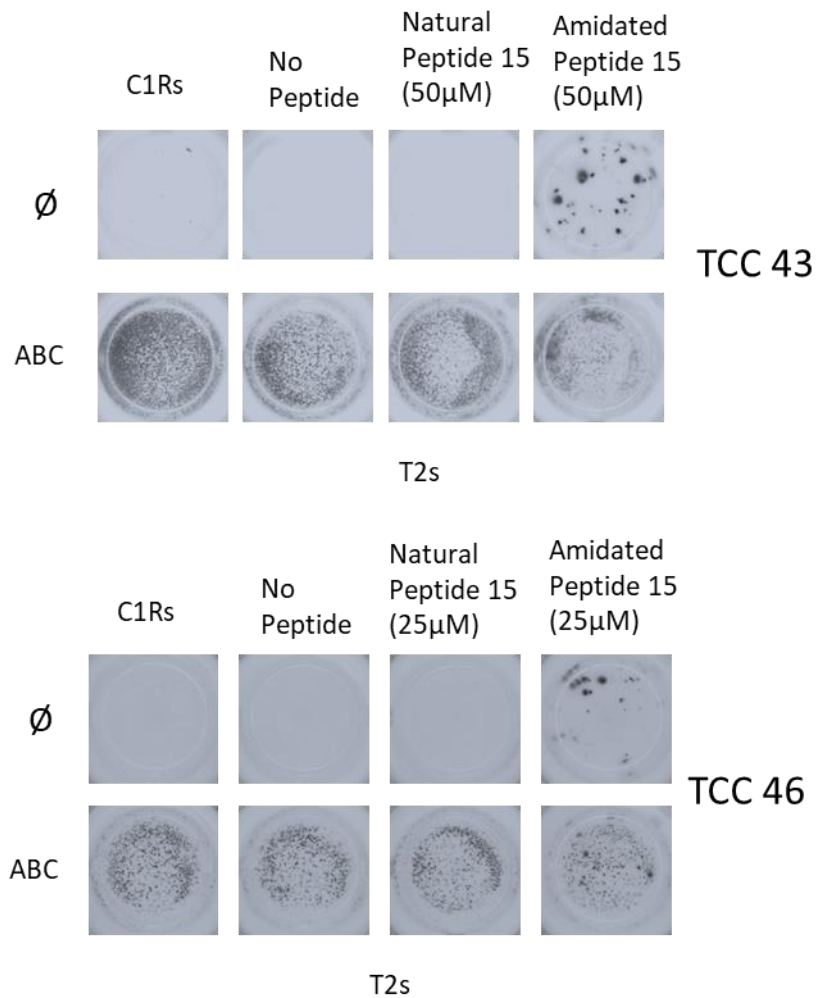
Figure 5.5. Repetition of T-cell induction by addition of peptide 15 in natural and amidated form. Abacavir (ABC)-responsive CD8^{+} T-cell clones were co-incubated with T2 APCs ± abacavir in the presence or absence of peptide 15 in the natural or amidated form (25-50μM). T-cells incubated with T2 APCs with no peptide were used as a negative control and T-cells co-incubated with C1R APCs ± abacavir were used as a positive control. (ABC used at concentrations of 1μM and 20μM for clones 43 and 46 respectively.

5.4.3. Dose dependency on T-cell activation by abacavir with the natural peptide 15.

To investigate whether the addition of peptide 15 would enhance the response to abacavir in clones at lower concentrations of the drug, dose titration assays were conducted. Initially, T-cell clones were incubated with C1R and T2 APCs at increasing concentrations of abacavir in the presence or absence of peptide 15 in both the natural and amidated forms ($25\mu M$) (Figure 5.6). No enhancement of T-cell activity was observed in clones incubated alongside T2 APCs with the natural form of peptide 15 in the presence of abacavir when compared with abacavir alone. Furthermore, low levels of T-cell activation were detected in clones co-incubated with T2 APCs in the presence of the amidated peptide. However, this level of T-cell activation was consistent at all doses, but also without drug, indicating that the presence of abacavir had no bearing on T-cell activation by the amidated peptide.

Next, the dose response assay was expanded to a broader range of abacavir-specific T-cell clones, using autologous EBVs in place of C1R and T2 APCs. T-cell clones were incubated with autologous EBVs at increasing concentrations of abacavir ($0\text{-}30\mu M$) in the presence or absence of the natural peptide 15. No distinguishable difference in T-cell activation was observed in response to abacavir across four of the five abacavir clones in the presence of the peptide, compared to abacavir alone. One clone (TCC 46) displayed an enhanced response to abacavir in the presence of the peptide at concentrations of $10\mu M$ and below (Figure 5.7). Based on these findings, this clone was selected for further study.
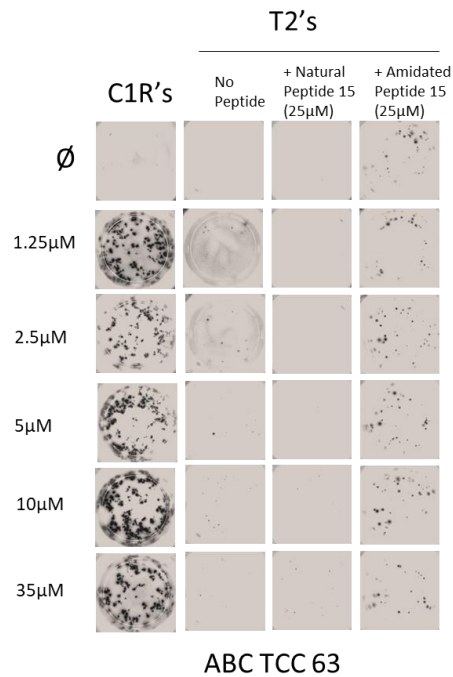
Figure 5.6. Effect of abacavir concentration on T-cell activity induced by peptide 15. Abacavir-responsive CD8$^+$ T-cell clones were co-incubated with T2 APCs at increasing concentrations of abacavir (0-35µM) in the presence or absence of peptide 15 in the natural or amidated form (25µM). T-cells incubated with T2 APCs with no peptide in the presence of abacavir (0-35µM) were used as a negative control and T-cells co-incubated with C1R APCs with the same abacavir concentrations were used as a positive control.
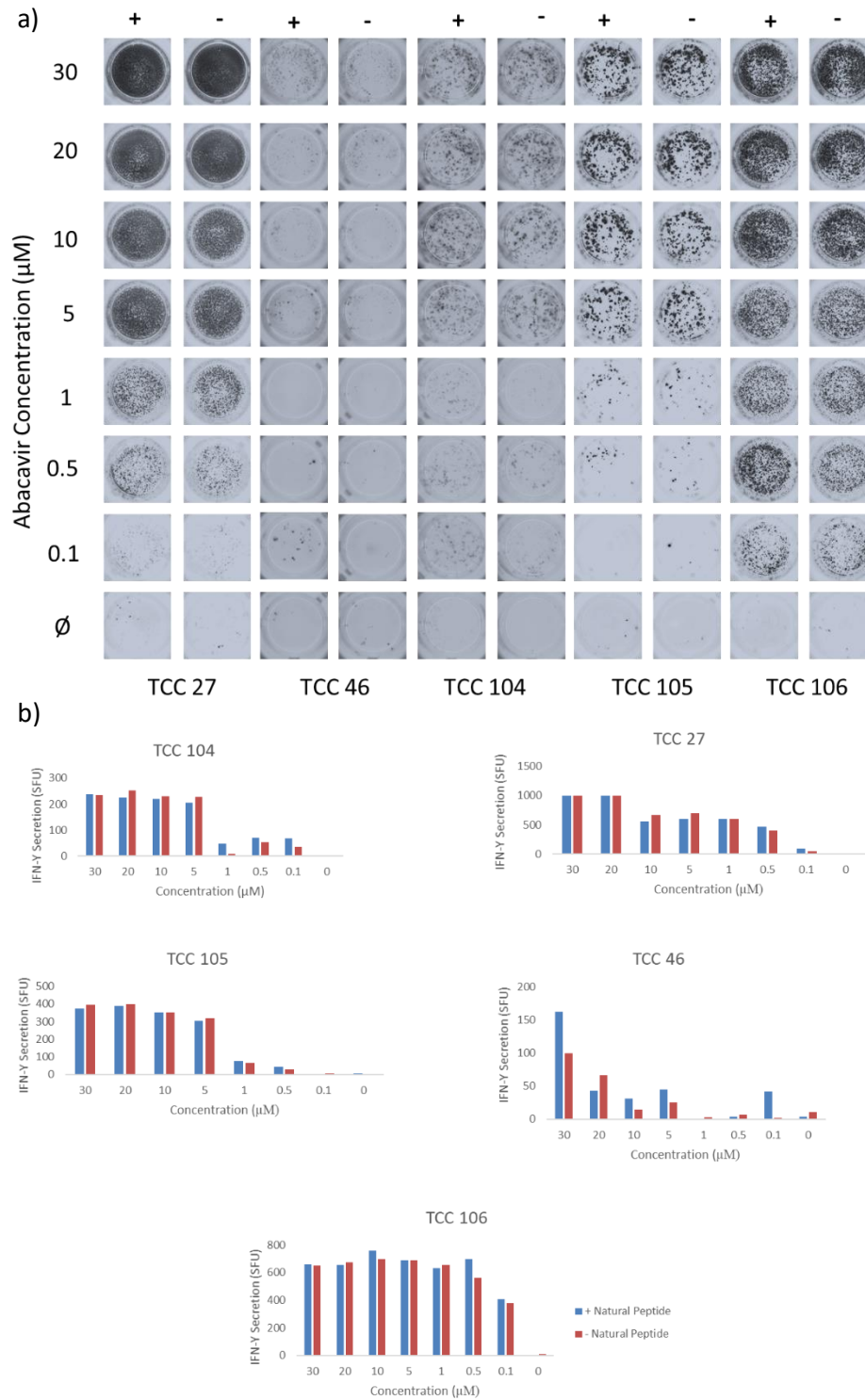
Figure 5.7. Abacavir-specific T-cell activation in the presence of abacavir and natural peptide 15.

a) IFN-γ ELIspot well images of five abacavir-specific CD8^{+}T-cell clones (TCC) co-incubated with autologous EBVs at abacavir concentrations of 0-30μM in the presence or absence of the natural peptide 15 (+ and -). b) T-cell activation quantified by IFN-γ secretion from T-cell clones and compared in the presence or absence of peptide 15.
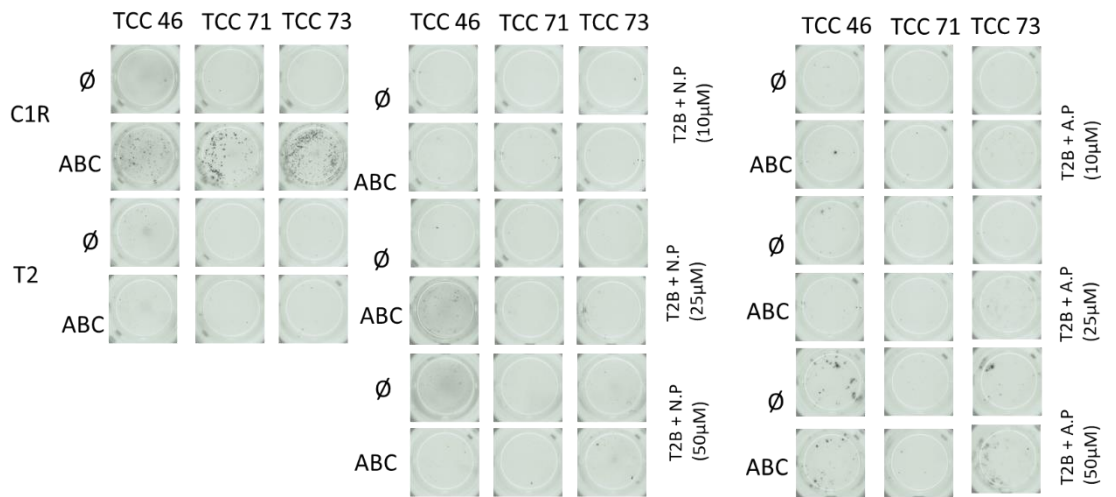
5.4.4. Dose dependency of CD8$^+$ T-cell activation in in response to increasing concentrations of peptide 15 in natural and amidated form.

Three CD8$^+$ T-cell clones were co-incubated with C1R and T2 APCs and peptide 15 in both forms at concentrations of 10µM, 25µM and 50µM in the presence or absence of abacavir. In all three clones used, the eradicated response to abacavir observed in T-cells incubated with the T2 APCs was not reinstated by the addition of natural peptide 15 at any concentration. Stimulation with the amidated peptide resulted in modest T-cell activation at 50µM in two of the clones, but the presence of the drug had no influence on induced T-cell activity (Figure 5.8).

Using T-cell clone 46, dose response assays to both natural peptide 15 and abacavir were conducted. T-cells were co-incubated with T2 APCs at increasing concentrations of abacavir (0-100µM) and the natural peptide (0-100µM). As expected, an increase in T-cell activation was observed with an increase in concentration of abacavir, however no enhanced T-cell activity was triggered by increasing the concentrations of natural peptide 15 compared to abacavir alone (Figure 5.9.).
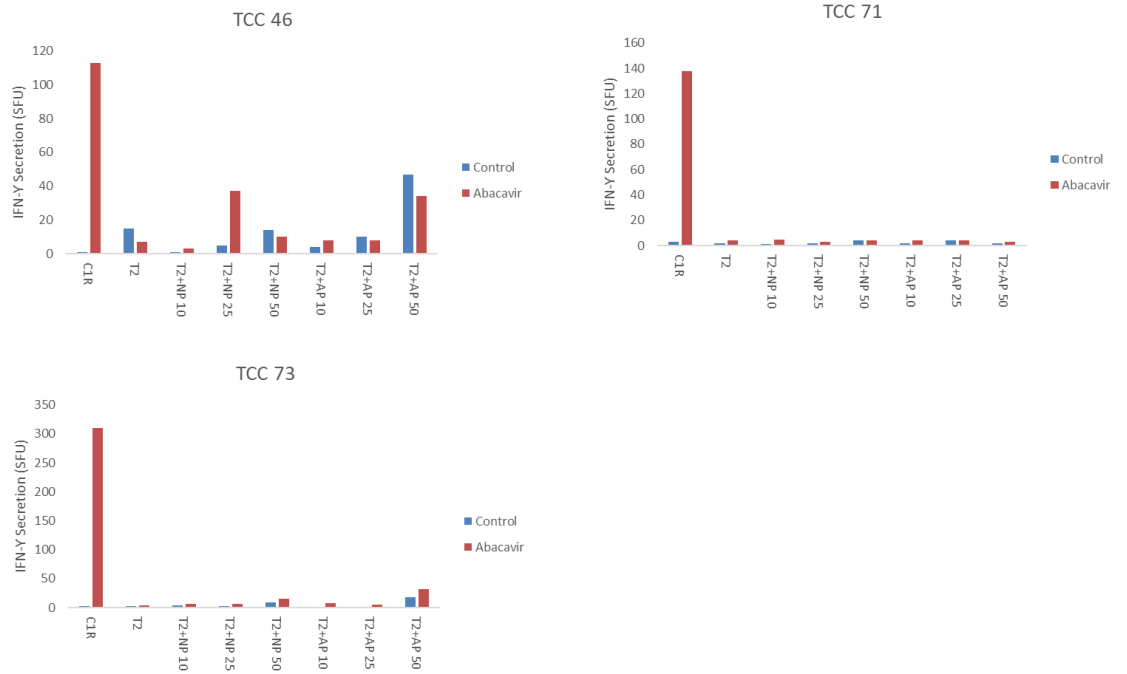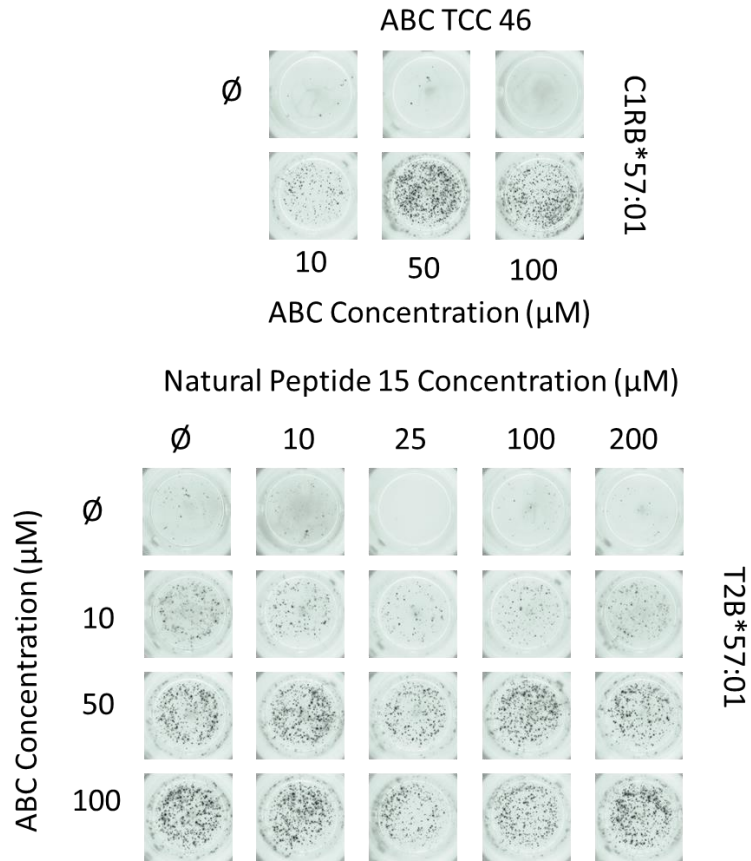
Figure 5.8. Dose dependency of T-cell activation on concentration of peptide 15 in the natural and amidated form (N.P and A.P. respectively). a) IFN-γ ELIspot well images and b) direct comparisons of three individual abacavir-responsive T-cell clones. T-cells were co-incubated with T2 APCs ± abacavir at increasing concentrations of peptide 15 in the natural or amidated form (10, 25, 50 μM).

Figure 5.9. T-cell activation dependency on concentration of abacavir and the natural peptide 15. Abacavir-responsive CD8^{+} T-cells were co-incubated with T2 APCs at increasing concentrations of both abacavir (ABC; 0-100μM) and natural peptide 15 (0-200μM). T-cell clones co-incubated with C1R APCs at increasing abacavir concentrations (0-100μM) were used as a positive control.

5.4.5. APC pulsing assays with peptide 15 in natural form.

Stimulating T-cells with 16 hour abacavir pulsed EBVs is shown in some clones to result in the induction of IFN-γ secretion (Chapter 2), indicating these clones employ the altered peptide model as a means of T-cell activation (Illing et al. 2012). Two abacavir-specific T-cell clones which demonstrated strong T-cell responses in the presence of abacavir pulsed EBVs, were co-incubated with C1R and T2 APCs pulsed for 16 hours in the presence of abacavir ± natural peptide 15. The observed T-cell response in the presence of C1Rs (TCC 46, *P<0.01*), (TCC 71, *P<0.05*) was abrogated in the presence of the T2 APCs. However, co-stimulation with natural peptide 15 and T2 APCs did not induce T-cell activation (Figure 5.10).
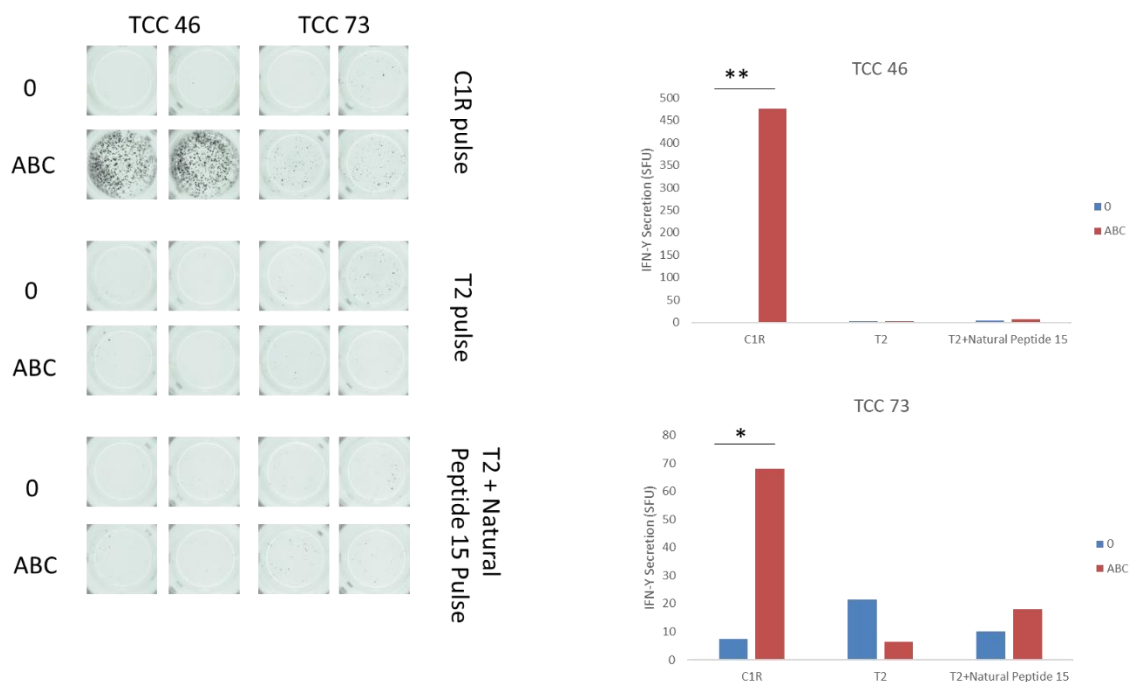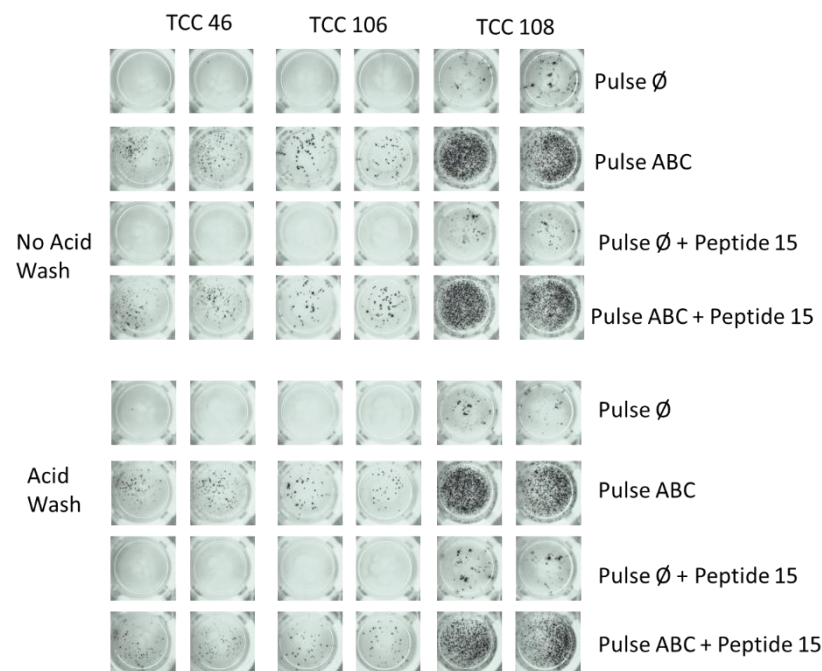

Figure 5.10. T2 APCs were pulsed with abacavir (ABC; 35μM) in the presence or absence of the natural peptide 15 (25μM) for 16h. Pulsed APCs were then co-incubated with abacavir-specific T-cells for 48h and T-cell activation was quantified using IFN-γ ELIspot. ABC pulsed C1R APCs were used as a positive control and APCs pulsed in just R9 medium were used as a negative control.
*P<0.05, **P<0.01, ***P<0.001.

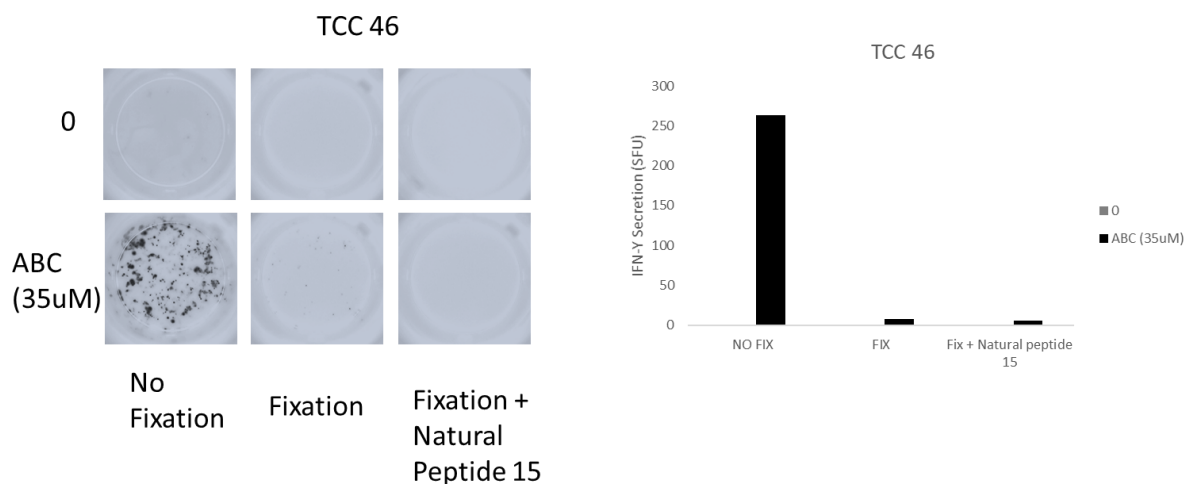## 5.4.6. Activation of abacavir T-cell clones in response to abacavir + peptide pulsed, acid washed APCs.

To assess if the introduction of a new peptide, following displacement of the peptide bound at the MHC, could result in an increased T-cell response in the presence of abacavir, autologous EBVs were incubated in cold citrate-phosphate buffer (0.131M citric acid/0.066M Na_2HPO_4, pH 3.0 containing 1% BSA) prior to pulsing with abacavir alone or abacavir ± natural peptide 15. Cells incubated with HBSS instead of citrate-phosphate buffer were used as a comparator. No comparable difference was observed in T-cells co-incubated with acid washed EBVs pulsed with abacavir in the presence of natural peptide 15 when compared to pulsing with abacavir alone. Furthermore, no measurable difference was observed across the three clones between cells washed with citrate-phosphate buffer prior to pulsing and those washed with HBSS instead.

Figure 5.11. CD8^{+} T-cell response of abacavir-specific clones with pulsed autologous EBVs. IFN-γ ELIspot well images of three abacavir-specific CD8^{+}T-cell clones co-incubated with autologous EBVs pulsed with abacavir (ABC) (35μM), peptide 15 (25μM) and abacavir + peptide 15. EBVs pulsed with cell culture media alone were used as a negative control. Acid wash: EBVs were washed with cold citrate-phosphate buffer (0.131M citric acid/0.066M Na_2HPO_4, pH 3.0 containing 1% BSA) prior to pulsing. No acid wash; EBVs were washed with HBSS prior to pulsing.

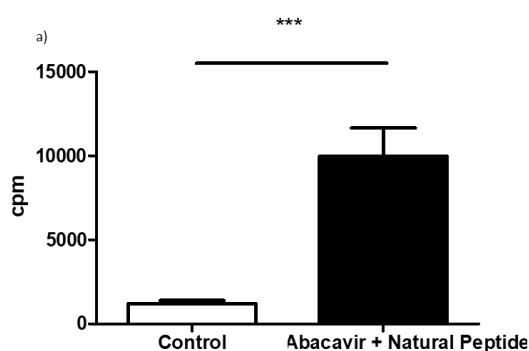### 5.4.7. T-cell activation to abacavir + natural peptide 15 in the presence of glutaraldehyde fixed APCs.

To remove the processing capabilities of the autologous EBVs, fixation with glutaraldehyde prior to co-incubation with T-cells was conducted. T-cells were co-incubated with the glutaraldehyde fixed EBVs in the presence of abacavir or abacavir + natural peptide 15. T-cells incubated with non-fixed EBVs in the presence of abacavir were used as a positive control. Indeed, fixation of the EBVs eradicated the T-cell response to abacavir, however addition of the natural peptide was not sufficient to evoke IFN-γ secretion in the presence or absence of the drug (Figure 5.12).

Figure 5.12. Activation of abacavir-specific T-cell clones co-incubated with autologous EBVs fixed with glutaraldehyde in the presence of abacavir (35 μM) and abacavir + natural peptide 15 (25 μM). T-cells incubated with unfixed APCs ± abacavir (35 μM) were used as a comparator.
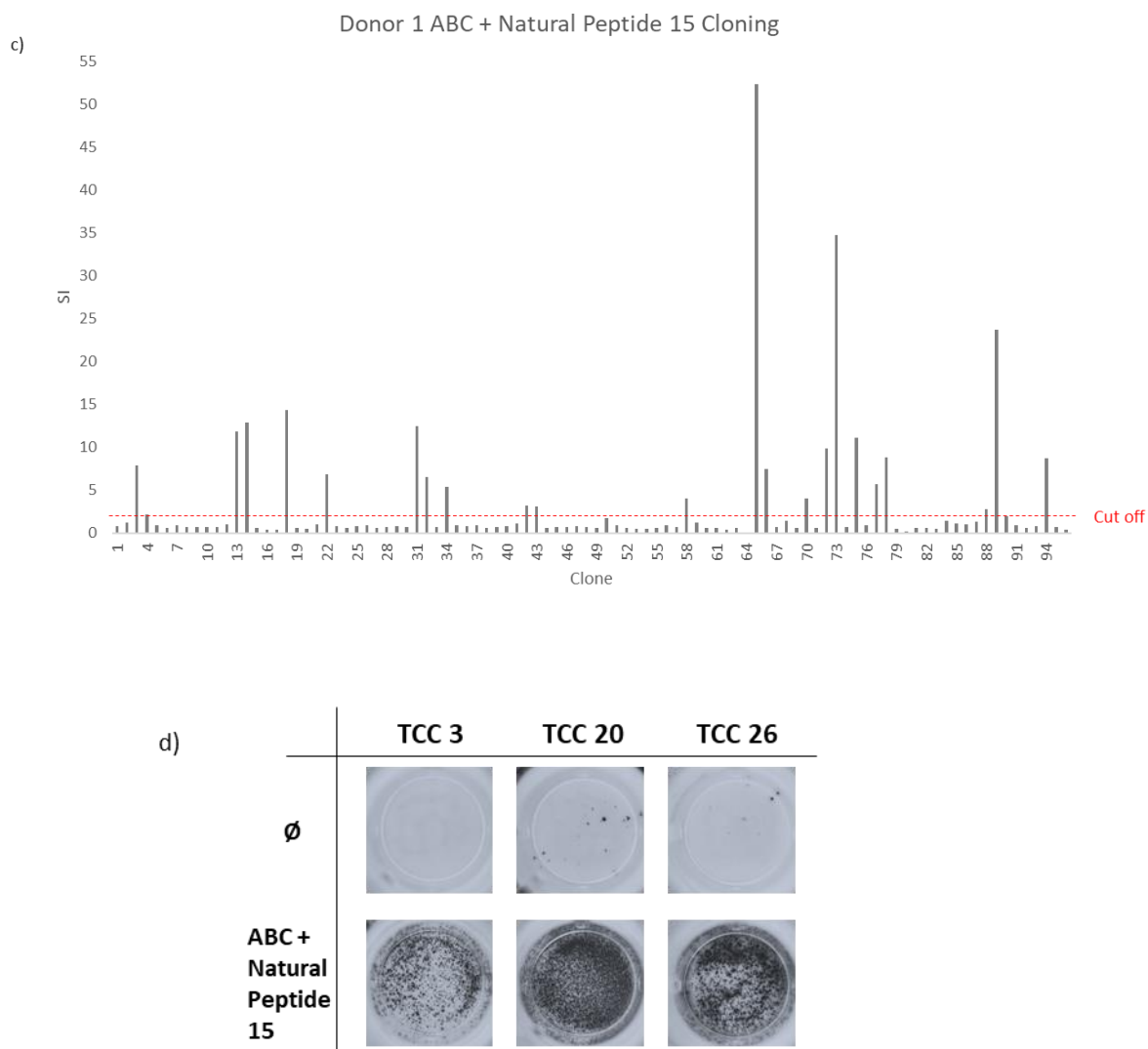
5.4.8. Generation of T-cell clones to the natural form of peptide 15 in the presence of abacavir.

To test the possibility of yielding T-cell clones responsive to abacavir and the natural form of peptide 15, T-cell cloning was carried out using established methods described in detail in section 2.3.5. The procedure was conducted following the same methods, only the natural peptide 15 (25µM) was added alongside abacavir at the priming and testing for antigen specificity stages. From a total of 96 clones tested, 25 proliferated in response to abacavir + the natural peptide on first testing (0, 1201 ± 189.4 cpm; abacavir (35µM) + natural peptide 15 (25µM), 9987 ± 1673 cpm; P<0.0001). Antigen specificity was confirmed by culturing the generated T-cell clones with abacavir and the natural peptide for 48 hours and measuring IFN-γ secretion via ELIspot (Figure 5.13). Only those clones producing significant increase in IFN-γ secretion between control and abacavir + natural peptide 15 were maintained in cell culture. All responsive clones to abacavir + the natural peptide 15 were phenotyped as CD8$^+$ (Figure 5.15).


a)

	Clones Tested	Specific	% Specific
Abacavir + Natural Peptide 15	96	25	26

c)

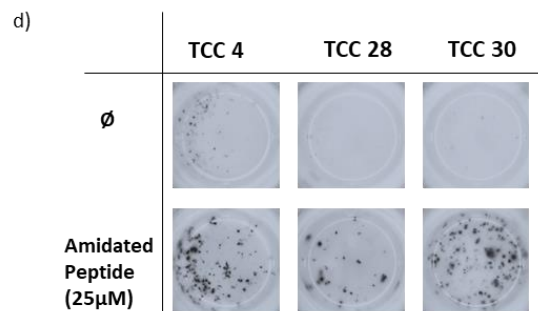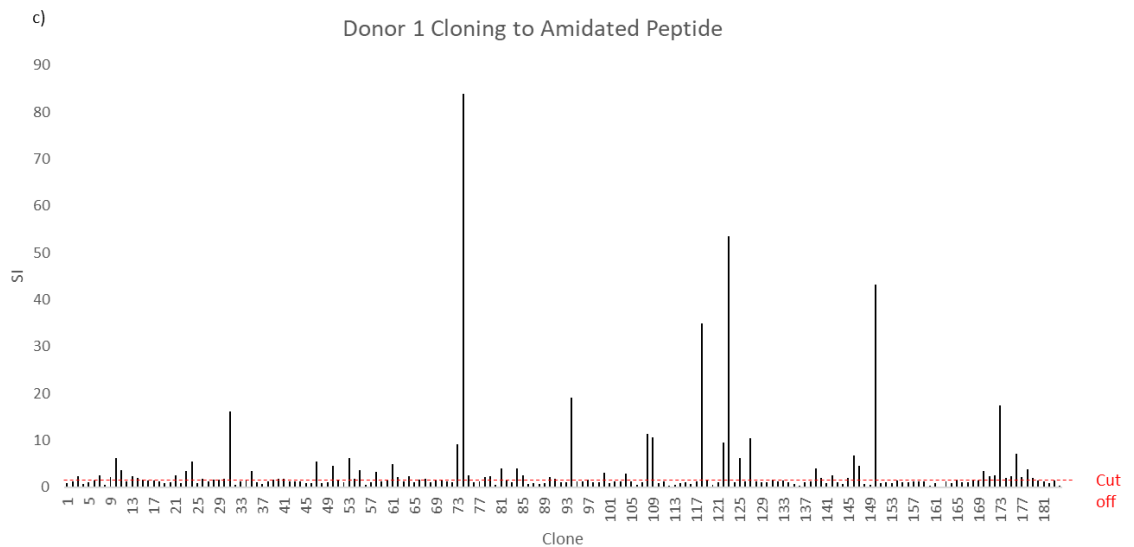Donor 1 ABC + Natural Peptide 15 Cloning

d)

Figure 5.13. Generation of T-cell clones responsive to abacavir and natural peptide 15. a) Mean proliferative response and b) Table showing percentage of responsive clones generated to abacavir in the presence of the natural peptide 15 from donor 1. c) Antigen specificity of T-cell clones generated to abacavir in the presence of natural peptide 15. T-cell clones (5×10^4) were cultured in the presence of irradiated autologous antigen presenting cells (1×10^4) in the presence or absence of abacavir (35µM) + natural peptide 15 (25µM) for 48 hours. Tritiated thymidine (0.5µCi) was added for 16 hours and proliferation was measured using scintillation counting. Clones yielding an SI<2 were considered positive. d) Representative ELIspot well images from three T-cell clones tested for antigen specificity in the presence of abacavir (35µM) + natural peptide 15 (25µM).

## 5.4.9. Generation of T-cell clones to amidated peptide 15.

T-cell cloning was carried out to the amidated form of peptide 15 using methods described in detail in section 2.3.5. Cloning was carried out using the same methods as before, with the amidated peptide 15 (25µM) used at the priming and testing for antigen specificity stages in the place of abacavir. From a total of 184 clones, 73 proliferated in response to the amidated peptide on first testing (0, 1619 ± 265.7 cpm, amidated peptide (25uM), 7321 ± 1417 cpm; P<0.0001). Antigen specificity was confirmed by culturing the generated T-cell clones with the amidated peptide for 48 hours and measuring IFN-γ secretion via ELIspot (Figure 5.14). All responsive clones to the amidated peptide 15 were phenotyped as CD8^{+} (Figure 5.15).

	Clones Tested	Specific	% Specific
Amidated Peptide	184	73	39.6

c)

d)
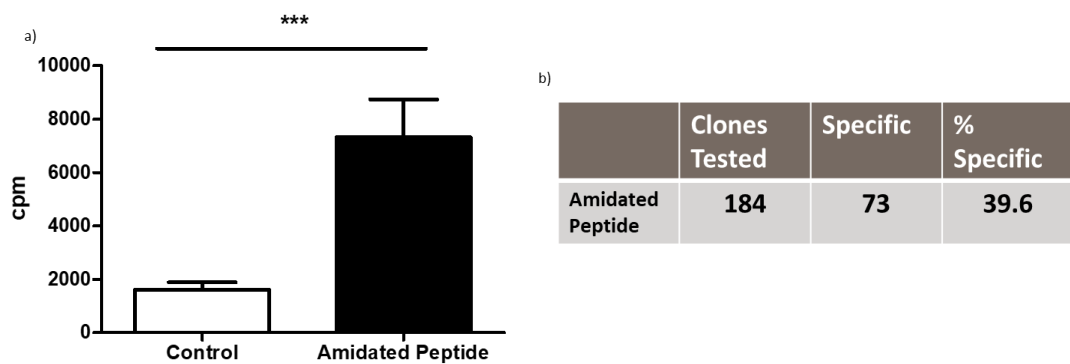
Figure 5.14. Generation of T-cell clones responsive to amidated peptide 15. a) Mean proliferative response and b) Table showing percentage of responsive clones generated to amidated peptide 15 from donor 1. c) Antigen specificity of T-cell clones generated to amidated peptide 15. T-cell clones ($5x10^4$) were cultured in the presence of irradiated autologous antigen presenting cells ($1x10^4$) in the presence or absence of the amidated peptide (25µM) for 48 hours. Tritiated thymidine (0.5µCi) was added for 16 hours and proliferation was measured using scintillation counting. Clones yielding an SI<2 were considered positive. d) Representative ELIspot well images from three T-cell clones tested for antigen specificity in the presence of amidated peptide 15 (25µM).
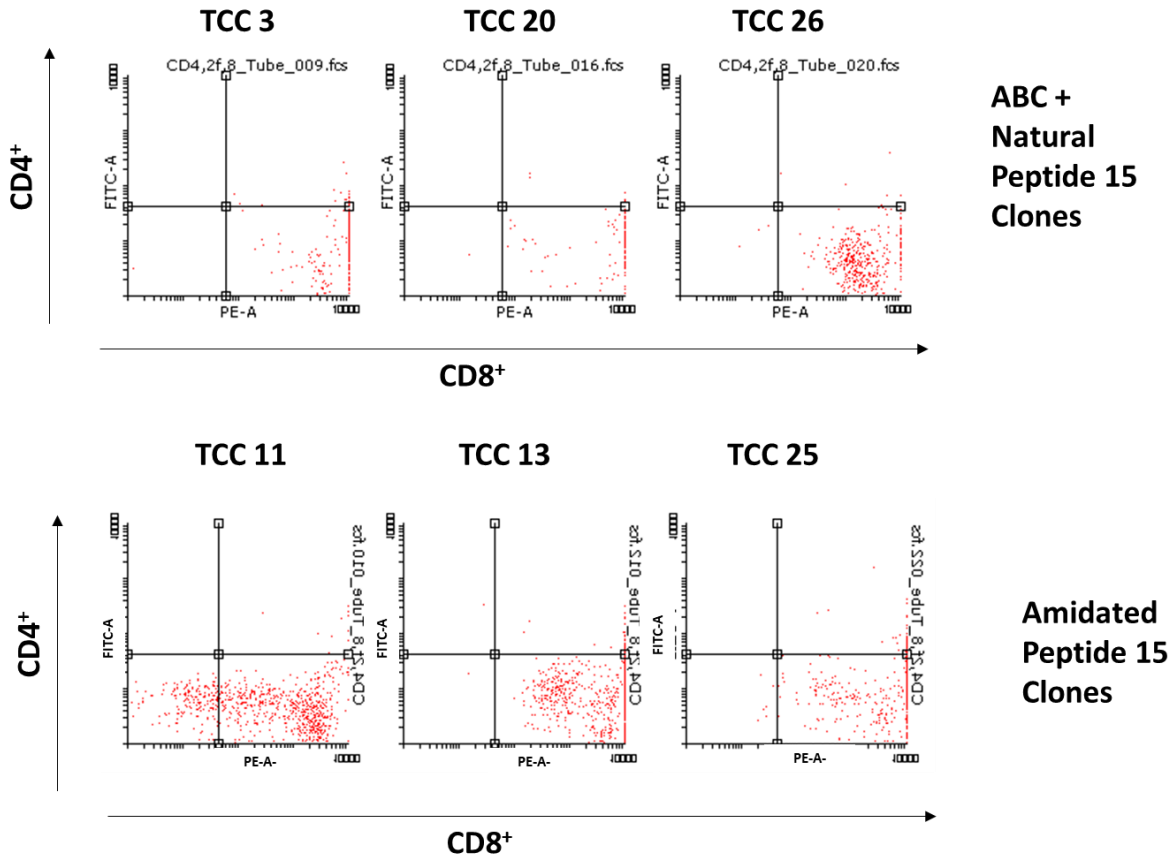
Figure 5.15. Cell phenotyping for expression of CD4 and CD8 on the surface of abacavir + natural peptide 15 or amidated peptide 15 T-cell clones. Cells (50μL) were stained with antibodies CD4-FITC and CD8-PE and incubated for 20 minutes at 4°C. Cells were then washed and flow cytometry used to analyse cellular phenotype (BD FACSCANTO II).

5.4.10. Activation of peptide specific T-cell clones with peptide 15 in natural and amidated form in the presence or absence of abacavir.

To test the responsiveness of the T-cell clones generated to either abacavir + natural peptide 15 or the amidated peptide 15 alone, a selection of clones were tested with the individual peptides in the presence or absence of abacavir, with abacavir alone as a comparator. Clones generated to abacavir + natural peptide 15 displayed no distinguishable difference in T-cell activation when incubated with abacavir in the presence of the natural peptide, compared to abacavir alone. Furthermore, these clones were activated by the amidated peptide but to a much lesser degree than with the amidated peptide in the presence of abacavir. No T-cell activity was observed in these clones when stimulated with the natural peptide 15 alone.

Clones generated to the amidated peptide produced strong T-cell activity when co-incubated with the peptide in its amidated form, but yielded no T-cell activity when stimulated with the natural form of peptide 15. Furthermore, these clones displayed no IFN-γ secretion when stimulated with abacavir. Interestingly, the observed response to the amidated peptide was diminished in the presence of abacavir in clone 11 (Figure 5.16).
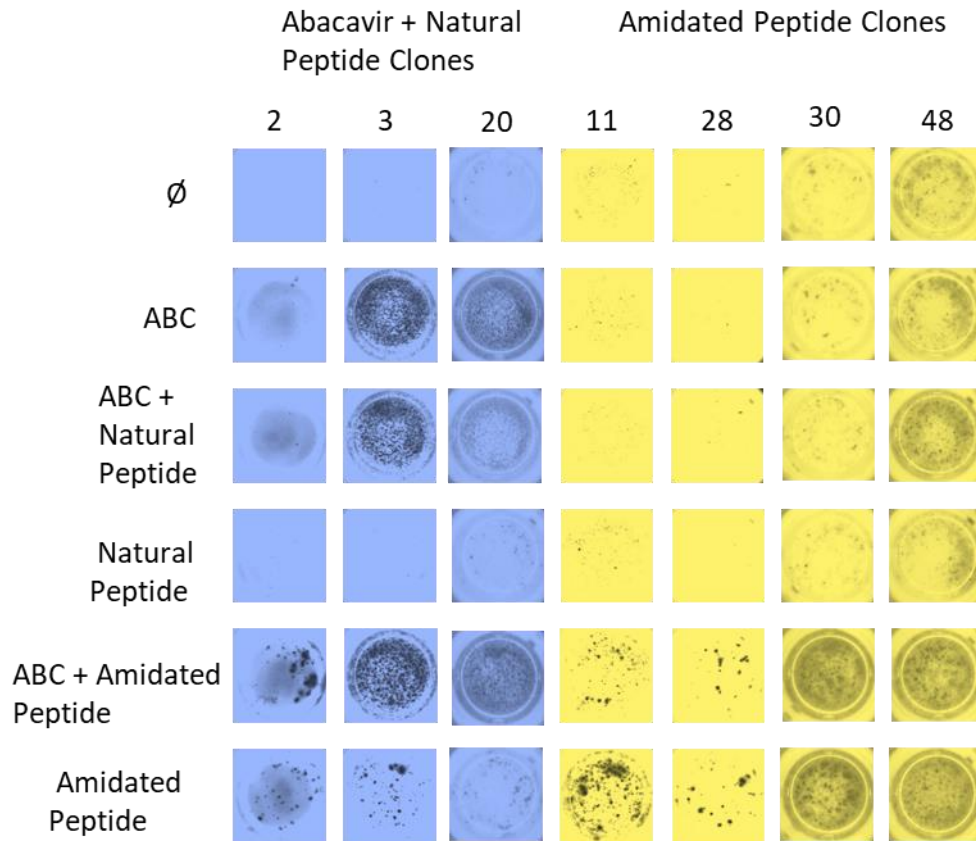
Figure 5.16. CD8^{+} T-cell activity of clones to natural peptide 15 + abacavir and amidated peptide 15. A panel of responsive clones generated to peptide 15 in the natural form + abacavir (blue) and the amidated peptide 15 in abacavirs absence (yellow) were exposed to six individual conditions. Abacavir alone (ABC, 35µM), natural peptide 15 (25µM) ± abacavir. Amidated peptide 15 (25µM) ± abacavir for 48h (37°C, 5% CO_2). T-cell activity was quantified by measuring IFN-γ secretion by means of the ELIspot assay.

5.4.11. Dose dependent activation of abacavir + natural peptide 15 specific clones.

Next, the dose dependent activation of clones with abacavir in the presence or absence of natural peptide 15 were assessed. Distinguishing between the T-cell responses observed in the presence of abacavir + natural peptide from the response to abacavir alone can be difficult, therefore, titrating the dose down a concentration gradient allows for easier distinction of T-cell activation. Two clones responsive towards abacavir + natural peptide 15 were co-incubated with autologous EBVs at increasing concentrations of abacavir (0-30μM) in the presence or absence of natural peptide 15 (25μM). Clone 3, displayed an enhanced T-cell response in the presence of the peptide at all concentrations within the range used (Figure 5.17), however the same distinction between peptide-treated and untreated cells was not as clearly observed with clone 20, particularly as at concentrations of 5μM and below higher T-cell activity to abacavir was observed in the absence of the peptide. Furthermore, upon repetition of the assay (Figure 5.18), the distinction in response to abacavir between peptide-treated and untreated cells with clone 3 was not observed. A small enhancement of T-cell activity in the presence of natural peptide 15 was observed at 2.5μM, but not at any of the concentrations below which would have been expected if the peptide was producing the enhanced T-cell response. The same absence of a distinguishable T-cell response between abacavir-treated and abacavir + natural peptide-treated cells was again observed with clone 20 (Figure 5.17).
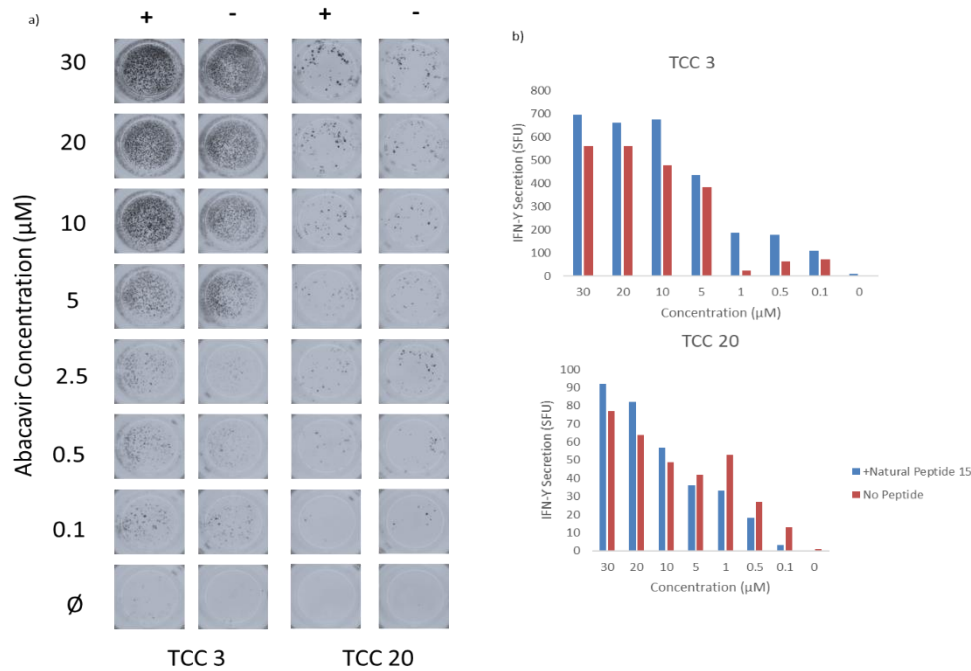
Figure 5.17. Abacavir-specific T-cell activation in the presence of abacavir and natural peptide 15. a) IFN-γ ELIspot well images of two abacavir + natural peptide 15 specific CD8^{+} T-cell clones co-incubated with autologous EBVs at abacavir concentrations of 0-30µM in the presence or absence of the natural peptide 15 (25µM). b) T-cell activation quantified by IFN-γ secretion from T-cell clones and compared in the presence or absence of peptide 15 (SFU).
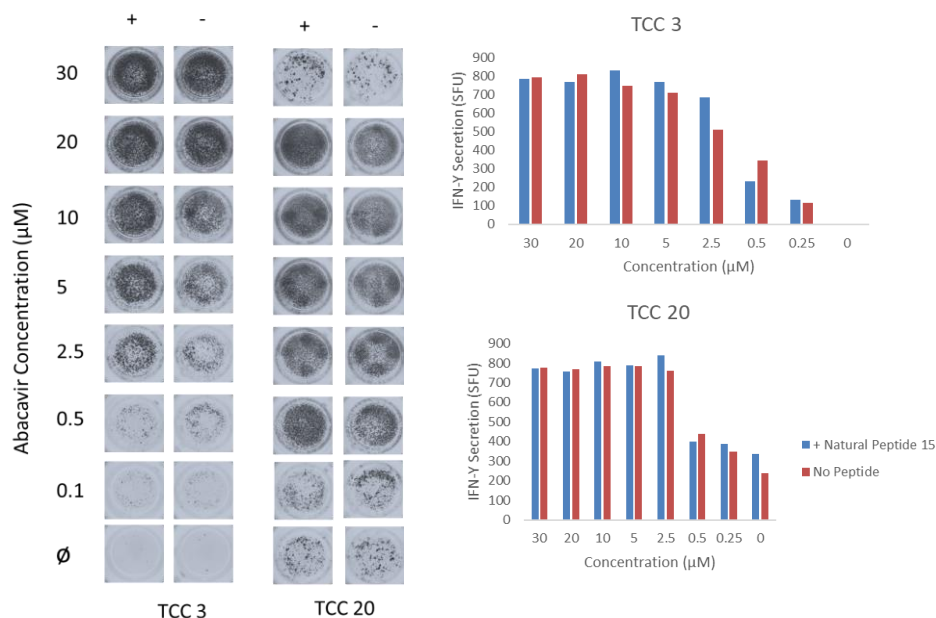
Figure 5.18. Abacavir-specific T-cell activation in the presence of abacavir and natural peptide 15. a) IFN-γ ELIspot well images of two abacavir + natural peptide 15 specific CD8^{+} T-cell clones co-incubated with autologous EBVs at abacavir concentrations of 0-30µM in the presence or absence of the natural peptide 15 (25µM). b) T-cell activation quantified by IFN-γ secretion from T-cell clones and compared in the presence or absence of peptide 15 (SFU).

5.4.12. Activation of T-cell clones with APCs pulsed with natural peptide 15 ± abacavir.

The APC pulsing assays to abacavir in the presence or absence of natural peptide 15 were repeated using the two specific T-cell clones generated to abacavir in the presence of peptide 15. All conditions were the same as described in section 5.4.6. Again, no comparable difference in IFN-γ secretion between cells co-incubated with abacavir pulsed EBVs and those co-incubated with EBVs pulsed with abacavir + natural peptide 15 was observed in either clone. Next, the assay was repeated, but prior to pulsing with abacavir or abacavir + peptide, EBVs were incubated in cold citrate-phosphate buffer to remove the bound peptides as described in section 5.4.2. As observed previously with abacavir clones, no increase in T-cell activation was observed in cells co-incubated with abacavir + peptide 15 pulsed APCs compared to those incubated with APCs pulsed with abacavir alone following acid washing of the cells.
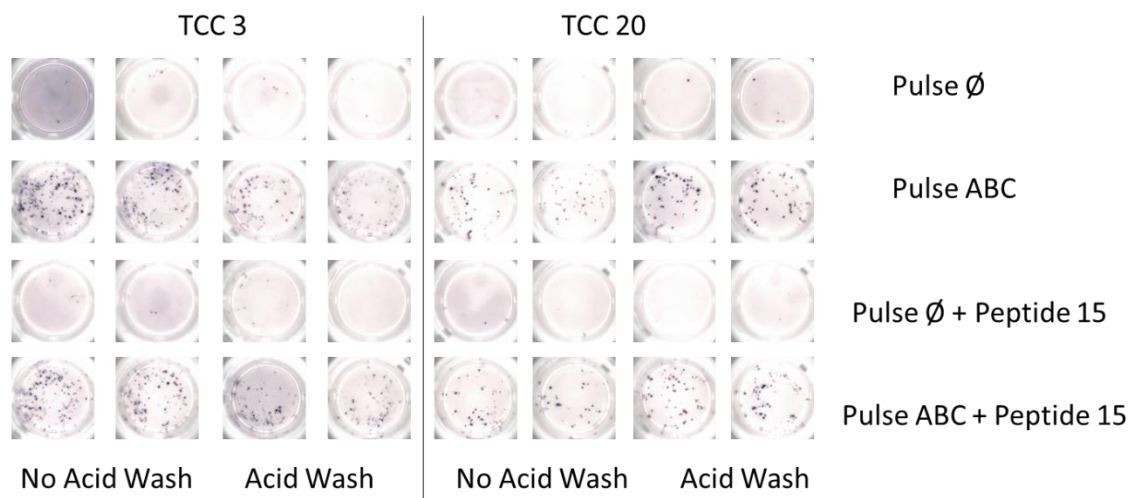
Figure 5.19. CD8$^+$ T-cell response of abacavir + natural peptide 15 specific clones with pulsed autologous EBVs. IFN-γ ELIspot well images of two abacavir + natural peptide 15 specific CD8$^+$ T-cell clones co-incubated with autologous EBVs pulsed with abacavir (ABC) (35μM), natural peptide 15 (25μM) and abacavir + natural peptide 15. EBVs pulsed with cell culture media alone were used as a negative control. Acid wash: EBVs were washed with cold citrate-phosphate buffer (0.131M citric acid/0.066M Na$_2$HPO$_4$, pH 3.0 containing 1% BSA) prior to pulsing. No acid wash; EBVs were washed with HBSS prior to pulsing.

5.4.13. APC dependency of amidated peptide 15 specific T-cell clones.

Three clones generated with specificity for peptide 15 in the amidated form were co-incubated with the peptide in the presence or absence of autologous EBVs with T-cell activation quantified via the IFN-γ ELIspot assay. T-cell activation in the presence of amidated peptide 15 was severely blunted in the absence of APCs in all three peptide specific T-cell clones. The assay was repeated using the same three amidated specific T-cell clones but with the natural form of peptide 15 in place of its amidated counterpart. Co-incubation with the natural peptide induced no activation of T-cells in either the presence or absence of APCs (Figure 5.20).
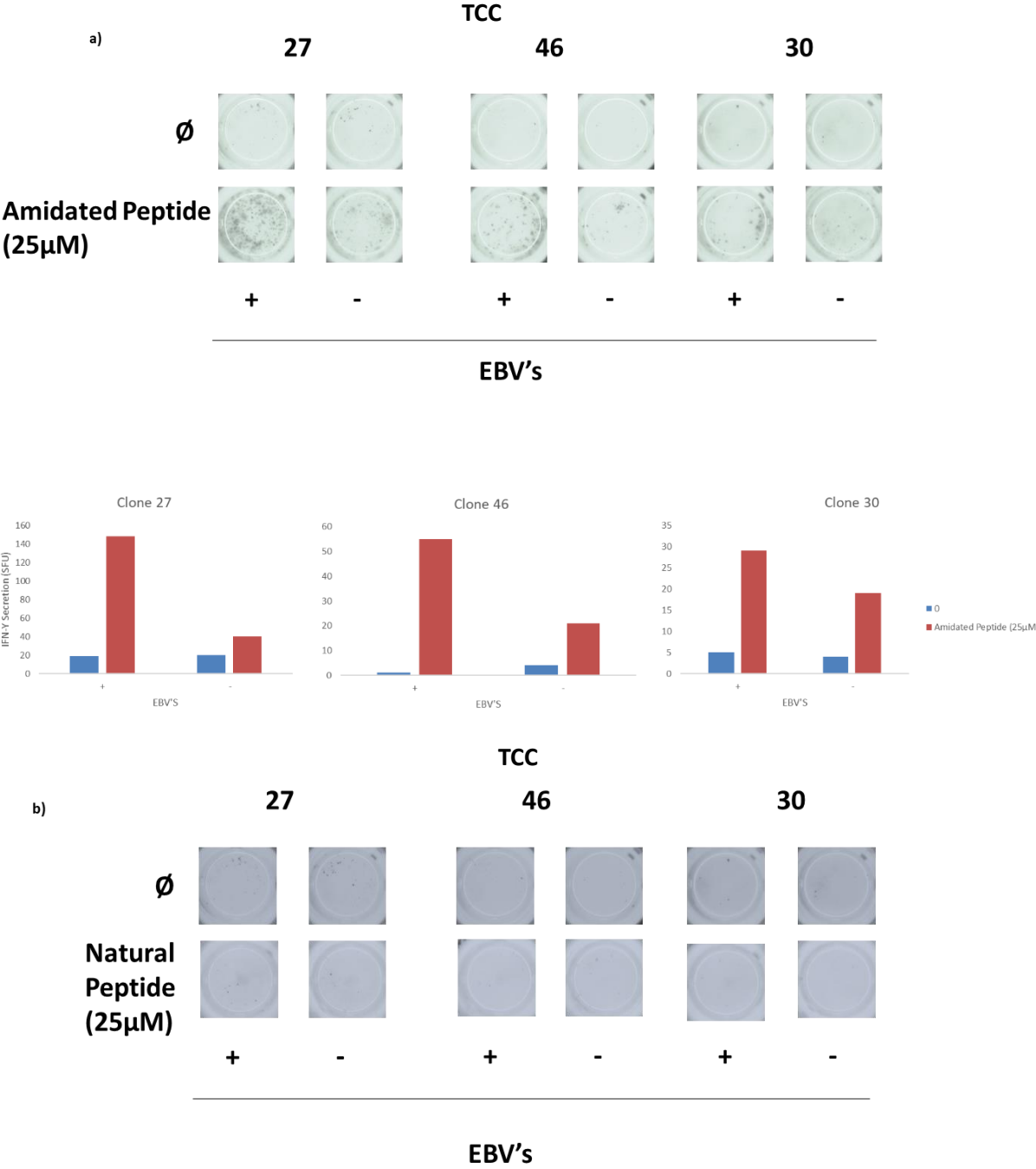
Figure 5.20. APC dependency of CD8^{+} T-cell activation to the amidated peptide 15. Three amidated peptide 15-specific T-cell clones were co-incubated with the amidated peptide 15 (25µM) for 48 hours in the presence or absence of EBVs (37°C; 5% CO_2). T-cell activation was measured by IFN-γ secretion via means of the ELIspot assay (SFU). b) The assay was repeated on the same three amidated peptide 15-specific T-cell clones but using the natural form of peptide 15 instead of the amidated version.

5.4.14. Activation of amidated peptide 15-specific T-cell clones is not dependent on abacavir.

To investigate the dependence on abacavir for the induction of CD8^{+} T-cells with specificity to the amidated form of peptide 15, two specific clones were co-incubated with autologous EBVs at increasing concentrations of the amidated peptide (0-200μM) in the presence or absence of abacavir (35μM) for 48 hours (37°C; 5% CO_2). T-cell activation was measured via quantification of IFN-γ secretion using the ELIspot assay. The presence of abacavir had little to no bearing on the magnitude of T-cell activation instigated by the amidated peptide 15 in the two specific clones (Figure 5.21). With one clone (TCC 11), an enhanced response was observed at 50μM of the amidated peptide in the presence of abacavir, compared to peptide alone. However, no enhancement was observed at any concentration below indicating that abacavir was unlikely to contribute to this response.
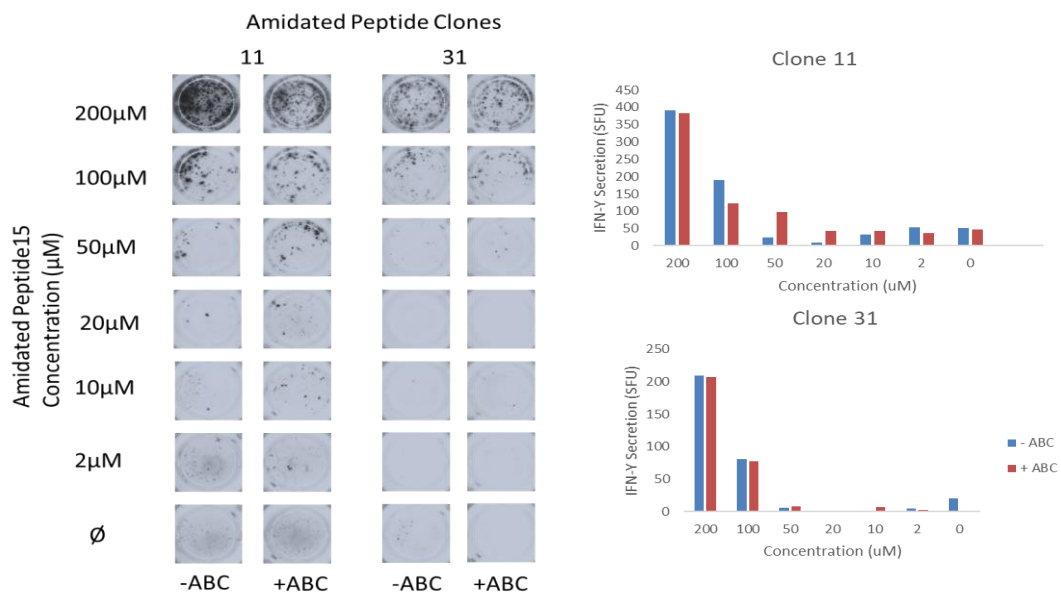
Figure 5.21. Dependency on dose and presence of abacavir on activation of amidated peptide specific CD8^{+} T-cell clones. Two amidated peptide 15 specific T-cell clones were co-incubated with autologous EBVs at increasing concentrations of the amidated peptide 15 (0-200μM) in the presence or absence of abacavir (35μM) for 48h (37°C; 5% CO_2). T-cell activation was measured using IFN-γ secretion as a readout via means of the ELIspot assay (SFU).

5.5. Discussion.

Abacavir hypersensitivity reactions in individuals expressing the HLA-B*57:01 allele present a major clinical problem due to the high prevalence of the risk allele, particularly in caucasian individuals. Indeed, prospective genotyping for HLA-B*57:01 expression is now common practice in the medical setting prior to treatment with abacavir, with those testing positive for the allele excluded from abacavir therapy (Mallal et al. 2008). However, the underlying mechanisms mediating the observed hypersensitivity reactions to abacavir remain a contested topic. Neither the hapten or the PI model have been able to sufficiently explain the T-cell mediated reactions observed in the presence of the drug due to abacavir co-eluting from MHC unbound to peptides and the requirement for antigen processing and presentation for T-cell responses to take place (Illing et al. 2012; Chessman et al. 2008).

The altered peptide repertoire model hypothesises that abacavir induces a change in the array of peptides presented on the surface of antigen presenting cells for recognition by T-cells. As T-cells would perceive these peptides to be foreign, due to no previous exposure, an immunological response would be initiated. Indeed, studies to investigate this found an overall shift in the prevalence of new altered self-peptides mainly terminating in small chain C-terminal anchors such as valine, isoleucine and leucine eluted from HLA-B*57:01 in the presence of abacavir, that were not detected in its absence (Illing et al. 2012; Ostrov et al. 2012; Norcross et al. 2012). This incepted the theory that abacavir-induced a conformational change in the shape and chemistry of the antigen binding cleft of HLA-B*57:01, leading to a reduction in its size which would accommodate the amino acids containing small C-terminal anchors, meaning their subsequent presentation to T-cells would initiate an immune response (Illing et al. 2012; Ostrov et al. 2012; Norcross et al. 2012).

A panel of 120 of these eluted abacavir-induced self-peptides were received by our research group from our collaborators in the Purcell Laboratory (Monash University, Melbourne)

which were subsequently tested for T-cell activating properties by Dr Mohammad Alhaidiri. From these 120 self-peptides, peptide 15 was initially found to activate T-cells in the presence of abacavir in its natural form, while in its amidated form T-cell activation was observed in the absence of abacavir.

NTVELRVKI (peptide 15) belongs to the dolichyl-diphosphooligosaccharide-protein glycosyltransferase subunit 2. This protein is located in the endoplasmic reticulum and plays a direct role in protein glycosylation which constitutes part of protein modification (http://www.uniprot.org/uniprot/P04844). In this chapter we sought to assess in detail the effect of this abacavir-induced self-peptide on a wider range of T-cell clones firstly using techniques previously employed, then expanding to a greater range of assays for further dissection between the properties of peptide 15 (NTVELRVKI) in the natural and amidated forms.

First, assays using C1R and T2s as APCs with and without the addition of the peptides and abacavir were repeated. In T2B*57:01 cells, the transporter associated with antigen presentation (TAP) is knocked out meaning they cannot process and present endogenously generated peptides to T-cells in the manner employed by C1Rs. Co-incubation of some abacavir-specific T-cell clones with T2 APCs blunted the T-cell response observed in the presence of abacavir. In some T-cell clones, exogeneous addition of natural peptide 15 to the T-cells enhanced the response to abacavir in the presence of T2 APCs to a similar level observed in the presence of C1Rs, however, this was not observed universally across all clones. Addition of peptide 15 in the amidated form resulted in a T-cell response in most clones tested, but activation was also observed in the absence of abacavir. Unfortunately, results obtained with some T-cell clones in the presence of natural peptide 15 were not observed in other abacavir-responsive T-cell clones, nor upon repetition with the same clones.

Distinguishing the T-cell response to abacavir in the presence of the natural peptide from that to abacavir alone proved to be difficult, therefore we next looked at co-incubating T-cells down a concentration gradient of abacavir in the presence or absence of the peptide in both forms. In the presence of the amidated peptide, the T-cell response was constant at all concentrations of abacavir used, but also without drug, indicating that the presence of abacavir had no influence on the induction of T-cell activity by the amidated form of peptide 15. Furthermore, no activation of T-cells was observed when they were co-incubated with T2 APCs in the presence of the natural peptide regardless of the abacavir concentration suggesting that addition of the natural peptide was not sufficient to reinstate the T-cell activity that was abrogated by the loss of antigen processing (Figure 5.6).

Next, we assessed if the use of autologous EBVs in place of the C1R and T2s may allow for a distinction between responses in the presence or absence of the peptide in dose titration assays. Abacavir-specific T-cell clones co-incubated with abacavir at increasing concentrations displayed no enhanced T-cell activity in the presence of the natural peptide compared to abacavir alone, again suggesting that the peptide has little influence on T-cell activity. Abacavir clones were then exposed to the natural and amidated peptides at increasing concentrations in the presence or absence of the drug to investigate if T-cell activity induced by the peptide was dependent on dose. However, in the presence of T2 APCs the inhibited response to abacavir was not altered via the addition of the natural peptide at any concentration, while some modest activation was observed in the presence of the amidated peptide, there was no distinguishable difference between the abacavir-treated and untreated cells. Finally, to investigate dose dependency of both the drug and the peptide, T-cells were co-incubated with increasing concentrations of abacavir and the natural peptide. While an increase in T-cell activation was observed with increasing abacavir concentration, no distinguishable enhancement of T-cell activity was noted with the

increasing concentrations of natural peptide 15 (Figure 5.9), again suggesting that the natural peptide plays little role in the activation of a T-cell response to abacavir.

Next, we investigated the effect of using C1R and T2 APCs pulsed with natural peptide 15 in the presence or absence of abacavir on T-cell activation. In chapter 2, we reported that T-cell activation was observed following co-incubation with abacavir-pulsed EBVs (16 hour), consistent with previous findings (Bell *et al.*, 2013). Strong T-cell responses were observed in cells co-incubated for 16 hour with abacavir pulsed C1R APCs, but not pulsed T2 APCs. Pulsing T2 APCs with abacavir in the presence of the natural peptide did not stimulate T-cells (Figure 5.10). Repetition of the assay using autologous EBVs in place of the C1Rs and T2s displayed no enhanced T-cell activation with abacavir when co-exposed to the natural peptide, compared to abacavir alone (Figure 5.11). This suggested that perhaps in the natural form, peptide 15 does not possess sufficient binding affinity to be able to bind to HLA-B*57:01 presented on the surface of the APC, nor to displace the peptide already bound. To investigate this, APCs were washed with the weak acid citrate-phosphate buffer prior to pulsing to displace the peptides bound to surface MHC (Burkhart et al. 2002; Sugawara et al. 1987). No enhanced T-cell activation was detected in cells pulsed with abacavir in the presence of the natural peptide compared to abacavir alone in any of the T-cell clones. Furthermore, no difference was observed in T-cell activation between clones incubated with the weak acid washed APCs and those incubated with APCs washed in HBSS instead. This suggests an inability of natural peptide 15 to bind to surface MHCs or alternatively that it binds but is not involved in T-cell activation. Finally, we investigated T-cell responses after glutaraldehyde fixation of EBVs. Glutaraldehyde fixation completely abrogated the T-cell response to abacavir, however, addition of the natural peptide did not reinstate the T-cell response (Figure 5.12).

Taken together, these findings suggest that abacavir-responsive T-cell clones possess little to no affinity for peptide 15 in its natural form, indicating that the peptide plays little to no role in the induction of T-cell responses or that the induction of T-cell responses by peptide 15 was limited to a small subset of T-cells.

The next step was to generate specific T-cell clones to the natural peptide in the presence of abacavir and to the amidated peptide in the absence of abacavir. T-cell clones were generated to the natural peptide in the presence of abacavir, yielding an overall 26% response rate of clones at the first testing stage. The return was much higher with the peptide in its amidated form with just under 40% of the clones tested displaying specificity for the peptide. Clones activated with the natural peptide in the presence of abacavir displayed no T-cell activation when incubated with the natural peptide alone. The clones were also activated by the amidated peptide in the presence of abacavir as well as in its absence, however, the latter was to a lesser degree.

We next sought to repeat the APC pulsing assays on T-cell clones generated to abacavir in the presence of the natural peptide. This assay was carried out firstly using autologous EBVs pulsed with the natural peptide in the presence or absence of abacavir. No increase in T-cell activity was observed in either clone co-incubated with abacavir in the presence of the natural peptide compared to abacavir alone. Furthermore, when EBVs were acid washed prior to pulsing in the respective conditions, co-incubation with abacavir clones again demonstrated no enhancement in T-cell activity in clones specific to abacavir + natural peptide 15 (Figure 5.19). These data suggest that natural peptide 15 possessed little to no T-cell stimulatory properties i.e. clones were only responding to abacavir and the repertoire of peptides generated endogenously.

Focus was next shifted to the responsive T-cell clones generated to the amidated form of peptide 15, many of which indicated strong CD8$^+$ T-cell activity when retested in the presence

of peptide in the ELIspot assay (Figure 5.14). Indeed, activation of clones to the amidated peptide were shown to be dependent on the presence of antigen presenting cells (Figure 5.20). The assay was repeated using amidated peptide-specific T-cell clones but co-incubated with the peptide in natural form instead of amidated. No T-cell activation was observed in either the presence or absence of APCs to the natural peptide, confirming the C-terminal amidation of the peptide to be the governing factor in the induction of a T-cell response.

The findings with the amidated peptide were intriguing if not related to the activation of T-cells with abacavir. Previous unpublished data has shown that the peptide activates clones with specificity to other drugs, including sulfamethoxazole which has no association with HLA-B*57:01. Such findings would indicate that the amidated peptide functions as a mimotope, which mimics the actions of an epitope to induce a T-cell response (Gevorkian et al. 2005a; Casey et al. 2006). Amidation of peptides is a technique employed to enhance the biological activity of synthesised peptides as it increases their ability to enter cells and protects against degradation via the actions of proteases (Nuijens et al. 2012; Wollack et al. 2009). Furthermore, studies have indicated that the C-terminal amidation of peptides can increase their potency for biological activity by at least 10-fold (Merkler 1994; Merkler et al. 1993), suggesting that the amidated peptide may have been capable of more aggressive binding and interactions with the MHC, allowing for the induction of a T-cell response.

These findings seem to suggest the inability of the NTVELRVKI peptide to induce a T-cell response to abacavir. However, the response may be limited to a small number of T-cells further expanding the variability of abacavir-responsive T-cell clones as explored in chapter 2. As this study focused solely on one abacavir-induced self-peptide, a wider range of peptides must be explored to fully gain a holistic insight into the role of abacavir-induced altered self-peptides in the induction of T-cell responses to abacavir.

Chapter 6 - Abacavir altered self-peptides can be recognised by CD8⁺ T-cells, leading to IFN-γ secretion.

6.1. Introduction.

Hypersensitivity reactions to abacavir observed exclusively in individuals expressing the HLA-B*57:01 allele are known to be mediated by CD8^{+} T-cells (Chessman *et al.*, 2008; Mallal *et al.*, 2008; Adam *et al.*, 2012; Bell *et al.*, 2013; Naisbitt *et al.*, 2015). As previously mentioned, neither the hapten/prohapten nor the PI models adequately explain the mechanisms of the immune-mediated hypersensitivity reactions observed with abacavir. Three separate studies in 2012, cast light on a new mechanism of hypersensitivity observed uniquely with abacavir (Illing et al. 2012; Norcross et al. 2012; Ostrov et al. 2012). These studies postulated that abacavir may induce a conformational change in the binding cleft of HLA-B*57:01 leading to an alteration in the range of peptides displayed on the surface of the APC for T-cell recognition. A shift in prevalence of the small C-terminal anchors including leucine, isoleucine and valine was observed in the presence of abacavir. This shift in prevalence was only observed at the C-terminal position of the peptides, corresponding to the F-pocket of HLA-B*57:01 (Illing et al. 2012), casting new light on the role that the peptides might play in the activation of T-cells in abacavir hypersensitivity.

Subsequent studies concerning abacavir hypersensitivity reactions have tended to focus on peptides as a mainstay for investigation into activation of T-cells induced by the drug. *Lucas et al* indicated that T-cell reactions observed to abacavir upon first exposure in some individuals were caused by the presence of memory T-cells previously primed to an unknown antigen which were capable of cross-reacting with the abacavir HLA-B*57:01-endogenous peptide ligand complexes (Lucas et al. 2015). *Metushi et al,* identified using the drug acyclovir, a relationship between the peptide binding affinity for HLA-B*57:01 in the presence of a drug and the observed CD8^{+} T-cell response. Acyclovir, found to be devoid of T-cell activity, induced an increase in peptide affinity for HLA-B*57:01 of around 2-5 fold, while an increase in the region of 1000 fold was observed with abacavir. This indicated a

relationship between the binding affinity of a drug within HLA-B*57:01 and the induction of T-cell responses (Metushi et al. 2015).

Furthermore, *Naisbitt et al* demonstrated via the use of abacavir substituted analogues that T-cell reactivity could be abolished via substitution at the 6-amino cyclopropyl moiety. Subsequent i*n silico* modelling of some analogues within HLA-B*57:01 indicated a binding conformation adopted that would not allow for the presentation of altered peptides to T-cells (Naisbitt et al. 2015). Indeed, in similar studies conducted in chapters 3 and 4 we demonstrated that compounds which do not activate T-cells will not bind HLA-B*57:01 in a manner to instigate a shift in peptide prevalence. Furthermore, using mass spectrometry we found that with non-activating abacavir analogues there was no apparent shift in the peptide repertoire presented to T-cells on the surface of APCs.

Using viral peptide sequences which displayed structural similarity to an immunogenic self – peptide, *Yerly et al 2017* explored the relationship between solvent exposure by the peptide side chains and TCR recognition (Yerly et al. 2017). One abacavir-specific transfectant was activated with peptide VTQQAQVRL in the absence of abacavir which corresponded to the Herpes Simplex Virus (HSV ½ 230-238). However, this response was only observed in one abacavir TCR transfectant indicating that the observed cross-reactions exclusivity to a small subset of abacavir memory T-cells (Yerly et al. 2017).

In the previous chapter we explored the ability of abacavir-induced self-peptides to activate T-cells. We focussed on a panel of 120 peptides received from our collaborators in the Purcell Laboratory (Monash University, Melbourne). One peptide from this panel was found to evoke T-cell responses in the presence or absence of abacavir in the amidated form. In chapter 5, this peptide was subjected to detailed analysis to further dissect the responses that were observed. It was found that in the natural form the peptide possessed no significant T-cell inducing ability in either the presence or absence of the drug. In the

amidated form the peptide possessed non-specific T-cell activating properties; however, the presence of abacavir bore no influence on the T-cell responses observed. Furthermore, T-cell clones specific to other drugs including those with no HLA-B*57:01 association (SMX) were activated by this peptide, suggesting the peptide may function as a mimotope (Casey et al. 2006).

6.2. Aims.

In this chapter we investigated a further panel of 39 abacavir-induced self-peptides received from the Purcell Laboratory (Monash University, Melbourne) which have underwent prior studies to examine the kinetics of peptide display on the surface of the APCs over a time course of abacavir exposure. Based on the results of these assays, a panel of five abacavir-induced self-peptides were selected to perform T-cell cloning in both the presence and absence of abacavir, with responsive clones generated being subjected to further T-cell assays, to assess their influence on the induction of T-cell responses to abacavir.

6.3. Methods.

6.3.1. Materials.

Abacavir was received as a gift from GlaxoSmithKline (GSK). Human AB serum and foetal bovine serum were obtained from Innovative Research (Michigan, USA) and Invitrogen (Paisley, UK), respectively. Interleukin-2 (IL-2) was purchased from Peprotech (London, UK). Multisort bead separation kits were supplied by Miltenyi Biotec (Surrey, UK). Antibodies for staining were purchased from BD Biosciences (Oxford, UK). ELIspot kits including the coating and detection antibodies, streptavidin alkaline phosphate conjugate and BCIP/NBT substrates were purchased from Mabtech (Stockholm, Sweden). Other reagents were purchased from Sigma-Aldrich (Dorset-UK) unless otherwise stated.

6.3.2. Cell Culture Medium

R9 medium for T-cells (R9) is composed of RPMI supplemented with 10% human AB serum, HEPES (25mM), penicillin (1000 U/mL), streptomycin (0.1mg/mL), L-glutamine (2mM) and transferrin (25µg/mL).

EBV transformed B-cells were cultured in F1 medium composed of RPMI supplemented with 10% foetal bovine serum, HEPES (25mM), penicillin (1000 U/mL), streptomycin (0.1mg/mL) and L-glutamine (2mM).

6.3.3. Maintaining C1R and T2 cells

Cells from the class I deficient lymphoblastoid cell lines, C1R and T2 were transfected with HLA-B*57:01 to be used in functional assays. Both cell lines were maintained as described in section 5.3.3.

6.3.4. Generation of abacavir-specific T-cell clones.

Generation of abacavir-specific T-cell clones was carried out as described in section 2.3.5, subsequent testing for antigen specificity of the T-cell clones was assessed using T-cell proliferation assays described in section 2.3.6. Antigen specificity of the abacavir clones was confirmed using the ELIspot assay described in section 2.3.7. Cellular phenotyping on abacavir-specific T-cell clones was investigated using methods described in section 2.3.8.

6.3.5. T-cell activation in the presence of abacavir-induced self-peptides.

Abacavir-induced self-peptides were assigned a number from 1 to 39 for identification in T-cell assays. Each peptide sequence with its corresponding number is displayed in Table 6.1.

Abacavir-responsive T-cells ($5x10^4$/50µL) were co-incubated with T2 APCs and the mixtures of self-peptides (2 peptides/well) in the presence and absence of abacavir (varying concentrations dependent on the T-cell clones used) for 48 hours (37^OC; 5% CO_2). T-cells were also co-incubated with C1R or T2 APCs in the absence of peptides ($1x10^4$/50µL) in the presence or absence of abacavir as positive and negative controls, respectively. T-cell responses were measured using the IFN-γ ELIspot assay, due to its superiority over the proliferation assay. Peptide mixes that produced a T-cell response with T2 APCs in the presence of abacavir which surpassed the response in T2 APCs to abacavir alone were selected for individual analysis.

PEPTIDE	SEQUENCE
1	KIADFGWSV
2	ATFKGIVRAI
3	ASAIIIQRW
4	IVFPGSTGHI
5	KTFIGTVRV
6	FAYDGKDYL
7	KVFKLQTSL
8	KSIARVLTV
9	HTIQIRQDW
10	KSIFVFTHV
11	ASSSQIIHI
12	VTTDIQVKV
13	GSFGKVFLV
14	YTDNLVRVW
15	RVLPPSHRVTW
16	LTSELITHI
17	KSTALQTWL
18	RTLLEDGTFKV
19	KTIETSPSL
20	KSYELPDGQVI
21	HSTDRVVLI
22	KTFTTQETI
23	LSSPVTKSF
24	KAIDYIRFL
25	KTLEGEFSV
26	ITKTVVENI
27	STIRLLTSL
28	SSAEVKVTI
29	NTVELRVKI
30	VSVKDIQAHL
31	RTLPVDFHI
32	KSYELPDGQVITI
33	KTIKLWNTL
34	IAINLFTNV
35	TSLKSRVTI
36	SGMGVIVHI
37	STLHLVLRL
38	GTYQDVGSLNI
39	KTFKDVGNLL

Table 6.1. A panel of abacavir-induced self-peptides eluted from HLA-B*57:01 in the presence of the drug.

6.3.6. Activation of T-cell clones with titrated concentrations of abacavir and abacavir-induced self-peptides.

Abacavir-responsive T-cells were co-incubated with T2 APCs at increasing concentrations of abacavir (0-100μM) and one representative abacavir self-peptide (peptide 4 (0-200μM)) for 48 hours (37°C; 5% CO_2). T-cells were co-incubated with C1R APCs in the presence of abacavir at the same concentration range as a positive control, with T-cell activity measured by means of IFN-γ ELIspot.

6.3.7. T-cell activation induced by abacavir self-peptides in the presence of pulsed APCs.

T2 APCs were incubated overnight with a selection of individual peptides (25μM) in the presence and absence of abacavir (35μM). APCs pulsed overnight in R9 medium alone were used as a negative control while abacavir pulsed C1R APCs were employed as a positive control. Following pulsing, the APCs were washed three times in R9 medium and diluted to a concentration of 1x10^4/ 50μL. The APCs were then co-incubated with abacavir-responsive CD8$^+$ T-cell clones (5x10^4/ 50μL) for a period of 48 hours (37°C; 5% CO_2). T-cell activity was measured using IFN-γ ELIspot.

6.3.8. T-cell activation induced by abacavir self-peptides in the presence of glutaraldehyde fixed EBVs.

Autologous EBVs (2x10^6 cells/mL) were washed and resuspended in 1mL of HBSS buffer. Glutaraldehyde (25%, 1μL) was added to the cells for 30 seconds, followed by 1mL of glycine (1M) for a further 45 seconds. The EBVs were then washed three times and resuspended in R9 medium to a concentration of (2x10^{5}cells/mL). Abacavir-specific T-cell clones (5x10^4/ 50μL) were co-incubated with the glutaraldehyde fixed EBVs (1x10^4/ 50μL) and individual abacavir self-peptides (25μM) in the presence and absence of abacavir for 48 hours (37°C; 5% CO_2). T-cells were co-incubated in the presence and absence of abacavir with non-fixed

EBVs as a positive control. T-cell activation was quantified using IFN-γ secretion by means of the ELIspot assay.

6.3.9. Self-peptide presentation over a time course of abacavir exposure.

Kinetic studies to analyse the presentation of peptides over a time course of abacavir exposure were conducted by Dr Patricia Illing at Monash University (Melbourne, Australia).

HLA class I molecules were isolated from 10^8 CIR.B*57:01 cells using solid phase bound pan class I antibody W6/32 (produced in house from hybridoma) and fractionated by RP-HPLC as described previously (Purcell et al. 2001; Tan et al. 2011). UV absorbance at 215 nm was used to monitor the elution of material from the column and the area under the curve for the β_2-microglobulin (β_2m) peak recorded as a measure of the purified HLA within the sample. 500 μL peptide containing fractions were combined into 3 pools, concentrated using a speed vacuum concentration system (LABCONCO, USA) and equalised to a volume of 30 μL with 0.1% formic acid (FA, Thermo Scientific). Liquid chromatography-multiple reaction monitoring (LC-MRM)-MS experiments were performed using a Tempo nanoLC (Eksigent) autosampler and cHiPLC nanoflex (Eksigent) coupled to an SCIEX QTRAP 5500 mass spectrometer. 10 μL samples were loaded onto a cHiPLC trap column (ChromXP C_{18}-CL column 0.5mm x 200μm i.d., 3 μm particle size, nominal pore size 120 Å) at a flow rate of 5 μL/min in 2% acetonitrile (ACN), 0.1% formic acid (FA) for 10 min, an analytical cHiPLC column (ChromXP C_{18}-CL 15cm x 75μm i.d., 3 μm particle size, nominal pore size 120 Å) switched in line, and the peptides eluted at 300 nL/min over a gradient of buffer A (0.1% FA) and B (98% ACN, 0.1.% FA) as follows: 0–1 min 2% B, 1-3 min 2–10% B, 3–40 min 10–35.5% B, 40–45 min 35.5–80% B, 45–50 min hold at 80% B, 50–53 min 80–2% B, re-equilibration at 2% B for 7 min. The QTRAP 5500 was operated in MRM mode in unit resolution for Q1 and Q3, with any MRM transition exceeding 600 counts triggering an Enhanced Product Ion (EPI) scan (10,000 Da/sec; rolling CE; unit resolution, 6 second exclusion window). MRM parent-product ion

transitions were designed based on the prominent product ions observed for targeted peptides in LC-MS/MS data acquired previously (Illing et al. 2012). Detection of these transitions overlapping at a particular retention time (RT) was used as an indicator of peptide presence. Peptide identity was validated through fragmentation observed in the EPI scan or comparison to synthetic peptides. Transitions were also designed for the detection of abacavir which is observed as a singly charged ion of mass:charge ratio (m/z) +287.2 with fragment ions of 190.9 (collision energy [CE] 30), 174.0 (CE 45), 164.1 (CE 39) and 150.0 (CE 46). A relative measure of peptide/abacavir abundance within the immunopeptidome was calculated as the total area under the curve for the detected transitions (using Skyline software 64bit 2.6.0.6851 [MacCoss Laboratory] (MacLean et al. 2010) for the peptides, and Peakview® Version 1.2 [SCIEX] for abacavir) divided by the area of the β_2m peak observed on RP-HPLC separation of the immunoaffinity eluate. Mean abundance was calculated from three biological replicates for each timepoint and normalised to the maximum mean detection of the peptide/abacavir.

6.3.10. Generation of specific T-cell clones to peptide mixes ± abacavir.

A selection of five individual abacavir-induced self-peptides were selected for T-cell cloning in one HLA-B*57:01 positive healthy drug naïve donor in both the presence and absence of the drug.

PBMCs isolated from a HLA-B*57:01 positive healthy drug naïve donor, HLA-0622 (Table 2.1), were incubated with the mixture of five selected abacavir self-peptides (5µM) in the presence and absence of abacavir (35µM) for a period of 14 days. On days 6 and 9 cells were maintained with R9 medium containing IL-2 (2µL/mL) to preserve the antigen-driven expansion of T-cells. On day 14, CD8$^+$ T-cells were positively selected using MultiSort kits (Miltenyi Biotec, Surrey UK) and T-cell clones were generated via means of serial dilution as described in section 2.3.5.

6.3.11. Testing for antigen specificity.

Approximately four weeks after beginning the serial dilutions T-cell specificity to the abacavir-induced peptides in the presence and absence of the drug was assessed via cellular proliferation in the presence of the peptides ± abacavir. This was conducted by analysing proliferation via ^{3}H thymidine incorporation. This process was carried out using the same methods as described in section 2.3.6 and antigen specificity was confirmed via the measurement of IFN-γ secretion using the ELIspot assay as described in section 2.3.7. For these steps the peptide mix (5μM) ± abacavir (35μM) was used as the antigen instead of abacavir alone.

T-cell clones which responded in the presence of the peptide mix ± abacavir were subsequently tested to the individual abacavir self-peptides from the mix in both the presence and absence of abacavir, using the same methods described above.

6.3.12. Dose dependency of abacavir ± peptide-specific T-cell clones.

T-cell clones were incubated with autologous EBVs at decreasing concentrations of abacavir (2-0.1μM) in the presence and absence of the individual abacavir self-peptides (5μM) for a period of 48 hours (37°C; 5% CO_2). T-cell activity was quantified via measuring IFN-γ secretion by means of the ELIspot assay.

6.3.13. APC pulsing assays to abacavir ± individual peptides.

Autologous EBVs were pulsed for time periods of 1, 4 and 16 hours with individual abacavir-induced self-peptides in the presence and absence of abacavir (35μM) (37°C; 5% CO_2). Following pulsing EBVs were washed three times, resuspended in R9 medium (0.2x10^6/mL) and co-incubated with T-cells for a period of 48 hours (37°C; 5% CO_2). T-cells were also co-

incubated with soluble abacavir as a positive control. Activation of T-cells was measured via the ELIspot assay.

6.3.14. T-cell activation by abacavir-induced self-peptides in the presence of glutaraldehyde fixed APCs.

Autologous EBVs underwent cellular fixation via the use of glutaraldehyde as described previously in section 5.3.10. Following cellular fixation, EBVs were co-incubated with T-cells and individual abacavir-induced self-peptides in the presence and absence of the drug for 48 hours (37^OC; 5% CO_2). T-cells were incubated with abacavir in the presence of non-fixed EBVs as a positive control. Activation of T-cells was measured by means of IFN-γ secretion via the ELIspot assay.

6.3.15. Statistical Analysis

For comparison between control and test values in proliferation assays the Mann-Whitney test was used.

6.4. Results

6.4.1. Generation of abacavir-specific T-cell clones.

T-cell clones specific to abacavir were generated by means of serial dilution assays described in section 2.3.5 – 2.3.7. From a total of 2279 clones tested across four HLA-B*57:01 positive donors, 101 proliferated in the presence of abacavir on first testing, (0, 1665 ± 188.5 cpm: Abacavir 35µM, 6940 ± 729 cpm; $P < 0.0001$). The abacavir-responsive T-cell clones used for assays in this chapter are displayed in Table 6.2 with their corresponding donor. Results for T-cell specificity assays of these abacavir clones and subsequent cellular phenotyping data is discussed in detail in section 2.3. All clones to donor 2 lost antigen specificity prior to commencement of assays in this chapter.

Donor 1 HLA-0617	Donor 2 HLA-0957	Donor 3 HVN-0158	Donor 4 HLA-0622
TCC 3*		TCC 46	TCC 119
		TCC 56	TCC 121

Table 6.2. Abacavir-specific T-cell clones used for assays in this chapter
* Denotes clone generated to abacavir in the presence of the natural peptide 15, T-cell specificity data and cellular phenotyping discussed in section 5.3.11.

6.4.2. T-cell activation in the presence of abacavir-induced self-peptides.

All 39 peptides were initially screened as mixes of 2/well with T2 APCs in the presence and absence of abacavir. C1R APCs (a fully functional APC expressing HLA-B*57:01) in the presence and absence of abacavir were used as a positive control. T2 APCs were used in order to abrogate the antigen processing capabilities of the cells, thereby investigating the ability of the exogenously added peptide (± abacavir) to activate T-cells. While the T-cell response to abacavir in the presence of T2 APCs was not completely abolished with some T-cell clones it was diminished when compared to the response in the presence of C1R APCs. Therefore, subtle increases in IFN-γ secretion observed in the presence of a peptide mix

when compared to T2 APCs with no peptides were selected for individual analysis (data not shown).

Figure 6.1 shows the results from a representative assay from two abacavir-responsive T-cell clones in the presence of a panel of selected individual self-peptides ± abacavir with T2 APCs. In both abacavir-responsive T-cell clones no response was observed in the presence of the individual peptides that was of greater magnitude than T-cells in the presence of T2 APCs and abacavir alone. This was mainly due to the self-presentation observed with one of the clones in the presence of abacavir, making the distinction between responses to abacavir in the presence of the peptides and the absence very difficult. Therefore, to investigate the dependency on concentration of the peptides and abacavir on T-cell activation, T-cells were co-incubated with T2 APCs at increasing concentrations of abacavir and one self-peptide. Peptide 4 was selected for use as it gave the strongest response in the individual peptide assays. The increasing abacavir concentrations enhanced the T-cell response observed in the presence of T2 APCs, but at lower concentrations and the absence of the drug, no T-cell activity was induced by the addition of peptide 4 (Figure 6.1).
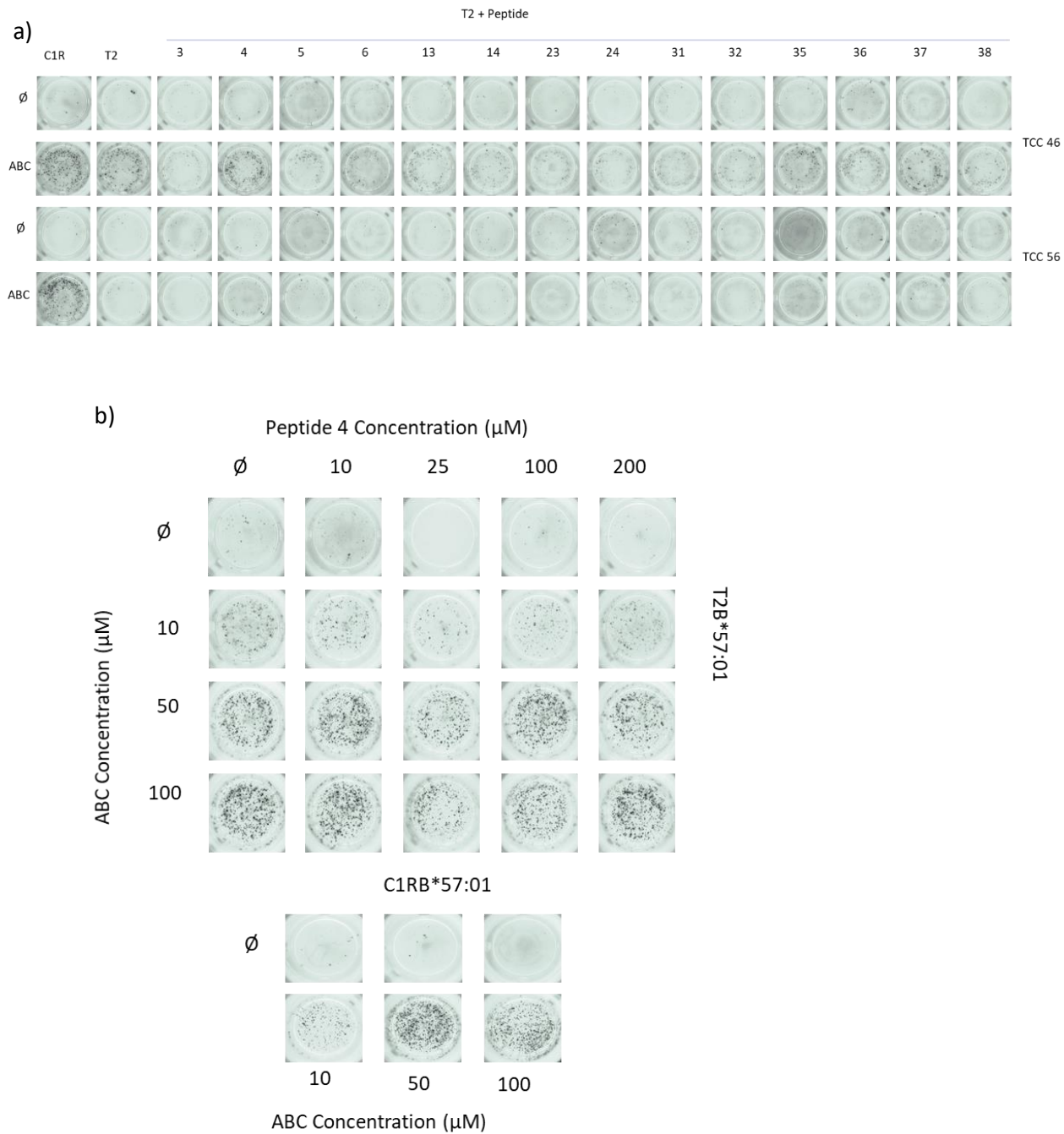
Figure 6.1. Drug-specific T-cell responses to abacavir in the presence of individual self-peptides. a) ELIspot well images of abacavir-responsive T-cell clones co-incubated with individual self-peptides in the presence and absence of the drug. C1R APCs were used as a positive control. b) Abacavir-specific T-cell clones co-incubated with T2 APCs at increasing concentrations of the drug (0-100µM) and one representative abacavir-induced self-peptide (peptide 4, 0-200µM). T-cells were incubated with C1R APCs at the same abacavir concentrations as a positive control.

6.4.3. T-cell activation induced by abacavir self-peptides in the presence of pulsed or glutaraldehyde fixed APCs

As the self-presentation of some abacavir clones was evident in the presence of T2 APCs, we next focussed on abrogating the IFN-γ secretion to abacavir via pulsing or glutaraldehyde fixation. The observed IFN-γ secretion in response to abacavir was not detected when T2 cells were used as APCs. However, pulsing of T2 APCs with the abacavir-induced-self-peptides in the presence and absence of the drug had no effect on the T-cell responses lost to abacavir (Figure 6.2). The effects of abacavir-induced peptides on activation of abacavir-specific T-cell clones was next investigated using EBVs previously fixed with glutaraldehyde with the individual peptides added exogenously in the presence and absence of abacavir. In the two abacavir-specific T-cell clones examined, T-cell activation with abacavir was abrogated via glutaraldehyde fixation of APCs. However, T-cell activity was not reinstated by the addition of the abacavir self-peptides in either the presence or absence of the drug.
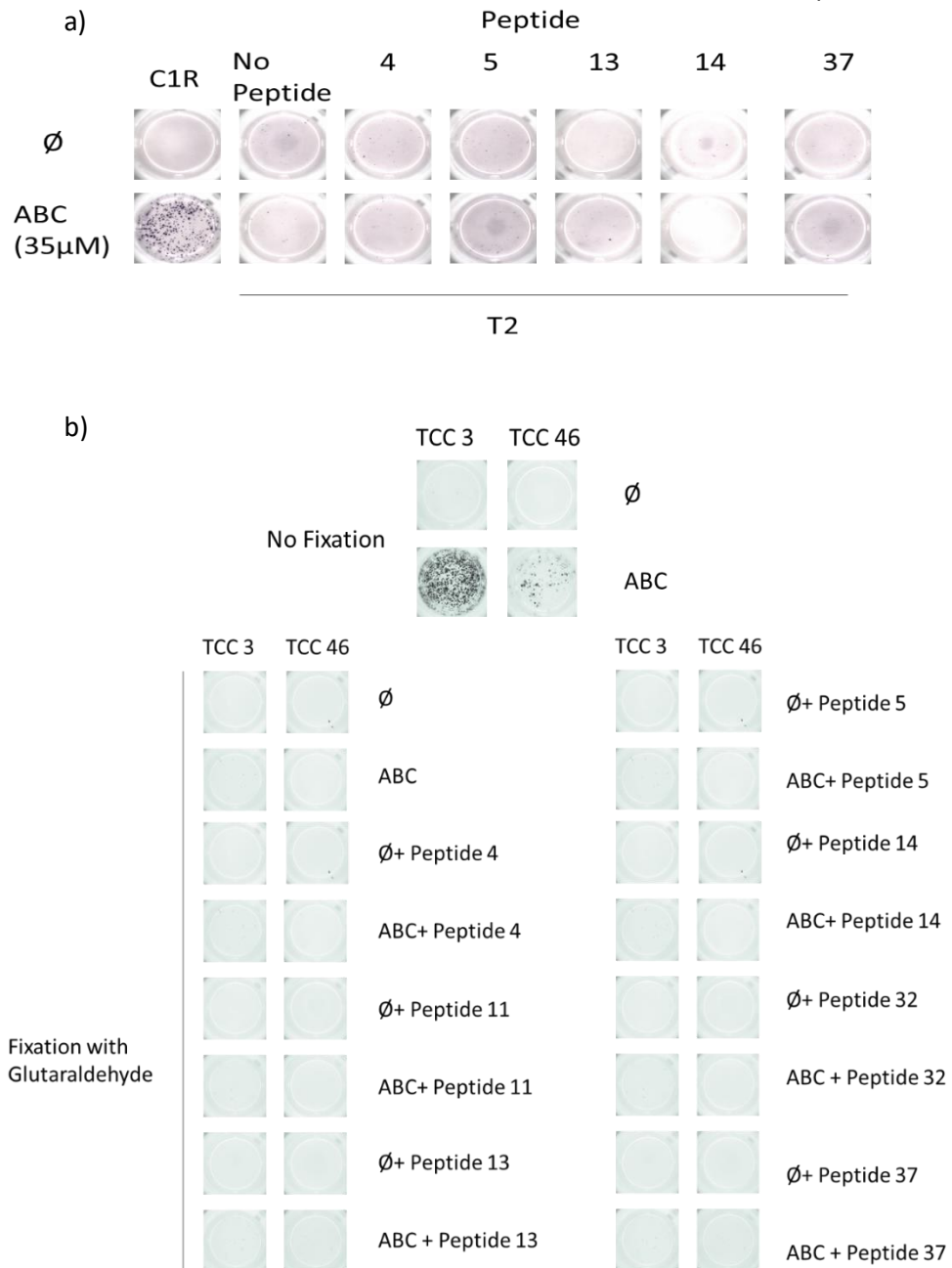
Figure 6.2. Abacavir-induced self-peptide responses in the presence of pulsed or fixed APCs. a) T-cell activity of abacavir-specific T-cell clones incubated with T2 APCs pulsed with the abacavir-induced self-peptides in the presence and absence of the drug. C1R APCs pulsed in the presence and absence of abacavir were used as a positive control. b) Two abacavir-responsive T-cell clones co-incubated with glutaraldehyde fixed autologous EBVs in the presence and absence of abacavir with the induced self-peptides (4, 5, 11, 13, 32 and 37) added exogenously. T-cell clones were incubated with abacavir in the presence of unfixed APCs as a positive control.

6.4.4. Change in peptides eluted from HLA-B*57:01 in the presence of abacavir.

Analysis of peptides eluted from HLA-B*57:01 over a time course of abacavir exposure was conducted using methods described in Illing *et al.*, 2012. The proportion of abacavir eluted (shaded area) spiked during the first five hours of exposure before sharply decreasing, most likely due to being internalized within the APC. The elution of abacavir then increases exponentially over the next ten hours of exposure as it is presented on the cellular surface (Figure 6.3). With the exception of peptide 24, all abacavir induced peptides increased in presentation on the APC surface over a time course of abacavir exposure, demonstrating a dependence on the presence of abacavir for their accommodation within the peptide binding groove of HLA-B*57:01. Conversely, peptides eluted from HLA-B*57:01 in the absence of abacavir (canonical motif) demonstrate little to no dependence on the presence of abacavir for their exposure on the surface of the antigen presenting cell, with many decreasing in exposure following the introduction of abacavir. Based on these findings five peptides were selected for T-cell cloning in the presence and absence of abacavir (Table 6.3). These peptides had multiple intracellular and extracellular origins (Table 6.4).

Peptide Number	Sequence
4	IVFPGSTGHI
13	GSFGKVFLV
24	KAIDYIRFL
32	KSYELPDGQVITI
37	STLHLVLRL

Table 6.3. Number and sequence of abacavir-induced self-peptides used for cloning assays in the presence and absence of the drug.
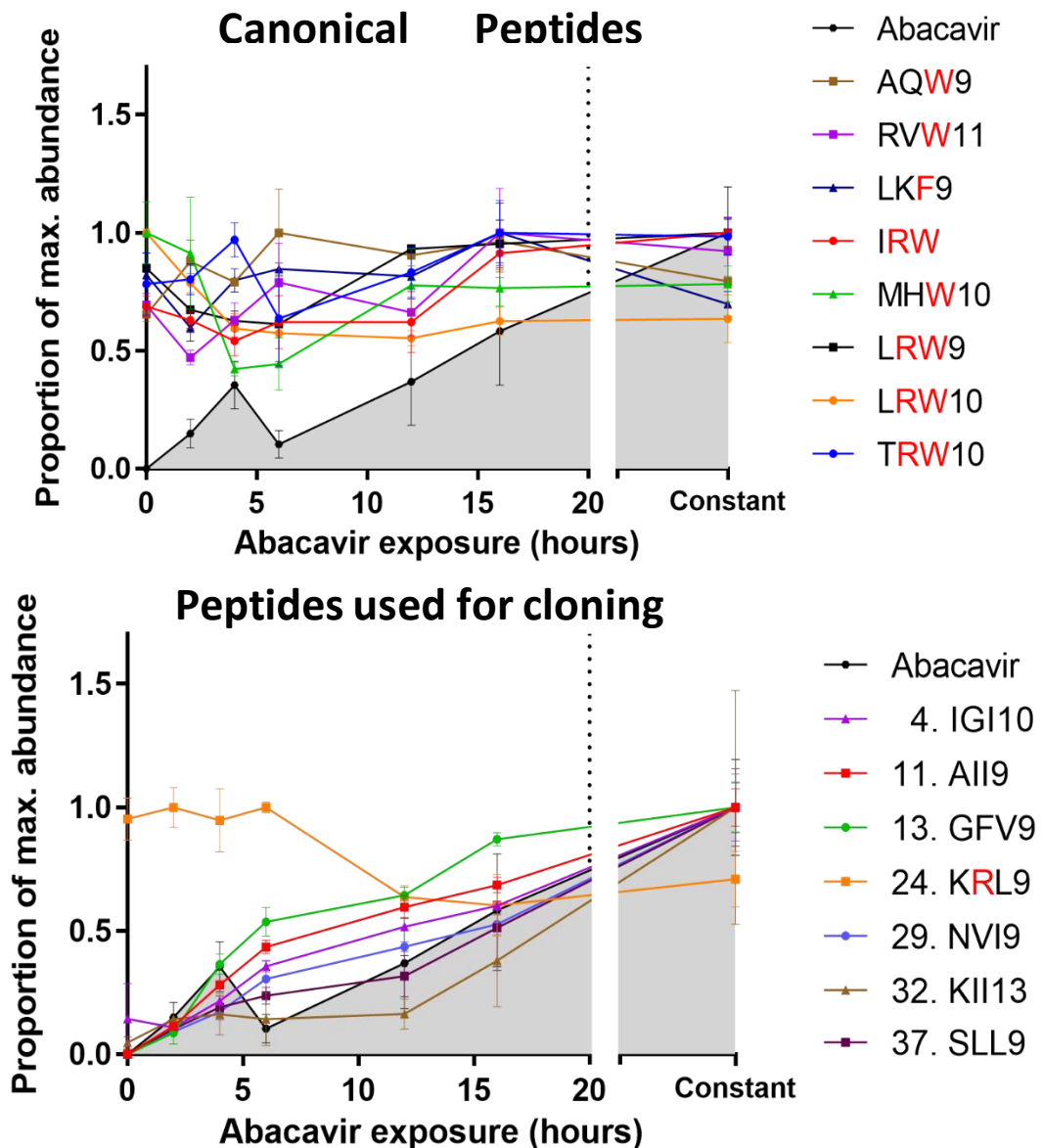
Figure 6.3. Presentation of self-peptides eluted from HLA-B*57:01 over time in the presence and absence of abacavir. MRM-MS analysis of peptide ligands isolated from HLA-B*57:01 of 10^8 CIR.B*57:01 cells after 0-16 hours, or constant, abacavir treatment (35 μM). Peptides were isolated as in *Illing et al. Nature 2012.* 4 MRM parent-product ion transitions were used to detect each peptide/abacavir. Detection of all 4 transitions at the same retention time, correlated with elution time of synthetic peptides or a transition triggered full MS/MS scan, was used as evidence of peptide identification. Peptide and abacavir abundances were calculated as the sum peak area of the transitions and normalised to the amount of β_2m isolated with the peptides. Peptide and abacavir abundances are shown as a proportion of the maximum normalised sum peak area detected across all experiments and are portrayed as the mean of the three biological replicates. Error bars depict the standard error of the mean. Peptide IDs: Residue 1, Ω-2, Ω and length. Residues that have key interactions with the antigen binding cleft that are blocked by abacavir are shown in red.

Sequence	Protein Name	Location	Accession
IVFPGSTGHI	Homeodomain-interacting protein kinase 2	Nucleus	http://www.uniprot.org/uniprot/Q9H2X6
ASSSQIIHI	ATPase family AAA domain-containing protein 2	Nucleus	http://www.uniprot.org/uniprot/Q6PL18
GSFGKVFLV	Ribosomal protein S6 kinase alpha-1, 3, 6	Nucleus	http://www.uniprot.org/uniprot/Q15418, Q9UK32, P51812
KAIDYIRFL	Sterol regulatory element-binding protein 1	Nucleus, ER, Golgi	http://www.uniprot.org/uniprot/P36956
KSYELPDGQVITI	Actin, cytoplasmic 1, 2. Actin, alpha cardiac muscle 1 Actin, gamma-enteric smooth muscle Actin, aortic smooth muscle Putative beta-actin-like protein 3 Actin, alpha skeletal muscle POTE ankyrin domain family member F, I, J, E	Cytoskeleton Extracellular	http://www.uniprot.org/uniprot/P60709, P68032, P63261, P63267, P62736, Q9BYX7, P68133, A5A3E0, P0CG38, P0CG39, Q6S8J3.
STLHLVLRL	Polyubiquitin-B, C Ubiquitin-40S ribosomal protein S27a, L40	Nucleus, Cytoplasm	http://www.uniprot.org/uniprot/P0CG47, P0CG48, P62979, P62987.

Table 6.4. Sequences, corresponding proteins and cellular locations of the abacavir-induced self-peptides used in the T-cell cloning assays.

6.4.5. Generation of T-cell clones responsive to the peptide mix ± abacavir.

Next to investigate if T-cell clones could be generated that were specific to the abacavir self-peptides in the presence and absence of the drug, a panel of five peptides were selected based on the results of the T-cell assays to undergo T-cell cloning in one HLA-B*57:01 positive healthy drug naïve donor, HLA-0622 (Table 2.1).

6.4.6. T-cell cloning to the abacavir self-peptide mix.

From a total of 148 clones tested, 34 proliferated weakly in response to the abacavir self-peptide mix alone on first testing (Control, 1031 ± 135.9 cpm; Peptide Mix (5µM), 2494 ± 378.7 cpm; P<0.0001). Second testing of the responsive T-cell clones via the ELIspot assay revealed no T-cell clones to possess antigen specificity toward the peptide mix in either the

presence or absence of abacavir. This confirmed these clones to have generated a false

positive result at the first testing stage (Figure 6.4).

a)

HLA-622 Cloning to Peptide Mix

b)

HLA-622 peptide mix clones 1st test

c)

Donor	Donor 4
Clones Tested	148
Responsive	34
Percentage responsive	22.9%

d)
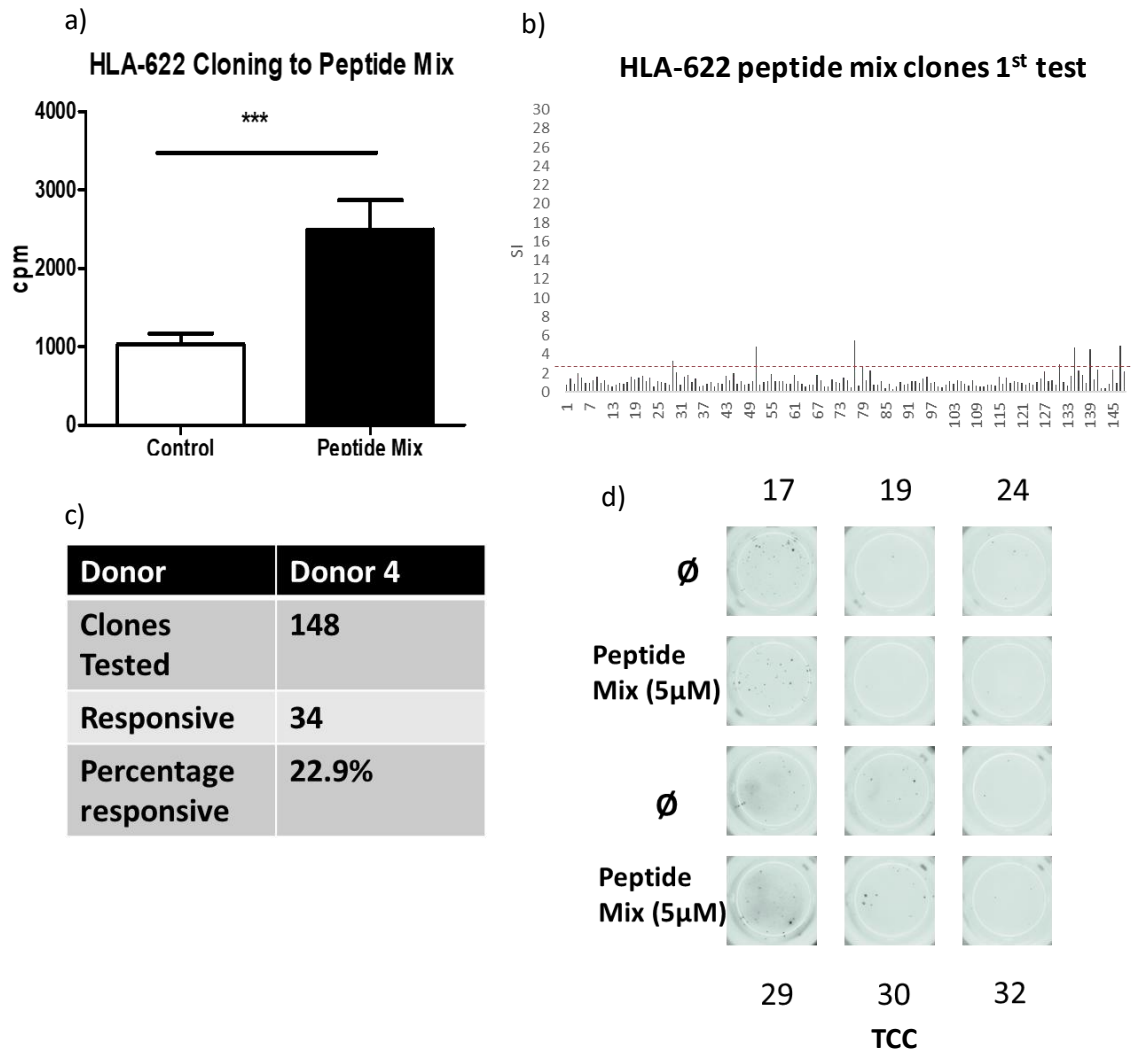
Figure 6.4. Generation of T-cell clones to the mix of abacavir-induced self-peptides in the absence of the drug. a) Mean proliferative response from T-cells tested to the abacavir-induced self-peptide mix (5µM) in the absence of the drug. Data shown as mean of all responsive clones vs control ± SEM, *P<0.05, **P<0.01, ***P<0.001. b) Antigen specificity of individual T-cell clones to the self-peptide mix. c) Table representative of total clones generated to the abacavir self-peptide mix. d) Representative ELIspot images of clones second test in response to the peptide mix (5µM) as a means of confirming antigen specificity.

6.4.7. T-cell cloning to the self-peptide mix + abacavir.

From a total of 88 clones tested, 9 proliferated in response to abacavir + the peptide mix upon first testing (Control, 497.4 ± 45.33 cpm; ABC (35µM) + peptide mix (5µM), 4393 ± 1325 cpm; P<0.0001). Second testing revealed strong activation of some T-cell clones in response to the peptide mix + abacavir. These clones were subjected to further analysis.

a)

b)

c)

Donor	Donor 4
Clones Tested	88
Responsive	9
Percentage responsive	10.2%

d)
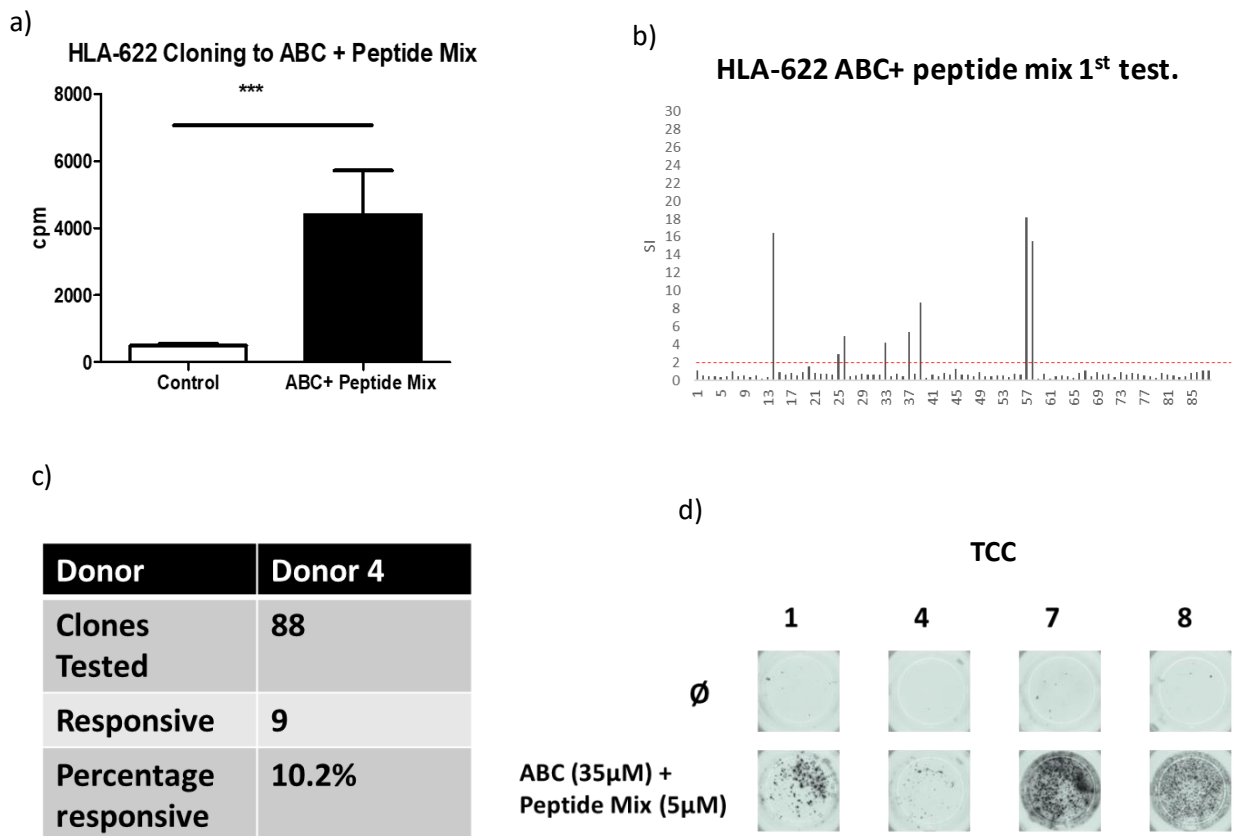
Figure 6.5. Generation of specific T-cell clones to the mix of abacavir-induced self-peptides in the presence of the abacavir. a) Mean proliferative response from T-cells tested to abacavir (35µM) + the induced self-peptide mix (5µM). b) Antigen specificity of individual T-cell clones to abacavir (35µM) + the self-peptide mix. c) Table representative of total clones generated to abacavir + the self-peptide mix. d) Representative ELIspot images of clones second test in response to abacavir + the peptide mix (5µM) as a means of confirming antigen specificity. *P<0.05, **P<0.01, ***P<0.001.

6.4.8. Cross reactivity of T-cell clones to abacavir, abacavir + peptide mix and the peptide mix alone.

A panel of T-cell clones specific to abacavir and abacavir + the peptide mix were tested across four conditions; 1) Ø, 2) abacavir (35µM), 3) abacavir (35µM) + peptide mix (5µM), 4) peptide mix alone (5µM) to assess their potential for cross-reactivity. T-cell clones generated to the peptide mix in the presence of abacavir produced strong IFN-γ secretion when co-incubated with the peptide mix in the presence of abacavir as well as when incubated with abacavir alone (Figure 6.6). Abacavir-responsive T-cell clones also secreted IFN-γ when co-incubated with the peptide mix in the presence of the drug and to the drug alone. Interestingly, two abacavir-specific T-cell clones (TCC 119 and 121) also secreted low levels of IFN-γ when incubated with the peptide mix in the absence of the drug (Figure 6.6).
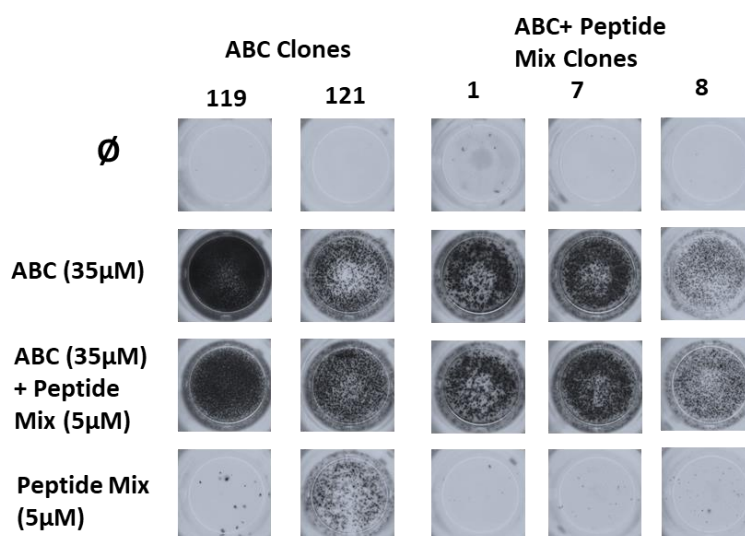
Figure 6.6. Cross reactivity of T-cell clones generated to abacavir and abacavir + peptide mix. Representative ELIspot images of T-cell clones generated to various conditions co-incubated with abacavir (35µM), abacavir (35µM) + peptide mix (5µM) and peptide mix alone (5µM).

6.4.9. T-cell activity in response to individual self-peptides in the presence and absence of abacavir.

To differentiate between the T-cell responses observed to abacavir in the presence of the peptides from those observed to abacavir alone, dose titration assays using decreasing concentrations of abacavir in the presence and absence of the individual self-peptides from the peptide mix were conducted. One T-cell clone specific to the peptide mix in the presence of abacavir was employed for this assay (TCC 8). This T-cell clone was tested in the presence and absence of the five individual abacavir-specific peptides (5μM) with abacavir at decreasing concentrations (0-2μM). The magnitude of IFN-γ secretion from the abacavir-treated clone decreased in line with the decrease in abacavir concentration as expected. However, in the presence of the abacavir-induced self-peptides, clear enhancement of IFN-γ secretion was observed at the low concentrations of the drug (Figure 6.7).
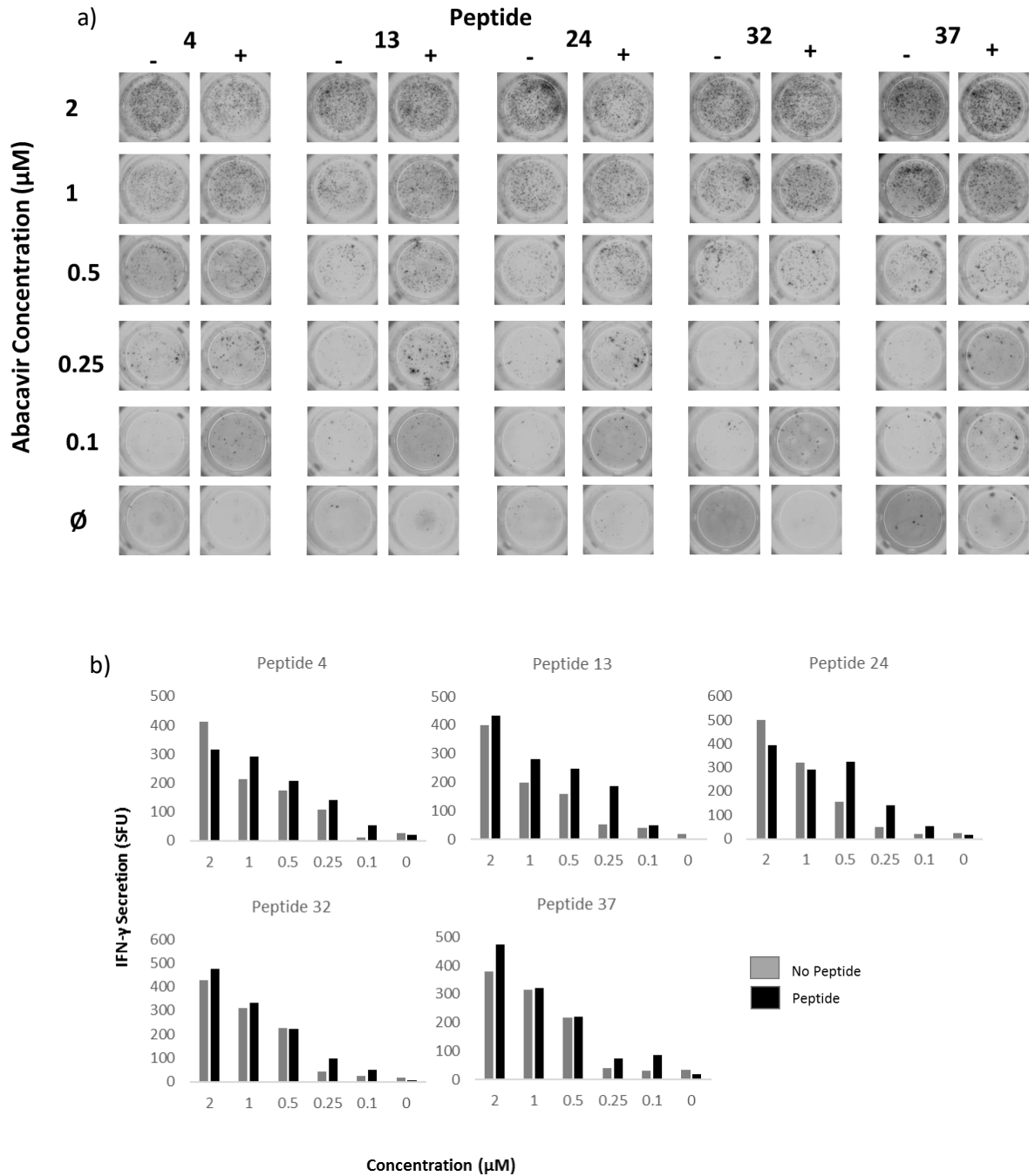
Figure 6.7. T-cell activity of abacavir + peptide mix-specific T-cell clones in the presence and absence of abacavir and the individual self-peptides. a) ELIspot well images and bar graphs comparing IFN-γ secretion to abacavir in the presence and absence of peptides. One clone specific to abacavir in the presence of the self-peptide mix co-incubated with abacavir at decreasing concentrations (2-0.1μM) in the presence and absence of the individual abacavir-induced self-peptides.

6.4.10. T-cell activity of abacavir clones to individual self-peptides in the absence of the drug.

Two abacavir-specific T-cell clones displayed strong T-cell activity when co-incubated with the peptide mix in the presence of the drug, while also secreting IFN-γ in response to the peptide mix in the absence of abacavir (Figure 6.6). Both clones were co-incubated with autologous EBVs in the presence of the individual peptides with no drug to examine if the individual peptides could induce a T-cell response. The natural form of peptide 15 (NTVELRVKI) from chapter 5 was also incorporated into this assay. Clone 119 secreted low levels of IFN-γ in the presence of peptide 37, but not the other peptides. However, T-cell clone 121 displayed clear T-cell responses when incubated with peptides 4 and 32 (Figure 6.8).
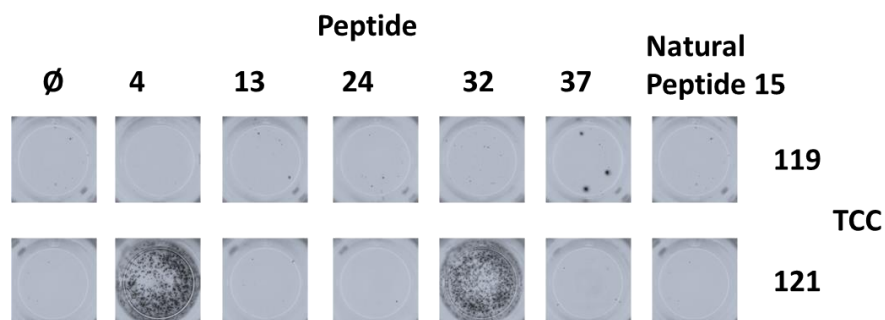
Figure 6.8. Secretion of IFN-γ by T-cell clones stimulated with abacavir-induced self-peptides. ELIspot well images from two abacavir-specific CD8+ T-cell clones co-incubated with abacavir-induced self-peptides 4, 13, 24, 32, 37 and the natural form of peptide 15 from Chapter 5.

6.4.11. Antigen presenting cell pulsing assays with individual abacavir self-peptides.

Using these abacavir-specific T-cell clones and the abacavir self-peptides 4 and 32, APC pulsing assays were carried out at time periods of 1, 4 and 16 hours to the individual peptides in the presence and absence of abacavir. As previously shown, 16 hours is the optimal pulsing time for a strong T-cell response for abacavir. Figure 6.9 shows the differences in abacavir response based on the duration of APC pulsing employed. At the 16 and 1 hour pulsing stage, little difference is observed between the responses to abacavir in the presence of the peptides and abacavir alone. However, at the 4 hour time point a clear increase in T-cell activity is observed in clones co-incubated with APCs pulsed to abacavir in the presence of peptide 32 when compared to pulsing with abacavir alone.

This experiment was then repeated at just the 4 hour timepoint using abacavir T-cell clone 119 in the presence of APCs pulsed to the individual peptides 4 and 32 in the presence and absence of abacavir. Strong T-cell activity is induced by co-incubation with APCs pulsed with both the individual abacavir self-peptides in the presence of the drug, compared with cells pulsed to the drug alone. This indicates a clear role for the peptides in the induction of a T-cell response to abacavir.
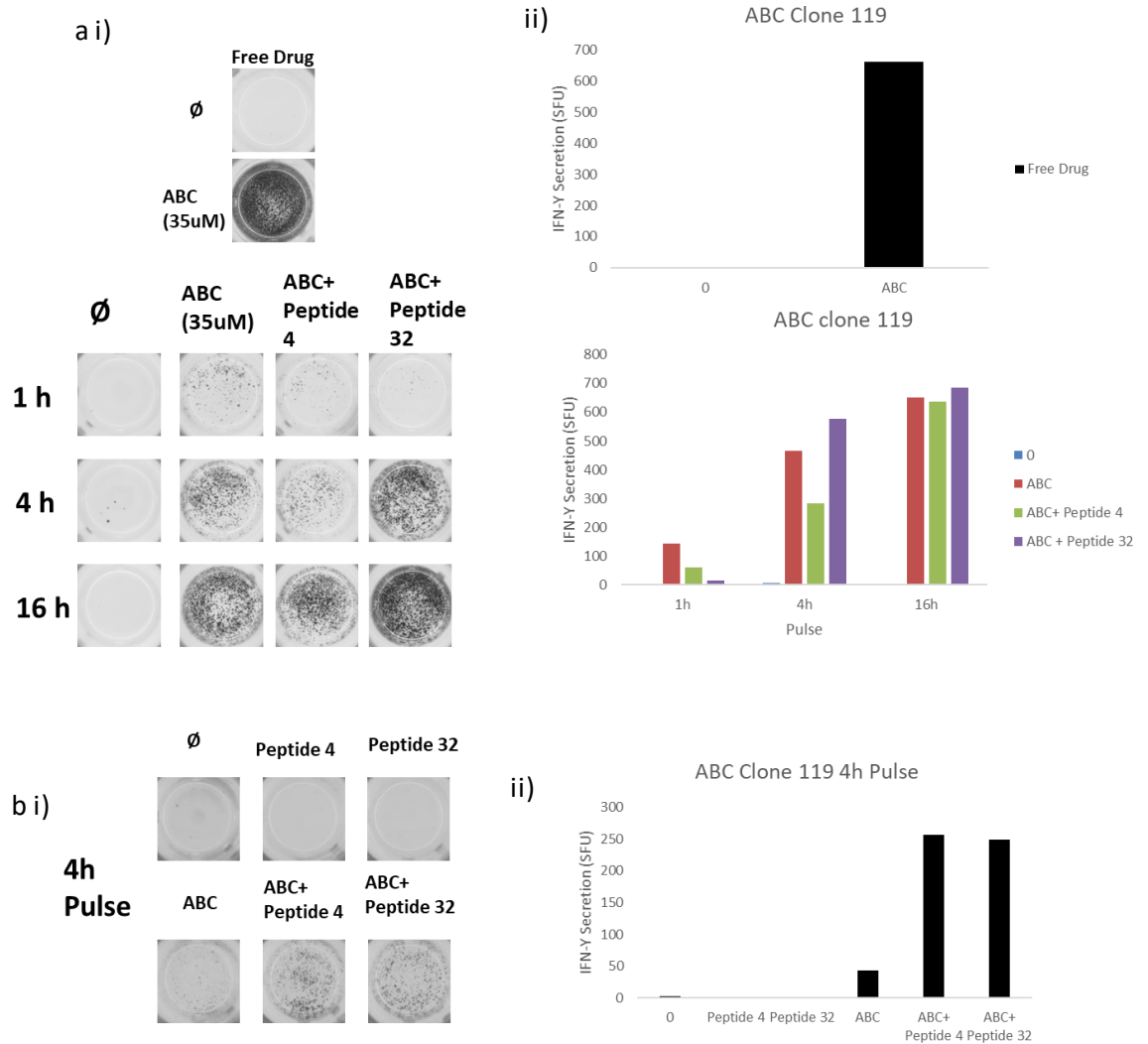
Figure 6.9. T-cell activation with abacavir pulsed APCs is enhanced in the presence of abacavir-induced self-peptides. a) i) ELIspot well images and ii) bar charts comparing the IFN-γ secretion from abacavir clone 119 co-incubated with APCs pulsed for periods of 1h, 4h and 16h in the presence of abacavir (ABC, 35µM), ABC + Peptide 4 (5µM) and ABC + Peptide 32 (5µM). b) A 4h pulse time was selected and the assay was repeated to examine the effects of peptides 4 and 32 (5µM) on T-cell activation in the presence of abacavir pulsed APCs with mock pulsed APCs as a comparator. i) ELIspot well images and ii) bar chart comparing IFN-γ secretion.

6.4.12. T-cell activation induced by abacavir self-peptides in the presence of glutaraldehyde fixed APCs.

Lastly, it was assessed whether exogenous addition of the abacavir self-peptides could reinstate the observed T-cell response to abacavir abolished via the glutaraldehyde fixation of APCs. Peptides 4 and 32 were again used along with abacavir T-cell clone 119. In the presence of fixed APCs, the T-cell response to abacavir was severely diminished compared to the response in the presence of unfixed APCs. However, exogenous addition of both peptides 4 and 32 enhanced IFN-γ secretion from T-cells in the presence of abacavir and fixed APCs. No T-cell activation was observed to either peptide in the absence of the drug.
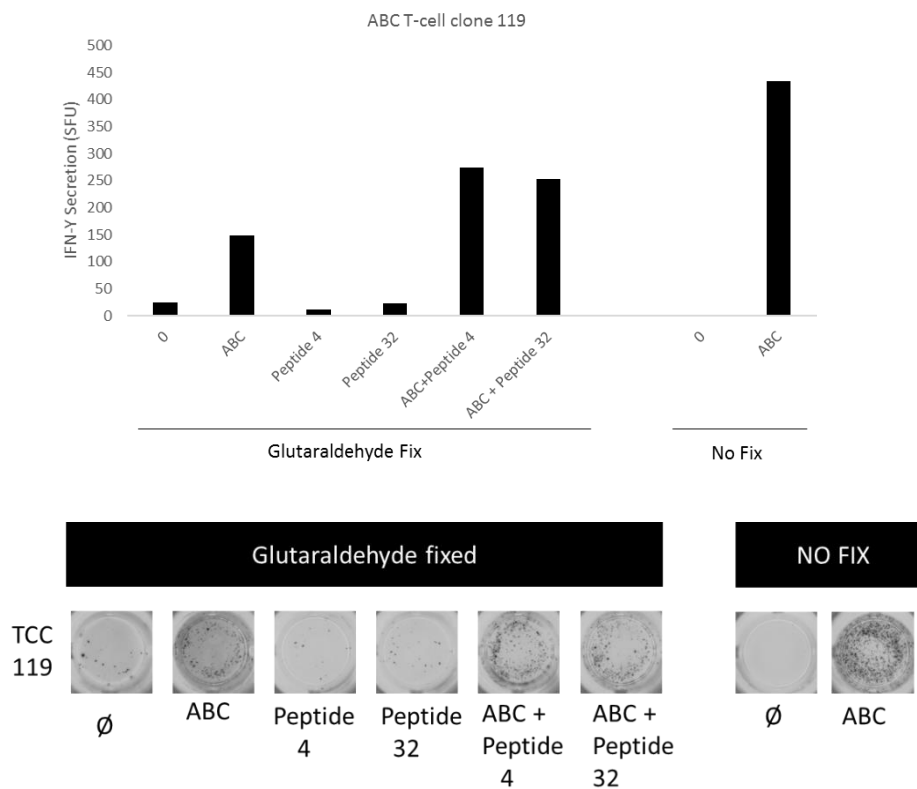
Figure 6.10. T-cell activation induced by peptides 4 and 32 in the presence of abacavir and glutaraldehyde fixed APCs. IFN-γ secretion from abacavir-specific T-cell clone 119 co-incubated with glutaraldehyde fixed APCs with peptides 4 and 32 in the presence and absence of abacavir. Abacavir alone was used as a comparator.

6.5. Discussion.

CD8^{+} T-cell responses elicited by abacavir occur via two independent mechanisms in a processing dependent manner and via direct interaction with HLA-B*57:01 on the surface of APCs (Chessman *et al.*, 2008; Bell *et al.*, 2013). The former is hypothesised to be initiated via a mechanism unique to abacavir. As previously described, abacavir binds non-covalently to HLA-B*57:01 altering the shape and chemistry of the antigen binding cleft thereby allowing for the binding and subsequent presentation of a range of neo self-peptides not previously presented to T-cells. This is believed to induce a T-cell response as T-cells are only tolerant to peptides they are previously exposed to during development in the thymus. This means that recognition of these altered peptides would be adjudged to be similar to a foreign antigen (Illing et al. 2012; Ostrov et al. 2012; Norcross et al. 2012; Llano & Brander 2012).

The use of C1R and T2 cells as APCs provided a strong mechanistic basis for the investigation of the abacavir self-peptides exogenously added to the assays. C1R cells comprise a fully functional B-cell line which in this case has been transfected to express the HLA-B*57:01 allele only. T2 cells also comprise a B-cell line which has been transfected to express the HLA-B*57:01 allele, however, the transporter associated with antigen presentation (TAP) was knocked out, meaning that MHC class I molecules remain in the ER, with only a small number transported to the cell surface (Wolpert et al. 1997; Kleijmeer et al. 1992). Therefore, co-incubation with T2 APCs should abolish or at least diminish the T-cell mediated response observed in the presence of the C1R APCs, allowing for investigation into whether the addition of altered self-peptides exogenously could reinstate the response to abacavir. However, some abacavir-specific T-cell clones display characteristics of self-presentation in the presence of the drug, thereby inducing an equal T-cell response with the T2 APCs observed with the positive control in C1Rs. This makes it impossible to distinguish responses to the drug in the presence of the peptides from those to the drug alone, reducing the

number of T-cell clones that can be effectively used for assays in this manner. While C1R and T2 APCs were used for some initial assays in this chapter the primary focus was shifted to the use of autologous EBVs with the antigen uptake and processing capabilities knocked out via glutaraldehyde fixation (Fonteneau et al. 2003) or interfered with by abacavir pulsing for short periods of time that do not allow for full antigen processing and presentation to occur (Bell *et al.*, 2013). This allowed for more accurate quantification of T-cell responses to abacavir in the presence of altered self-peptides compared to the drug alone (Chessman et al. 2008).

Figure 6.3 displays the results of a kinetics study conducted by Dr Patricia Illing at Monash University in Melbourne. It compares the changes in presentation of abacavir-induced self-peptides with those eluted from HLA-B*57:01 in the absence of the drug (canonical motif) and in the presence of abacavir, thereby demonstrating dependence on abacavir for presentation of these altered self-peptides. With the exception of peptide 24 (KAIDYIRFL) all abacavir-induced self-peptides increased in presentation over time when exposed to abacavir. While those peptides eluted from a canonical motif, demonstrated little to no increase in presentation over a timecourse of abacavir exposure, with many showing a decrease in prevalence. This shows that abacavir plays no role on the increased prevalence of the peptides eluted from a canonical motif, while the abacavir-induced self-peptides were wholly dependent on abacavir for their presentation, apart from peptide 24. This led us to focus on generating specific T-cell clones to the five abacavir-induced self-peptides (4, 13, 24, 32 and 37) in the presence and absence of abacavir.

Responsive T-cell clones could not be generated to the self-peptides in the absence of abacavir. Conversely, in the presence of abacavir, responsive T-cell clones were generated to the peptides, with clones producing strong IFN-γ secretion upon second testing with abacavir and the peptides. As the responsive clones demonstrated strong T-cell activity to

the peptides in the presence of abacavir but also to the drug alone, it was difficult to accurately distinguish between the responses at the optimal concentration of abacavir. Therefore, dose titration assays were conducted using decreasing concentrations of abacavir in the presence and absence of the individual peptides. Indeed, secretion of IFN-γ in response to abacavir was diminished at lower concentrations of the drug, however, addition of the individual abacavir self-peptides enhanced the response to abacavir in the T-cell clones (Figure 6.7). This indicates that the peptides eluted from HLA-B*57:01 in the presence of abacavir (Illing et al. 2012) play a key role in the induction of T-cell responses to abacavir. However, as no T-cell response was observed in the presence of the peptides without abacavir, abacavir appears to be imperative for the binding and presentation of these altered peptides in order to initiate a T-cell response, most likely by altering the peptide binding groove to allow for the stable accommodation of the peptides for presentation to T-cells (Ostrov et al. 2012).

Two abacavir-responsive T-cell clones generated were found to evoke T-cell activation in response to the abacavir self-peptide mix in the presence and the absence of the drug (Figure 6.8). Clone 119, produced low levels of T-cell activation to self-peptide 37 in the absence of abacavir. However, using both pulsing and cellular fixation assays, to remove or reduce antigen processing, robust levels of IFN-γ were observed to peptides 4 and 32 in the presence of abacavir compared to the low T-cell activity observed with T-cells incubated with abacavir alone. Abacavir-specific T-cell clone 121 secreted high levels of IFN-γ in the presence of the same two self-peptides in the absence of abacavir. Unfortunately due to issues with cell numbers with this clone, the fixation and pulsing assays could not be utilized. These findings were surprising, due to the fact that neither clone had been exposed to the abacavir self-peptides exogenously during the priming stage, indicating that the previous exposure to these peptides must have occurred naturally during the T-cell priming to abacavir, suggesting

a distinct role for the presentation of altered peptides in the T-cell responses to abacavir (Illing et al. 2012; Ostrov et al. 2012; Norcross et al. 2012; Yerly et al. 2017).

IFN-γ secretion was observed with peptide 24 in the presence of abacavir at lower concentrations of the drug when compared to the drug alone in the dose titration assays (Figure 6.7). This peptide contains an arginine residue at the Ω-2 position, which would normally have interactions with the binding cleft in the absence of abacavir. These interactions are blocked following abacavirs binding to HLA-B*57:01, therefore it is likely that presentation of this peptide in the presence of the drug would be in an altered conformation which may account for the T-cell activation observed (Illing et al. 2013). This peptide also possesses multiple intracellular origins including ER and Golgi (Table 6.4), which may explain its expression in the absence of abacavir as it can be easily loaded onto MHCs on canonical motifs.

T-cell responses to the abacavir self-peptides in the absence of the drug had not previously been observed with other abacavir-responsive T-cell clones. From chapter 2 and previous studies it is known that abacavir clones possess differing properties including sensitivity to the drug, the mechanism of activation employed and the repertoire of cytokines secreted upon activation (Adam *et al.*, 2012, 2014; Bell *et al.*, 2013). Therefore the notion that differing characteristics of T-cell clones could extend as far as some possessing the ability to respond to individual peptides while others do not is not inconceivable (Adam et al. 2012; Lucas et al. 2015; Yerly et al. 2017). These findings are in line with a recent study from *Yerly et al* in which a T-cell response was found to take place in response to a peptide in the absence of abacavir. However this was exclusive to T-cells transfected with only one specific TCR, indicating that polyclonal T-cell responses comprise multiple T-cell subsets each with different activation characteristics (Yerly et al. 2017). Indeed, the fact that T-cell responses to individual peptides in the absence of abacavir was found on one clone would agree with

these findings, warranting further study to investigate structural characteristics of the interactions of the peptide with T-cells.

The natural form of peptide 15 from chapter 5 (peptide 29) also increased in prevalence in the presence of abacavir, despite having no T-cell activation properties (Chapter 5). This suggests that peptide interactions with T-cells play an important role in the governance of an induction of T-cell responses. This casts light on TCR expression, which we know from chapter 2 displays considerable variation across abacavir clones (Yerly et al. 2017). Indeed, TCR expression is already known to be pivotal in other drugs associated with hypersensitivity reactions such as carbamazepine (Ko et al. 2011). Finally, the fact that two abacavir-specific clones were able to recognise self-peptides which they had not been exposed to previously suggests a strong role for these peptides in immune reactions to abacavir, however as this was only observed in two clones, casts strong light on the variability in T-cell responses between abacavir clones as described in chapter 2.

The successful use of the pulsing and glutaraldehyde assays to analyse the effect of the addition of some abacavir-induced self-peptides represents a promising assay for future research. The successful reinstatement of IFN-γ secretion by the addition of two self-peptides presents as exciting data for the research into the ever increasing role of peptides in the T-cell-mediated hypersensitivity reactions to abacavir.

Here we conclude that the elucidation of the contribution of abacavir and the self-peptides to the induction of T-cell responses remains difficult to define as the endogenous peptides are constantly displayed on the surface of APCs naturally. However our data shows that the abacavir-dependent self-peptides do seem to contribute to the activation of T-cells.

Chapter 7.

Final Discussion.

Adverse drug reactions (ADRs) represent a major clinical problem due to their association with increases in morbidity and mortality in patients, which contributes to a major financial burden on the NHS (Pirmohamed et al. 2004). ADRs can be broadly classified into two categories; Type A and Type B reactions. Type A reactions (augmented) comprise those reactions which are predictable, usually dose-dependent and are related to the primary or secondary pharmacology of the drug. Type B reactions (bizarre) are unpredictable, dose independent reactions which are usually immune-mediated meaning many of the reactions will be off target. Unlike type A, type B reactions are often severe leading to immediate cessation of the offending drug as continued use could be fatal. This represents a major impediment to the drug discovery and development process.

The involvement of HLA-alleles in the mediation of an individual's susceptibility to ADRs has been demonstrated across a range of drugs including carbamazepine (Chung et al. 2004; Ozeki et al. 2011; McCormack et al. 2011), allopurinol (Hung et al. 2005), flucloxacillin (Daly et al. 2009), dapsone (Zhang et al. 2013) and lamotrigine (Man et al. 2007; McCormack et al. 2012). However, perhaps the most commonly known association of risk HLA alleles with immune-mediated reactions is the hypersensitivity reactions experienced to the antiretroviral agent abacavir, linked exclusively with HLA-B*57:01 (Mallal et al. 2002; Hetherington et al. 2002). Indeed, studies focussing on genetic screening for HLA-B*57:01 prior to the commencement of abacavir therapy has been conducted (Hughes et al. 2008; Mallal et al. 2008). *Hughes et al* randomized patients into two distinct groups, one which underwent prospective genotyping for HLA-B*57:01 while the other did not. The incidence of clinically suspected HSR was almost 50% reduced in the genetic screening arm of the study in comparison with the control group (Hughes et al. 2008). Furthermore, a prospective

randomized study conducted by *Mallal et al* completely eradicated immune-mediated hypersensitivity reactions to abacavir, yielding a NPV of 100%, while the incidence of clinically diagnosed HSR was significantly abrogated by prospective genotyping (Mallal et al. 2008). Due to the high frequency of the HLA-B*57:01 risk allele, particularly in the Caucasian population, the practice of prospective genotyping for the allele in patients prior to prescription of abacavir, demonstrated to be a cost effective measure, is now a common application in the clinical setting (Schackman et al. 2008).

T-cell clones responsive to abacavir have been generated from PBMCs of healthy, drug naïve individuals positive for HLA-B*57:01 (Adam *et al.*, 2012, 2014; Bell *et al.*, 2013; Lucas *et al.*, 2015; Naisbitt *et al.*, 2015). These responsive abacavir clones were exclusively CD8$^+$ T-cells which were capable of interacting via processing dependent and independent pathways yielding an overall varied expression of TCR V$_\beta$ (Bell *et al.*, 2013).

Prior to the commencement of my PhD studies, Dr Mohammad Alhaidiri conducted experiments on abacavir focusing on two primary research arms. Firstly, the generation of sixteen abacavir 6-amino substituted analogues. The replacement of the cyclopropyl moiety with N-linked branched carbon chains at the 6-amino position of the compound abrogated the CD8$^+$-mediated T-cell reactions observed with abacavir. Two of these compounds retained antiviral activity, albeit to a lesser degree than abacavir (Naisbitt et al. 2015). Due to the reduced antiviral activity of these compounds however, none were sufficient for the replacement of abacavir in the therapeutic setting, leading to the synthesis of a further eighteen analogues in total for my studies to be analysed.

The second arm of Dr Alhaidiri's work focused on the induction of T-cell responses by abacavir clones to a range of self-peptides whose expression on the surface of APCs is induced by the presence of abacavir. From a panel of 120 peptides received from our collaborators at Monash University in Melbourne Australia, one peptide (NTVELRVKI) was

identified as being able to induce a T-cell mediated immune response in the presence of abacavir in its natural form, while in amidated form the peptide evoked T-cell responses in both the presence and absence of abacavir. However, responses to the natural peptide were observed in the presence of abacavir, only in a select number of clones.

Therefore, my studies focussed on three primary objectives: 1) to generate a panel of abacavir-responsive T-cell clones, which would undergo subsequent analysis of their cellular phenotype and their profiles of T-cell activation in response to the drug; 2) to generate and test a series of novel structural analogues of abacavir, this study investigated the potential for further modifications to be made to the structure of the drug, to eradicate the undesirable T-cell mediated hypersensitivity reactions, without loss of the antiviral potency of the drug; and 3) identify the contribution of the abacavir-induced self-peptides eluted from HLA-B*57:01 on the induction of T-cell responses to the drug.

The successful generation of abacavir-specific T-cell clones was heavily dependent on the expression of HLA-B*57:01 in the healthy donors. The yield of clones responsive at the first testing stage was varied across the four donors employed in this study, ranging from as low as 0.4% in donor 2 (HLA-0957) to a high of 12.5% in donor 4 (HLA-0622). Some donors yielded no responsive T-cell clones at the first testing stage (data not shown). Across the four HLA-B*57:01[+] donors the overall percentage of responsive clones at the first testing stage was 4.5% which was slightly lower than previous studies but this figure was skewed by the low yield of responsive clones from donor 2 (HLA-0957). Indeed, activation of abacavir-responsive T-cell clones was consistent with previous findings where the clones may interact via 2 pathways, which relied on and were exclusive of antigen processing (Bell *et al.*, 2013). Some abacavir-responsive clones became reliant on antigen processing mechanisms as the concentration of the drug decreased. However, this was not true for all abacavir-responsive clones as in many cases T-cell activation was observed at fractional concentrations of the

drug in the absence of antigen processing. This suggests that these clones interact directly with the drug and possess self-presenting capabilities. APC pulsing assays discriminate between these two pathways of T-cell activation, clones which respond via the altered peptide model present strong IFN-γ secretion in this presence of APCs pulsed for 16 hours, ample time for antigen processing and presentation to occur. Clones which respond via direct interaction display a far diminished secretion of IFN-γ in the presence of pulsed APCs when compared to soluble abacavir. For my studies clones utilizing both pathways of T-cell activation were used in assays with the abacavir analogues, while those activated only in the presence of APCs were used for the peptide studies. However, as previously mentioned, due to the short life span of a T-cell clone in culture as well as the potential for losing antigen specificity, self-presenting clones were used for some assays involving peptides, but low concentrations of the drug were used where the need for APCs was apparent.

Consistent with previous findings all T-cell clones generated in the presence of abacavir were CD8$^+$ and the TCR V$_\beta$ expression was varied across all the clones tested (Adam *et al.*, 2012; Bell *et al.*, 2013). Unfortunately, due to limitations with the cost of TCR V$_\beta$ phenotyping kits and the relatively short life of a T-cell clone in cell culture, it was not possible to carry out TCR V$_\beta$ analysis on all responsive abacavir clones. A varied T-cell cytokine secretion profile was noted across the abacavir clones tested (Figure 2.14). While consistency was observed across clones with regard to secretion of the proinflammatory cytokine IFN-γ and the effector molecule granzyme B, there was also a consistent lack of secretion of the anti-inflammatory cytokine IL-10 or the cytokines IL-17 or IL-22, indicating a strong inflammatory response to abacavir. Variation was observed in the secretion of other cytokines and effector molecules. Secretion of IL-5 was observed in one clone tested while some clones secreted IL-13. Secretion of the effector molecules perforin and FasL was also varied across the clones

indicating the employment of multiple mechanisms for instigation of cell death across the range of abacavir clones utilized.

As mentioned above the concept of eradicating the undesirable T-cell activity exhibited in response to abacavir via substitution of the 6-amino cyclopropyl moiety of the compound, known to be imperative for abacavirs interactions within the F-pocket of HLA-B*57:01, has previously been explored (Daluge *et al.*, 1997; Faletto *et al.*, 1997; Naisbitt *et al.*, 2015). Continuing from *Naisbitt et al*, eighteen further abacavir substituted analogues were synthesised to assess the potential to generate structures that may replace abacavir in the therapeutic setting. Through the introduction of azetidine ring variant structures, the responses were eradicated in abacavir-specific T-cell clones. However, while compounds deficient in T-cell responses retained antiviral activity (Figure 7.1), it was not to the same degree as abacavir, making these analogues unsuitable for implementation into drug discovery. Nevertheless, introduction of the azetidine ring demonstrated the potential to generate abacavir substituted analogues with the ability to retain antiviral activity (Figure 7.1).
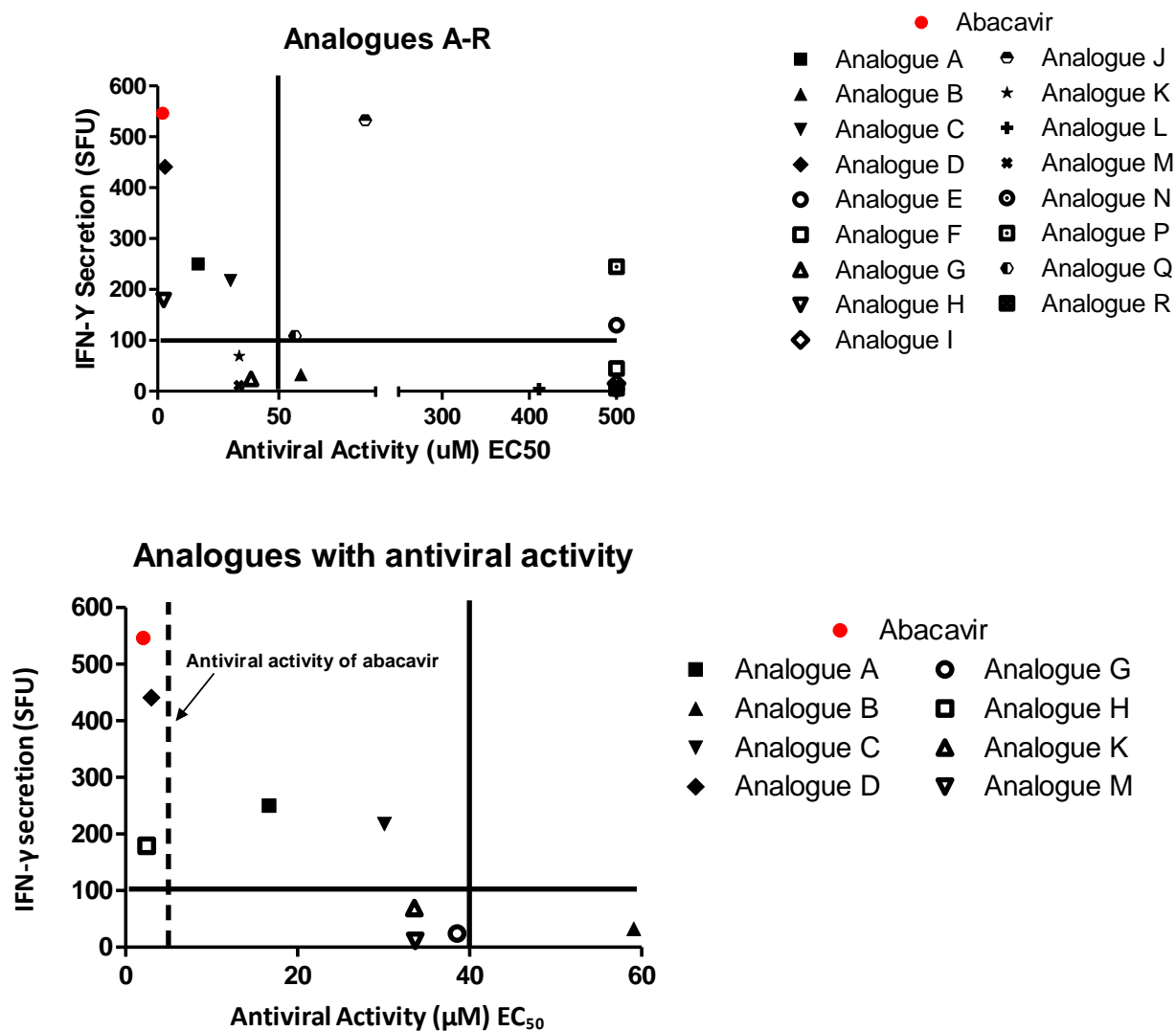
Figure 7.1. Comparison of antiviral and T-cell activity of the eighteen abacavir substituted analogues with abacavir as a comparator. Compounds with antiviral activity of 40 μM or below were considered to have retained antiviral activity. T-cell activity above 100 SFU was considered as activation of T-cells.

Conversely, analogues with equipotency to abacavir with regard to antiviral activity (**D** and **H)** evoked the activation of CD8^{+} T-cells in a similar manner to abacavir. While T-cell activity to analogue **H** was only detected at the higher concentrations of the drug, T-cell cloning to the analogue itself produced responsive CD8^{+} T-cells which were activated by both the analogue and abacavir at lower concentrations. This suggested that analogue **H** possesses similar chemical properties to abacavir with respect to HLA binding and T-cell activation.

The next step in our research was to analyse the interactions of the compounds within HLA-B*57:01 and the relationship with the induction of T-cell activity. Analogues with the ability to induce T-cell activation were found to bind within HLA-B*57:01 in a similar conformation to that of abacavir, allowing for the repertoire of induced self-peptides described in 2012 (Illing et al. 2012; Ostrov et al. 2012; Norcross et al. 2012) to be presented on the antigen presenting cell surface for T-cell recognition. Analogues with no T-cell activation potential, were found to bind HLA-B*57:01 in a hindered manner, making it unlikely that a repertoire of neo self-peptides could bind in their presence, illustrated by the unsustainable steric clashes between the functional groups of analogues **X**, **G, M** and **R** and the residues of the HLA binding peptide or amino acids within the F-pocket of HLA-B*57:01 (Naisbitt et al. 2015). Interestingly, we demonstrated that activation of abacavir-specific CD8^{+} T-cells was not only dependent on the functional group at the 6-amino cyclopropyl position of the compound, but on the chiral state of the functional group in question. Analogues **Q** and **R**, which differed only in their enantiomeric state, activated and were devoid of T-cell responses in abacavir clones, respectively. While studies have seldom been conducted to analyse the effect of enantiomers on T-cell activity, these findings concur with other results which indicate the enantioselectivity of T-cells (Naisbitt et al. 2005). Unfortunately, the enantiomeric state of each analogue bore little effect on their respective antiviral activities presenting the sec-butyl amino functional group to be unsuitable for implementation into the structure of

abacavir for replacement in therapy. However, these findings cast light on a new avenue for focus with regard to the synthesis of further abacavir analogues. If the chiral state of the sec-butyl amino group yields such a polar effect on the induction of T-cell activity then it would be sensible to assume that chiral variants of other functional groups may also possess this effect. Therefore, enantiomers of functional groups such as the azetidine ring (analogue **D**) and azetidine-fluro (analogue **H**) could conceivably be analysed to investigate the bearing on T-cell activation. However, chiral modification at the 6-amino cyclopropyl region of abacavir was not the only modification that was capable of eradicating the unwanted CD8$^+$ mediated T-cell activity experienced in HLA-B*57:01 positive individuals. The abacavir enantiomer **1R, 4S** abacavir, which differed in the chiral state of the cyclopentyl moiety located at the opposite end of the compound was also found to be completely free of T-cell activation when incubated with abacavir-specific T-cell clones. While this compound did not yield any antiviral potency, due to the enantioselective nature of enzyme adenosine phosphotransferase, responsible for the metabolism of the prodrug (Faletto et al. 1997), *in silico* modelling within HLA-B*57:01 revealed an unfavourable binding conformation of the compound. This indicated that the enantiomer was unable to interact within the F-pocket of HLA-B*57:01, presumably due to loss of interactions between the cyclopurine moiety and amino acids, thus preventing the cyclopropyl moiety from protruding into the F-pocket to induce the conformational change. This again incepts a new avenue to pursue in research into the construction of the benchmark abacavir analogue which can possess optimal antiviral activity whilst being devoid of the adverse CD8$^+$ mediated T-cell activity. It is likely that alteration of other parts of the abacavir molecule would hinder the binding of the compound within HLA-B*57:01 to prevent the induction of such T-cell responses. Indeed, such a theory has been postulated (*Ostrov, unpublished data)* via the introduction of modifications to the cyclopurine moiety of abacavir. This suggests the generation of two separate abacavir analogues comprising of firstly substitution of the amine group protruding

from the cyclopurine moiety with a methyl group. The second of these analogues comprised

substitution of the nitrogen groups in the cyclohexane ring with carbon atoms (Figure 7.2).

Abacavir
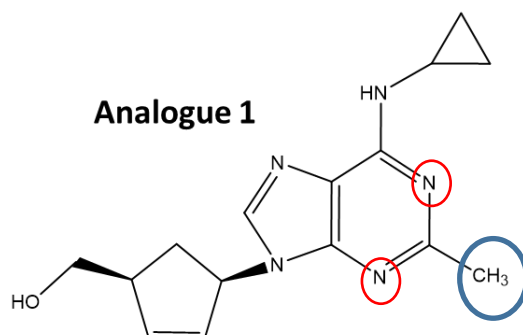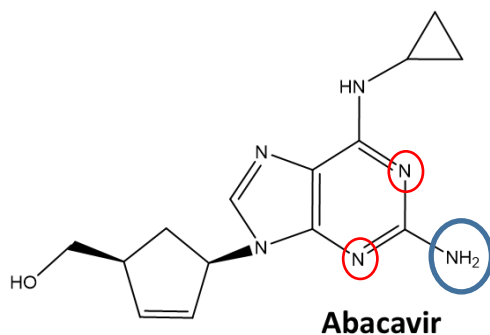
Analogue 1

((1*S*,4*R*)-4-(6-(cyclopropylamino)-2-methyl-9*H*-purin-9-yl)cyclopent-2-en-1-yl)methanol
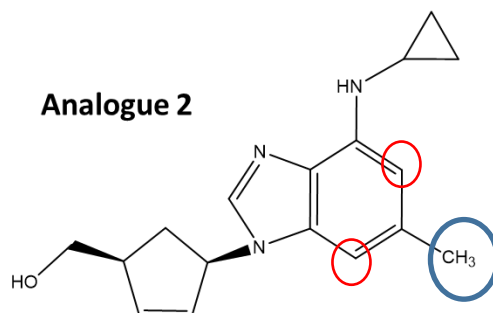
Analogue 2

((1*S*,4*R*)-4-(4-(cyclopropylamino)-6-methyl-1*H*-benzo[*d*]imidazol-1-yl)cyclopent-2-en-1-yl)methanol

Figure 7.2. Structures of currently unsynthesised potential abacavir analogues with substitutions in the cyclopurine moiety *(Ostrov, unpublished data).*

As mentioned earlier, the predicted hindered binding of abacavir analogues within HLA-B*57:01 results in the inhibition of an altered repertoire of self-peptides being presented to T-cells, observed in the presence of abacavir. This was confirmed via use of peptide elution assays conducted in chapter 3 by our collaborators in the Purcell Laboratory (Monash University, Melbourne). Indeed, the presentation of neo self-peptides on the surface of APCs was detected in the presence of the abacavir substituted analogues which induced T-cell activity, while those with no T-cell activity did not induce an increase in the prevalence of the smaller chain C-terminal anchors isoleucine and leucine, confirming our findings with regard to interactions of these compounds within HLA-B*57:01 and the relationship with the induction of CD8+ mediated T-cell activity. Based on these findings, it would be safe to presume that analogues **G**, **M** and **X** would be safe and well tolerated compounds. However, incorporation of analogues **G** and **X** into T-cell cloning assays produced results which were somewhat unexpected. Analogue **G** was well tolerated within the T- cell cloning assays generating no responsive T-cell clones, confirming this compounds safety and lack of immunogenicity. On the other hand, while analogue **X** evoked no activation of abacavir-specific T-cell clones, cloning to analogue **X** itself yielded a plethora of responsive T-cell clones which were not only capable of generating strong responses to the analogue, but also produced potent cross-reactivity with abacavir. At first glance these findings were perplexing, given the fact that analogue **X** had previously represented the benchmark of abacavir analogues with regard to lack of T-cell activity. Also, analogue **X** did not induce an increase in the prevalence of C-terminal anchors leucine or isoleucine, one could have presumed that it may have interacted via a different mechanism. However, closer analysis of the peptides eluted from HLA-B*57:01 in the presence of analogue **X** and abacavir, cast light on these surprising findings. As mentioned in chapter 3, co-incubation of C1R-B*57:01 cells with analogue **X** induces an increase in the prevalence of peptides terminating in the amino acid alanine. Given the similar properties of alanine to isoleucine and leucine (Biro 2006),

replacement at the C-terminal with this amino acid would possess similar properties. Furthermore, the alanine terminating amino acids prevalent in the presence of **X** are also observed in the presence of abacavir meaning that T-cell clones with specificity to the alanine terminating peptides would also recognise these peptides in the presence of abacavir, hence a T-cell response would be evoked. Although given the massive shift in isoleucine abundance in the presence of abacavir, it is likely that most abacavir clones will possess specify only to peptides terminating in isoleucine suggesting why the T-cell responses to analogue **X** are absent in abacavir clones.

These peptide elution studies may be important in the screening of new compounds. However, based on their low throughput, they present as logistically difficult experiments to carry out readily, and as previously stated require a large quantity of the compounds in question, hence why some compounds from this study could only be screened in singlet (**D, H, M**) and others were excluded (**G**). Taken together, these findings demonstrated the ability to generate abacavir substituted analogues which could retain antiviral activity and were devoid of T-cell activation. Further studies using a selected panel of these compounds highlighted the pivotal role of their interactions within HLA-B*57:01 and the effect this had on the peptides presented to T-cells. Based on this, it would seem sensible to investigate the interactions of potential new compounds within HLA-B*57:01 using the methods mentioned, prior to their synthesis, considerably reducing the number of compounds generated with T-cell activating properties. This would refine the process for the design and synthesis of the next panel of abacavir analogues allowing for easier deduction of whether a compound will activate abacavir-specific T-cells then allowing compounds devoid of T-cell activity to be forwarded for further analysis such as peptide elution work and T-cell cloning to the compounds themselves (Figure 7.3).
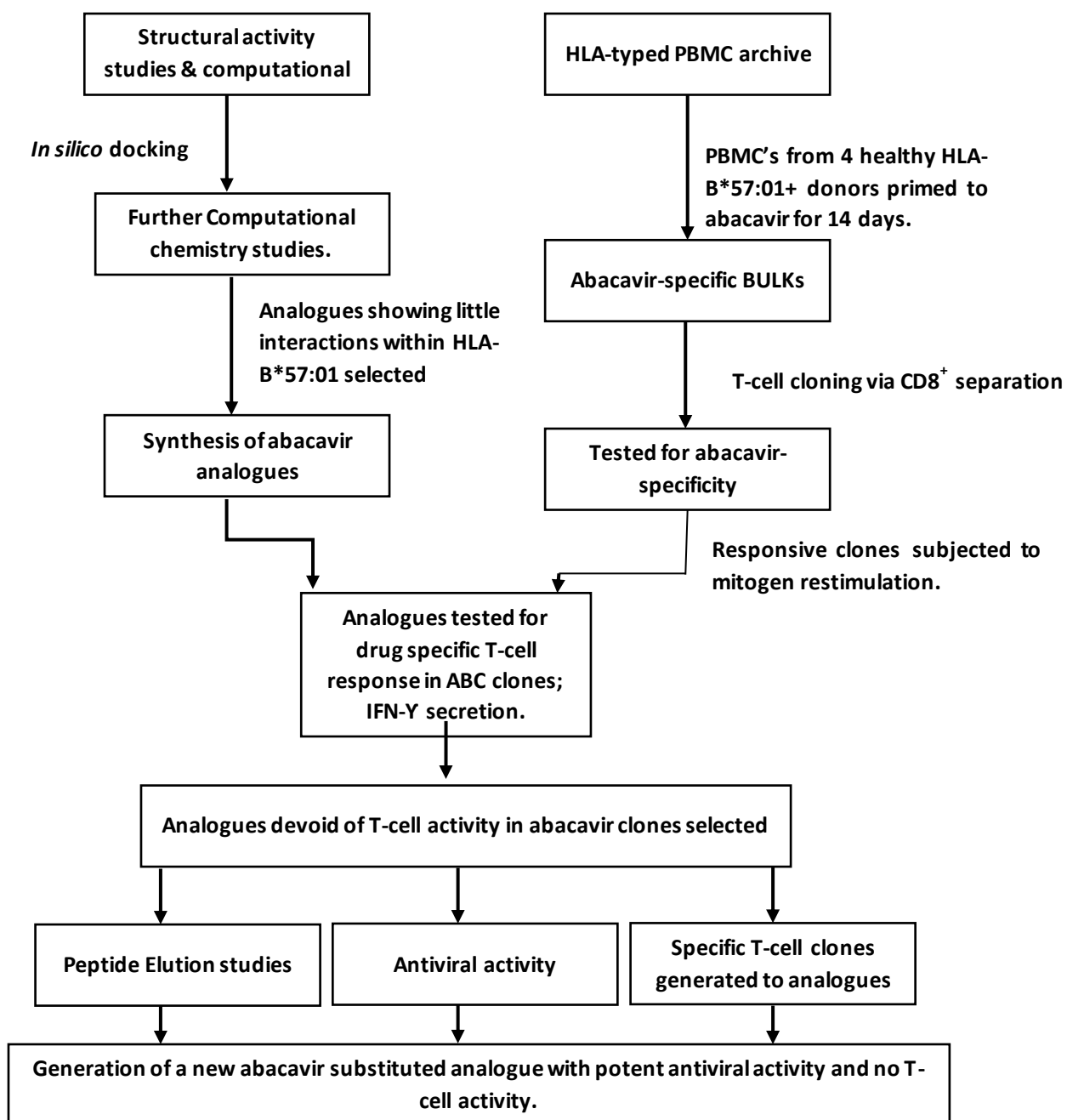
Figure 7.3. New experimental design and synthesis of abacavir substituted analogues.

Figure 7.3 presents an updated paradigm for the synthesis and generation of abacavir substituted analogues, with the emphasis on computational chemistry carried out in more detail before the synthesis of the analogues. This would refine the number of analogues synthesised to only those expected to be devoid of T-cell activity with a degree of certainty, then allowing for further studies to be conducted on the promising analogues in a much shorter period of time. Furthermore, the use of *in silico* docking could be expanded on promising analogues with no T-cell activity and strong antiviral properties to examine the effect of the compounds on other alleles, to assess if the T-cell burden is merely shifted to another allele.

Since the elegant studies carried out by three independent groups in 2012 (Illing et al. 2012; Norcross et al. 2012; Ostrov et al. 2012), the primary focus of abacavir hypersensitivity research has been directed towards the analysis of the neo self-peptides presented on the surface of the antigen presenting cell. Indeed, prior to my studies Dr Mohamad Alhaidiri identified one peptide (NTVELRVKI) that was capable of initiating T-cell activation in the presence of abacavir in the natural form, while in the amidated form T-cell activity was observed in the absence of the drug. Unfortunately, expansion of these studies to our T-cell clones was unable to detect T-cell activation in the presence of peptide 15 in its natural form, whilst in the amidated form strong T-cell activity was again detected. This may have presented the opportunity for the amidation of peptides for use in the assays, however the amidated form of peptide 15 was shown to activate T-cell clones to other drugs in a non-specific manner suggesting it to function as a mimotope (Hartmann et al. 2010; Casey et al. 2006; Gevorkian et al. 2005b). Carrying on from this work a panel of 39 abacavir-induced self-peptides were received, which underwent prior studies to examine their presentation on the surface of HLA-B*57:01 in the presence of abacavir over time. Initial T-cell assays with these peptides proved for the most part fruitless, they revealed a small number of peptides

which may have indicated an enhancement of T-cell activity in their presence. These peptides were investigated further via the use of the T-cell cloning assay to the peptides in both the presence and absence of abacavir. While it was consistently demonstrated that T-cell clones specific to the peptides in the absence of the drug could not be generated, in the presence of abacavir, a panel of responsive clones were detected. Furthermore, at low concentrations of abacavir the addition of the peptides individually yielded an enhancement in the T-cell response to abacavir, demonstrating that the peptides seem to play a role in the activation of T-cells. Perhaps most interestingly, two abacavir-specific CD8$^+$ T-cell clones were found to respond to some self-peptides in the absence of abacavir. Considering these clones were not exposed to the self-peptides exogenously during the priming stage of the experiment, exposure must have taken place naturally with the altered peptides presented in the presence of abacavir. Indeed, exogenous addition of these peptides reinstated the blunted response to abacavir achieved via the use of either short time point APC pulsing or APC fixation with glutaraldehyde. Expansion of the fixation assay to clones primed to the peptide mix + abacavir revealed a modest increase in T-cell activity in the presence of most of the peptides. However, this was not as strong a response as observed with the two abacavir clones. Since these responses were not observed in previous abacavir clones, this suggested that the TCR expression of abacavir clones plays a pivotal role on the ability to interact with peptides presented on the APC surface. The expression of TCRs is known to be a major factor in T-cell reactions to the anti-epileptic drug carbamazepine with the expression of the $V_\beta 11$ and $V_\alpha 22$ subtypes being the most prominent among the patients with CBZ induced SJS/TEN (Ko et al. 2011). With abacavir, the TCR expression is less restricted given that responsive abacavir clones possess a varied repertoire of TCRs (Figure 2.15) (Bell *et al.*, 2013). However, the expression of TCRs could be imperative for the mediation of responses to some abacavir self-peptides and not others. Unsurprisingly, the two abacavir T-cell clones capable of responding to peptides in the absence of the drug, expressed rare TCRV$_\beta$ which were not

detected in previous abacavir clones, one of which was not detectable by the $TCRV_{\beta}$ kit which constitutes around 85% of $TCRV_{\beta}$ repertoire. Consistent with reports from *Yerly et al,* it is likely that the T-cell reactions directed against the abacavir-induced self-peptides is restricted to multiple subsets of abacavir-specific T-cells and is mediated by the TCR expression on the T-cell (Yerly et al. 2017).

The aim of my studies was to gain a further insight into the mechanisms involved in the hypersensitivity reactions experienced to the antiretroviral drug abacavir. Here, we have demonstrated a pivotal role for the abacavir-induced self-peptides only present at HLA-B*57:01 in the presence of the drug. Furthermore, reactions directed against these self-peptides can take place even in the absence of abacavir, suggesting a critical role for the TCR expression on T-cells. While we were not able to synthesise an abacavir analogue which sufficiently met all the criteria to be considered as a replacement for abacavir in therapy, we demonstrated that it is possible to generate such analogues which can retain antiviral activity and not activate T-cells. Our findings have now led the incorporation of new avenues in the analogue field, including the consideration of a functional groups chiral state and also not restricting the modification of the abacavir structure to just the cyclopropyl moiety. Taking all these factors into consideration, it seems only a matter of time before the optimal analogue is discovered, with no T-cell activity and an equipotent antiviral activity to abacavir.

Studies have demonstrated the ability to use mouse models for investigation into drug hypersensitivity reactions with drugs including abacavir, carbamazepine, lamotrigine and phenytoin among others (Whritenour et al. 2014; Zhu et al. 2015), however to determine the underlying mechanisms and the role of viral load in hypersensitivity reactions to abacavir, transgenic mice expressing HLA-B*57:01 should be considered. Indeed, some success was observed via the use of HLA-B*57:01 transgenic mice, to analyse the role of abacavir and the innate immune system in the induction of idiosyncratic liver injury (Song et al. 2018).

Regulatory factors of the immune system have long been considered as responsible elements for the variation in immune responses to an antigen. For instance, the overexpression of PD-1 is apparent in the CD8^{+} virus specific T-cells in HIV infected mice. Furthermore, the blockade of the PD ligand restores the CD8^{+} T-cell function and thereby reduces viral load (Day et al. 2006). The presence of HIV infection results in a reduction in CD4^{+} T-cells, including Tregs. Therefore, as immune tolerance relies in part on cell extrinsic mechanisms such as those provided by CD4^{+} Tregs, this presented as a promising target for research. Indeed, a study conducted by the Norcross group looked to address this matter (Cardone et al. 2018) via the generation of transenic mice (Tg) expressing the HLA-B*57:01 risk allele. While CD8^{+} T-cells isolated from drug naïve HLA-B*57:01 Tg mice were activated *in vitro,* the addition of abacavir to the same Tg mice *in vivo* yielded little to no T-cell activity. However, the depletion of CD4^{+} T-cells via the use of anti-mouse CD4^{+} mAb (anti-CD4) prior to abacavir treatment, resulted in clear signs of hypersensitivity reactions in the Tg mice characterised by scarring, infiltration of CD8^{+} T-cells, in both the dermis and epidermis as well as increased ear thickness. This was not observed in wild type mice or non-CD4 depleted (Cardone et al. 2018).

Hypersensitivity reactions to abacavir yield a 100% NPV, but only a PPV of 55% meaning that just more than half of the HLA-B*57:01 expressing individuals will develop a hypersensitivity reaction when exposed to the drug (Mallal et al. 2008). To date, while the contribution of both genetic and non-genetic factors have been suggested as a reason for this, no definitive factor has been identified. Based on the results discussed, the answer to this question may simply lie in immune tolerance, in one such instance by the presence of CD4^{+} Tregs known to have strong immunosuppressive abilities (Gibson et al. 2017). As depletion of CD4^{+} T-cells results in the amplification of CD8^{+} mediated T-cell responses to abacavir in Tg mice, it does not seem inconceivable that this may also play a role in humans, suggesting that the viral

load of HIV itself, which severely diminishes $CD4^+$ cells in patients, could play a critical role in the regulation of the on the induction of T-cell responses to abacavir in individuals expressing the HLA-B*57:01 risk allele, with those possessing a lower viral load being more tolerant. However, while an association with HIV infection and cutaneous reactions exists (Coopman et al. 1993) no association between HIV viral load and susceptibility to cutaneous reactions has been found with other anti-infectious agents such as sulfonamides (Eliaszewicz et al. 2002). Therefore, it is likely that a complex interplay between both the innate and the adaptive immune system coupled with exogenous factors governs the susceptibility to hypersensitivity reactions with abacavir, accounting for why just under half of those expressing HLA-B*57:01 will not experience hypersensitivity reactions upon exposure and why some individuals experience such reactions on first exposure to the drug.

Since its identification as an agent to induce hypersensitivity reactions and the subsequent association of these hypersensitivity reactions with HLA-B*57:01 (Mallal et al. 2008; Hetherington et al. 2002; Mallal et al. 2002), abacavir has remained the gold standard of a HLA-associated drug hypersensitivity reaction. Here, we set out to gain a greater understanding of the T-cell mediated reactions to abacavir in HLA-B*57:01 expressing individuals with a view to designing safer therapeutics which retain the antiviral potency of abacavir but not the T-cell activating properties. In this thesis we have demonstrated the ability to generate stable substituted analogues of abacavir which retain antiviral activity, but lack the propensity to induce an undesirable T-cell response. Furthermore, we demonstrated that the induction of such T-cell responses showed considerable dependency on the chirality of the compounds structure, not just at the 6-amino cyclopropyl moiety but at other regions of the compound.

To conclude, numerous advances have been made in the study of abacavir-induced hypersensitivity reactions over the years; however, the story remains far from finished. We

demonstrate the importance of a holistic approach into both the understanding of these reactions and the design and analysis of newly generated therapeutics. Incorporation of multiple research paradigms are paramount for the studies into a drug's potential to induce T-cell mediated ADRs in susceptible individuals. This will ultimately lead to a greater likelihood of predicting and subsequently eradicating such reactions, ultimately removing the need for personalised therapy regimens.

Bibliography

Abe, R. et al., 2003. Toxic epidermal necrolysis and Stevens-Johnson syndrome are induced by soluble Fas ligand. *The American journal of pathology*, 162(5), pp.1515–20.

Aberer, W. et al., 2003. Drug provocation testing in the diagnosis of drug hypersensitivity reactions: general considerations. *Allergy*, 58(9), pp.854–863.

Adam, J. et al., 2014. Abacavir induced T cell reactivity from drug naive individuals shares features of allo-immune responses. *PLoS ONE*, 9(4).

Adam, J. et al., 2012. Avidity determines T-cell reactivity in abacavir hypersensitivity. *European Journal of Immunology*, 42, pp.1706–1716.

Adam, J., Pichler, W.J. & Yerly, D., 2011. Delayed drug hypersensitivity: models of T-cell stimulation. *British journal of clinical pharmacology*, 71(5), pp.701–7.

Aderem, A. & Underhill, D.M., 1999. Mechanism of Phagocytosis in Macrophages. *Annual Review of Immunology*, 17(1), pp.593–623.

Ahmed, R. & Branley, H.M., 2009. Reversible bronchospasm with the cardio-selective beta-blocker celiprolol in a non-asthmatic subject. *Respiratory Medicine CME*, 2(3), pp.141–143.

Aihara, M. et al., 2001. Anticonvulsant hypersensitivity syndrome associated with reactivation of cytomegalovirus. *British Journal of Dermatology*, 144, pp.1231–1234.

Akira, S., Uematsu, S. & Takeuchi, O., 2006. Pathogen recognition and innate immunity. *Cell*, 124(4), pp.783–801.

Albert, E. et al., 1978. Nomenclature for factors of the HLA system. *Tissue antigens*, 11(1), pp.81–86.

Alfirevic, A. et al., 2006. HLA-B locus in Caucasian patients with carbamazepine hypersensitivity. *Pharmacogenomics*, September(7), pp.813–8.

Alfirevic, A. & Pirmohamed, M., 2010. Drug-induced hypersensitivity reactions and pharmacogenomics : past, present and future. *Pharmacogenomics*, 11(4), pp.497–499.

Almeida, C.-A.M. et al., 2008. Cytokine profiling in abacavir hypersensitivity patients Original article Cytokine profiling in abacavir hypersensitivity. *Antiviral Therapy*, 13(October 2016), pp.281–288.

Alzahrani, A. et al., 2017. Dapsone and Nitroso Dapsone Activation of Naïve T-Cells from Healthy Donors. *Chemical Research in Toxicology*, p.acs.chemrestox.7b00263.

Amali, M.O. et al., 2017. Detection of drug-responsive B lymphocytes and antidrug IgG in patients with β-lactam hypersensitivity. *Allergy: European Journal of Allergy and Clinical Immunology*, 72(6), pp.896–907.

Amin, K., 2012. The role of mast cells in allergic inflammation. *Respiratory Medicine*, 106(1), pp.9–14.

Amir, A.L. et al., 2010. Allo-HLA reactivity of virus-specific memory T cells is common Allo-HLA reactivity of virus-specific memory T cells is common. *Blood*, 115(15), pp.3146–3157.

Andrews, E. & Daly, A.K., 2008. Flucloxacillin-induced liver injury. *Toxicology*, 254(3), pp.158–163.

Anon, 1972. WHO. International drug monitoring: the role of international centres. *WHO Tech Rep Ser*, 498.

Aronson, J.K. & Ferner, R.E., 2003. Joining the DoTS : new approach to classifying adverse drug reactions. *British Medical Journal*, 327(November), pp.1222–1225.

Baggiolini, M. & Clark-Lewis, I., 1992. Interleukin 8, a chemotactic and inflammatory. *FEBS letters*, 307(I), pp.97–101.

Banchereau, J. & Steinman, R.M., 1998. Dendritic cells and the control of immunity. *Nature*, 392(March), pp.245–252.

Baramki, D. et al., 2002. Modulation of T-cell function by (R)- and (S)-isomers of albuterol: Anti-inflammatory influences of (R)-isomers are negated in the presence of the (S)-isomer. *Journal of Allergy and Clinical Immunology*, 109(3), pp.449–454.

Barbarino, J.M. et al., 2014. PharmGKB summary: abacavir pathway. *Pharmacogenomics and Genomics*.

Bastuji-Garin, S. et al., 1993. Clinical Classification of Cases of Toxic Epidermal Necrolysis, Stevens-Johnson Syndrome, and Erythema Multiforme. *Archives of Dermatology*, 129(1), pp.92–96.

Beeler, A. et al., 2008. CD69 upregulation on T cells as an in vitro marker for delayed-type drug hypersensitivity. *Allergy: European Journal of Allergy and Clinical Immunology*, 63(2), pp.181–188.

Bell, C.C. et al., 2013. Oxidative bioactivation of abacavir in subcellular fractions of human antigen presenting cells. *Chemical Research in Toxicology*, 26(7), pp.1064–1072.

Bell, C.C. et al., 2013. T-Cells from HLA-B*57:01+ Human Subjects Are Activated with Abacavir through Two Independent Pathways and Induce Cell Death by Multiple Mechanisms. *Chemical research in Toxicology*, 26, pp.759–766.

Bewtra, M. & Lewis, J.D., 2011. therapy for inflammatory bowel disease. *Journal of clinical immunology*, 6(4), pp.621–631.

Bickel, M., 1993. The role of interleukin-8 in inflammation and mechanisms of regulation. *Journal of periodontology*, May(64), pp.456–60.

Biro, J.C., 2006. Amino acid size, charge, hydropathy indices and matrices for protein structure analysis. *Theoretical Biology and Medical Modelling*, 3(1), pp.1–12.

Blum, J.S., Wearsch, P.A. & Cresswell, P., 2013. Pathways of antigen processing. *Annual Review of Immunology*, 31, pp.443–73.

Boniface, K. et al., 2007. A role for T cell-derived interleukin 22 in psoriatic skin inflammation. *Clinical and Experimental Immunology*, 150(3), pp.407–415.

Bouchery, T. et al., 2014. The differentiation of CD4+ T-helper cell subsets in the context of helminth parasite infection. *Frontiers in Immunology*, 5(OCT), pp.1–13.

Bousquet, P.J. et al., 2008. Oral challenges are needed in the diagnosis of β-lactam hypersensitivity. *Clinical and Experimental Allergy*, 38(1), pp.185–190.

Bradding, P., Walls, A.F. & Holgate, S.T., 2006. The role of the mast cell in the pathophysiology of asthma. *Journal of Allergy and Clinical Immunology*, 117(6), pp.1277–1284.

Broeke, T., Wubbolts, R. & Stoorvogel, W., 2013. MHC Class II Antigen Presentation by Dendritic Cells Regulated through Endosomal Sorting. *Cold Spring Harbor Perspectives in Biology*, pp.1–21.

Burkhart, C. et al., 2002. Non-covalent presentation of sulfamethoxazole to human CD4+ T cells is independent of distinct human leucocyte antigen-bound peptides. *Clinical and Experimental Allergy*, 32(11), pp.1635–1643.

Bux, J. et al., 2000. Neutropenia and anaemia due to carbimazole-dependent antibodies. *British journal of haematology*, 109, pp.243–247.

Caligiuri, M. a., 2008. Human natural killer cells. *Bone*, 112(3), pp.461–469.

Callreus, T., 2006. Use of the Dose , Time , Susceptibility (DoTS) Classification Scheme for Adverse Drug Reactions in Pharmacovigilance Planning. *Drug Safety*, 29(7), pp.557–566.

Cârcu-Dobrin, M. et al., 2017. Enantioselective analysis of fluoxetine in pharmaceutical formulations by capillary zone electrophoresis. *Saudi Pharmaceutical Journal*, 25(3), pp.397–403.

Cardone, M. et al., 2018. A transgenic mouse model for HLA-B*57:01-linked abacavir drug tolerance and reactivity. *The Journal of clinical investigation*, 128(7), pp.2819–2832.

Carr, D.F. et al., 2013. Association of human leukocyte antigen alleles and nevirapine hypersensitivity in a Malawian HIV-infected population. *Clinical Infectious Diseases*, 56(9), pp.1330–1339.

Caruso, A. et al., 1997. Flow cytometric analysis of activation markers on stimulated T cells and their correlation with cell proliferation. *Cytometry*, 27(1), pp.71–76.

Casey, J.L. et al., 2006. Peptide Mimotopes Selected from a Random Peptide Library for Diagnosis of Epstein-Barr Virus Infection Peptide Mimotopes Selected from a Random Peptide Library for Diagnosis of Epstein-Barr Virus Infection. *JOURNAL OF CLINICAL MICROBIOLOGY*, 44(3), pp.764–771.

Castrejon, J.L. et al., 2010. Stimulation of human T cells with sulfonamides and sulfonamide metabolites. *Journal of Allergy and Clinical Immunology*, 125(2), p.411–418.e4.

Cella, M., Sallusto, F. & Lanzavecchia, A., 1997. Origin, maturation and antigen presenting function of dendritic cells. *Current Opinion in Immunology*, 9(1), pp.10–16.

Chamberlain, P.P. et al., 2014. Structure of the human Cereblon-DDB1-lenalidomide complex reveals basis for responsiveness to thalidomide analogs. *Nature Structural and Molecular Biology*, 21(9), pp.803–809.

Chaplin, D.D., 2010. Overview of the Immune Response. *Journal of Allergy and Clinical Immunology*, 125(5), pp.213–223.

Charneira, C. et al., 2011. Reactive aldehyde metabolites from the anti-HIV drug abacavir: Amino acid adducts as possible factors in abacavir toxicity. *Chemical Research in Toxicology*, 24(12), pp.2129–2141.

Chen, P. et al., 2011. Carbamazepine-Induced Toxic Effects and HLA-B*1502 Screening in Taiwan. *New England Journal of Medicine*, 364(12), pp.1126–1133.

Chen, Z. & O'Shea, J.J., 2008. Th17 cells: A new fate for differentiating helper T cells. *Immunologic Research*, 41(2), pp.87–102.

Chesnut, R. & Grey, H., 1985. Antigen presenting cells and mechanisms of antigen presentation. *Critical Reviews in Immunology*, 5(3), pp.263–316.

Chessman, D. et al., 2008. Human leukocyte antigen class I-restricted activation of CD8+ T cells provides the immunogenetic basis of a systemic drug hypersensitivity. *Immunity*, 28(6), pp.822–32.

Chipinda, I., Hettick, J.M. & Siegel, P.D., 2011. Haptenation: Chemical Reactivity and Protein Binding. *Journal of Allergy*, 2011, pp.1–11.

Cho, S.H., Hartleroad, J.Y. & Oh, C.K., 2001. (S)-albuterol increases the production of histamine and IL-4 in mast cells. *International Archives of Allergy and Immunology*, 124(4), pp.478–484.

Choquet-Kastylevsky, G. et al., 1998. Increased levels of interleukin 5 are associated with the generation of eosinophilia in drug-induced hypersensitivity syndrome. *British Journal of Dermatology*, 139(6), pp.1026–1032.

Chung, W.-H. et al., 2004. A marker for Stevens–Johnson syndrome. *Nature*, 428(6982), p.2501.

Chung, W.H. et al., 2008. Granulysin is a key mediator for disseminated keratinocyte death in Stevens-Johnson syndrome and toxic epidermal necrolysis. *Nature Medicine*, 14(12), pp.1343–1350.

Clark, C. & Dalmasso, A.., 1982. Delayed hypersensitivity responses to human IgG and methylated bovine serum albumin are regulated by different mechanisms. *Immunology*, 47(19), pp.19–29.

Le Cleach, L. et al., 2000. Blister fluid T lymphocytes during toxic epidermal necrolysis are functional cytotoxic cells which express human natural killer (NK) inhibitory receptors. *Clinical and Experimental Immunology*, 119(1), pp.225–230.

Coopman, S. et al., 1993. Cutaneous disease and drug reactions in HIV infection. *The New England Journal of Medecine*, 328(23), pp.1670–1674.

Cox, J.H., Ferrari, G. & Janetzki, S., 2006. Measurement of cytokine release at the single cell level using the ELISPOT assay. *Methods*, 38(4), pp.274–282.

Cribb, A.E. & Spielberg, S.P., 1992. Sulfamethoxazole is metabolized to the hydroxylamine in humans. *Clinical Pharmacology and Therapeutics*, 51(5), pp.522–526.

Curtsinger, J.M. et al., 1999. Inflammatory cytokines provide a third signal for activation of naive CD4+ and CD8+ T cells. *Journal of immunology (Baltimore, Md. : 1950)*, 162(6), pp.3256–62.:

Cuthbert, R., Ch, B. & Speirs, A.L., 1962. THALIDOMIDE INDUCED MALFORMATIONS--A RADIOLOGICAL SURVEY. *Clinical Radiology*, 14, pp.163–199.

Czerkinsky, C. et al., 1988. Reverse ELISPOT assay for clonal analysis of cytokine production I. Enumeration of gamma-interferon-secreting cells. *Journal of Immunological Methods*, 110(1), pp.29–36.

D'Arcy, P., 1986. Drug interactions with oral contraceptives. *Drug Intelligence & Clinical Pharmacy*, 20(May), pp.353–62.

Dalod, M. et al., 2014. Dendritic cell maturation: Functional specialization through signaling specificity and transcriptional programming. *EMBO Journal*, 33(10), pp.1104–1116.

Daluge, S.M. et al., 1997a. 1592U89 , a Novel Carbocyclic Nucleoside Analog with Potent , Selective Anti-Human Immunodeficiency Virus Activity. *ANTIMICROBIAL AGENTS AND CHEMOTHERAPY*, 41(5), pp.1082–1093.

Daluge, S.M. et al., 1997b. 1592U89 , a Novel Carbocyclic Nucleoside Analog with Potent , Selective Anti-Human Immunodeficiency Virus Activity analog with potent , selective anti-human immunodeficiency virus activity . *ANTIMICROBIAL AGENTS AND CHEMOTHERAPY*, 41(5), pp.1082–1093.

Daly, A.K. et al., 2009. HLA-B5701 genotype is a major determinant of drug-induced liver injury due to flucloxacillin. *Nature Genetics*, 41(7), pp.816–819.

Dausset, J., Delafontaine, P. & Fleuriot, Y., 1952. Agglutination and destruction in vitro of normal blood platelets by serum from a patient with purpura thrombopenica; inhibition of cloth retraction by serum. *Sang*, 5(373–84).

Day, C.L. et al., 2006. PD-1 expression on HIV-specific T cells is associated with T-cell exhaustion and disease progression. *Nature*, 443(7109), pp.350–354.

Descamps, V. et al., 2003. Drug-induced hypersensitivity syndrome associated with Epstein – Barr virus infection. *British Journal of Dermatology*, 148, pp.1032–1034.

DeVane, C. & Boulton, D., 2002. Great expectations in stereochemistry: focus on antidepressants. *CNS spectrums*, April(7), pp.28–33.

DJ, P. et al., 2015. Cost-effectiveness analysis of HLA-B5801 genotyping in the treatment of gout patients with chronic renal insufficiency in Korea. *Arthritis Care & Research*, Feburary, pp.280–7.

Donohugh, D.L., 1996. Medicine Eosinophils and Losinophilia. *CALIFORNIA MEDICINE*, Febuary, pp.421–427.

Drain, K.L. & Volcheck, G.W., 2001. Preventing and Managing Drug-Induced Anaphylaxis. *Drug Safety*, 24(11), pp.843–853.

Dudek, N.L. et al., 2012. Constitutive and inflammatory immunopeptidome of pancreatic β-cells. *Diabetes*, 61(11), pp.3018–3025.

Echizen, H., Manz, M. & Eichelbaum, M., 1988. Electrophysiologic effects of dextro- and levo-verapamil on sinus node and AV node function in humans. *Journal of Cardiovascular Pharmacology*, 12, pp.543–6.

Edwards, I.R. & Aronson, J.K., 2000. Adverse drug reactions Adverse drug reactions : definitions, diagnosis, and management. *Adverse Drug Reactions*, 356, pp.1255–1259.

Eliaszewicz, M. et al., 2002. Prospective evaluation of risk factors of cutaneous drug reactions to sulfonamides in patients with AIDS. *Journal of the American Academy of Dermatology*, 47(1), pp.40–46.

Elzagallaai, A.A. et al., 2009. In Vitro Testing for the Diagnosis of Anticonvulsant Hypersensitivity Syndrome A Systematic Review. *Molecular Diagnosis and Therapy*, 13(5), pp.313–330.

Elzagallaai, A.A. & Rieder, M.J., 2015. In vitro testing for diagnosis of idiosyncratic adverse drug reactions : Implications for pathophysiology. *British Journal of Clinical Pharmacology*, 80(4), pp.889–900.

Erkes, D. a. & Selvan, S.R., 2014. Hapten-induced contact hypersensitivity, autoimmune reactions, and tumor regression: Plausibility of mediating antitumor immunity. *Journal of Immunology Research*, 2014, pp.1–28.

Estelle, B. et al., 2006. Reciprocal developmental pathways for the generation of pathogenic effector TH17 and regulatory T cells. *Nature*, 441, pp.235–238.

Eyerich, S. et al., 2009. Th22 cells represent a distinct human T cell subset involved in epidermal immunity and remodeling. *Journal of Clinical Investigation*, 119(12), pp.3573–3585.

Faletto, M.B. et al., 1997. Unique intracellular activation of the potent anti-human immunodeficiency virus agent 1592U89. *Antimicrobial Agents and Chemotherapy*, 41(5), pp.1099–1107.

Farcas, A. & Bojita, M., 2009. Adverse Drug Reactions in Clinical Practice : a Causality Assessment of a Case of Drug-Induced Pancreatitis. *Journal of Gastrointestine Liver Disease*, 18(3), pp.353–358.

Farrell, R.J. et al., 2000. Increased incidence of non-Hodgkin's lymphoma in inflammatory bowel disease patients on immunosuppressive therapy but overall risk is low. *Gut*, 47(4), pp.514–519.

Faulkner, L. et al., 2016. Detection of Primary T Cell Responses to Drugs and Chemicals in HLA-Typed Volunteers: Implications for the Prediction of Drug Immunogenicity. *Toxicological sciences : an official journal of the Society of Toxicology*, 154(2), pp.416–429.

Faulkner, L. et al., 2012. The development of in vitro culture methods to characterize primary t-cell responses to drugs. *Toxicological Sciences*, 127(1), pp.150–158.

Fonteneau, J.F. et al., 2003. Characterization of the MHC class I crosspresentation pathway for cell associated antigens by human dendritic cells. *Blood.*, in press(13), pp.4448–4455.

Fraser, L.-A. & Adachi, J.D., 2009. Glucocorticoid-induced osteoporosis: treatment update and review. *Therapeutic advances in musculoskeletal disease*, 1(2), pp.71–85.

Fujihashi, K. et al., 1993. Cytokine-specific ELISPOT assay single cell analysis of IL-2, IL-4 and IL-6 producing cells. *Journal of Immunological Methods*, 160(2), pp.181–189.

Fujita, H., 2013. The role of IL-22 and Th22 cells in human skin diseases. *Journal of Dermatological Science*, 72(1), pp.3–8.

Galli, S.J. & Tsai, M., 2013. IgE and mast cells in allergic disease. *Nature medicine*, 280(21), pp.20814–20823.

Gallucci, S. & Matzinger, P., 2001. Danger signals: SOS to the immune system. *Current Opinion in Immunology*, 13(1), pp.114–119.

Gevorkian, G. et al., 2005a. Peptide mimotopes of Mycobacterium tuberculosis carbohydrate immunodeterminants. *The Biochemical journal*, 387(Pt 2), pp.411–7.

Gevorkian, G. et al., 2005b. Peptide mimotopes of Mycobacterium tuberculosis carbohydrate immunodeterminants. *The Biochemical journal*, 387(Pt 2), pp.411–7.

Gibson, A. et al., 2014. Negative Regulation by PD-L1 during Drug-Specific Priming of IL-22-Secreting T Cells and the Influence of PD-1 on Effector T Cell Function. *The Journal of Immunology*, 192(6), pp.2611–2621.

Gibson, A. et al., 2017. The Effect of Inhibitory Signals on the Priming of Drug Hapten–Specific T Cells That Express Distinct Vβ Receptors. *The Journal of Immunology*, 199(4), pp.1223–1237.

Gidal, B.E., 2011. Carbamazepine hypersensitivity: Progress toward predicting the unpredictable. *Epilepsy Currents*, 11(6), pp.189–191.

Guo, H. et al., 2014. HIV-1 infection induces interleukin-1β production via TLR8 protein-dependent and NLRP3 inflammasome mechanisms in human monocytes. *Journal of Biological Chemistry*, 289(31), pp.21716–21726.

Gyuris, A., Vajda, G. & Földes, I., 1992. Establishment of an MT4 cell line persistently producing infective HIV-1 particles. *Acta Microbiol Hung*, 39(3–4), pp.271–9.

Han, T.H. et al., 2009. Evaluation of Three Clinical Dendritic Cell Maturation Protocols Containing Lipopolysaccharide and Interferon-gamma. *Journal of Immunotherapy*, 32(4), pp.399–407.

Harding, C. V & Unanue, E.R., 1990. Cellular mechanisms of antigen processing and the function of class I and II major histocompatibility complex molecules. *Cell regulation*, 1(7), pp.499–509.

Harr, T. & French, L.E., 2010. Toxic epidermal necrolysis in Stevens Johnson syndrome. *Orphanet Journal of Rare Diseases*, 5(39), pp.1–11.

Hartigan-Go, K. & Wong, J., 2000. Inclusion of therapeutic failures as adverse drug reactions. *Side effects of drugs annual*, 23(12), pp.8006–9.

Hartmann, C. et al., 2010. Peptide mimotopes recognized by antibodies cetuximab and matuzumab induce a functionally equivalent anti-EGFR immune response. *Oncogene*, 29(32), pp.4517–4527.

Henderson, W.R., Banerjee, E.R. & Chi, E.Y., 2005. Differential effects of (S)- and (R)-enantiomers of albuterol in a mouse asthma model. *Journal of Allergy and Clinical Immunology*, 116(2), pp.332–340.

Hervey, P.S. & Perry, C.M., 2000. Abacavir: A Review of its Clinical Potential in Patients with HIV Infection. *Drugs*, 60(2), pp.447–479.

Hetherington, S. et al., 2002. Genetic variations in HLA-B region and hypersensitivity reactions to abacavir. *THE LANCET*, 359, pp.1121–1122.

Hetherington, S. et al., 2001. Hypersensitivity reactions during therapy with the nucleoside reverse transcriptase inhibitor abacavir. *Clinical Therapeutics*, 23(10), pp.1603–14.

Hewitt, E.W., 2003. The MHC class I antigen presentation pathway: Strategies for viral immune evasion. *Immunology*, 110(2), pp.163–169.

Hirata, K. et al., 2008. Ticlopidine-induced hepatotoxicity is associated with specific human leukocyte antigen genomic subtypes in Japanese patients: A preliminary case-control study. *Pharmacogenomics Journal*, 8(1), pp.29–33.

Hiro, i T. et al., 1994. Characterization of cytokine-producing cells in mucosal effector sites: CD3+ T cells of Th1 and Th2 type in salivary gland-associated tissues. *European Journal of Immunology*, 24(11), pp.2653–8.

Huang, Y.F. et al., 1998. Cardiovascular and central nervous system effects of intravenous levobupivacaine and bupivacaine in sheep. *Anesth Analg*, 86(4), pp.797–804.

Hubo, M. et al., 2013. Costimulatory molecules on immunogenic versus tolerogenic human dendritic cells. *Frontiers in Immunology*, 4(APR), pp.1–14.

Hughes, D.A. et al., 2004. Cost-effectiveness analysis of HLA B * 5701 genotyping in preventing abacavir hypersensitivity. *Pharmacogenomics*, 14(6), pp.335–342.

Hughes, S. et al., 2008. PREDICT-1 (CNA106030): the first powered , prospective trial of pharmacogenetic screening to reduce drug adverse events. *Pharmaceutical Statistics*, 7(May), pp.121–129.

Hung, S. et al., 2006. Genetic susceptibility to carbamazepine-induced cutaneous adverse drug reactions. *Pharmacogenomics and Genomics*, 16(4), pp.297–306.

Hung, S. et al., 2005. HLA-B*5801 allele as a genetic marker for severe cutaneous adverse reactions caused by allopurinol. *PNAS*, 102(17), pp.4134–4139.

Hunziker, T. et al., 1997. Comprehensive hospital drug monitoring (CHDM): adverse skin reactions, a 20-year survey. *Allergy*, 52(4), pp.388–93.

Illing, P.T. et al., 2013. Human leukocyte antigen-associated drug hypersensitivity. *Current Opinion in Immunology*, 25(1), pp.81–89.

Illing, P.T. et al., 2012. Immune self-reactivity triggered by drug-modified HLA-peptide repertoire. *Nature*, 486(7404), pp.554–8.

Jacobsen, E. a et al., 2012. Review article The expanding role (s) of eosinophils in health and disease. *Blood*, 120(19), pp.3882–3890.

Kägi, D. et al., 1994. Cytotoxicity mediated by T cells and natural killer cells is greatly impaired in perforin-deficient mice. *Nature*, 369, pp.31–37.

Kalinski, P., 2009. Dendritic cells in immunotherapy of established cancer: Roles of signals 1, 2, 3 and 4. *Current opinion in investigational drugs (London, England : 2000)*, 10(6), pp.526–535.

Kanhere, A. et al., 2012. T-bet and GATA3 orchestrate Th1 and Th2 differentiation through lineage-specific targeting of distal regulatory elements. *Nature Communications*, 3, p.1268.

Kaniwa, N. et al., 2008. HLA-B locus in Japanese patients with anti-epileptics and allopurinol-related Stevens-Johnson syndrome and toxic epidermal necrolysis. *Pharmacogenomics*, 9(11), pp.1617–22.

Kaniwa, N. & Saito, Y., 2013. The risk of cutaneous adverse reactions among patients with the *HLA-A* 31:01* allele who are given carbamazepine, oxcarbazepine or eslicarbazepine: a perspective review. *Therapeutic Advances in Drug Safety*, 4(6), pp.246–253.

Kapsenberg, M.L., 2003. Dendritic-cell control of pathogen-driven T-cell polarization. *Nature Reviews Immunology*, 3(12), pp.984–993.

Keane, N.M. et al., 2014. HLA Class I restricted CD8+ and Class II restricted CD4+ T cells are implicated in the pathogenesis of nevirapine hypersensitivity. *Aids*, 28(13), pp.1891–1901.

Khalifian, S., Raimondi, G. & Brandacher, G., 2015. The Use of Luminex Assays to Measure Cytokines. *Journal of Investigative Dermatology*, 135(4), p.e31.

Khazen, W. et al., 2005. Expression of macrophage-selective markers in human and rodent adipocytes. *FEBS Letters*, 579(25), pp.5631–5634.

Kim, J.H. & Scialli, A.R., 2011. Thalidomide: the tragedy of birth defects and the effective treatment of disease. *Toxicological sciences : an official journal of the Society of Toxicology*, 122(1), pp.1–6.

Kischkel, F.C. et al., 1995. Cytotoxicity-dependent APO-1 (Fas/CD95)-associated proteins form a death-inducing signaling complex (DISC) with the receptor. *The EMBO journal*, 14(22), pp.5579–88.

Kleijmeer, M.J. et al., 1992. Location of MHC-encoded transporters in the endoplasmatic reticulum and cis-Golgi. *Nature*, 357, pp.342–344.

Ko, T.M. et al., 2011. Shared and restricted T-cell receptor use is crucial for carbamazepine-induced Stevens-Johnson syndrome. *Journal of Allergy and Clinical Immunology*, 128(6), p.1266–1276.e11.

Ko, T.M. et al., 2015. Use of HLA-B∗58:01 genotyping to prevent allopurinol induced severe cutaneous adverse reactions in Taiwan: National prospective cohort study. *BMJ (Online)*, 351, pp.1–7.

Kolaczkowska, E. & Kubes, P., 2013. Neutrophil recruitment and function in health and inflammation. *Nature Reviews Immunology*, 13(3), pp.159–175. A

Koldsø, H. et al., 2010. The Two Enantiomers of Citalopram Bind to the Human Serotonin Transporter in Reversed Orientations. *Journal of American Chemical Society*, 132(9), pp.1311–1322.

Korey R. Demers, Morgans A. Reuter, M.R.B., 2013. CD8+ T-cell effector function and transcriptional regulation during HIV pathogenesis. *Immunological reviews*, 254(1), pp.190–206.

Lakehal, F. et al., 2001. Indirect cytotoxicity of flucloxacillin toward human biliary epithelium via metabolite formation in hepatocytes. *Chemical research in toxicology*, 14(6), pp.694–701.

Landsteiner, K. & Jacobs, J., 1936. Studies on the Sensitization of Animals With Simple Chemical Compounds. Ii. *The Journal of experimental medicine*, 64(10), pp.643–657.

Lanier, L.L., 2008. Up on the tightrope: natural killer cell activation and inhibition. *Nature Immunology*, 9(5), pp.495–502.

Larsen, J.M. et al., 2009. IL-23 and TH17-mediated inflammation in human allergic contact dermatitis. *Journal of Allergy and Clinical Immunology*, 123(2), p.486–492.e1.

Lazarou, J., Pomeranz, B.H. & Corey, P.N., 2015. Incidence of Adverse Drug Reactions in Hospitalized Patients A Meta-analysis of Prospective Studies. *The Journal of the American Medical Association*, 279(15).

Lehmann, P. V & Zhang, W., 2012. Handbook of ELISPOT. , 792, pp.3–23.

Leischner, C. et al., 2015. Nutritional immunology: function of natural killer cells and their modulation by resveratrol for cancer prevention and treatment. *Nutrition Journal*, 15(1), p.47.

Leone, P. et al., 2013. MHC class i antigen processing and presenting machinery: Organization, function, and defects in tumor cells. *Journal of the National Cancer Institute*, 105(16), pp.1172–1187.

Li, J. & Uetrecht, J.P., 2010. The Danger Hypothesis Applied to Idiosyncratic Drug Reactions. *Adverse Drug Reactions*, 196, pp.493–509.

Lichtenfels, M. et al., 2014. HLA restriction of carbamazepine-specific T-cell clones from an HLA-A*31:01-positive hypersensitive patient. *Chemical Research in Toxicology*, 27(2), pp.175–177.

Llano, A. & Brander, C., 2012. Mechanisms involved in the Abacavir-mediated hypersensitivity syndrome. *Cell research*, 22(12), pp.1637–9.

Locharernkul, C. et al., 2008. Carbamazepine and phenytoin induced Stevens-Johnson syndrome is associated with HLA-B*1502 allele in Thai population. *Epilepsia*, 49(12), pp.2087–2091.

Lonjou, C. et al., 2008. A European study of HLA-B in Stevens-Johnson syndrome and toxic epidermal necrolysis related to five high-risk drugs. *Pharmacogenetics and Genomics*, 18(2), pp.99–107.

Lucas, A. et al., 2015. Abacavir-reactive memory T cells are present in drug naïve individuals. *PloS one*, 10(2), p.e0117160.

Lucena, M.I. et al., 2011. Susceptibility to amoxicillin-clavulanate-induced liver injury is influenced by multiple HLA class i and II alleles. *Gastroenterology*, 141(1), pp.338–347.

Luckheeram, R.V. et al., 2012. CD4 +T cells: Differentiation and functions. *Clinical and Developmental Immunology*, 2012.

Luque, I. et al., 2001. In vitro T-cell responses to beta-lactam drugs in immediate and nonimmediate allergic reactions. *Allergy*, 56(7), pp.611–618.

MacLean, B. et al., 2010. Skyline: An open source document editor for creating and analyzing targeted proteomics experiments. *Bioinformatics*, 26(7), pp.966–968.

Mallal, S. et al., 2002. Association between presence of HLA-B*5701, HLA-DR7, and HLA-DQ3 and hypersensitivity to HIV-1 reverse-transcriptase inhibitor abacavir. *The Lancet*, 359, pp.727–732.

Mallal, S. et al., 2008. HLA-B*5701 Screening for Hypersensitivity to Abacavir. *New England Journal of Medicine*, 358(6), pp.568–79.

Man, C.B.L. et al., 2007. Association between HLA-B*1502 allele and antiepileptic drug-induced cutaneous reactions in Han Chinese. *Epilepsia*, 48(5), pp.1015–1018.

Manel, N., Unutmaz, D. & Littman, D.R., 2008. The differentiation of human T(H)-17 cells requires transforming growth factor-beta and induction of the nuclear receptor RORgammat. *Nature immunology*, 9(6), pp.641–9.

Maria, V.A. & Victorino, R.M., 1997. Diagnostic value of specific T cell reactivity to drugs in 95 cases of drug induced liver injury. *Gut*, 41(4), pp.534–40.

Marsh, S.G.E. et al., 2010. Nomenclature for factors of the HLA system, 2010. *Tissue Antigens*, 75(4), pp.291–455.

Martin, A. et al., 2005. Predisposition to nevirapine hypersensitivity associated with HLA-DRB1*0101 and abrogated by low CD4 T-cell counts. *AIDS*, January(3), pp.97–99.

Martin, A.M. et al., 2007. Immune responses to abacavir in antigen-presenting cells from hypersensitive patients. *AIDS*, 21(October 2006), pp.1233–1244.

Martin, A.M. et al., 2004. Predisposition to abacavir hypersensitivity conferred by HLA-B * 5701 and a haplotypic Hsp70-Hom variant. *PNAS*, 101(12), pp.4180–4185.

Martin, M.A. & Kroetz, D.L., 2013. Abacavir pharmacogenetics - From initial reports to standard of care. *Pharmacotherapy*, 33(7), pp.765–775.

Matzinger, P., 2002. The Danger Model: A Renewed Sense of Self. *Science*, 296(5566), pp.301–305.

Matzinger, P., 1994. TOLERANCE, DANGER, DANGER, AND AND THE THE EXTENDED FAMILY. *Annual Review of Immunology*, 12, pp.991–1045.

McConathy, J. & Owens, M.J., 2003. Stereochemistry in Drug Action. *Prim Care Companion J Clin Psychiatry*, 5(2), pp.70–73.

McCormack, M. et al., 2012. Genome-wide mapping for clinically relevant predictors of lamotrigine- and phenytoin-induced hypersensitivity reactions. *Pharmacogenomics*, 13(4), pp.399–405.

McCormack, M. et al., 2011. HLA-A*3101 and Carbamazepine-Induced Hypersensitivity Reactions in Europeans. *New England Journal of Medicine*, 364(12), pp.1134–1143.

McDowell, J. a et al., 1999. Pharmacokinetics of [(14)C]abacavir, a human immunodeficiency virus type 1 (HIV-1) reverse transcriptase inhibitor, administered in a single oral dose to HIV-1-infected adults: a mass balance study. *Antimicrobial Agents and Chemotherapy*, 43(12), pp.2855–2861.

Medzhitov, R. & Janeway, C.A., 1997. Innate immunity : impact on the adaptive immune response. *Current Opinion in Immunology*, 9, pp.4–9.

Mekori, Y. a & Metcalfe, D.D., 2000. Mast cells in innate immunity. *Immunological reviews*, 173(Il), pp.131–140.

Mellman, I., 2013. Dendritic Cells: Master Regulators of the Immune Response. *Cancer Immunology Research*, 1(3), pp.145–149.

Meng, X. et al., 2014. Abacavir forms novel cross-linking abacavir protein adducts in patients. *Chemical Research in Toxicology*, 27(4), pp.524–535.

Merk, H.F., 2005. Diagnosis of drug hypersensitivity : lymphocyte transformation test and cytokines. *Toxicology*, 209, pp.217–220.

Merkler, D.J., 1994. C-Terminal amidated peptides: Production by the in vitro enzymatic amidation of glycine-extended peptides and the importance of the amide to bioactivity. *Enzyme and Microbial Technology*, 16(6), pp.450–456.

Merkler, D.J. et al., 1993. The Enzymology of Peptide Amidation. *Bioinorganic Chemistry of Copper*, pp.196–209.

Metushi, I.G. et al., 2015. Acyclovir Has Low but Detectable Influence on HLA-B*57:01 Specificity without Inducing Hypersensitivity. *PloS one*, 10(5), p.e0124878.

Monshi, M.M. et al., 2013. Human leukocyte antigen (HLA)-B*57:01-restricted activation of drug-specific T cells provides the immunological basis for flucloxacillin-induced liver injury. *Hepatology*, 57(2), pp.727–739.

Mosmann, T.R. et al., 1986. Two types of murine helper T cell clone. I. Definition according to profiles of lymphokine activities and secreted proteins. *Journal of immunology (Baltimore, Md. : 1950)*, 136(7), pp.2348–57.

Muller, J. et al., 2016. Ketamine enantiomers in the rapid and sustained antidepressant effects. *Therapeutic Advances in Psychopharmacology*, 6(3), pp.185–192.

Münz, C., 2016. Autophagy proteins in antigen processing for presentation on MHC molecules. *Immunological Reviews*, 272(1), pp.17–27.

Naisbitt, D.J. et al., 2001. Antigenicity and immunogenicity of sulphamethoxazole: demonstration of metabolism-dependent haptenation and T-cell proliferation *in vivo*. *British Journal of Pharmacology*, 133(2), pp.295–305.

Naisbitt, D.J. et al., 2003. Characterization of drug-specific T cells in lamotrigine hypersensitivity. *Journal of Allergy and Clinical Immunology*, 111(6), pp.1393–1403.

Naisbitt, D.J. et al., 2005. Characterization of the T-cell response in a patient with phenindione hypersensitivity. *The Journal of pharmacology and experimental therapeutics*, 313(3), pp.1058–1065.

Naisbitt, D.J. et al., 2002. Covalent binding of the nitroso metabolite of sulfamethoxazole leads to toxicity and major histocompatibility complex-restricted antigen presentation. *Mol Pharmacol*, 62(3), pp.628–637.

Naisbitt, D.J. et al., 2000. Immunological Principles of Adverse Drug Reactions The Initiation and Propagation of Immune Responses Elicited by Drug Treatment. *Drug Safety*, 23(6), pp.483–507.

Naisbitt, D.J. et al., 2015. Towards depersonalized abacavir therapy : chemical modification eliminates HLA-B M 57 : 01-restricted CD8 R T-cell activation. *AIDS*, 00(00), pp.1–12.

Nau, C. & Strichartz, G.R., 2002. Drug chirality in anesthesia. *Anesthesiology*, 97(2), pp.497–502.

Neefjes, J. et al., 2011. Towards a systems understanding of MHC class I and MHC class II antigen presentation. *Nature Reviews Immunology*, 11(12), pp.823–836.

Nguyen, L.A., He, H. & Pham-Huy, C., 2006. Chiral drugs: an overview. *International journal of biomedical science : IJBS*, 2(2), pp.85–100.

Nograles, K.E. et al., 2010. IL-22 producing "T22" T-cells account for up-regulated IL-22 in atopic dermatitis (AD), despite reduced IL-17 producing Th17 T- cells. *J Allergy Clin Immunol.*, 123(6), pp.1–16.

Norcross, M.A. et al., 2012. Abacavir induces loading of novel self-peptides into HLA-BM 57:01: an autoimmune model for HLA-associated drug hypersensitivity. *AIDS*, 18(9), pp.1199–1216.

Nowak, R. et al., 2006. A comparison of levalbuterol with racemic albuterol in the treatment of acute severe asthma exacerbations in adults. *American Journal of Emergency Medicine*, 24(3), pp.259–267.

Nuijens, T. et al., 2012. Enzymatic C-terminal amidation of amino acids and peptides. *Tetrahedron Letters*, 53(29), pp.3777–3779.

Nyfeler, B. & Pichler, W.J., 1997. The lymphocyte transformation test for the diagnosis of drug allergy : sensitivity and specificity. *Clinical and Experimental Allergy,*, 27, pp.175–181.

Ostrov, D. a et al., 2012. Drug hypersensitivity caused by alteration of the MHC-presented self-peptide repertoire. *Proceedings of the National Academy of Sciences of the United States of America*, 109(25), pp.9959–64.

Overgaard, N.H. et al., 2015. CD4+/CD8+ double-positive T cells: more than just a developmental stage? *Journal of Leukocyte Biology*, 97(1), pp.31–38.

Ozeki, T. et al., 2011. Genome-wide association study identifies HLA-A*3101 allele as a genetic risk factor for carbamazepine-induced cutaneous adverse drug reactions in Japanese population. *Human Molecular Genetics*, 20(5), pp.1034–1041.

Padda, M.S. et al., 2012. DRUG INDUCED CHOLESTASIS. *Hepatology*, 53(4), pp.1377–1387.

Padial, A. et al., 2008. Non-immediate reactions to β-lactams: Diagnostic value of skin testing and drug provocation test. *Clinical and Experimental Allergy*, 38(5), pp.822–828.

Padovan, E. et al., 1997. Penicilloyl peptides are recognized as T cell antigenic determinants in penicillin allergy. *European Journal of Immunology*, 27(6), pp.1303–1307.

Park, B.K. et al., 2001. Metabolic activation in drug allergies. *Toxicology*, 158(1–2), pp.11–23.

Parkin, J. & Cohen, B., 2001. An overview of the immune system. *Lancet*, 357(9270), pp.1777–1789.

Pavlos, R. et al., 2015. T Cell–Mediated Hypersensitivity Reactions to Drugs. *Annual Review of Medicine*, 66(1), pp.439–454.

Pegram, H.J. et al., 2011. Activating and inhibitory receptors of natural killer cells. *Immunology and Cell Biology*, 89(2), pp.216–224.

Phillips, E. & Mallal, S., 2011. Pharmacogenetics of drug hypersensitivity. *Pharmacogenomics*, 11(7), pp.973–987.

Phillips, E.J. & Mallal, S.A., 2011. HLA-B * 1502 Screening and Toxic Effects of Carbamazepine. *The New England journal of medicine*, August, pp.672–673.

Pichler, W.J., 2007. Drug Hypersensitivity Reactions : Classification and Relationship to T-Cell Activation. *Drug Hypersensitivity*, pp.168–178.

Pichler, W.J., 2002a. Pharmacological interactions of drugs with antigen-specific immune receptors: the p-i concept. *Curr Opin Allergy Clin Immunol*, 2(June), pp.301–5.

Pichler, W.J., 2002b. T cells in drug allergy. *Current allergy and asthma reports*, 2(1), pp.9–15.

Pichler, W.J., 2008. The p-i Concept: Pharmacological Interaction of Drugs With Immune Receptors. *World Allergy Organization*, pp.96–102.

Pichler, W.J. & Tilch, J., 2004. The lymphocyte transformation test in the diagnosis of drug hypersensitivity. *Allergy*, 59, pp.809–820.

Pirmohamed, M. et al., 2004. Adverse drug reactions as cause of admission to hospital : *British Medical Journal*, 329(July), pp.15–19.

Pirmohamed, M., 2005. Anticipating , investigating and managing the adverse effects of drugs CME Clinical pharmacology. *Clinical Medicine*, 5(1), pp.23–26.

Pirmohamed, M. et al., 2002. The danger hypothesis—potential role in idiosyncratic drug reactions. *Toxicology*, 181–182, pp.55–63.

Pirmohamed, M. & Park, B.K., 2003. Adverse drug reactions : back to the future. *British journal of clinical pharmacology*, 55(January), pp.486–492.

Plumpton, C.O. et al., 2017. Cost effectiveness analysis of HLA-B*58:01 genotyping prior to initiation of allopurinol for gout. *Rheumatology (Oxford, England)*, 56(10), pp.1729–1739.

Porebski, G., Gschwend-Zawodniak, A. & Pichler, W.J., 2011. In vitro diagnosis of T cell-mediated drug allergy. *Clinical and Experimental Allergy*, 41(4), pp.461–470.

Pradeu, T. & Cooper, E.L., 2012. The danger theory: 20 years later. *Frontiers in Immunology*, 3(SEP), pp.1–9.

Pritchett, J.C., Nanau, R.M. & Neuman, M.G., 2012. The Link between Hypersensitivity Syndrome Reaction Development and Human Herpes Virus-6 Reactivation. *International Journal of Hepatology*, 2012, pp.1–19.

Purcell, a W. et al., 2001. Quantitative and qualitative influences of tapasin on the class I peptide repertoire. *Journal of immunology (Baltimore, Md. : 1950)*, 166(2), pp.1016–1027.

Pymm, P. et al., 2017. MHC-I peptides get out of the groove and enable a novel mechanism of HIV-1 escape. *Nature Structural and Molecular Biology*, 24(4), pp.387–394.

Quah, B.J.C., Warren, H.S. & Parish, C.R., 2007. Monitoring lymphocyte proliferation in vitro and in vivo with the intracellular fluorescent dye carboxyfluorescein diacetate succinimidyl ester. *Nature Protocols*, 2(9), pp.2049–2056.

Rasmussen, S.B. et al., 2013. Peptide pool immunization and CD8+ T cell reactivity. *Immunology Letters*, 151(1–2), pp.48–53.

Rescigno, M. et al., 1998. Dendritic Cell Survival and Maturation Are Regulated by Different Signaling Pathways. *Journal of Experimental Medicine*, 188(11), pp.2175–2180.

Robinson, J.H. & Delvig, A.A., 2002. Diversity in mhc class ii antigen presentation. *Immunology*, 105(3), pp.252–262.

Roche, P.A. & Furuta, K., 2015. The ins and outs of MHC class II-mediated antigen processing and presentation. *Nature Reviews Immunology*, 15(4), pp.203–216.

Rodriguez-Pena, R. et al., 2006. Potential involvement of dendritic cells in delayed-type hypersensitivity reactions to β-lactams. *Journal of Allergy and Clinical Immunology*, 118(4), pp.949–956.

Rohilla, A. & Yadav, S., 2013. Adverse drug reactions : An Overview. *International Journal of Pharmacological Research*, 3(1), pp.10–12.

Romano, A. et al., 2004. Diagnosis of nonimmediate reactions to β-lactam antibiotics. *Allergy: European Journal of Allergy and Clinical Immunology*, 59(11), pp.1153–1160.

Roujeau, J.-C., 2005. Clinical heterogeneity of drug hypersensitivity. *Toxicology*, 209(2), pp.123–129.

Roujeau, J.-C. et al., 1995. Medication Use and the Risk of Stevens–Johnson Syndrome or Toxic Epidermal Necrolysis. *New England Journal of Medicine*, 333(24), pp.1600–1608.

Rouvier, E., Luciani, M.F. & Golstein, P., 1993. Fas involvement in Ca(2+)-independent T cell-mediated cytotoxicity. *The Journal of experimental medicine*, 177(1), pp.195–200.

Rudensky, a Y., 2011. Regulatory T cells and Foxp3. *Immunol Rev*, 241(1), pp.260–268.

Russmann, S. et al., 2005. Risk of cholestatic liver disease associated with flucloxacillin and flucloxacillin prescribing habits in the UK: Cohort study using data from the UK General Practice Research Database. *British Journal of Clinical Pharmacology*, 60(1), pp.76–82.

Rzany, B. et al., 1996. Epidemiology of Erythema Exsudativum Multiforme Majus , Stevens-Johnson Syndrome , and Toxic Epidermal Necrolysis in Germany (1990- 1992): Structure and Results of a Population-Based Registry. *ELSEVIER*, 49(7), pp.769–773.

Salehi, M. et al., 2016. Th1, Th2 and Th17 Cytokine Profile in Patients with Multiple Sclerosis Following Treatment with Rapamycin. *Iranian journal of immunology : IJI*, 13(2), pp.141–7.

Sanderson, J.P. et al., 2007. Sulfamethoxazole and Its Metabolite Nitroso Sulfamethoxazole Stimulate Dendritic Cell Costimulatory Signaling. *The Journal of Immunology*, 178(9), pp.5533–5542.

Saokaew, S. et al., 2014. Cost-effectiveness analysis of HLA-B*5801 testing in preventing allopurinol-induced SJS/TEN in Thai population. *PLoS ONE*, 9(4), pp.1–9.

Satoh, K., T, Y. & Taira, N., 1980. Coronary vasodilator and cardiac effects of optical isomers of verapamil in the dog. *Journal of Cardiovascular Pharmacology*, 2, pp.309–18.

Schackman, B.R. et al., 2008. The cost-effectiveness of HLA-B*5701 genetic screening to guide initial antiretroviral therapy for HIV. *AIDS (London, England)*, 22(15), pp.2025–33.

Schnyder, B. et al., 1997. Direct, MHC-dependent presentation of the drug sulfamethoxazole to human T cell clones. *Journal of Clinical Investigation*, 100(1), pp.136–141.

Schnyder, B. et al., 2013. HLA-B*57:01+abacavir-naive individuals have specific T cells but no patch test reactivity. *Journal of Allergy and Clinical Immunology*, 132(3), pp.756–758.

Segal, A.W., 2005. How Neutrophils Kill Microbes. *Annual Review of Immunology*, 23(1), pp.197–223.

Sharma, S.T. & Nieman, L.K., 2011. Cushing's Syndrome: All variants, detection, and treatment. *Endocrinology and Metabolism Clinics of North America*, 40(2), pp.379–391.

Shiohara, T., Inaoka, M. & Kano, Y., 2006. Drug-induced hypersensitivity syndrome (DIHS): a reaction induced by a complex interplay among herpesviruses and antiviral and antidrug immune responses. *Allergology international : official journal of the Japanese Society of Allergology*, 55(1), pp.1–8.

Shipkova, M. & Wieland, E., 2012. Surface markers of lymphocyte activation and markers of cell proliferation. *Clinica Chimica Acta*, 413(17–18), pp.1338–1349.

Simms, P.E. & Ellis, T.M., 1996. Utility of Flow Cytometric Detection of CD69 Expression as a Rapid Method for Determining Poly- and Oligoclonal Lymphocyte Activation. *CLINICAL AND DIAGNOSTIC LABORATORY IMMUNOLOGY*, 3(3), pp.301–304.

Singer, J.B. et al., 2010. A genome-wide study identifies HLA alleles associated with lumiracoxib-related liver injury. *Nature Genetics*, 42, pp.711–714.

Siracusa, M.C. et al., 2013. Basophils and allergic inflammation. *Journal of Allergy and Clinical Immunology*, 132(4), pp.789–801.

Sivagnanam, S. & Deleu, D., 2003. Red man syndrome. *Critical Care*, 7, pp.119–121.

Song, B. et al., 2018. An animal model of abacavir-induced HLA-mediated liver injury. *Toxicological Sciences*, 162(2), pp.713–723.

Spriet, S. & Banks, T.A., 2015. Drug reaction with eosinophilia and systemic symptoms syndrome. *Allergy and Asthma Proceedings*, 36(6), pp.501–505.

Stone, K.D., Prussin, C. & Metcalfe, D.D., 2011. IgE, Mast Cells, Basophils, and Eosinophils. *Journal of Allergy and Clinical Immunology*, 125(2), pp.1–16.

Sugawara, S., Abo, T. & Kumagai, K., 1987. A simple method to eliminate the antigenicity of surface class I MHC molecules from the membrane of viable cells by acid treatment at pH 3. *Journal of Immunological Methods*, 26(100), pp.83–90.

Sukasem, C., 2014. Pharmacogenomics of drug-induced hypersensitivity reactions : challenges, opportunities and clinical implementation. *Asian Pacific Journal of Allergy and Immunology*, 32, pp.111–23.

Sullivan, A. et al., 2016. β-Lactam hypersensitivity involves expansion of circulating and skin-resident TH22 cells. *Journal of Allergy and Clinical Immunology*.

Symonds, W. et al., 2002. Risk Factor Analysis of Hypersensitivity Reactions to Abacavir. *Clinical Therapeutics*, 24(4), pp.565–573.

Tait, B.D., 2011. The ever-expanding list of HLA alleles: Changing HLA nomenclature and its relevance to clinical transplantation. *Transplantation Reviews*, 25(1), pp.1–8.

Tan, C.T. et al., 2011. Direct quantitation of MHC-bound peptide epitopes by selected reaction monitoring. *Proteomics*, 11(11), pp.2336–2340.

Tanguay, S. & Killion, J., 1994. Direct comparison of ELISPOT and ELISA-based assays for detection of individual cytokine-secreting cells. *Lymphokine Cytokine Research.*, Aug 13(4), pp.259–63.

Tassaneeyakul, W. et al., 2009. Strong association between HLA-B*5801 and allopurinol-induced Stevens-Johnson syndrome and toxic epidermal necrolysis in a Thai population. *Pharmacogenetics and genomics*, 19(9), pp.704–9.

Terasaki, P.I. & McLelland, J.D., 1964. Microdroplet Assay of Human Serum Cytotoxins. *Nature*, 204, pp.998–1000.

Thijssen, H.H.W., 1979. Identification of the active metabolites of the isoxazolyl penicillins by means of mass-spectrometry. *The Journal of Antibiotics*, XXXII(10).

Thorsby, E. et al., 1970. The HL-A system: evidence of a third sub-locus. *Scandinavian Journal of Haematology*, 7(3), pp.195–200.

Toksoy, A. et al., 2017. Potent NLRP3 inflammasome activation by the HIV reverse transcriptase inhibitor abacavir. *Journal of Biological Chemistry*, 292(7), pp.2805–2814.

Torres, M.A. & Moraes, M.E.H., 2011. Nomenclature for factors of the HLA system. *Einstein*, 9(11), pp.2010–2012.

Triggle, D.J., 1997. Stereoselectivity of drug action. *Drug Discovery Today*, 2(4), pp.138–147.

Trinchieri, G., Pflanz, S. & Kastelein, R.A., 2003. The IL-12 family of heterodimeric cytokines: New players in the regulation of T cell responses. *Immunity*, 19(5), pp.641–644.

Uetrecht, J. & Naisbitt, D.J., 2013. Idiosyncratic Adverse Drug Reactions: Current Concepts. *Pharmacological Reviews*, 65(2), pp.779–808.

Unanue, E.R., 1984. ANTIGEN-PRESENTING FUNCTION OF THE MACROPHAGE. *Annu. Rev. Immunol.*, 2, pp.395–428.

Vargesson, N., 2015. Thalidomide-induced teratogenesis: History and mechanisms. *Birth Defects Research Part C - Embryo Today: Reviews*, 105(2), pp.140–156.

Veldhoen, M. et al., 2006. TGFβ in the context of an inflammatory cytokine milieu supports de novo differentiation of IL-17-producing T cells. *Immunity*, 24(2), pp.179–189.

Verma, R., Vasudevan, B. & Pragasam, V., 2013. Severe cutaneous adverse drug reactions. *Medical Journal Armed Forces India*, 69(4), pp.375–383.

Vignali, D.A.A., Collison, L.W. & Workman, C.J., 2008. How regulatory T cells work. *Nature Reviews Immunology*, 8(7), pp.523–532.

Villadangos, J.A. et al., 1999. Proteases involved in MHC class II antigen presentation. *Immunological reviews*, 172(1), pp.109–200.

Vitovec, J. & Spinar, J., 2000. First-dose hypotension after angiotensin-converting enzyme ž (ACE) inhibitors in chronic heart failure : a comparison of enalapril and perindopril. *The European Journal of Heart Failure*, 2, pp.299–304.

Vojdani, A. & Erde, J., 2006. Regulatory T cells, a potent immunoregulatory target for CAM researchers: Modulating tumor immunity, autoimmunity and alloreactive immunity (III). *Evidence-based Complementary and Alternative Medicine*, 3(3), pp.309–316.

Voskoboinik, I., Whisstock, J.C. & Trapani, J.A., 2015. Perforin and granzymes: Function, dysfunction and human pathology. *Nature Reviews Immunology*, 15(6), pp.388–400.

Wall, E.E. Van Der, Ph, D. & Meulen, J. Van Der, 1996. Angiology Nitrate-Induced Headache in Patients with Stable Angina Pectoris : Beneficial Effect of Starting on a Low Dosage. *The Journal of Vascualar Diseases*, 47(7), pp.679–685.

Walsh, J.S., Reese, M.J. & Thurmond, L.M., 2002. The metabolic activation of abacavir by human liver cytosol and expressed human alcohol dehydrogenase isozymes. *Chem Biol Interact*, 142(1–2), pp.135–154.

Wang, Z. et al., 1994. CD4+ effector cells default to the Th2 pathway in interferon gamma-deficient mice infected with *Leishmania major*. *The Journal of experimental medicine*, 179(4), pp.1367–71.

Weaver, C.T., 2009. Th17: The ascent of a new effector T-cell subset. *European Journal of Immunology*, 39(3), pp.634–636.

Wei, C.Y., Chung, W.H., et al., 2012. Direct interaction between HLA-B and carbamazepine activates T cells in patients with Stevens-Johnson syndrome. *Journal of Allergy and Clinical Immunology*, 129(6), pp.1562–1569.

Wei, C.Y., Michael lee, M.T. & Chen, Y.T., 2012. Pharmacogenomics of adverse drug reactions: Implementing personalized medicine. *Human Molecular Genetics*, 21(R1), pp.58–65.

Whritenour, J. et al., 2014. Development and partial validation of a mouse model for predicting drug hypersensitivity reactions. *Journal of Immunotoxicology*, 11(2), pp.141–147.

Wieczorek, M. et al., 2017. Major histocompatibility complex (MHC) class I and MHC class II proteins: Conformational plasticity in antigen presentation. *Frontiers in Immunology*, 8(MAR), pp.1–16.

Williams, D.P. et al., 2000. Induction of metabolism-dependent and -independent neutrophil apoptosis by clozapine. *Molecular Pharmacology*, 58(1), pp.207–216.

Wing, K. et al., 2017. Quantification of the risk of liver injury associated with flucloxacillin: a UK population-based cohort study. *Journal of Antimicrobial Chemotherapy*, 27(July 2017), pp.374–9.

Wollack, J.W. et al., 2009. Multifunctional prenylated peptides for live cell analysis. *Journal of the American Chemical Society*, 131(21), pp.7293–7303.

Wolpert, E.Z. et al., 1997. Generation of CD8+ T cells specific for transporter associated with antigen processing deficient cells. *Proceedings of the National Academy of Sciences of the United States of America*, 94(21), pp.11496–501.

Wortmann, R.L., 2002. Gout and hyperuricemia. *Current Opinion in Rheumatology.*, 14(3), pp.281–286.

Wu, Y. et al., 2006. Activation of T cells by carbamazepine and carbamazepine metabolites. *Journal of Allergy and Clinical Immunology*, 118(1), pp.233–241.

Wuillemin, N. et al., 2013. HLA Haplotype Determines Hapten or p-i T Cell Reactivity to Flucloxacillin. *The Journal of Immunology*, 190(October), pp.4956–4964.

Yang, J. et al., 2008. Antigen activation and impaired Fas-induced death-inducing signaling complex formation in T-large-granular lymphocyte leukemia. *Blood*, 111(3), pp.1610–1616.

Yaseen, F.S. et al., 2015. Promiscuous T-cell responses to drugs and drug-haptens. *Journal of Allergy and Clinical Immunology*, 136(2), pp.474–476.

Yerly, D. et al., 2017. Structural Elements Recognized by Abacavir-Induced T Cells. *International journal of molecular sciences*, 18(1464), pp.1–10.

Yip, V.L. et al., 2012. HLA genotype and carbamazepine-induced cutaneous adverse drug reactions: A systematic review. *Clinical Pharmacology and Therapeutics*, 92(6), pp.757–765.

Yun, J. et al., 2013. Allopurinol hypersensitivity is primarily mediated by dose-dependent oxypurinol-specific T cell response. *Clinical and Experimental Allergy*, 43(11), pp.1246–1255.

Yun, J. et al., 2014. Oxypurinol Directly and Immediately Activates the Drug-Specific T Cells via the Preferential Use of HLA-B*58:01. *The Journal of Immunology*, 192(7), pp.2984–2993.

Zanni, M.P., von Greyerz, S., Schnyder, B., Wendland, T., et al., 1998. Allele-unrestricted presentation of lidocaine by HLA-DR molecules to specific alphabeta+ T cell clones. *Int Immunol*, 10(4), pp.507–515.

Zanni, M.P. et al., 1998. HLA-restricted, processing- and metabolism-independent pathway of drug recognition by human αβ T lymphocytes. *Journal of Clinical Investigation*, 102(8), pp.1591–1598.

Zanni, M.P., von Greyerz, S., Schnyder, B., Brander, K. a, et al., 1998. HLA-restricted, processing-and metabolism-independent pathway of drug recognition by human alpha beta T lymphocytes. *Journal of Clinical Investigation*, 102(8), p.1591.

Zanni, M.P. et al., 1999. Recognition of local anesthetics by alphabeta+ T cells. *The Journal of investigative dermatology*, 112(2), pp.197–204.

Zeilhofer, H. et al., 1992. Differential effects of ketamine enantiomers on NMDA receptor currents in cultured neurons. *European Journal of Pharmacology*, March(213), pp.115–8.

Zhang, F.-R. et al., 2013. *HLA-B*13:01* and the Dapsone Hypersensitivity Syndrome. *New England Journal of Medicine*, 369(17), pp.1620–1628.

Zhao, D. et al., 2017. Role of perforin secretion from CD8+ T-cells in neuronal cytotoxicity in multiple sclerosis. *Neurological Research*, 6412(November), pp.1–6.

Zhu, J., Yamane, H. & Paul, W., 2010. Differentiation of effector CD4 T cell populations. *Annu Rev Immunol.*, 28(1), pp.445–489.

Zhu, X. et al., 2015. Characterization of the draining lymph node response in the mouse drug allergy model: A model for drug hypersensitivity reactions. *Journal of Immunotoxicology*, 12(4), pp.376–384.

Appendix

Appendix Section 1

Amino acid sequence differences between HLA-B*57:01 and the abacavir insensitive alleles HLA-B*57:03 and HLA-B*58:01.

Appendix Table 1. **Comparison of amino acid sequences between HLA-B*57:01 and abacavir insensitive alleles HLA-B*57:03 and HLA-B*58:01.** Sequences were determined using sequence alignment tool of the EMBL European Bioinformatics Institute (www.ebi.ac.uk). Red boxes indicate amino acid differences at positions 114 and 116 between HLA-B*57:01 and HLA-B*57:03. Blue boxes highlight amino acid differences between HLA-B*57:01 and HLA-B*58:01.

Appendix Section 2. Synthesis of chapter 3 substituted abacavir analogues.

The abacavir substituted analogues used in chapter 3 were synthesised following a general procedure outlined in section 3.3.2. Synthesis of individual analogues was carried out as described below.
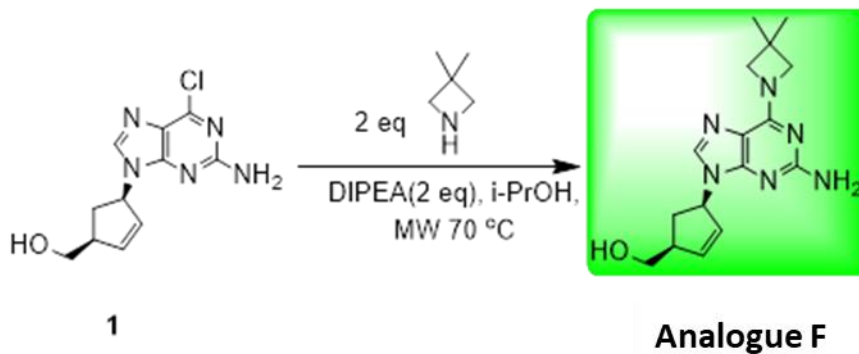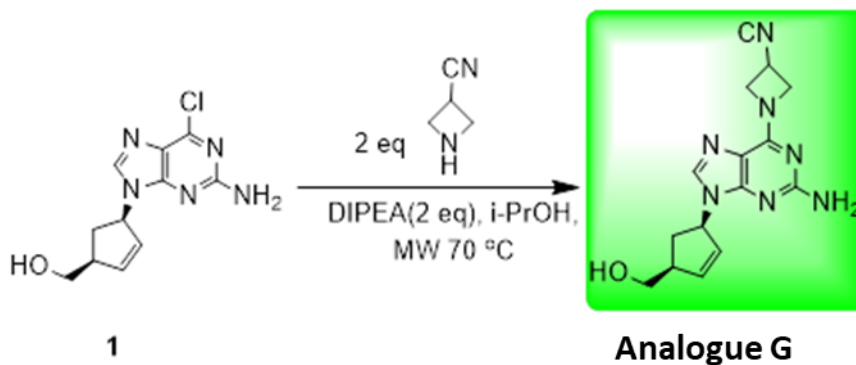
Analogue A
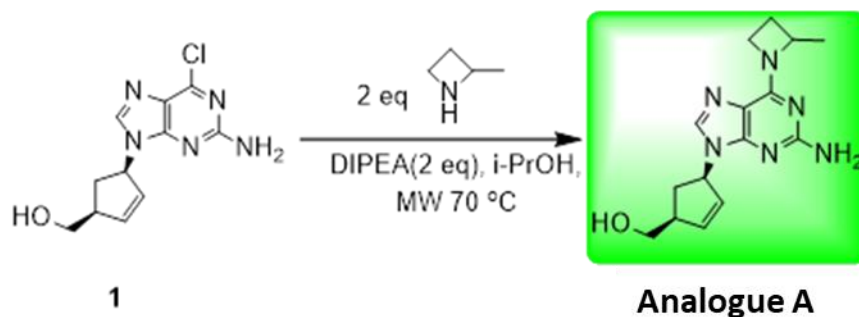
The crude product was purified by prep.TLC purification to give **Analogue A** (54.8 mg, 182.4 umol, 32 % yield) as a white solid.

LCMS: ET4430-1-P1A6 (M+H$^+$): 301.1

^{1}H NMR: ET4430-1-P1A1 400 MHz MeOD

δ7.70 (s, 1H), 6.15 (t, J = 3.6 Hz, 1H), 5.88 (t, J = 2.4 Hz, 1H), 5.47-5.51 (m, 1H), 4.80 (s, 1H), 4.35 (s, 1H), 4.21 (s, 1H), 3.61-3.65 (m, 2H), 2.98 (s, 1H), 2.76-2.98 (m, 1H), 2.73-2.75 (m, 1H), 1.68-2.02 (m, 1H), 1.65-1.67 (m, 1H), 1.57 (d, J = 6.4 Hz, 3H).
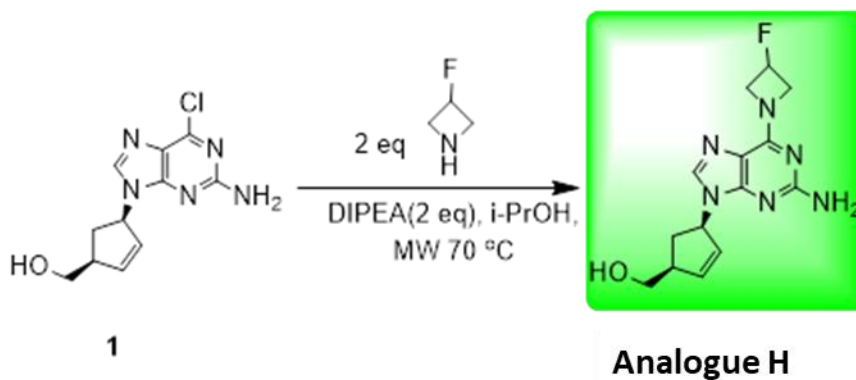
Analogue B
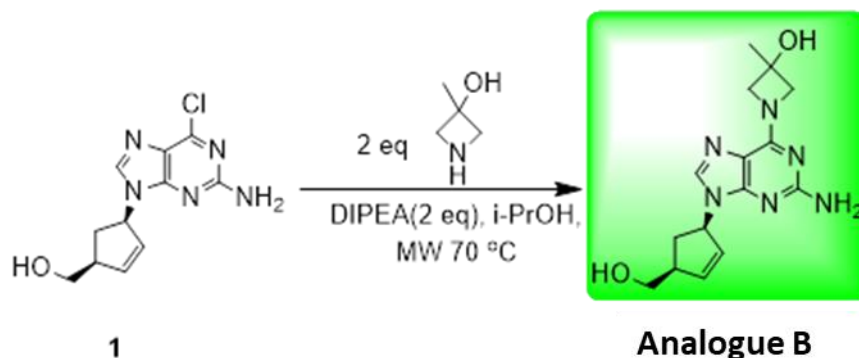
The crude product was purified by prep.TLC purification to give **Analogue B** (104.8 mg, 331.3 umol, 58 % yield) as a white solid.

LCMS: ET4430-5-P1A6 (M+H$^+$): 317.1

^{1}H NMR: ET4430-5-P1A2 400 MHz MeOD

δ7.73 (s, 1H), 6.15 (t, J = 3.6 Hz, 1H), 5.88 (t, J = 2.4 Hz, 1H), 5.48-5.49 (m, 1H), 4.20 (s, 1H), 3.57-3.65 (m, 2H), 3.54 (s, 2H), 2.98 (s, 1H), 2.73-2.76 (m, 1H), 1.65-1.70 (m, 1H), 1.63 (d, J = 5.6 Hz, 3H).

Analogue C
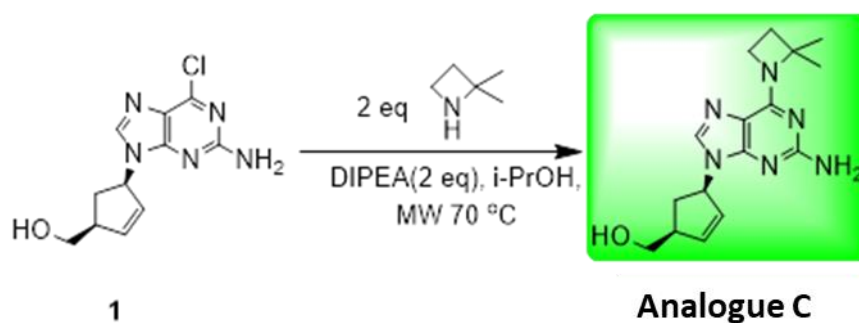
The crude product was purified by prep. TLC purification to give **Analogue C** (109.5 mg, 348.3 umol, 62% yield) as a white solid.

LCMS: ET4430-17-P1A5 (M+H$^+$): 315.2

^{1}H NMR: ET4430-17-P1A1 400 MHz MeOD

δ7.64 (s, 1H), 6.12-6.15 (m, 1H), 5.86 (t, J = 2.4 Hz, 1H), 5.45-5.47 (m, 1H), 4.38 (s, 1H), 3.56-4.00 (m, 2H), 2.96-2.97 (m, 1H), 2.72-2.75 (m, 1H), 2.18-2.21 (m, 1H), 1.62-1.68 (m, 6H).
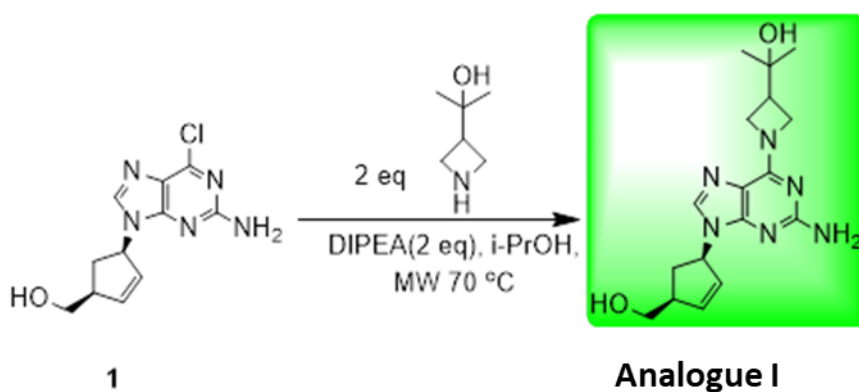
Analogue D
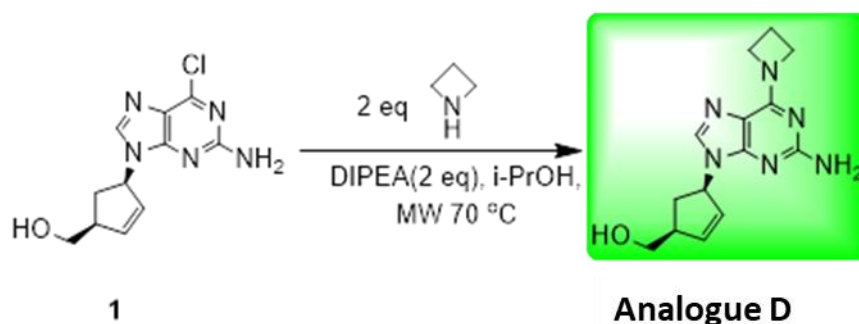
The crude product was purified by prep. TLC purification to give **Analogue D** (57.3 mg, 200.1 umol, 35% yield) as a white solid.

LCMS: ET4430-5-P1A6 (M+H$^+$): 287.1

^{1}H NMR: ET4430-2-P1A5 400 MHz MeOD

δ7.71 (s, 1H), 6.14-6.16 (m, 1H), 5.86-5.88 (m, 1H), 5.47-5.50 (m, 1H), 4.80 (s, 1H), 3.56-3.65 (m, 2H), 2.98 (s, 1H), 2.72-2.76 (m, 1H), 2.44-2.47 (m, 2H), 1.63-1.69 (m, 1H)
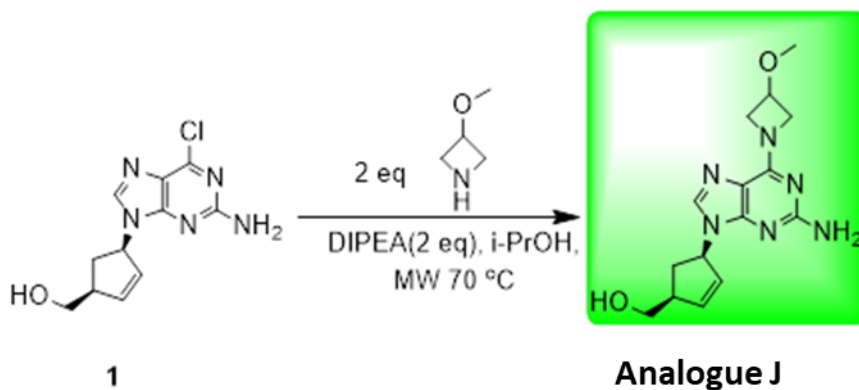
Analogue E
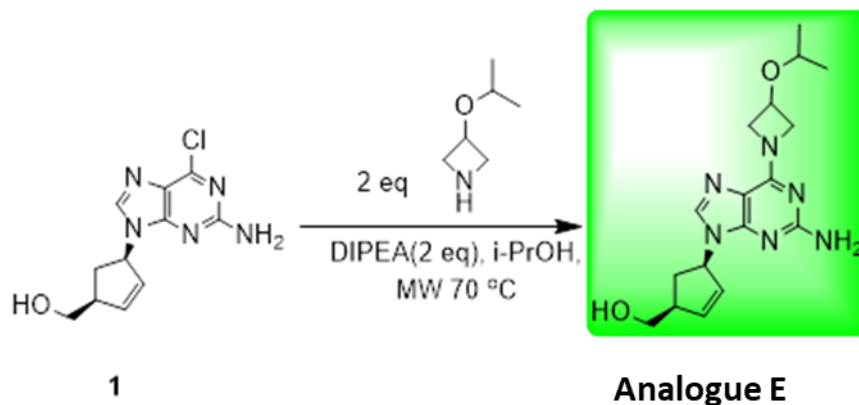
The crude product was purified by prep.TLC purification to give **Analogue E** (126.1 mg, 366.1 umol, 65% yield) as a white solid.

LCMS: ET4430-24-P1A5 (M+H$^+$): 301.2

^{1}H NMR: ET4430-24-P1A3 400 MHz MeOD

δ7.73 (s, 1H), 6.14-6.16 (m, 1H), 5.86-5.88 (m, 1H), 5.47-5.51 (m, 1H), 4.57 (s, 2H), 4.14 (s, 1H), 3.61-3.71 (m, 3H), 2.98-3.32 (m, 1H), 2.72-2.98 (m, 1H), 1.64-1.70 (m, 1H), 1.16 (d, J = 6.0 Hz, 6H)

Analogue F

The crude product was purified by prep.TLC purification to give **Analogue F** (71.0 mg, 225.8 umol, 40% yield) as a yellow solid.

LCMS: ET4430-6-P1A6 (M+H$^+$): 315.2

^{1}H NMR: ET4430-6-P1A5 400 MHz MeOD

δ7.71 (s, 1H), 6.14-6.16 (m, 1H), 5.86-5.88 (m, 1H), 5.47-5.51 (m, 1H), 4.03 (s, 1H), 3.57-3.65 (m, 2H), 2.97-2.98 (m, 1H), 2.72-2.76 (m, 1H), 1.64-1.70 (m, 1H), 1.35 (s, 6H)

Analogue G

Analogue G

 The crude product was purified by prep.TLC purification to give **Analogue G** (79.9 mg, 256.6 umol, 45% yield) as a white solid.

LCMS: ET4430-18-P1A (M+H$^+$): 312.2

^{1}H NMR: ET4430-18-P1A6 400 MHz MeOD

δ7.63 (s, 1H), 6.08-6.09 (m, 1H), 6.02 (s, 2H), 5.82-5.83 (m, 1H), 5.34-5.37 (m, 1H), 4.68-4.71 (m, 1H), 4.48-4.52 (m, 2H), 4.32-4.33 (m, 1H), 3.88-3.92 (m, 1H), 3.40 (t, J = 5.6 Hz, 2H), 2.56-2.83 (m, 1H), 2.42-2.54 (m, 1H), 1.50-1.55 (m, 1H)

Analogue H

Analogue H

The crude product was purified by prep.TLC purification to give **Analogue H** (65.0 mg, 213.6 umol, 38% yield) as a white solid.

LCMS: ET4430-7-P1A5 (M+H$^+$): 305.2

^{1}H NMR: ET4430-7-P1A1 400 MHz MeOD

δ7.75 (s, 1H), 6.14-6.16 (m, 1H), 5.87-5.88 (m, 1H), 5.50-5.86 (m, 2H), 4.65 (s, 2H), 4.36-4.42 (m, 2H), 3.56-3.65 (m, 2H), 3.28-3.54 (m, 1H), 2.73-2.98 (m, 1H), 1.64-1.71 (m, 1H)

Analogue I

The crude product was purified by prep.TLC purification to give **Analogue I** (134.5 mg, 390.2 umol, 69% yield) as a white solid.

LCMS: ET4430-25-P1A (M+H$^+$): 345.2

^{1}H NMR: ET4430-25-P1A3 400 MHz MeOD

δ7.73 (s, 1H), 6.15 (s, 1H), 5.87 (s, 1H), 5.50 (s, 1H), 3.57-3.65 (m, 2H), 3.32 (s, 1H), 2.98 (s, 1H), 2.83-2.87 (m, 1H), 2.72-2.76 (m, 1H), 1.65-1.68 (m, 1H), 1.28-1.34 (m, 1H), 1.17 (s, 6H)

Analogue J

The crude product was purified by prep.TLC purification to give **Analogue J** (83.4 mg, 263.6 umol, 47% yield) as a white solid.

LCMS: ET4430-8-P1A6 (M+H$^+$): 317.2

^{1}H NMR: ET4430-8-P1A2 400 MHz MeOD

δ7.73 (s, 1H), 6.15 (t, J = 3.6 Hz, 1H), 5.88 (t, J = 2.0 Hz, 1H), 5.50 (t, J = 5.6 Hz, 1H), 4.53 (s, 1H),4.37-4.39 (s, 1H), 4.36 (s, 1H), 3.57-3.65 (m, 2H), 3.55 (s, 3H), 2.98 (s, 1H), 2.73-2.78 (m, 1H), 1.63-1.70 (m, 1H).

Analogue K
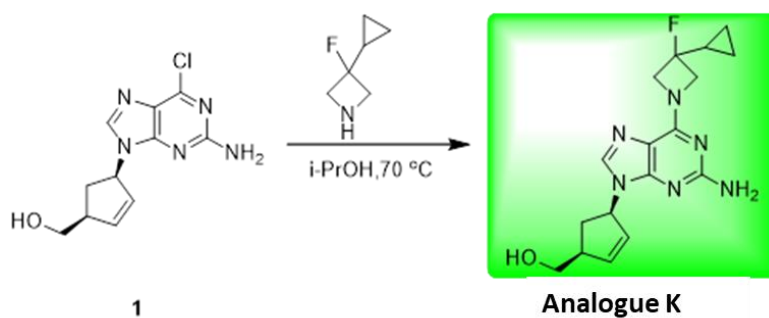
Analogue K

Compound **1** (135 mg, 447 umol, 1.0 *eq*), **Analogue K** (135 mg, 894 umol, 2.0 *eq*) and DIPEA (289 mg, 2.2 mmol, 5.0 *eq*) were dissolved in i-PrOH (3 mL). The solution was heated at 70 °C under microwave for 2 hr. LC-MS showed the reaction was completed. The reaction solution was concentrated and the residue was dissolved in EtOAc (20 mL). The organic phase was washed with water (20 mL). The water phase was extracted with EtOAc (10 mL*3). The combined organic layers were washed with brine (10 mL), dried over Na_2SO_4, filtrated and concentrated to give **Analogue K** (100 mg, 290 umol, 65% yield) as an off white solid.

¹HNMR: ET5353-5-P1A 400 MHz MeOD

δ 7.78 (s, 1H), 6.17-6.18 (m, 1H), 5.89-5.91 (m, 1H), 5.51-5.55 (m, 1H), 4.33 (d, *J* = 16 Hz, 4H), 3.57-3.68 (m, 2H), 3.00-3.01 (m, 1H), 2.75-2.81 (m, 1H), 1.67-1.73 (m, 1H), 1.41-1.45 (m, 1H), 0.65-0.70 (m, 2H), 0.50-0.53 (m, 2H).

LCMS: ET5353-5-p1a (M+H)⁺: 345.2

SFC: ET5353-5-P1: 100%

Analogue L
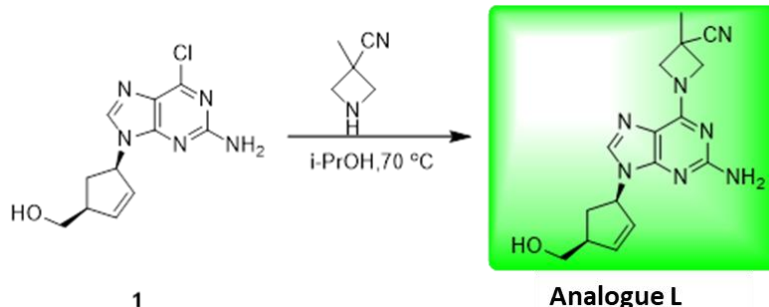
Analogue L

Compound **1** (135 mg, 447 umol, 1.0 *eq*), **Analogue L** (118 mg, 894 umol, 2.0*eq*) and DIPEA (289 mg, 2.2 mmol, 5.0 *eq*) were dissolved in i-PrOH (3.0 mL). The solution was heated at 70 °C under microwave for 2 hr. LC-MS showed the reaction was completed. The reaction solution was concentrated and the residue was dissolved in EtOAc (20 mL). The organic phase was washed with water (20 mL). The water phase was extracted with EtOAc (10 mL*3). The combined organic layers were washed with brine (10 mL), dried over Na_2SO_4, filtrated and concentrated to give the crude product. The crude product was purified by prep-TLC (Dichloromethane: Methanol =10:1) to give **Analogue L** (75 mg, 231 umol, 52% yield) as a white solid.

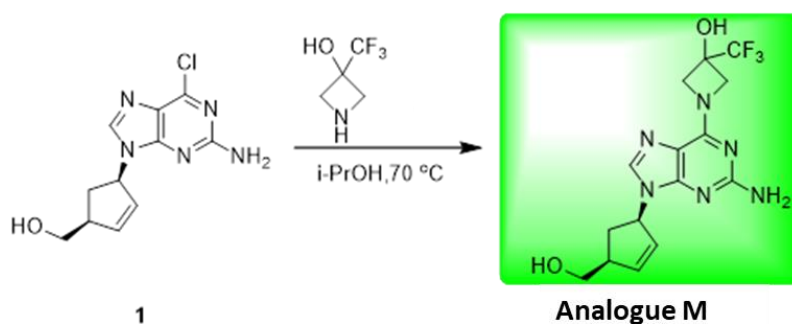**¹HNMR:** ET5353-6-p1a 400 MHz MeOD

δ 7.79 (s, 1H), 6.17-6.19 (m, 1H), 5.89-5.91 (m, 1H), 5.52-5.55 (m, 1H), 4.65 (d, *J* = 8 Hz, 2H), 4.29 (d, *J* = 8 Hz, 2H), 3.57-3.68 (m, 2H), 3.00 (s, 1H), 2.73-2.81 (m, 1H), 1.74 (s, 3H), 1.68-1.73 (m, 1H).

LCMS: ET5353-6-p1 (M+H)⁺: 326.2

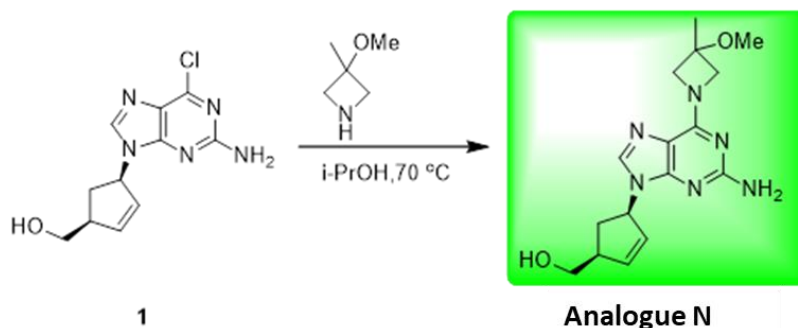**SFC:** ET5353-6-P1A: 100%

Analogue M

Compound **1** (135 mg, 447 umol, 1.0 *eq*), **Analogue M** (159 mg, 894 umol, 2.0 *eq*) and DIPEA (289 mg, 2.2 mmol, 5.0 *eq*) were dissolved in i-PrOH (3 mL). The solution was heated at 70 °C under microwave for 2 hr. LC-MS showed the reaction was completed. The reaction solution was concentrated and the residue was dissolved in EtOAc (20 mL). The organic phase was washed with water (20 mL). The water phase was extracted with EtOAc (10 mL*3). The combined organic layers were washed with brine (10 mL), dried over Na$_2$SO$_4$, filtrated and concentrated to give the crude product. The crude product was purified by prep-TLC (Dichloromethane: Methanol =10:1) to give **Analogue M** (65 mg, 176 umol, 39% yield) as a white solid.

¹HNMR: ET5353-7-p1c 400 MHz MeOD

δ 7.79 (s, 1H), 6.17-6.19 (m, 1H), 5.90-5.91 (m, 1H), 5.50-5.54 (m, 1H), 4.60 (s, 2H), 4.29 (d, 2H), 3.57-3.68 (m, 2H), 3.00 (s, 1H), 2.73-2.81 (m, 1H), 1.67-1.74 (m, 1H).

LCMS: ET5353-7-p1a (M+H)⁺: 371.2

SFC: ET5353-7-P1A: 100%

Analogue N

Compound **1** (135 mg, 447 umol, 1.0 *eq*), **Analogue N** (123 mg, 894 umol, 2.0 *eq*) and DIPEA (289 mg, 2.2 mmol, 5.0 *eq*) were dissolved in i-PrOH (3 mL) in a microwave tube. The solution was heated at 70 °C under microwave for 2 hr. LC-MS showed the reaction was completed. The reaction solution was concentrated and the residue was dissolved in EtOAc (20 mL). The organic phase was washed with water (20 mL). The water phase was extracted with EtOAc (10 mL*3). The combined organic layers were washed with brine (10 mL), dried over Na$_2$SO$_4$, filtrated and concentrated to give the crude product. The crude product was purified by prep-TLC (Dichloromethane: Methanol =10:1) to give **Analogue N** (65 mg, 197 umol, 44% yield) as a white solid.

¹HNMR: ET5353-8-p1a 400 MHz MeOD

δ 7.76 (s, 1H), 6.17-6.19 (m, 1H), 5.91-5.94 (m, 1H), 5.22 (s, 1H), 4.28 (s, 2H), 4.16 (s, 2H), 3.57-3.68 (m, 2H), 3.32 (s, 3H), 3.00 (s, 1H), 2.75-2.81 (m, 1H), 1.66-1.73 (m, 1H), 1.55 (s, 3H).
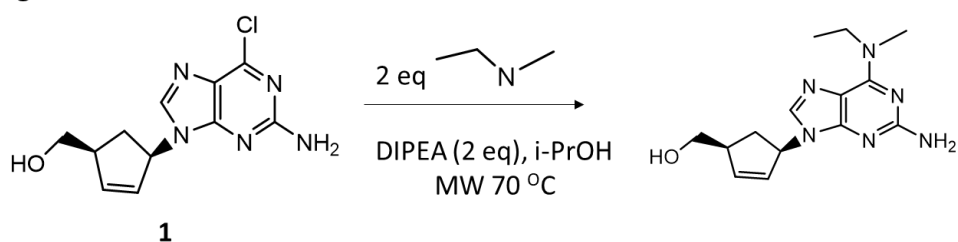
**LCMS:** ET5353-8-p1a (M+H)⁺: 331.2

SFC: ET5353-8-P1: 100%

Appendix Section 3. Synthesis of chapter 4 substituted abacavir analogues

The abacavir substituted analogues processed in chapter 4 were synthesised following the same procedure as described in section 3.3.2. Synthesis of individual abacavir analogues is outlined below.
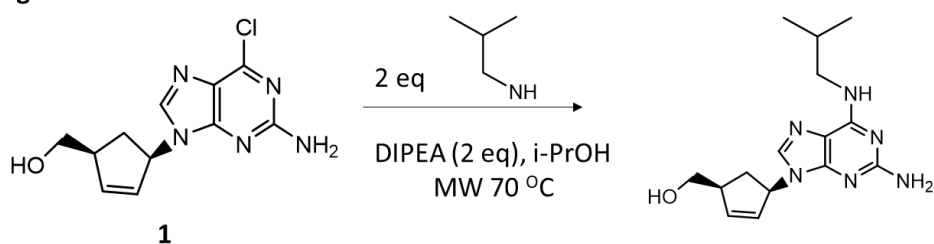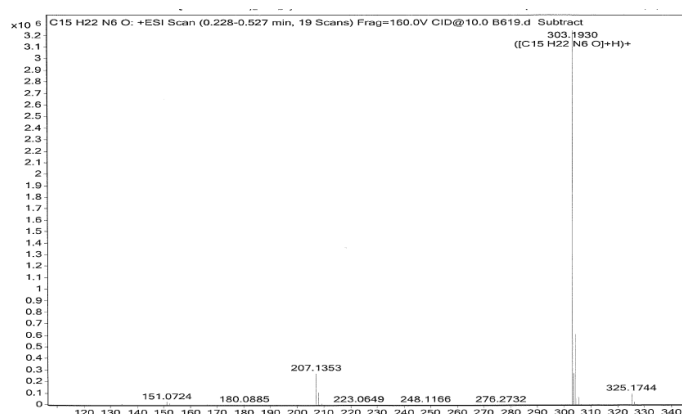
Analogue O

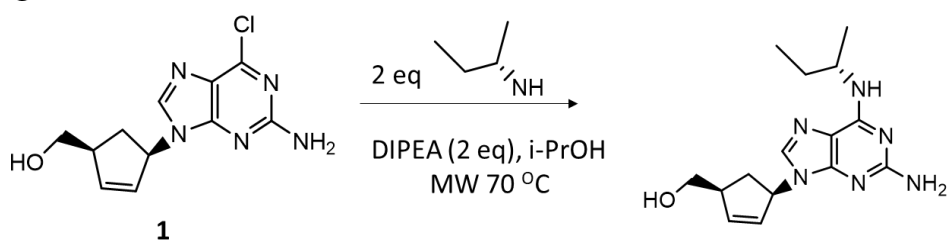The crude product was purified by prep.TLC purification to give **Analogue O** (136.9mg) as a white solid.
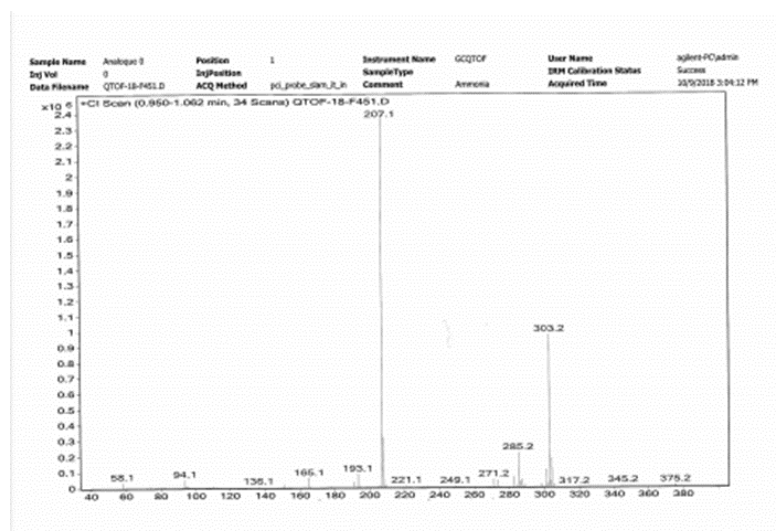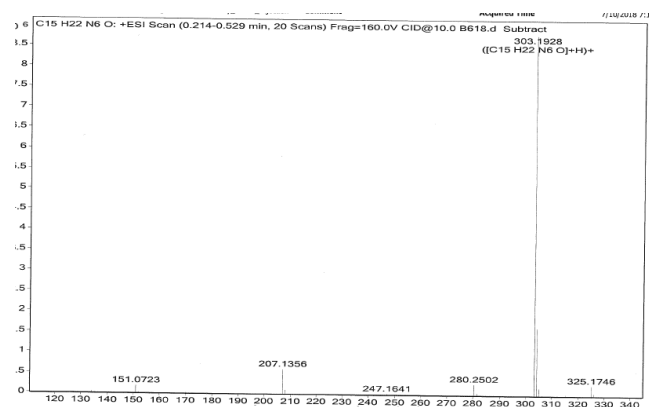
Analogue P

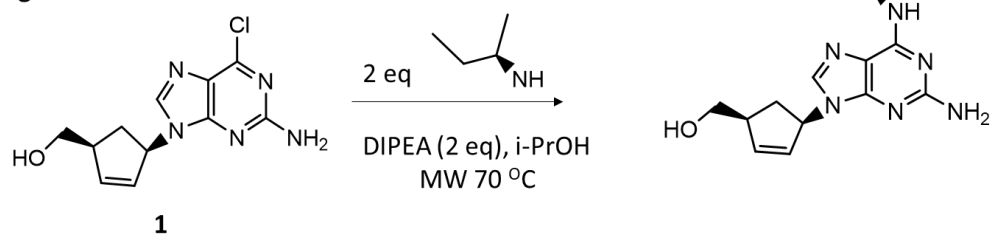The crude product was purified by prep. TLC purification to give **Analogue P** (100mg) as a white solid.

Analogue Q

The crude product was purified by prep. TLC purification to give **Analogue Q** (97.6mg) as a white solid.

Analogue R

The crude product was purified by prep.TLC purification to give **Analogue R** (56.8mg) as a white solid.